The Synthesis and Evaluation of Potential anti-*Mycobacterium tuberculosis* and Apoptotic agents

Sunil Sagar

A thesis submitted in partial fulfillment of the requirements for the degree of Doctor Philosophiae in the Department of Chemistry, University of the Western Cape.

Supervisor: Prof. Ivan R. Green

Co-Supervisor: Prof. F. Ameer

April 2007

Keywords

2-(1´,4´-Benzoquinon-2´-yl)-5-hydroxy-7-methyl-1,4-naphthoquinone

2,2´-Bis(7-methyl-1,4-naphthoquinone)

2,5-Dibromobenzoquinone

Apopercentage

Apoptosis

Boronic acid

Cancer

Caspases

Cell cycle

Cytotoxicity

Diospyrin

DNA fragmentation

Glutathione

Isoniazid

MDR-TB

Mycobacterium tuberculosis

Reductive alkylation

Suzuki coupling

Topoisomerases

Abstract

Tuberculosis (TB) and Cancer are among the most devastating and therapeutically challenging diseases that need to be addressed in South Africa today. The development of muti-drug resistance in TB causing bacteria, *Mycobacterium tuberculosis* and cancerous cells has prompted the search for effective novel compounds. The present study focuses on the synthesis and the evaluation of different analogues of diospyrin, a proven anti-TB and anti-cancer agent. Two binaphthoquinone compounds viz., 2,2′-bis(7-methyl-1,4-naphthoquinone) and 2,2′-bis(5-methoxy-7-methyl-1,4-naphthoquinone) were synthesized by using Suzuki methodology. Two naphthoquinone-benzoquinone compounds viz., 2-(1′,4′-benzoquinon-2′-yl)-7-methyl-1,4-naphthoquinone and 2-(1′,4′-benzoquinon-2′-yl)-5-hydroxy-7-methyl-1,4-naphthoquinone, which differ only in the hydroxyl group at C-5 position were synthesized in fairly good yields by using the same methodology. Several other naphthoquinone-naphthalene biaryl compounds were also synthesized by using commercially available boronic acids.

Initially 7 analogues were evaluated for their biological activity against fast growing bacteria viz., *M. smegmatis* and *M. aurum* using the broth microdilution method. These compounds were found to be very potent against these strains. Since different strains of mycobacteria behave differently to the same compounds so these analogues were evaluated against a clinical strain of *M. tuberculosis* using the BACTEC method, where 2-(6′-hydroxynaphthalen-2′-yl)-5-hydroxy-7-methyl-1,4-naphthoquinone and 2-(5′,10′-dioxydithianthren-1′-yl)-7-methyl-1,4-naphthoquinone demonstrated promising results and need further investigation to check their potential to be considered for drug trials.

Four different analogues 2-(1′,4′-benzoquinon-2′-yl)-5-hydroxy-7-methyl-1,4-naphthoquinone, 2-(5′,10′-dioxydithianthren-1′-yl)-7-methyl-1,4-naphthoquinone, 2-(1′,4′,5′-trimethoxy-7′-methylnaphthalen-2′-yl)-5-methoxy-7-methyl-1,4-naphthoquinone and 2-(1′,4′-benzoquinon-2′-yl)-7-methyl-1,4-naphthoquinone were evaluated for their ability to induce apoptosis in three cancer cell lines viz., HeLa, MCF7, MG63 and one non-transformed cell line i.e. CHO. The various methods employed to assess the apoptotic potential of the compounds were the APOpercentage, DNA fragmentation and Cell cycle. APOpercentage revealed that the compounds 2-(1′,4′-benzoquinon-2′-yl)-5-hydroxy-7-methyl-1,4-naphthoquinone and 2-(5′,10′-dioxydithianthren-1′-yl)-7-methyl-1,4-naphthoquinone were active apoptosis inducers. Since 2-(1′,4′-benzoquinon-2′-yl)-5-hydroxy-7-methyl-1,4-naphthoquinone was the most active inducer in three cell lines under investigation, it was further tested for its ability to induce apoptosis via the DNA fragmentation, which confirmed the induction of apoptosis in the malignant cells in response to 2-(1′,4′-benzoquinon-2′-yl)-5-hydroxy-7-methyl-1,4-naphthoquinone, after 24 hours and at a concentration of 10 μM.

Thus several analogues of diospyrin were successfully synthesized in fairly good yield and were identified to have anti-mycobacterial and anti-cancer activities. This preliminary investigation has created an interest to synthesize more structurally modified quinonoids in order to develop and establish them as potent drugs against mycobacterium and cancer.

DECLARATION

I declare that *The Synthesis and Evaluation of Potential anti-Mycobacterium tuberculosis and Apoptotic agents* is my own work, that it has not been submitted before for any degree or examination in any other university, and that all the sources I have used or quoted have been indicated and acknowledged as complete references.

Sunil Sagar April 2007

Signed: ……..

Acknowledgements

I would like to take this opportunity to express my sincere gratitude to Prof. I. R. Green for his advice, guidance, encouragement and support throughout the course of this work.

My thanks also go to Prof. F. Ameer for the much-appreciated assistance given to me during part of this project.

Thanks also go to:

Department of Chemistry, UWC, for the facilities provided during course of study.

Prof. Ian Wiid, Medical School, Stellenbosch University and Tracy Seaman, at UCT for evaluation of compounds against mycobacteria.

Department of Chemistry, WITS University for their technical assistance in high resolution mass spectra and Prof. Jasper Rees and Dr Mervin Meyer of the Department of Biotechnology for their appreciated assistance.

My friends and colleagues at UWC for their support and encouragement.

Finally, I would like to thank my family for their unstinting support during my years of study, and for encouraging me in my academic pursuits.

The acknowledgements are also due to National Research Foundation for financial support.

TABLE OF CONTENTS

List of Tables

Chapter 1

Chapter 5

Chapter 7

List of Figures

Chapter 1

Chapter 5

Chapter 6

Chapter 7

Abbreviations

AIDS	Acquired Immuno Deficiency Syndrome
APAF1	Apoptotic protease-activating factor 1
ATP	Adenosine triphosphate
CAD	Caspase-activated deoxyribonuclease
CARD	Caspase activated recruitment domains
CHO	Chinese Hamster Ovaries
CPFX	Ciprofloxacin
DCM	Dichloromethane
DD	Death domain
DEDs	Death effector domains
DISC	Death inducing signaling complex
DMSO	Dimethyl sulfoxide
DNA	Deoxyribonucleic acid
DSBs	Double-strand breaks
EAC	Ehrlich Ascites Carcinoma
ED_{50}	50% Effective dose
EMB	Ethambutol
EtOAc	Ethyl acetate
FACS	Flourescent Activated Cell Sorting
FADD	Fas-activated Death Domain
GI	Growth Index
GSTs	Glutathione transferases
GTFX	Gatifloxacin
h	Hours

HIV	Human Immunodeficiency Virus
HRMS	High Resolution Mass Spectrum
Hz	Hertz
IAPs	Inhibitors of Apoptosis proteins
IC_{50}	50% Inhibitory concentration
ICAD	Inhibitor of CAD
INH	Isoniazid
INT	Iodonitrotetrazolium salt
LVFX	Levofloxacin
M. tuberculosis	*Mycobacterium tuberculosis*
MDR-TB	Multi-drug Resistance Tuberculosis
MIC	Minimum inhibitory concentration
MRC	Medical Research Council
MXFX	Moxifloxacin
NMR	Nuclear Magnetic Resonance
NR	Neutral Red
OD	Optical Density
OFLX	Ofloxacin
PBS	Phosphate buffer saline
PEG	Polyethylene glycol
PI	Propidium Iodide
PZA	Pyrazinamide
RIF	Rifampicin
ROS	Reactive Oxygen Species
SM	Streptomycin

SPFX	Sparfloxacin
STFX	Sitafloxacin
TB	Tuberculosis
TNFR	Tumor necrosis factor receptor
TRADD	Toll receptor activated death domain
XDR-TB	Extensively Drug Resistant TB

Chapter 1: Introduction

Tuberculosis (TB) is as old as mankind.[1] Archaeologists have identified skeletal tuberculosis of the spine in prehistoric populations from Egypt, Peru, Canada, Germany, Denmark and in Britain. A German doctor, Robert Koch (1881) first identified, the organism that causes TB in humans. He named the organism *Mycobacterium tuberculosis*, which means 'fungus-bacterium' because of the fungus-like membrane that the bacteria produce when grown on liquid media. Mycobacteria are aerobic, non-endospore-forming, non-motile, slightly curved or straight rods. These bacteria are relatively resistant to normal staining procedures. Once stained, however, mycobacteria are not easily decolourised, even with acid-alcohol and are therefore classified as acid-fast.[2] This characteristic reflects on the unusual composition of the cell wall, which contains mycolic acids together with free lipids. There are approximately 70 other species in the genus *Mycobacterium*, many of which are opportunistic pathogens in animals and humans.

Fig 1.1 Scanning electron micrograph of *Mycobacterium tuberculosis*

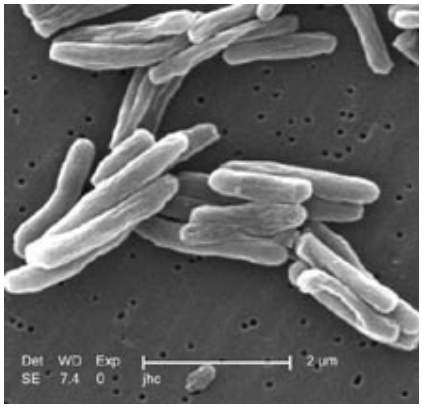

Mycobacterium tuberculosis is an intracellular pathogen, which has a predilection for lung tissue, which has a rich oxygen supply. TB is spread through the air from one person to

another. When infectious people cough, sneeze, talk or spit, they propel TB germs, known as bacilli, into the air. The tubercle bacilli enter the body via the respiratory route. The bacilli spread from the site of initial infection in the lung through the lymphatics or blood to other parts of the body with the apex of the lung and the regional lymph node being favoured sites. Extrapulmonary TB of the pleura, lymphatics, bone, genito-urinary system, meninges, peritoneum, or skin occurs in about 15% of TB patients.[3]

A person needs only to inhale a small number of bacilli to be infected. Left untreated, each person with the active TB disease will infect on average between 10 and 15 people every year. However, people infected with TB bacilli will not necessarily become sick with the disease. The immune system "walls off" the TB bacilli, which, protected by a thick waxy coat, can lie dormant for years. When someone's immune system is weakened, the chances of becoming sick are greater. Most people who become infected with TB are able to fight the bacteria and stop them from multiplying. The bacteria become inactive, but they remain alive in the body and can become active later. This is called latent TB infection. The diagnosis of TB includes medical history, a chest X-ray, physical examination and a microbiological test of a person's mucus coughed up from the lungs.

According to the World Health Organization, TB infection is currently spreading at the rate of one person per second. The disease kills more young people and adults than any other infectious disease and is the world's biggest killer of women. Each year, an estimated 8 to 10 million people contract the disease and about two million people die from it. About one-third of the world's population or approximately two billion people carry the TB bacteria but most never develop the active disease. Around 10% of people infected with TB actually develop the disease at some point during their lives, but this proportion is changing because of HIV. HIV severely weakens the human immune system and makes people much more vulnerable to TB infection. It is estimated that between now and 2020, nearly 1 billion more people will be

newly infected, 200 million will become sick and 70 million will die from TB if control is not strengthened.[4]

Table1.1 Estimated incidence, prevalence and TB mortality, 2004[4]

	Incidence*			Prevalence*	Mortality
	All forms		Smear-positive*		
WHO region	(% of global total)	per 100000 population	per 100000 population	per 100000 population	per 100000 population
Africa	29	356	152	518	81
The Americas	4	41	18	53	5.9
Eastern Mediterranean	7	122	55	206	27
Europe	5	50	23	65	7.8
South-East Asia	33	182	81	304	33
Western Pacific	22	111	50	216	18
Global	100	140	62	229	27

*Incidence - new cases arising in given period; *prevalence - the number of cases, which exist in the population at a given point in time. *Smear-positive cases are those confirmed by smear microscopy, and are the most infectious cases.

The TB epidemic in South Africa has been documented as one of the worst in the world, with disease rates more than double those observed in other developing countries and up to 60 times higher than those currently seen in the USA or Western Europe. It is the fifth largest cause of death among the black population (South African Tuberculosis Association, 1998). At the current pace of the epidemic, nearly one out of every twelve South Africans will become sick with TB in the next ten years. About ten thousand people die of TB every year.

The 11 countries of the Southern Africa sub region contribute approximately 275,000 cases every year to the total caseload in Africa. Almost half of these come from South Africa. The MRC (Medical Research Council, South Africa, 1998) estimated that the country had an estimated 180,507 cases (55% reported) in 1997, or 419 per 100,000 of the total population.[5] Of these, 32.8% (73,679 cases) were probably infected with HIV. Estimates by the MRC National Tuberculosis Programme indicate that current trends in the epidemic will continue unless effective control is achieved, resulting in 3,5 million new cases of tuberculosis over the next decade and at least 90,000 patients dying. The financial implications are staggering: Given that more than US$100 million is spent annually on tuberculosis in South Africa, in excess of US$3 billion would be required over the next 10 years if current increases in tuberculosis rates are allowed to continue unabated.

Multi-drug Resistance Tuberculosis (MDR-TB) is caused by *Mycobacterium tuberculosis* which is resistant to both isoniazid **1.1** and rifampicin **1.2** with or without resistance to other drugs.[4] MDR-TB is among the most worrisome elements of the pandemic of antibiotic resistance because TB patients that fail treatment have a high risk of death.[6] While host genetic factors may contribute, drug resistance can occur when, a) TB patients do not adhere to their prescribed drug regimens, b) health professionals prescribe an incorrect treatment regimen, c) an unreliable drug supply interrupts patient's treatment. This means that the drug can no longer kill the bacteria. Only 3% of all the new tuberculosis cases that arise worldwide every year are estimated to be multi-drug resistant.[6] There are several hotspots around the world where MDR-TB prevalence is high. These Include Estonia, Latvia and two Russian oblasts (territories) in Europe; Henan and Zhejiang province in China; Argentina and the Dominican Republic in the Americas; and Cote d'Ivoire in Africa. People with MDR-TB disease must be treated with specific drugs that often are much more expensive (>US$250 000 per case) than conventional therapy.

Extensively Drug Resistant TB (XDR-TB) is a form of MDR-TB that is resistant to any fluoroquinolone, and at least one of the three injectable second-line drugs (capreomycin, kanamycin, and amikacin).[4] XDR-TB can develop when these second-line drugs are also misused or mismanaged and therefore also become ineffective. Because XDR-TB is resistant to first- and second-line drugs, treatment options are seriously limited. Recent findings from a survey conducted by WHO and US centres for Disease Control and Prevention, on data from 2000-2004 found that XDR-TB has been identified in all regions of the world but is most frequent in the countries of the former Soviet Union and in Asia. In the United States, 4% and in Latvia, a country with one of the highest rates of MDR-TB, 19% of MDR-TB cases met the criteria of XDR-TB. Separate data on a recent outbreak of XDR-TB in an HIV-positive population in Kwazulu-Natal in South Africa was characterized by alarmingly high mortality rates.[7]

HIV/AIDS and TB are so closely connected that the term "co-epidemic" or "dual epidemic" is often used to describe their interrelationship. TB and HIV infections are both intracellular and known to have a profound influence on the progression of each other. HIV infection brings about the reduction in CD4+ T cells, which play a major role in immunity to TB. HIV also can facilitate both the progression of latent TB infection to active disease status and relapse of the disease in previously treated patients.

TB kills up to half of all AIDS patients worldwide. People who are co-infected with HIV and TB are up to 50 times more likely to develop active TB in a given year compared to people who are HIV-negative. An estimated 33% of the 40 million people living with HIV/AIDS worldwide are co-infected with TB. Furthermore, without proper treatment, approximately 90% of people living with HIV/AIDS die within months of contracting TB. The majority of people who are co-infected with both diseases live in sub-Saharan Africa, where up to 70% of TB patients are co-infected with HIV in some countries.

Drug treatment for TB has been available since streptomycin was produced in 1944. This was followed by isoniazid (INH) **1.1** in 1952, and rifampicin (RIF) **1.2** in1966. Pyrazinamide (PZA) **1.3** was added later, and is of value especially in the initial phase of treatment. The most common medicines used to treat TB patients are**:** isoniazid **1.1**, rifampicin **1.2**, pyrazinamide **1.3**, ethambutol (EMB) **1.4,** and streptomycin (SM) **1.5**.

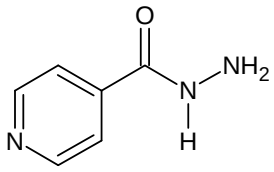

1.1

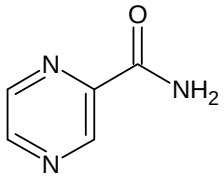

1.3

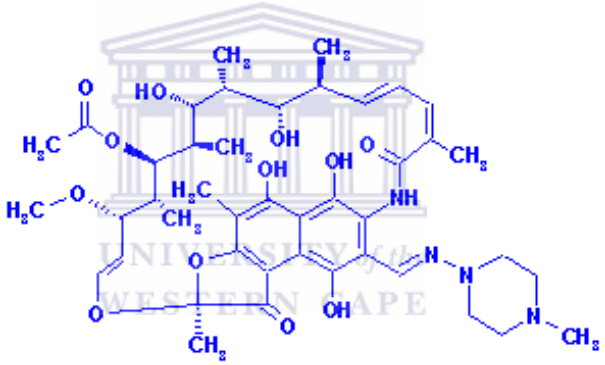

1.2

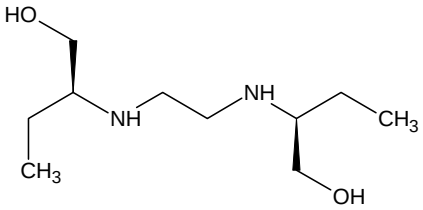

1.4

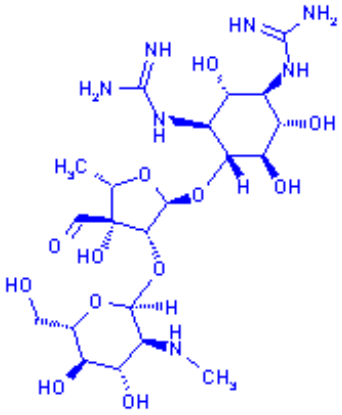

1.5

Treatment of TB depends on whether a person has either the active TB or latent TB form of the infection. A person who has become infected with TB but who does not have active TB might be given preventive therapy; the usual prescription is a daily dose of INH. The person takes INH for six to nine months, possibly for up to a year for some patients. However, when a patient has active TB, several different medicines are needed. Patients commonly receive a combination of several drugs, most frequently INH plus two to three others, usually for at least six months.[8]

Table 1.2 Current regimens for treatment of drug susceptible tuberculosis

Regimen	Initial Phase	Continuation Phase
Daily	2 months of isoniazid, rifampicin, pyrazinamide with or without ethambutol	4 months of isoniazid and rifampicin
Intermittent	2 weeks of daily isoniazid, rifampicin, pyrazinamide and streptomycin or ethambutol	24 weeks of twice weekly isoniazid and rifampicin
	8 weeks of thrice weekly isoniazid, rifampicin, pyrazinamide and streptomycin or ethambutol	18 weeks of thrice weekly isoniazid and rifampicin

When MDR-TB is suspected on the basis of history or epidemiological information, the patient's sputum must be subjected to culture and anti-tuberculosis drug sensitivity testing. If there is resistance to isoniazid and rifampicin (with or without resistance to streptomycin), or there is resistance to isoniazid, rifampicin and ethambutol (with or without resistance to streptomycin), the following are the suggested treatments (Table 3).[9]

Baseline liver function tests and periodic and regular monitoring are advocated in view of the potential hepatotoxicity of isoniazid **1.1**, rifampicin **1.2**, and pyrazinamide **1.3**. The risk of liver damage is less than 1%, but mild asymptomatic increase in transaminase blood concentrations are seen in up to 20% of the patients. Doses of ethambutol **1.4** should be carefully adjusted in patients with renal impairment.[10] Regimens containing thiacetazone also have a greater risk causing potentially lethal cutaneous drug reactions in people with AIDS.[11]

Table 1.3 Suggested treatments for MDR-TB

Resistance pattern	Initial Phase		Continuation Phase	
	Drugs	Minimum duration (months)	Drugs	Minimum duration (months)
Resistance to isoniazid and rifampicin with or without resistance to streptomycin	Aminoglycoside Ofloxacin or Levofloxacin Pyrazinamide Ethambutol Ethionamide	3	Ofloxacin or Levofloxacin Ethambutol Ethionamide	18-24
Resistance to isoniazid, rifampicin and ethambutol with or without resistance to streptomycin	Aminoglycoside Ofloxacin or Levofloxacin Pyrazinamide Ethionamide Cycloserine	3	Ofloxacin or Levofloxacin Ethionamide Cycloserine	18-24

New quinolones are being recommended for use as second-line drugs in the treatment of MDR-TB, since they have potent anti-*Mycobacterium tuberculosis* activity and good pharmacokinetics, in terms of tissue and cellular distribution, and have few adverse effects.[12, 13] Ofloxacin **1.6** (OFLX), sparfloxacin (SPFX), and levofloxacin **1.7** (LVFX), ciprofloxacin **1.8** (CPFX) have good therapeutic efficacies against experimental *M. tuberculosis* infection in mice[14] and are efficacious in the clinical control of tuberculosis, including MDR-TB, when given in combination with other antituberculous drugs.[12] A new fluoroquinolone HSR-903 **1.9**, (S)-(-)-5-Amino-7-(7-amino-5-azaspiro[2,4]hept-5-yl)-1-cyclopropyl-6-fluoro-1,4-dihydro-8-methyl-4-oxoquinoline-3-carboxylic acid, has a broad spectrum of action against both gram-positive and gram-negative bacteria.[15] The *in vitro* antimicrobial activity of HSR-903 **1.9** against *M. tuberculosis* was compared with those of several other fluoroquinolones, including LVFX **1.7**, sitafloxacin (STFX) **1.10** and gatifloxacin (GTFX) **1.11**, which possess potent *in vitro* and *in vivo* antimycobacterial activities.[14, 16] The MIC_{50} and MIC_{90} of test quinolones were distributed over a range from 0.1 to 0.78 mg/ml and 0.39 to 25 mg/ml for

non-MDR *M. tuberculosis* and MDR *M. tuberculosis* strains, respectively. Their MICs were in the order STFX **1.10** ≈ GTFX < LVFX **7** ≤ HSR-903 **1.9**.[17] The minimal inhibitory concentration (MIC) is defined as the lowest concentration of the compound that inhibits more than 99% of the bacterial population. The MICs of RMP **1.2** and INH **1.1** were lowest among test drugs for non-MDR *M. tuberculosis* strains, but markedly increased in the case of MDR-*M. tuberculosis* strains. Notably, the MICs of test quinolones for MDR-*M. tuberculosis* isolates were 4 to 32 times higher than their MICs for non-MDR-*M. tuberculosis* strains.

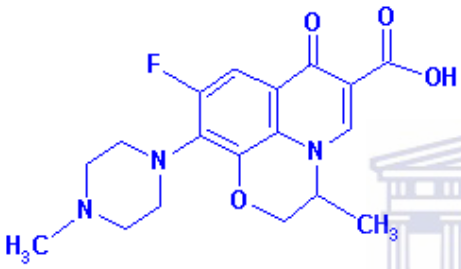

1.6

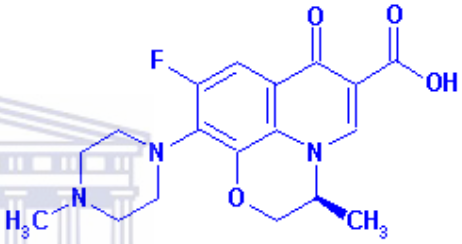

1.7

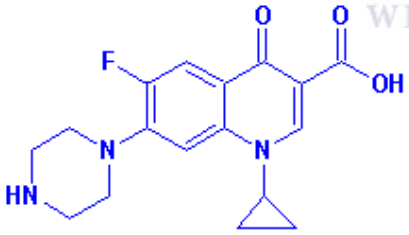

1.8

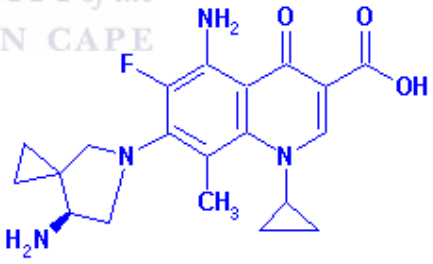

1.9

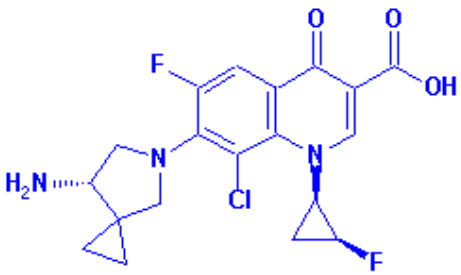

1.10

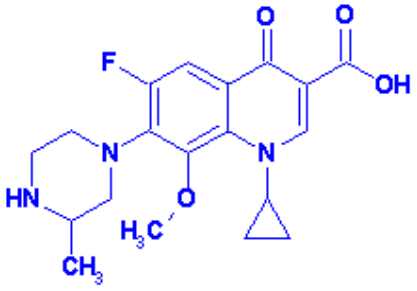

1.11

The fluoroquinolones are by far the most promising new agents for treatment of tuberculosis. The most potent of the currently available drugs in descending order of *in vitro* activity are moxifloxacin (MXFX) **1.12**, gatifloxacin **1.11**, levofloxacin **1.7**, ofloxacin **1.6** and ciprofloxacin **1.8**.[18] While recent studies suggested that moxifloxacin **1.12** is particularly active, the long term tolerability and safety of third generation fluoroquinolones like moxifloxacin **1.12** or gatifloxacin **1.11** have not been established as they have for ofloxacin **1.6** and levofloxacin **1.7**.[19] The oxazolidinones are also a novel group of antimicrobials.[20] One member of the family, linezolid **1.13**, has been used in the management of extensive drug resistance TB and it has shown some apparent efficacy (unreported data).[21] However, its utility is compromised by its toxicity and high cost. Nitroimidazopyrans have also been shown to be active compared to static *M. tuberculosis* populations, and replicate bacilli.[22] After activation by a mechanism dependent on the *M. tuberculosis* F420 cofactor, nitroimidazopyrans inhibited the synthesis of protein and cell wall lipid. Bacille Calmette-Guerin vaccine is currently the only vaccine available for treatment against TB. Although it does appear to lessen disease, particularly extrapulmonary TB in young people following primary infection, it has had very meagre effects upon adult pulmonary disease. Efforts to develop a more effective TB vaccine are underway, and researchers hope to make such a vaccine available within a decade.

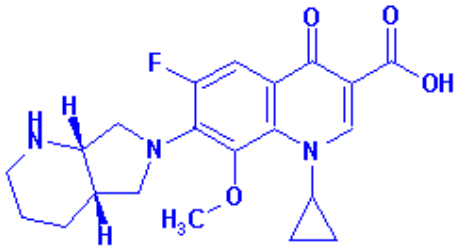

1.12

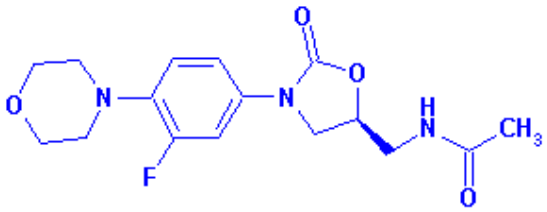

1.13

Currently available second-line drugs used to treat MDR-TB are four to ten times more likely to fail than standard therapy for drug-susceptible tuberculosis.[23] After the initial introduction of rifampicin **1.2** almost 30 years ago, no worthwhile anti-tuberculosis drug with a new mechanism of action has been developed. Moreover, no new drugs that might be effective in the treatment of MDR-TB are currently undergoing clinical trials. It appears that effective new drugs for tuberculosis are at least a decade away.[24]

The resurgence of tuberculosis as a major disease in many parts of the world is prompting the search for novel compounds, active against the causative organism, *Mycobacterium tuberculosis*. Over the past decade, there has been a proliferation in the literature on the antimycobacterial properties of plant extracts. The quinones exhibiting inhibitory activity against *M. tuberculosis* were found to be multiortho-quinone and 12-demethylmultiorthoquinone isolated from *Salvia multicaulis*.[25] The compounds such as allicin isolated from garlic oil,[26] Hypargenin F, from the roots of *Salvia hypargeia*,[27] triterpenes from *Borrichia frutescens*,[28] ambroxol, a semi-synthetic derivative of vasicine from the Indian shrub *Adhatoda vasica*,[29] alkaloids isolated from *Galipea officinalis*[30] were found to have good activity against *M. tuberculosis*. These compounds act bactericidally by denying access of essential metabolites through the membrane into the interior of the cell.[31]

A naphthoquinone, kigelinone **1.14**, isolated from *Kigelia pinnata* synonymous with *K. africana* has been shown to be active against Gram-positive bacteria at concentrations ranging from 0.05 to 0.2 mg/ml. This activity has been attributed to the position of the hydroxyl group on the aromatic ring of the naphthoquinone nucleus. The position of the hydroxyl group relative to the quinone carbonyl as in kigelinone **1.14** advances its ability of chelation with an active site.[32] The compound known as pinnatin **1.15** (4-Methoxy-7-phenyl-6,7-dihydrofuro[3,2-*g*]-chromen-5-one), was isolated from *Derris indica*, a mangrove plant belonging to the *Leguminosae* family, showed moderate antimycobacterial activity against

Mycobacterium tuberculosis H37Ra with a minimum inhibition concentration of 12.5 *m*g/ml.[33]

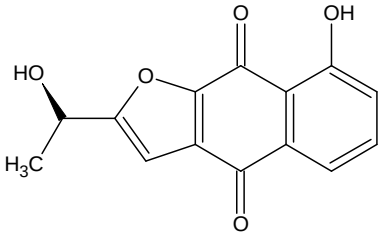

1.14

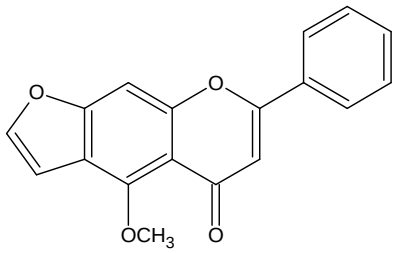

1.15

Twenty South African medicinal plants used to treat pulmonary diseases were screened for activity against drug-resistant and a drug-sensitive strain of *M. tuberculosis*.[34] A preliminary screening of acetone and water plant extracts, against a drug-sensitive strain of *M. tuberculosis*; H37Rv was done by the agar plate method. Acetone as well as water extracts of *Cryptocarya latifolia*, *Euclea natalensis, Helichrysum melanaome, Nidorella anomala* and *Thymus valgaris* inhibited the growth of *M. tuberculosis*. These active acetone extracts were screened using rapid radiometric method, against the H37Rv strain as well as a strain resistant to the drugs, isoniazid **1.1** and rifampin **1.2**. The minimal inhibitory concentration of *Croton pseudopulchellus, Ekebergia capensis, Euclea natalensis, Nidorella anomala* and *Polygala myrtifolia* was 0.1 mg/ml against the H37Rv strain.[34] Out of 20 medicinal plants investigated, *Euclea natalensis* exhibited the best activity against drug-sensitive and drug-resistant strains of *M. tuberculosis*. *E. natalensis*, a tree of the *Ebenaceae* family is used extensively in oral health care, for chest complains, bronchitis, pleurisy, chronic asthma, urinary tract infections, venereal diseases etc. by the indigenous people of South Africa. It was found that the MIC of a crude extract of *E. natalensis* against M. tuberculosis was 100 μg/ml.[35]

The large subtropical genus *Euclea* is well known as a source for naphthoquinones; monomers, complex dimers and trimers such as 7-methyljuglone **1.16**, diospyrin **1.22** and

mamegakinone. Lall and Meyer,[34] first reported the inhibitory effect of the crude extract of *E. natalensis* against the drug-sensitive and two drug-resistant strains of *M. tuberculosis*. They also reported the isolation and identification of the active principle from *E.natalensis*, viz., a binaphthoquinone, diospyrin **1.22**. Diospyrin **1.22** and methyljuglone **1.16** have been found to inhibit several antibiotic resistant as well as antibiotic susceptible strains of *M. tuberculosis*. The traditional use *of E. natalensis* extract against sores, purulent lesions and skin infections and cough could possibly be attributed to the activity of diospyrin against S. *aureus* and *M. tuberculosis*. This might explain the plant's use in traditional remedies against TB. The antimycobacterial properties of the root extract, probably, provide the reason for its use in folk medicines also, to treat leprosy, which is caused by another mycobacterial species.

Twenty-eight compounds were screened for activity against Mycobacteria.[36] The 1,4-diketone quinone motif has strong inhibitory activity, while the 1,2-naphthoquinone motif was 8-fold less active than 1,4-naphthoquinone **1.17**. Compounds without this quinone structure had much lower activity. Activity fell, when the 1,4-diketone moiety itself was retained but not part of the aromatic ring as with benzil (1,2-diphenylethanedione).[36] Thus the ketone group themselves are not toxic. While adding a second conjugated ring mildly improved activity (*M. smegmatis* MIC of benzoquinone 463 μM, while that of **1.17** 316 μM), adding a third ring strongly decreased activity (anthraquinone MIC of 30,700 μM). Plumbagin **1.18** was reported to be one of the most potent synthesized compounds against RGM (rapidly growing Mycobacteria) and MAC (*M. avium* complex), with an MIC of 66 μM, while juglone **1.19** had an MIC against MAC of 72 μM. For comparison, kanamycin **1.20** has an MIC against *M. smegmatis* of 4 μM, and against *M. avium* of 26 μM. Not only are compounds **1.18** and **1.19** the most toxic examined, their mechanism of killing may be novel.[36]

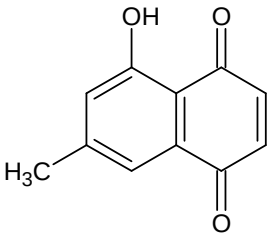

1.16

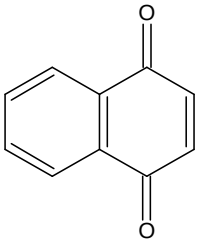

1.17

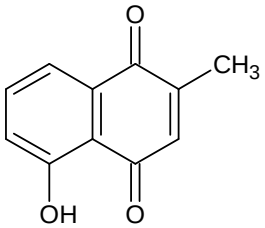

1.18

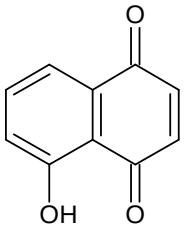

1.19

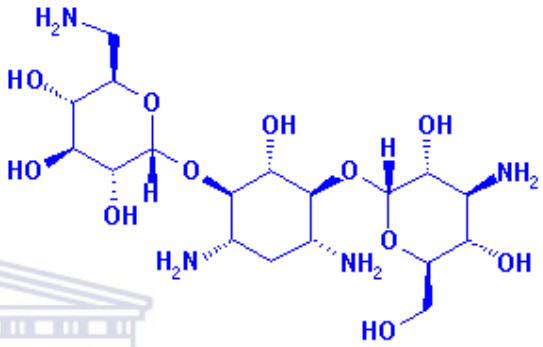

1.20

Six compounds were isolated from *D. piscatorial* and identified as isodiospyrin **1.21**, diospyrin **1.22**, bisisodiospyrin, an unidentified tetrameric form of plumbagin **1.18**, betulinic acid and an unidentified oily compound.[37] It was observed that activity of diospyrin **1.22** and isodiospyrin **1.21** were significant especially on *M. chelonae*, which is a pathogenic organism. The MICs of isodiospyrin **1.21** for the eight Gram-positive organisms ranged between 0.78 to 50 μg/ml, while those against the four Gram-negative organisms ranged between 50 μg/ml and 100 μg/ml.[37] On the other hand, the MICs of diospyrin **1.22** for the eight Gram-positive bacteria ranged between 1.56 to above 100 μg/ml. It is however, interesting to note that the two compounds were effective against *M. chelonae*, with isodiospyrin **1.21** being more potent (MICs of 6.26 to 25 μg/ml) than diospyrin **1.22** (MICs of 25 to 100 μg/ml).[37] Diospyrin **1.22** has also been isolated from other species of *Euclea* such as *E. pseudebenus*, *E. crispa*,

E. divinorum, and *E. schimper*, and from *Diospyros* species, *D. mannii*, *D. montana* and *D. chamaethamus*.

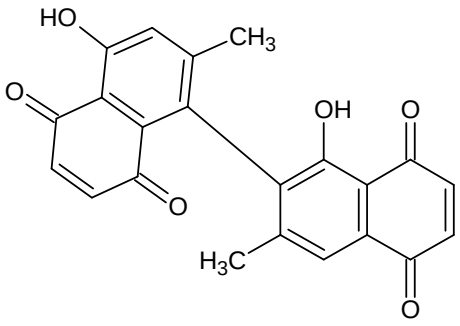

1.21

Diospyrin **1.22** was first isolated in 1961 by Kapil and Dhar as an orange-red constituent of *Diospyros Montana*, a small or medium-sized tree found throughout India.[38] Its structure was proposed by Ganguly and Govindachari in 1966 as a dimer of 7-methyljuglone **1.16** linked between C-2 and C-3′.[39] Subsequent studies by Sidhu and Pardhasaradhi led to the correct structure of diospyrin **1.22** with a linkage between C-2 and C-6′.[40] Diospyrin **1.22** is optically inactive and thus there is no restricted rotation around the connecting bond between C-2 and C-6′.

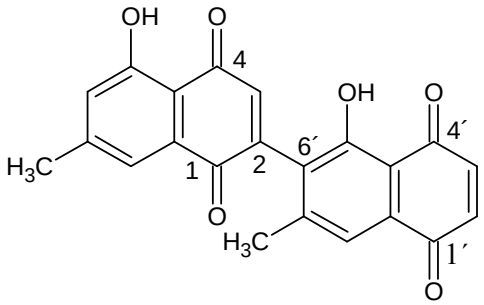

1.22

Arguments based on NMR spectra[40] indicated that diospyrin **1.22** has the structure with a 2-6′ linkage present between the naphthoquinonyl units, and its synthesis[41] has provided support for this hypothesis. It is now established crystallographically that diospyrin **1.22** does indeed have the 2-6′ structure.[42] In the crystal, the two ring systems are not coplanar, the angle between their least-squares planes being 59.74˚. The length of the inter-ring C9-C12 bond (1.494 A˚) suggests that it is essentially a single bond. A somewhat surprising feature is that the bulky C11 methyl group lies close to atom O4 rather than, as might be expected, close to the much smaller H atom attached to atom C13. As a result, atom O4 is significantly displaced (by 0.387 A˚) from the least-squares plane of its naphthoquinonyl unit (C12-C22/O5-O6). Conversely, atom C11 shows no significant deviation (displacement = 0.018 A˚) from the C1-C11/O1-O3 least-squares plane.

Fig 1.2 Crystal structure of diospyrin showing intra-molecular H-bonding

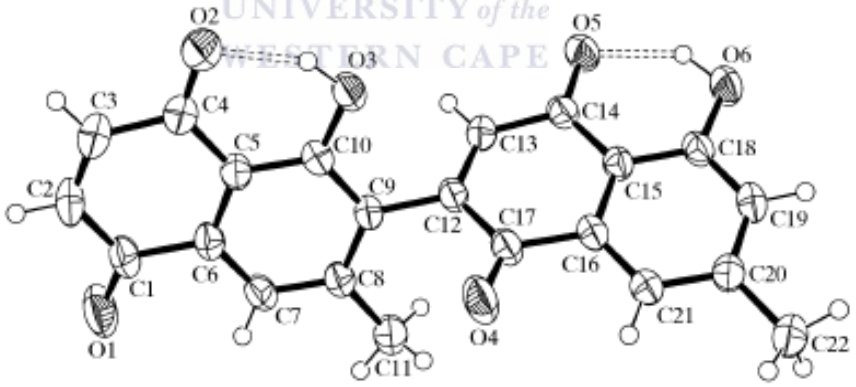

Both OH groups participate in bifurcated intra/intermolecular hydrogen bonds to C=O acceptors. The intra-molecular OH---O bonds are much shorter and stronger than the intermolecular links. This difference results in an `unbalanced' hydrogen-bonding network, in which atoms O2 and O5 accept two hydrogen bonds each (one intra-molecular and one intermolecular), and atoms O1 and O4 do not accept any conventional hydrogen bonds.

Together the OH---O bonds generate infinite stacks of molecules of **1.22**, The structure shown is dissymmetric, but crystal symmetry generates a racemic mixture that is consistent with the lack of optical activity shown by **1.22** in solution.[43] The inter-conversion of the two enantiomeric forms would be expected to occur readily in solution by analogy with the behaviour of trisubstituted biphenyls, which undergo rapid racemization in solution. [44]

Fig 1.3 Crystal structure of diospyrin showing intra-molecular and intermolecular H-bonding

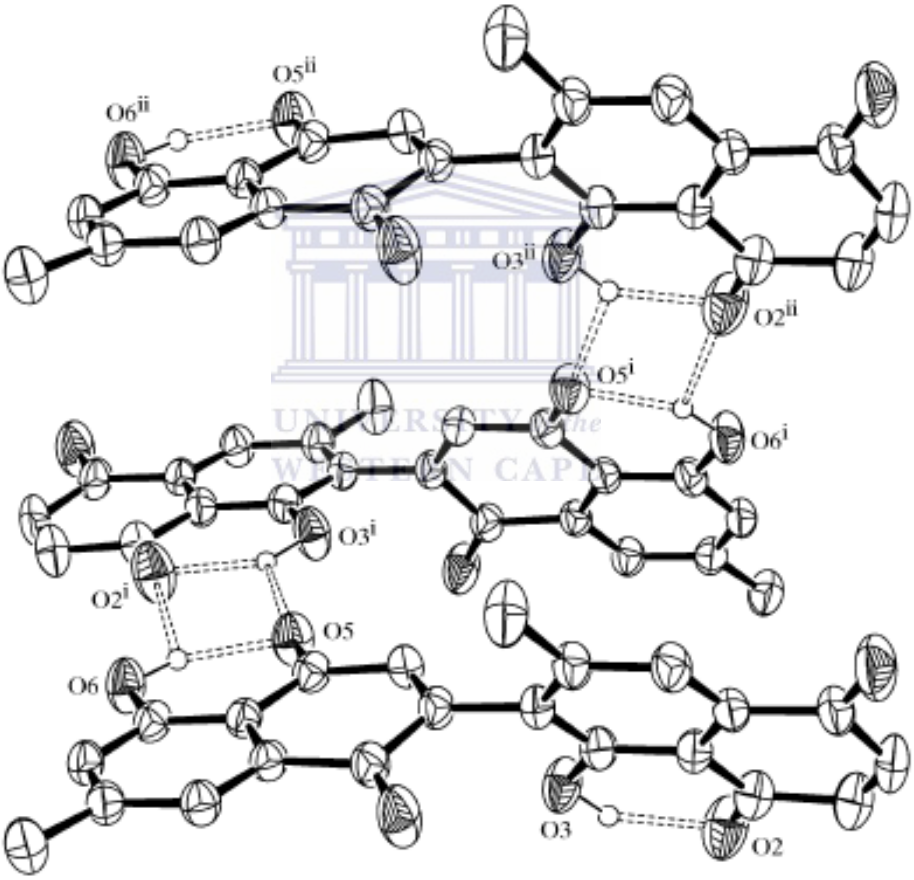

Three derivatives and one structural analogue of diospyrin **1.22** were synthesized and investigated for their inhibitory activity against *M. tuberculosis*.[45] A novel aminoacatate derivative **1.23** (of diospyrin dimethyl ether) was found to be more active than the diospyrin **1.22**, the MIC's being 10-50 and 100 mg/L, respectively, for a drug-susceptible strain,

H37Rv, of *M. tuberculosis*.[45] This derivative also exhibited an MIC of 50 mg/L, for a few multidrug-resistant strains of *M. tuberculosis*. The other three analogues i.e. diospyrin dimethyl ether hydroquinone **1.24**, diospyrin diethyl ether **1.25** and the dimer of lawsone **1.26** did not show any activity against any strain at the highest concentration tested. However, the reported tuberculostatic activity of *Lawsonia inermis* would indicate the probable involvement of lawsone, i. e. 2-hydroxynaphthoquinone, which is known to be the major bioactive contituent of this herb.[46] This observation is consistent with the enormous influence of structural modification on the biological activity of the bisnaphthoquinonoid, diospyrin.

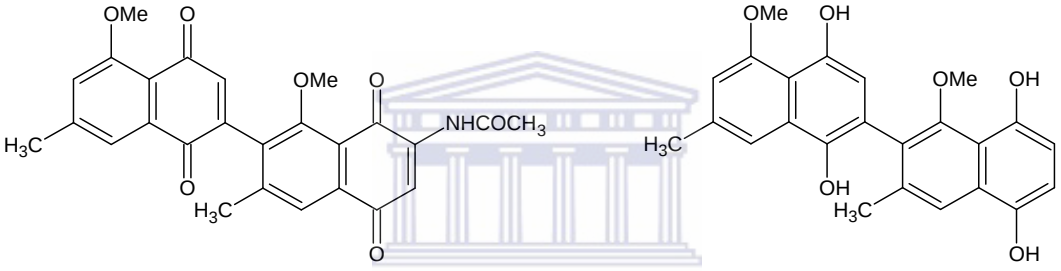

1.23 **1.24**

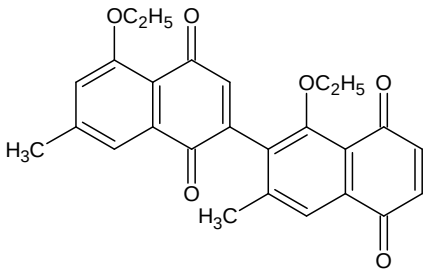

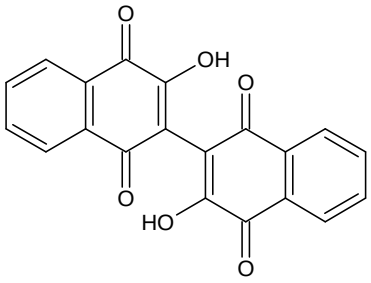

1.25 **1.26**

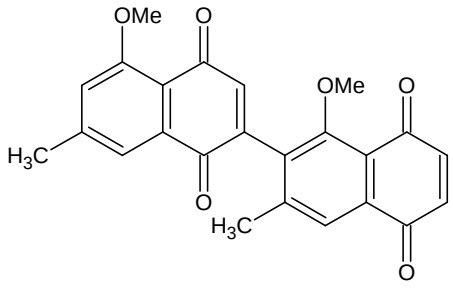

1.27

The broad spectrum of action of diospyrin **1.22** invoked research into various other disciplines. A limited number of studies highlighting anti-tumour activity of diospyrin **1.22** are available. The stem bark of *Diospyros montana* was first reported to be useful in the treatment of tumours.[47] It has been shown that crude ethanolic extract of the bark produces significant regression in the growth of *Ehrlich Ascites Carcinoma* (EAC) in Swiss Albino mice and the haematological parameters of tumour bearing mice could be significantly restored towards the normal range.[48] Later, diospyrin **1.22** has been identified as a biologically active principle present in the bark extract of *Diospyros montana*.[49] The *in vitro* studies indicated marked effects of small doses of diospyrin **1.22** on EAC cell surfaces, leading to agglutination and exocytosis. Higher doses caused disruption of the whole cell resulting in the expulsion of intracellular material leading to total lysis. Several experiments showing the significant inhibition of *in vivo* growth of EAC and increase in the life span of the tumour bearing mice confirmed the effect of diospyrin **1.22** against EAC.

Diospyrin **1.22** and its two derivatives viz., **1.24** and **1.27** were tested for their inhibitory activities towards EAC *in vivo*.[50] The growth of EAC *in vivo* was significantly inhibited by all three compounds. However, the derivatives **1.24** and **1.27** were far more effective than diospyrin **1.22**. One other tetraacetate derivative **1.28** and **1.24** were also checked for their activity against EAC and Sarcoma 180 and it was noted that the activity of **1.28** was less than that of **1.24**.[51]

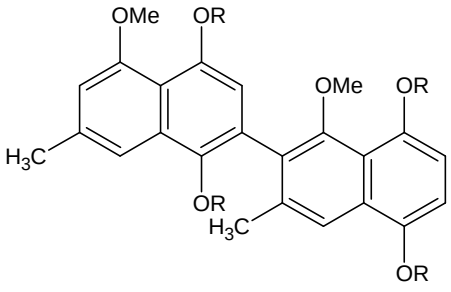

R = $COCH_3$

1.28

Diospyrin **1.22** and its three synthetic derivatives i.e. diospyrin dimethyl ether **1.27**, diospyrin dimethyl ether hydroquinone **1.24** and diospyrin diethyl ether **1.25** have been tested for their activity on four human cancer cell lines viz., acute myeloblastic leukemia (HL-60), chronic myelogenic leukemia (K-562), breast adenocarcinoma (MCF-7) and cervical epithelial carcinoma (HeLa).[52] Diethyl ether derivative **1.25** was most effective in this regard while the parent compound diospyrin **1.22** was least active. A concentration-dependent response in leukemic cell lines showed maximum growth inhibition with **1.25**. Thus, IC_{50} (50% inhibitory concentration) values in HL- 60 cells were >100 μM for **1.22**, 64 μM for **1.27**, 54 μM for **1.24** and 30 μM for **1.25**, and the corresponding values in K-562 cells were >100 μM, >100 μM, 65 μM and 40 μM, respectively. Compound **1.25** was not cytotoxic toward normal human lymphocytes, suggesting its action is specific for tumor cells. On microscopic examination, **1.25** treated cells exhibited characteristic morphological features of apoptosis, such as cell shrinkage and formation of apoptotic bodies. In earlier studies, diospyrin **1.22**, was found to show significant tumor-inhibitory effects against Ehrlich ascites carcinoma *in vivo*.[53] Subsequently, synthesis of some derivatives of diospyrin **1.22** led to the isolation of more potent inhibitors against murine tumors.[54]

A series of aminonaphthoquinones was synthesized for the first time in fairly good yield, starting with diospyrin **1.22**, isolated from *Diospyros montana*. The aminoacetate derivative **1.29** showed the maximum (~93%) increase in life-span with respect to the untreated control in Swiss A. mice bearing Ehrlich Ascites Carcinoma (EAC) and exhibited the lowest

inhibitory concentrations (IC_{50} of **1.29** = 0.06 μM, of **1.30** = 0.07 μM and of **1.31** = 0.09 μM) *in vitro*.[55] (Please refer to chapter 5 for detailed introduction to apoptosis).

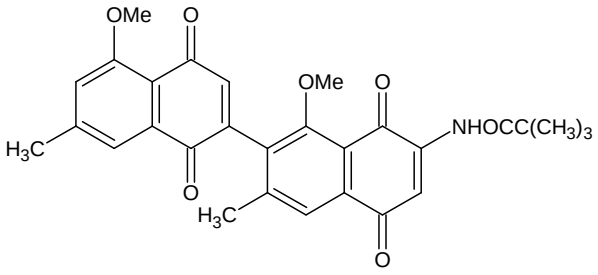

1.29

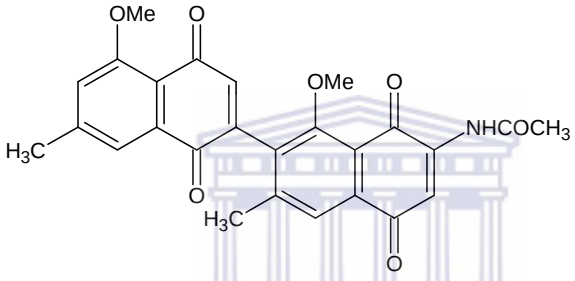

1.30

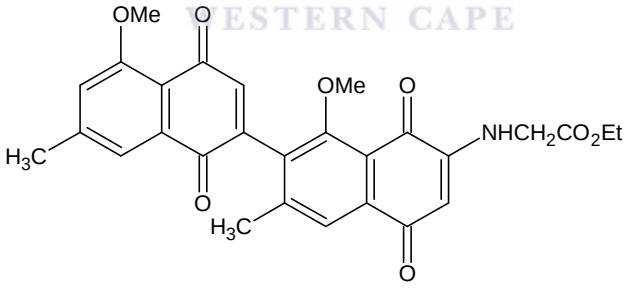

1.31

Diospyrin **1.22** and three other compounds i.e. Atovaquone **1.32**, Diospyrin dimethyl ether **1.27** and Diospyrin dimethyl ether hydroquinone **1.24** were also tested for their effect on cellular ATP of P. carinii.[56] Of the napthoquinone drugs tested in this study, atovaquone **1.32** was the most effective in reducing ATP (Adenosine triphosphate) levels after 24 h, but this inhibitory effect then remained stable through the duration of the 3-day study. The average 50% inhibitory concentration (IC_{50}) after 24 to 72 hours of exposure was 1.5 μg/ml (4.2 μM).

In contrast, the diospyrin-based quinoid drugs were ineffective in reducing cellular ATP levels after 24 h of exposure. These compounds were able to reduce ATP pools in *P. carinii* only after 48 h of exposure, and this effect dramatically increased after 72 h of exposure. All of the diospyrin **1.22** type compounds had greater activity, expressed as the IC_{50}, than atovaquone **1.32** at the 72 h time point. When considered individually, the diospyrin dimethyl ether **1.27** analog exhibited greater activity against *P. carinii* than the other quinoid compounds at 48 and 72 h of exposure with IC_{50} of 1.67 μg/ml (6.71 μM) and 0.31 μg/ml (1.25 μM) respectively.

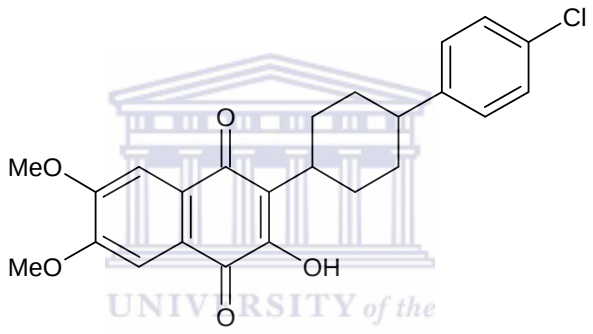

1.32

Exposure of *P. carinii* to the diospyrin analogues caused a continual decrease in ATP levels over time. In contrast, the decrease in ATP levels at all concentrations of atovaquone **1.32** remained the same from 24 to 72 h. Since all the compounds targeted the electron transport chain, as evidenced by the decrease in ATP, these differences in the kinetics likely involve effects on other cellular processes. Diospyrins have been reported to inhibit protistan topoisomerase activity.[57] Topoisomerases are enzymes involved in many cellular processes and are classified into two groups by virtue of the nicks made in single stranded (type I) or double stranded (type II) DNA. These breaks relax the DNA strands during replication and chromosomal separation. Since *P. carinii* replicates very slowly in the *in vitro* setting,

deleterious effects from the inhibition of topoisomerases may require longer exposure to manifest.

Diospyrin **1.22** and its two synthetic derivatives viz., **1.24** and **1.27** were tested *in vitro* against intracellular amastigotes of *Leishmania donovani* and *Trypanosoma cruzi* in macrophages and extracellular *Trypansoma brucei brucei* bloodstream form trypomastigotes.[58] Diospyrin **1.22** was inactive against *L. donovani* but had ED_{50} (50% effective doses) values of 27 and 50 μM, respectively, against *T. cruzi* and *T.b. brucei*. The dimethyl ether **1.27** derivative was more active than the parent compound **1.22** against *T. cruzi* and *T.b. brucei*, but the hydroquinonoid **1.24** form was the most active antiparasitic agent with ED_{50} values of 2.2 and 0.7 μM, respectively, against *L. donovani* and *T.b. brucei*. Studies suggested that diospyrin **1.22** exerts its action by interacting with type I DNA topoisomerase of leishmania and stabilizing the "cleavable complex". The inhibition by diospyrin **1.22** is relatively specific as the compound requires 10-fold higher concentrations to inhibit DNA topoisomerase I from calf thymus and it does not inhibit DNA topoisomerase II of *L. donovani* at this concentration. Results suggested that diospyrin **1.22** is a novel inhibitor of type I DNA topoisomerase of *L. donovani*. Like camptothecin **6.3**, a class I inhibitor, it also stabilizes the cleavable complex. However it differs from camptothecin **6.3** with respect to its mode of action. Camptothecin **6.3** does not bind with the enzyme alone, but diospyrin **1.22** does; this interaction is reversible.[57]

Diospyrin **1.22** and its derivatives, viz., alkyl ethers **1.25, 1.27**, hydroquinonoid **1.24** and amino **1.33** were tested for their activity against *Leishmania major*.[59] Diospyrin **1.22** was only slightly active at a dose of 5 μg/ml, causing only 22% inhibition of the parasite growth, while all of its derivatives produced more than 98% inhibition under comparable conditions. Thus, modifications in the structure of diospyrin **1.22** could produce marked enhancement of its antileishmanial activity whereas **1.34**, the dimeric naphthoquinonoid analogue (dimer of

lawsone), did not show any inhibitory activity up to 5μg/ml concentration. Among the derivatives, the dimethyl ether **1.27** and its hydroquinonoid analogue **1.24** were the most active compounds, causing nearly 98% inhibition at a dose of 2.5 μg/ml. The lower activity of the compounds **1.22** and **1.33** may be explained on the basis of H-bonding between the phenolic –OH and their adjacent quinonoid moieties. However studies on some more analogues are needed in order to elucidate the specific role of these structural features.

The insolubility of naphthoquinonoid compounds, including diospyrin **1.22** and its derivatives, in aqueous medium poses a major problem in the evaluation of their activities in biological systems. The polyethylene glycol (PEG) conjugated technique used in this study[59] could effectively solubilise the compound **1.24** in aqueous medium, which might have a significant impact on the pharmacological profile and future applications. In preliminary experiments, this conjugate showed significantly higher (~10 fold) inhibitory activity on the growth of the leishmanial parasite as compared to the 'free' drug, when tested at a dose of 1.2 μg/ml, thereby indicating a potential advantage of this modification. PEG as a carrier polymer is known to be non-toxic, non-antigenic and biocompatible. Conjugation to PEG is expected to increase the water-solubility and therapeutic effect of hydrophobic compounds like naphthoquinonoids with concomitant reduction in the toxicity.

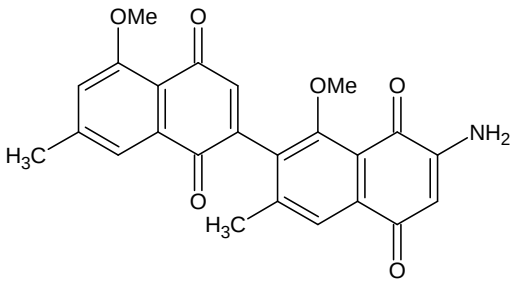

1.33

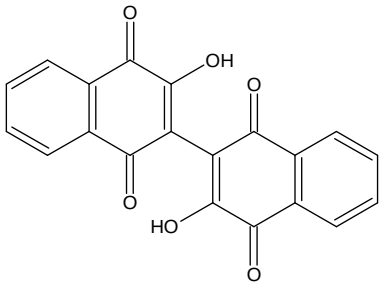

1.34

Plumbagin **1.18**, a naphthoquinone isolated from many species of the genus *Plumbago*, has been reported to have an activity (IC_{50}) of 0.42 and 1.1 μg/ml against amastigotes of *L. donovani* and *L. amazonensis*, respectively.[60] Plumbagin **1.18**, and the dimeric products 3,3-

biplumbagin **1.35** and 8,8-biplumbagin **1.36**, have been isolated from the bark of *Pera benensis*, a plant used in Bolivia for the treatment of cutaneous leishmaniasis. While **1.18** and **1.36** show activity against promastigotes of *L. braziliensis*, *L. amazonensis*, and *L. donovani* at a concentration (IC_{90} = 90% Inhibitory concentration) of 5 μg/ml, **1.35** shows a lower activity (IC_{90} =50 μg/ml) against the same *Leishmania* species.

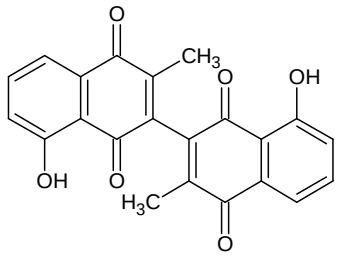

1.35

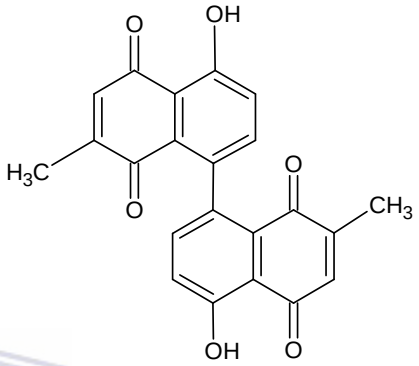

1.36

Two novel hydroquinoid analogues derived from diospyrin **1.22** also show enhanced inhibitory effects against *Plasmodium falciparum, in vitro*, and may be a useful model for the development of novel antimalarial drugs.[61]

The evidences accumulated to date suggest that diospyrin **1.22** is a potent inhibitor against a variety of organisms' viz., *Mycobacterium tuberculosis*, *Leishmania donovani, Leishmania major, P. carinii, Trypanosoma brucei, Trypanosoma cruzi, Plasmodium falciparum* as well as various cancer cell lines. Tuberculosis and cancer are among the most devastating diseases with few therapeutic options available. Both diseases develop resistance against the drugs being administered, thus demanding a continuous and exhaustive search for potential new drugs.

AIMS and OBJECTIVES

Diospyrin, a naturally occurring bisnaphthoquinone compound, has been shown to exhibit significant antimycobacterial and anti-tumour activity. By considering diospyrin as a lead compound, the present study is aimed at the synthesis of similar types of biaryl systems and the evaluation of their biological activity against different strains of *Mycobacterium tuberculosis* and certain cancer cell lines. The initial target was the synthesis of quinone-quinone biaryl systems, which one may think of as bisnaphthoquinone compounds or naphthoquinone-benzoquinone compounds having different substituent groups. The envisaged route towards the synthesis of these compounds would involve Suzuki methodology for C-C bond formation between two quinone moieties. Following on from this it was then further planned to synthesize several other naphthoquinone-naphthalene biaryl compounds from precursors available as it was envisaged that from the results of the evaluations of the activities of these compounds it would help in deducing their structure and activity relationship.

It was proposed that the evaluation of the different analogues against fast growing bacteria viz., *Mycobacterium smegmatis* and *Mycobacterium aurum* will be done by using the broth microdilution method at the facility available at the University of the Cape Town. Further evaluation against a clinical strain 1432 (sensitive to all front line drugs i.e. Isoniazid, Rifampicin, Ethambutol, Streptomycin) of *M. tuberculosis* using the BACTEC method at the Stellenbosch Medical School facility was also proposed. These were considered to be the preliminary studies. Depending on the results the possibility for further investigation to check their potential to be considered for drug trials was a strong possibility.

Further investigation of the potential of these compounds to induce apoptosis in three cancer cell lines viz., HeLa, MCF7, MG63 and one normal cell line i.e. CHO was also envisaged.

The various methods, which will be employed to assess the apoptotic potential of the compounds, are APOpercentage, DNA fragmentation and Cell cycle. The APOpercentage assay will help to identify the apoptosis inducing potential of the compounds. This is considered to be one of the basic and preliminary tests. DNA fragmentation will also be measured since this is a confirmatory test for detecting cell death mediated by apoptosis. Cell cycle analysis will help us to identify the phase during which cell growth arrests in response to the induced compound.

Chapter 2

Section 2.1: An investigation into the synthesis of diospyrin 1.22

In 2000, Masao Yoshida and Kenji Mori first reported the synthesis of diospyrin **1.22** as illustrated in Scheme **2.1, 2.2** and **2.3.**[41] The two-naphthoquinone moieties **2.1** and **2.2** were synthesized separately and then coupled by using Suzuki coupling via an organoboronic acid intermediate. The first stage of the synthesis was to prepare the naphthalene building blocks **2.1** and **2.2** obtained in the retrosynthetic analysis of Scheme **2.1**.

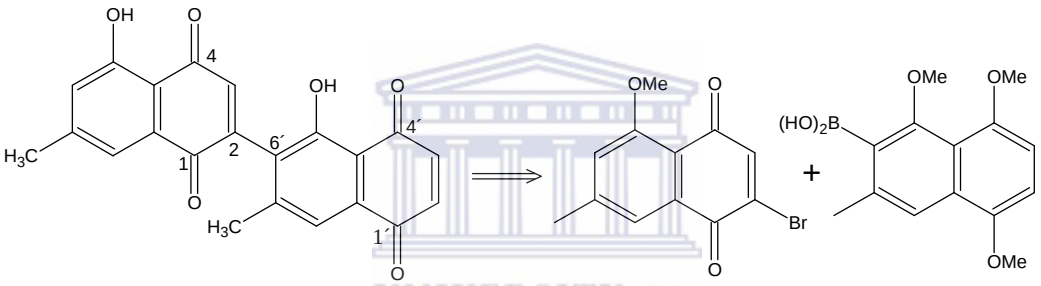

1.22 **2.1** **2.2**

Scheme 2.1

A Diels-Alder reaction between the known 1-methoxy-3-methyl-1-trimethylsilyloxy-1,3-butadiene **2.3** and 2,5-dibromo-1,4-benzoquinone **2.4** afforded 2-bromo-5-hydroxy-7-methyl-1,4-naphthoquinone **2.5**. This was further methylated with methyl iodide and silver oxide to give 2-bromo-5-methoxy-7-methyl-1,4-naphthoquinone **2.1** and is illustrated in Scheme **2.2**.

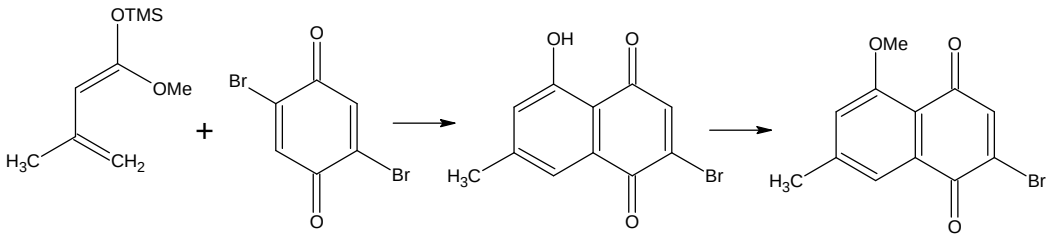

2.3 **2.4** **2.5** **2.1**

Scheme 2.2

For the synthesis of boronic acid **2.2**, another Diels-Alder reaction was executed. For that purpose, 2-bromo-1-methoxy-3-methyl-1-trimethylsilyloxy-1,3-butadiene **2.7** was prepared from the known methyl 2-bromosenecioate **2.6**. A Diels-Alder reaction between **2.7** and 1,4-benzoquinone **2.8** proceeded in dichloromethane, and the resulting mixture was treated with dilute hydrochloric acid to remove the partly remaining trimethylsilyl group, giving a mixture of 6-bromo-5-hydroxy-7-methyl-1,4-naphthoquinone **2.9** and 6-bromo-5-methoxy-7-methyl-1,4-naphthoquinone **2.10**. This mixture was subsequently fully methylated with methyl iodide and silver oxide to afford pure **2.10**. Reduction of **2.10** with tin(II) chloride furnished naphthalenediol **2.11,** which was then methylated to give 6-bromo-1,4,5-trimethoxy-7-methylnaphthalene **2.12**. The conversion of **2.12** to the corresponding tributyltin derivative by lithiation followed by stannylation was first attempted. These attempts, however, were unsuccessful, and the use of Stille methodology for coupling of the two naphthalene units was abandoned. The alternative approach was to employ Suzuki coupling. The desired boronic acid **2.2** was prepared by lithiation of **2.12** and subsequent reaction with trimethyl borate.

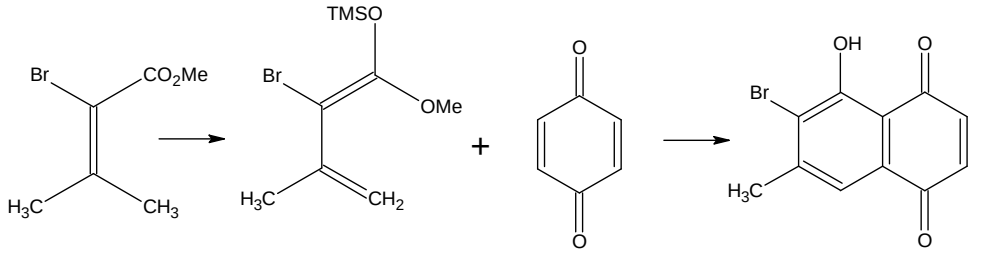

2.6 **2.7** **2.8** **2.9**

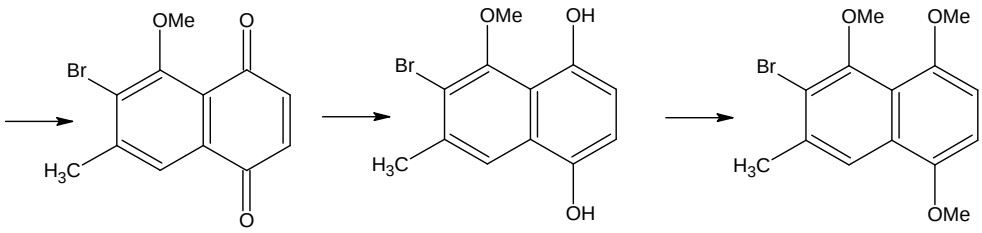

2.10 **2.11** **2.12**

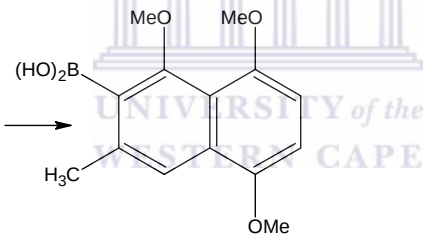

2.2

Scheme 2.3

The coupling of **2.1** and **2.2** was successfully done under the standard conditions, employing tetrakis(triphenylphosphine)palladium(0) as the catalyst in the presence of aqueous sodium carbonate to give the coupling product **2.13** as oranges red needles in 53% yield. Oxidative demethylation of **2.13** with ceric ammonium nitrate furnished diospyrin dimethyl ether **2.14** as yellow needles. Further demethylation of **2.14** with aluminium chloride in dichloromethane at room temperature yielded diospyrin **1.22** in 19% yield based on **2.13**.

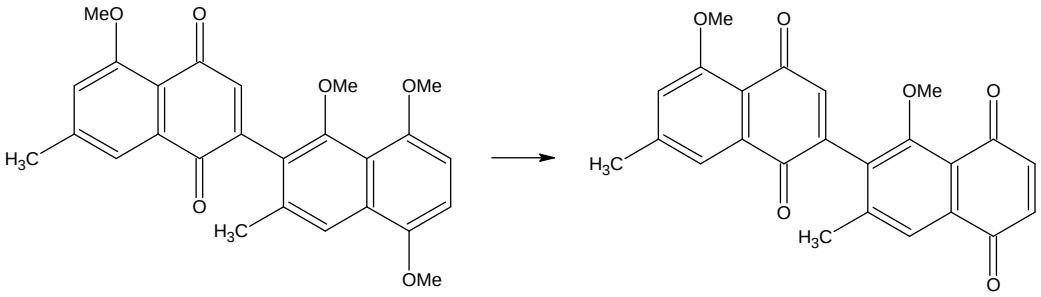

2.13 **2.14**

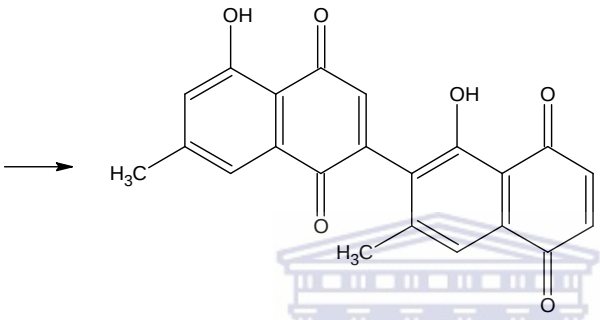

1.22

Scheme 2.4

Section 2.2: The Suzuki coupling between a Boronic acid and an Aryl halide

The Suzuki reaction, which was discovered by Akira Suzuki in 1979, is one of the most common cross-coupling methods in organic synthesis and allows C-C bonds to be formed between aryl or alkenyl halides and aryl, alkenyl or alkyl borates in the presence of a palladium(0) catalyst. Suzuki chemistry provides an efficient, cost effective, mild and environmentally safe methodology for the selective formation of C-C bonds. As opposed to the Stille coupling,[62] Suzuki reagents do not involve highly toxic (tin) reagents.

This transformation utilizes palladium catalyzed coupling between two reactants: an organohalide and an organoborane as shown in Scheme **2.5**. The organohalide is normally aryl or alkenyl, but the organoborane can be practically anything, as long as it can be prepared and is relatively stable.

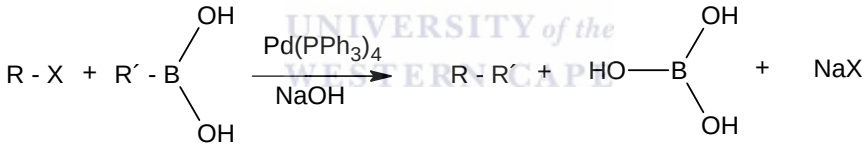

Scheme 2.5

Aryl halides are treated with butyl lithium to form the corresponding lithiated reagents, which are then reacted with trimethylborate $B(OMe)_3$ to form the boronic acid esters and these are hydrolyzed with either aqueous HCl or aqueous NH_4Cl to form the corresponding boronic acids as shown in Scheme **2.6**.

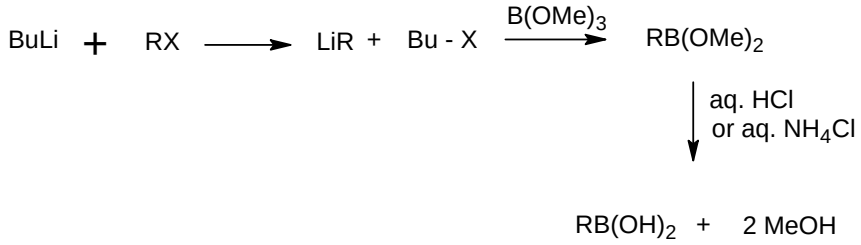

Scheme 2.6

Aryl halides function as electrophiles whose reactivity order is Ar-I > Ar-Br >> Ar-Cl. Aryl chlorides are usually not reactive enough, with the exception of those having heteroaromatic rings and electron-withdrawing groups. This is because the oxidative addition of aryl chlorides to palladium complexes is too slow to develop the catalytic cycle. A recent paper showed that the use of nickel catalysts for the cross-coupling reaction with aryl chlorides produced favourable results.[63]

Arylboronic acids are stable and easy to handle. They are normally stable in air and to a limited amount of heat, and can be recrystallised from water and alcohol. Various arylboronic acids are prepared relatively easily by functionilization reactions of the parent arylboronic acid since the boronic acid group is inert to many chemical reactions.

In 1981, Suzuki and Miyaura *et al*. reported that the cross-coupling reaction of phenylboronic acid with any aryl bromide in the presence of palladium catalysts and an aqueous base provides the corresponding biaryl molecules in good yields as shown in Scheme **2.7**.[64] The Suzuki reaction is tolerant to a wide variety of functional groups so that variously substituted aromatic rings can be used. By-products from homocoupling are limited because of the selective reaction involved.

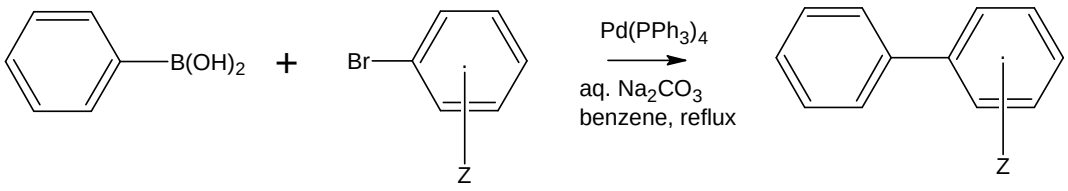

Scheme 2.7

The mechanism of the Suzuki process essentially involves three steps. The first step is the oxidative addition of the alkyl or aryl halide to the palladium(0) atom of a two-coordinate complex. This species is generated by a series of equilibria in which triphenylphosphine ligands dissociate from the metal. The oxidation state of the palladium does not change until reaction with either the alkyl or aryl halide occurs. Alkyl or aryl halides react very slowly in the oxidative addition step as shown in Scheme **2.8**.

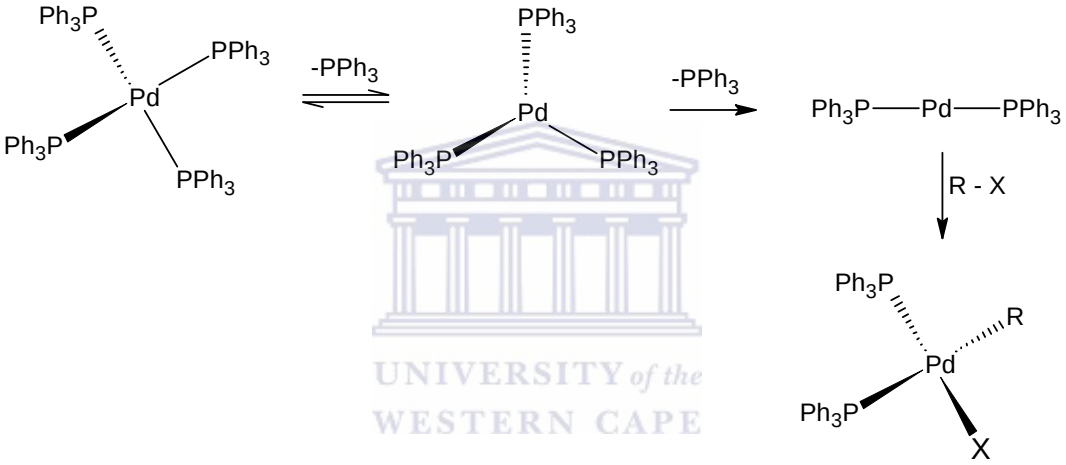

Scheme 2.8

The coupling reaction of organic boron compounds proceeds only in the presence of base. This is due to the fact that the organic group on boron is not nucleophilic enough for the transfer from boron to the palladium in the transmetallation step because of the strong covalent character of the B-C bond in boron compounds. Therefore, it is necessary to increase the carbanion character of organic groups by the formation of an organoborate having a tetravalent boron atom upon treatment with base (Scheme **2.9**).

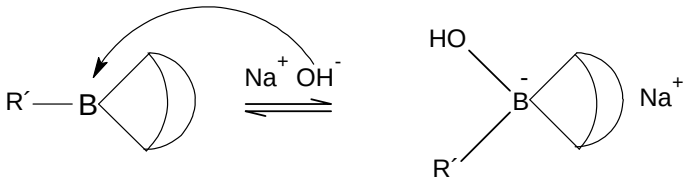

Scheme 2.9

In the next step, a substitution reaction occurs at the metal ion. The organic group attached to boron is transferred to palladium(II) ion, replacing the halide ion. The intermediate five-coordinate Pd(II) ion is sterically crowded, which facilitates the dissociation of the halide ion to produce the four-coordinate (diorgano) palladium(II) species.

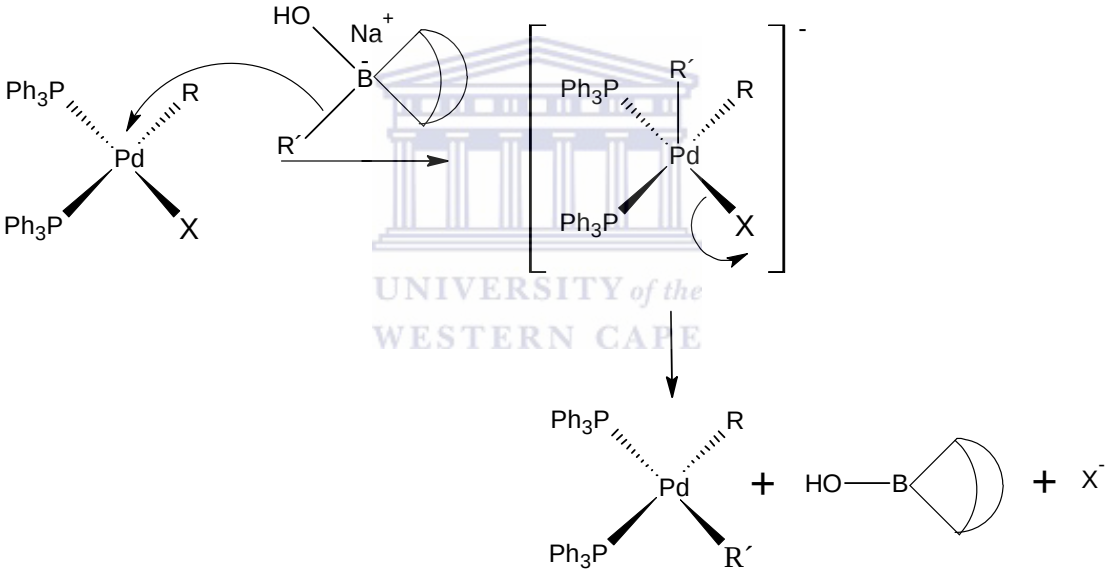

Scheme 2.10

This complex then immediately undergoes reductive elimination, yielding the coupled organic product and regenerating the two-coordinated palladium complex as shown in Scheme **2.11**.

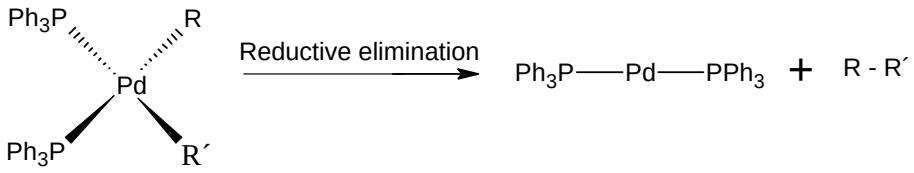

Scheme 2.11

Although the catalyst most often used in the Suzuki reaction is $Pd(PPh_3)_4$, various other palladium catalysts have been employed, viz., $Pd(dppb)Cl_2$, $PdCl_2(PPh_3)_2$, $Pd(OAc)_2$ and $PdCl_2$.

Bases are always required in the Suzuki reaction as opposed to the coupling reaction using organotin or organozinc reagents. The best results are achieved with the use of relatively weak bases of which Na_2CO_3 is most frequently used. However, other bases, such as Et_3N, $NaHCO_3$ and K_3PO_4, have also successfully been employed. In the case of sterically hindered boronic acids, strong bases for example aqueous $Ba(OH)_2$ or NaOH, accelerate the coupling reaction, while weak bases are more favorable in the case of sterically unhindered boronic acids since hydrolytic deboronation is suppressed. In some cases, anhydrous K_3PO_4 or CsF in aprotic solvents, such as dimethoxyethane (DME), have been used.[65]

Chapter 3: Results and Discussion

Section 3.1: Synthesis of 2,2´-bis(7-methyl-1,4-naphthoquinone) 3.1

In deciding on analogues of diospyrin **1.22**, we considered the most convenient one from the point of view of easily accessible starting materials and synthetic procedures. Thus the first analogue that we decided to synthesize was the binaphthoquinone **3.1** in which the two retrosynthons were quinone **3.2** and boronic acid **3.3**, shown in the retro Scheme **3.1**. It was thus clear that the two naphthalene moieties were to be synthesized separately and then coupled together by using Suzuki methodology via the organoboronic acid **3.3** and naphthoquinone **3.2**.

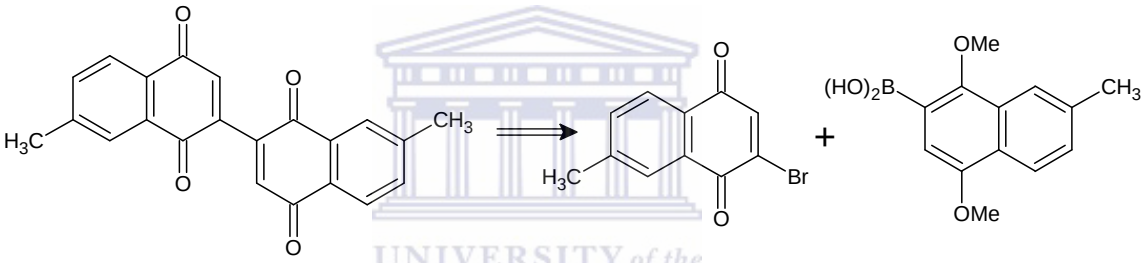

3.1 **3.2** **3.3**

Scheme 3.1

Section 3.1.1: Synthesis of 2-Bromo-7-methyl-1,4-naphthoquinone 3.2

The proposed synthetic protocol of the target naphthoquinone **3.2** is illustrated in Scheme **3.2** below.

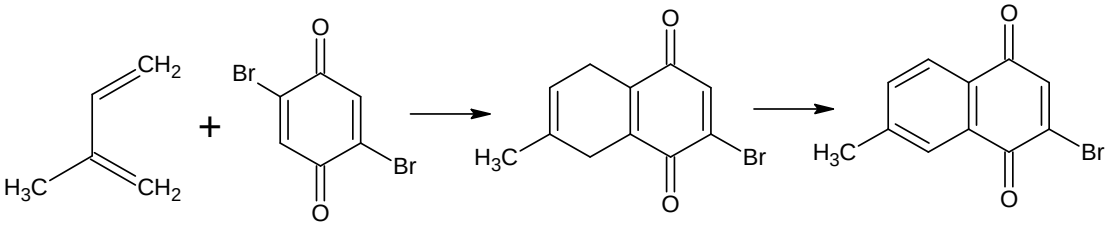

3.4 **3.5** **3.6** **3.2**

Scheme 3.2

The first step was to synthesize the one starting material viz., dibromobenzoquinone **3.5** by using the method reported by Lopez-Alvarado *et al.*,[66] depicted in Scheme **3.3** below.

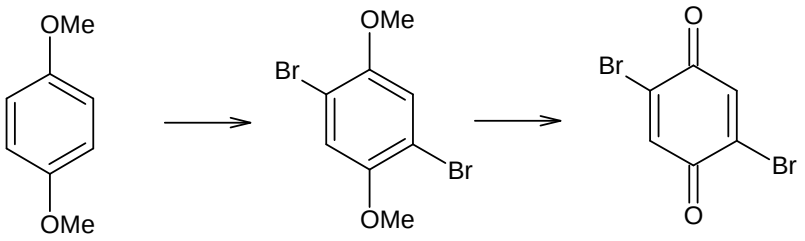

3.7 **3.8** **3.5**

Scheme 3.3

A solution of 1,4-dimethoxybenzene **3.7** in acetic acid was treated with 2 mole equivalents of bromine in acetic acid to afford the corresponding 2,5-dibromo-1,4-dimethoxybenzene **3.8** which on oxidation with cerium ammonium nitrate (CAN) afforded the corresponding dibromobenzoquinone **3.5** with 82% yield. The resulting material was assigned the structure **3.5** based on a singlet at 7.48ppm, which is due to the two symmetrical quinone hydrogens in the ^{1}H nmr spectrum and a m.p. of 159-160˚C (Lit.[66] m.p. is 160-161˚C).

Diels-Alder reaction between dibromobenzoquinone **3.5** and 2-methyl-1,3-butadiene (isoprene) **3.4**, commercially available from Acros Organics, afforded the expected adduct **3.6** (64%) in refluxing THF as shown in Scheme **3.4** below as reported by Ho *et al.*[67]

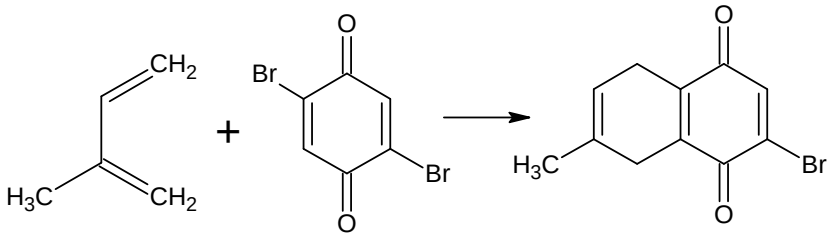

3.4 **3.5** **3.6**

Scheme 3.4

The assigned structure for **3.6** is based on the following spectral evidence. The HRMS of 251.9787 demonstrated a molecular formula of $C_{11}H_9BrO_2$ (^{79}Br) (required 251.9785). In the ^1H nmr spectrum, a 4-proton multiplet at 3.05ppm is due to H-5 and H-8 and a 1-proton multiplet at 5.48ppm is due to the H-6. In the ^{13}C nmr spectrum, signals at 179.3ppm and 184.5ppm are due to the two quinone carbonyls.

Bromonaphthoquinone **3.6** was then oxidized with chloranil in benzene under reflux for 30h to afford 75% yield of the 2-bromo-7-methyl-1,4-naphthoquinone **3.2** as shown in Scheme **3.5** below.[67]

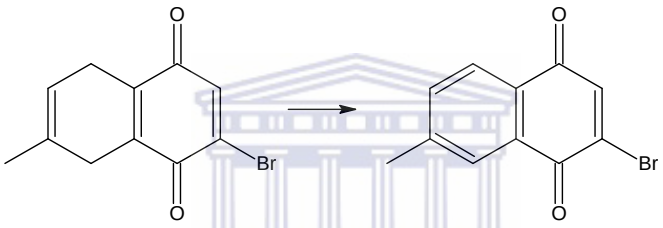

3.6 **3.2**

Scheme 3.5

The disappearance of the 4-proton multiplet at 3.05ppm and replaced by only signals in the aromatic region in the ^1H nmr spectrum supported aromatisation. A HRMS of 251.9631 supported the molecular formula $C_{11}H_7BrO_2$ (^{81}Br) (required 251.9629).

It was noted that even after the 30h reflux period some starting material was still present in the reaction mixture but by careful chromatographic separation using EtOAc: hexane (5: 95) as eluent the fully aromatised product **3.2** was obtained in pure form.

The proposed general mechanism for oxidation of unsaturated alicyclic rings with chloranil is shown in scheme **3.6** below.

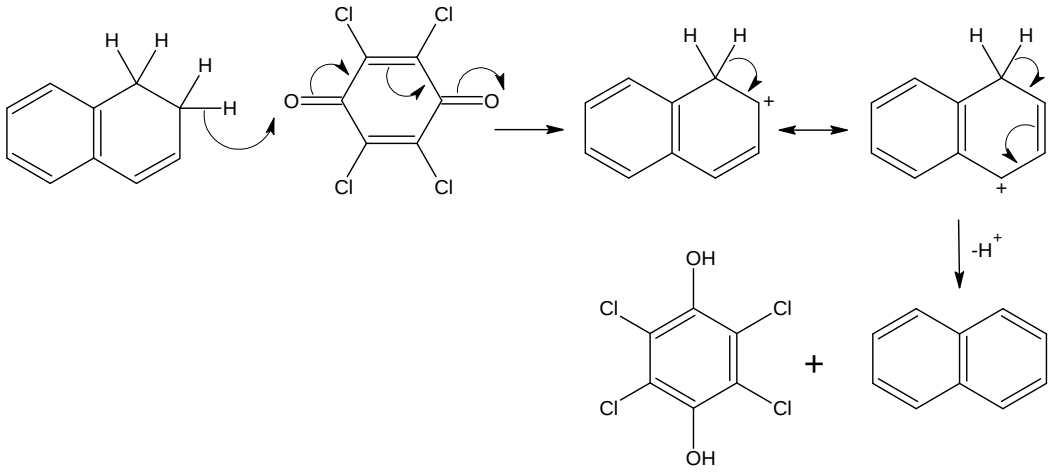

Scheme 3.6

Section 3.1.2: Synthesis of 1,4-dimethoxy-7-methylnaphthalene-2-boronic acid 3.3

The next step was the synthesis of boronic acid **3.3**, which was to be coupled to **3.2** by Suzuki coupling methodology. The envisaged route to **3.3** was expected to proceed according to Scheme **3.7** as shown below.

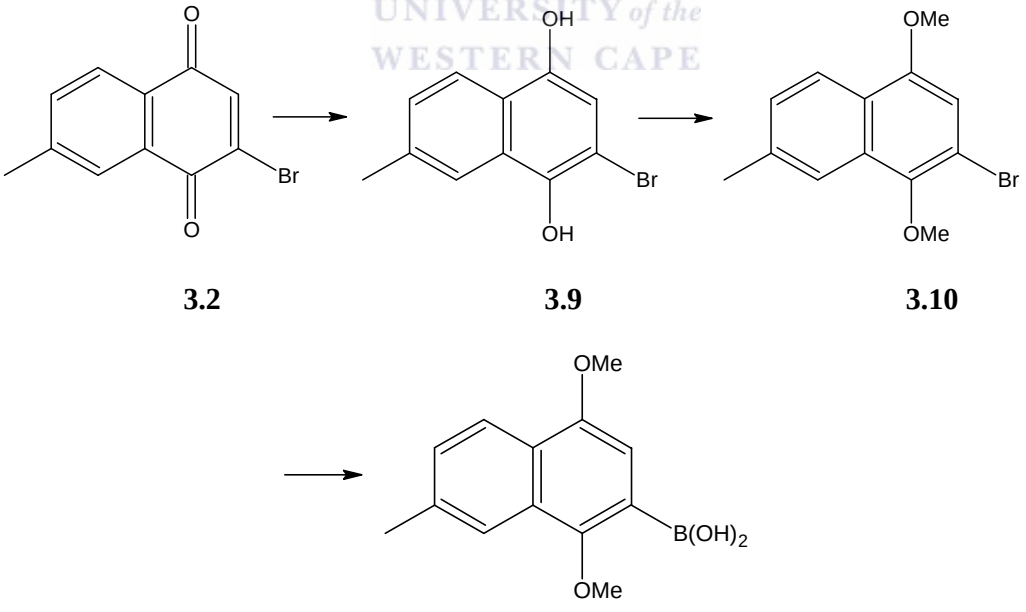

3.2 **3.9** **3.10**

3.3

Scheme 3.7

The first step was the reduction of quinone **3.2** to 2-bromo-7-methyl-1,4-naphthalenediol **3.9** as reported by Kesteleyn *et al.*,[68] as shown in Scheme **3.8** below.

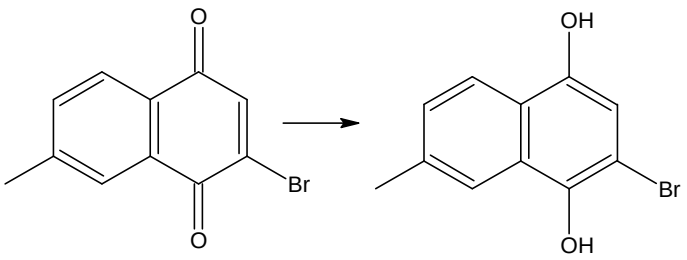

3.2 **3.9**

Scheme 3.8

A suspension of 2-bromo-7-methyl-1,4-naphthoquinone **3.2** in ethanol was treated with a solution of tin(II) chloride in concentrated HCl, poured into cold water and then filtered to afford 77% of the product **3.9**. The resulting material was assigned the structure **3.9** based on the following spectral evidence. The infrared spectrum showed the –OH stretching frequency at 3297 cm^{-1}. In the ^{1}H nmr spectrum a 2-proton broad singlet at 5.56ppm is assigned to the two hydroxyl protons. However in the ^{1}H nmr spectrum (d_6-acetone), the two peaks for the hydroxyl groups appeared at 7.77 and 8.83ppm for the 4-OH and 1-OH groups respectively. In the ^{13}C spectrum, C-4 and C-1 appeared at 133.8 and 138.9ppm respectively. The naphthol is immediately used in further reactions since it undergoes aerial oxidation to afford a blue residue.

The next step was the methylation of **3.9** to afford 2-bromo-1,4-dimethoxy-7-methylnaphthalene **3.10** as reported by Jung *et al.*,[69] and is shown in Scheme **3.9**.

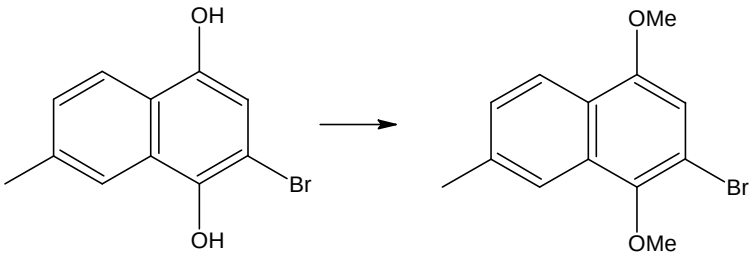

3.9 **3.10**

Scheme 3.9

A solution of naphthalenediol **3.9** in acetone was treated with anhydrous potassium carbonate and dimethyl sulphate and heated under reflux for 20h and filtered. The residue obtained by removal of solvent then dissolved in ether and treated with triethylamine to afford 77% of the product **3.10**. The spectral evidence for the structure **3.10** of the product includes the disappearance of hydroxyl peak in the infrared spectrum. In the ^{1}H nmr spectrum, two methoxy signals appeared at 3.94 and 3.96ppm respectively. In the ^{13}C nmr spectrum, C-1 and C-4 appeared at 150.6 and 152.4ppm.

Great difficulty was experienced in transforming bromonaphthalene **3.10** into boronic acid **3.3** following the method of Yoshida et al.[41] Eventually it was found that addition of HCl to hydrolyse the initial borate has to be very carefully performed and thus the method of Alo *et al*.,[70] was subsequently followed as illustrated in Scheme **3.10**.

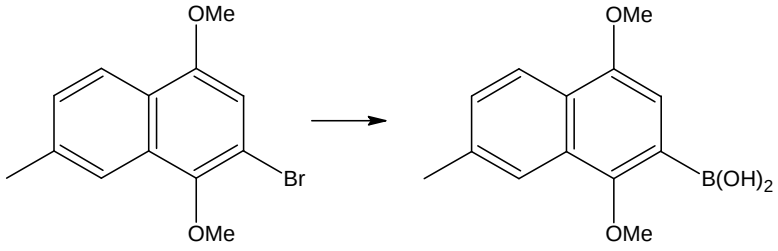

3.10 **3.3**

Scheme 3.10

A solution of 2-bromo-1,4-dimethoxy-7-methylnaphthalene **3.10** in THF was treated with n-butyllithium and trimethyl borate at -78˚C and then stirred for 20h at room temperature. The reaction mixture was then cooled to 0˚C and aqueous HCl (5% v/v) was added until the pH was approximately 6 to afford a 70% yield of **3.3**. The spectral evidence includes two methoxy peaks at 3.55 and 3.81ppm and a 2-proton singlet at 5.58ppm assigned to $B(OH)_2$ in the ^1H nmr spectrum. The boronic was not characterized further by spectroscopy and was used immediately in the next biaryl-coupling reaction.

Section 3.1.3: Coupled product

In the next step, naphthoquinone **3.2** and boronic acid **3.3** were coupled together to provide 2-(1´,4´-dimethoxy-7´-methylnaphthalen-2´-yl)-7-methyl-1,4-naphthoquinone **3.11** by using Suzuki coupling as reported by Miyaura *et al.*,[64, 65] and is shown in Scheme **3.11** below.

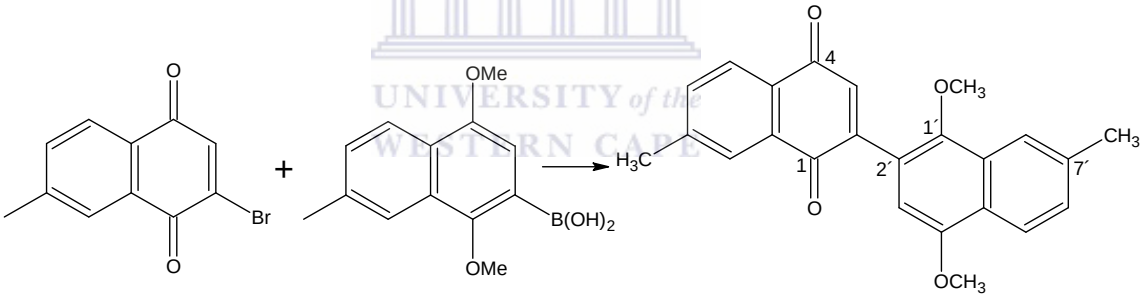

3.2 **3.3** **3.11**

Scheme 3.11

A mixture of naphthoquinone **3.2** and $Pd(PPh_3)_4$ (catalytic amount) in benzene was treated with an aqueous solution of sodium carbonate and boronic acid **3.3** in benzene at 24˚C and then heated under reflux for 16h to afford a 41% yield of product **3.11**. The resulting material was assigned the structure **3.11** based on the following spectral evidence. In the infrared spectrum, two peaks at 1664 and 1657 cm^{-1} shows carbonyl stretching frequencies for the

quinone moiety. In the ^{1}H nmr spectrum, signals for the two methyl groups appeared at 2.53 and 2.55ppm. A 1-proton singlet at 6.56ppm is assigned to H-3´ because of the electron donating resonance effect of the methoxy groups attached to the same ring. A 1-proton dd at 7.38ppm with *J* 8.4 and 1.4 Hz was assigned to H-6´ and a 1-proton dd at 7.59ppm with *J* 7.6 and 1.0 Hz was assigned to H-6. In the ^{13}C spectrum, C-1´ and C-4´ appeared at 145.0 and 151.7ppm while the two quinone carbonyl peaks, C-1 and C-4 appeared at 184.4 and 185.1ppm. A HRMS of 372.1299 supported the molecular formula $C_{24}H_{20}O_4$ (required 372.1361).

The last step in the synthesis of 2,2´-bis(7-methyl-1,4-naphthoquinone) **3.1**, required oxidative demethylation of the **3.11** and the method reported by Syper *et al.*,[71] was chosen as shown in Scheme **3.12** below.

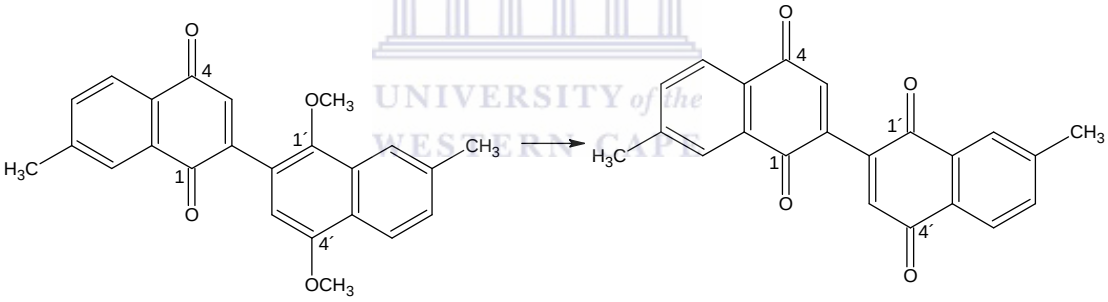

3.11 **3.1**

Scheme 3.12

A suspension of naphthoquinone **3.11** in a mixture of acetonitrile and water at 0˚C was treated with cerium(IV) ammonium nitrate in a mixture of acetonitrile and water and stirred for 30 min at 24˚C to afford a 15% yield of product **3.1** with m.p. 179-181°C (from ethanol), (lit.[72] 240°C). Spectral evidence for the structure **3.1** includes two aryl methyl peaks at 2.52 and 2.54ppm and the absence of methoxy peaks in the ^{1}H nmr spectrum. In the ^{13}C nmr spectrum,

the peaks for the quinone carbonyls, (C-1´, C-4´, C-1 and C-4)[a] appeared at (177.3, 180.0, 182.0 and 183.8ppm)[a]. A HRMS of 342.0627 supported the molecular formula $C_{22}H_{14}O_4$ (required 342.0892).

Laatsch[72] as illustrated in Schemes **3.13** and **3.14** below also reported a synthesis of **3.1**.

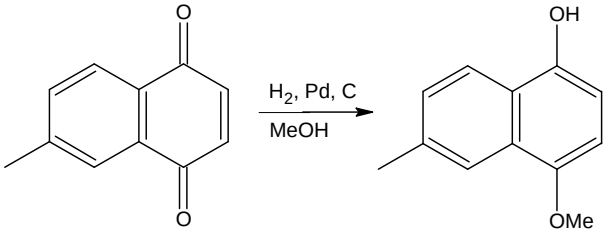

Scheme 3.13

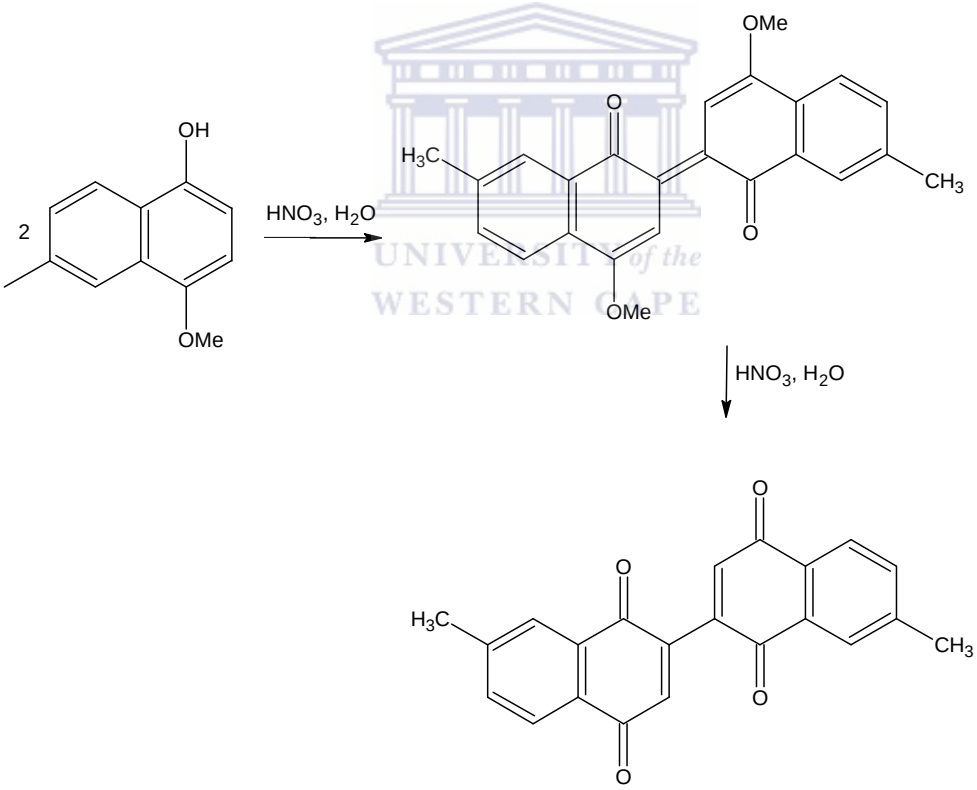

3.1

Scheme 3.14

Section 3.2: Synthesis of 2,2´-bis(5-methoxy-7-methyl-1,4-naphthoquinone) 3.12

The second molecule that we decided to synthesize was the bisnaphthoquinone with two methoxy groups **3.12**. It was reported that the dimethyl ether derivative of diospyrin **1.27** is more biologically active than diospyrin **1.22**, against *Ehrlich Ascites Carcinoma* (EAC) in Swiss Albino mice[50] and human cancer cell lines.[52] Based on the previous references in the thesis, molecule **3.12** could also act as an effective anti-cancer agent. Two possible retrosynthons of this target molecule were quinone **3.13** and boronic acid **3.14**, as shown in Scheme **3.15**.

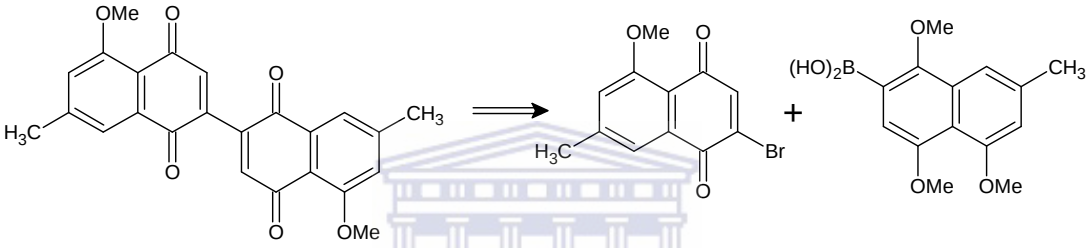

3.12 **3.13** **3.14**

Scheme 3.15

Section 3.2.1: Synthesis of 2-Bromo-5-methoxy-7-methyl-1,4-naphthoquinone 3.13

The synthetic protocol of the target naphthoquinone **3.13** is illustrated in Scheme **3.16**.

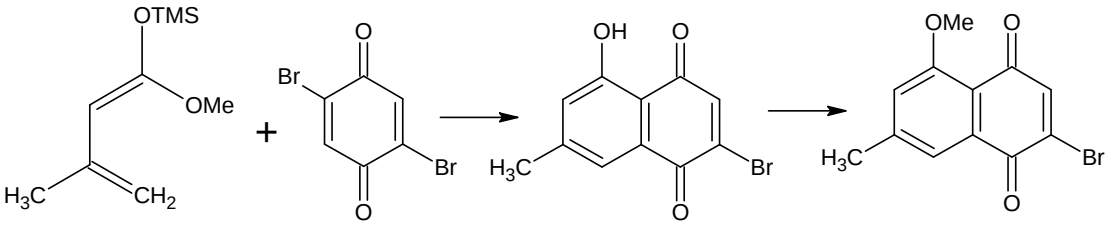

3.15 **3.5** **3.16** **3.13**

Scheme 3.16

The synthesis of butadiene **3.15** was successfully carried out using the method reported by Casey *et al.*,[73] depicted in Scheme **3.17**.

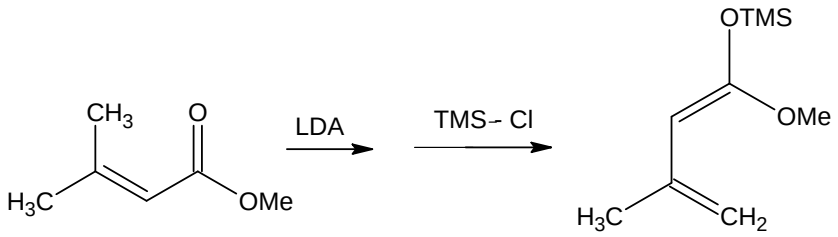

3.17 **3.15**

Scheme 3.17

Methyl-3-methyl-2-butenoate **3.17** in THF was treated with a solution of lithiumdiisopropylamide at –78˚C followed by addition of trimethylsilyl chloride and triethylamine. The temperature was allowed to rise to 24˚C to afford an 80% yield of the diene **3.15,** which was immediately allowed to react with dibromobenzoquinone **3.5**, and afforded the hydroxynaphthoquinone **3.16** in a 57% yield as illustrated in Scheme **3.18** below.[41]

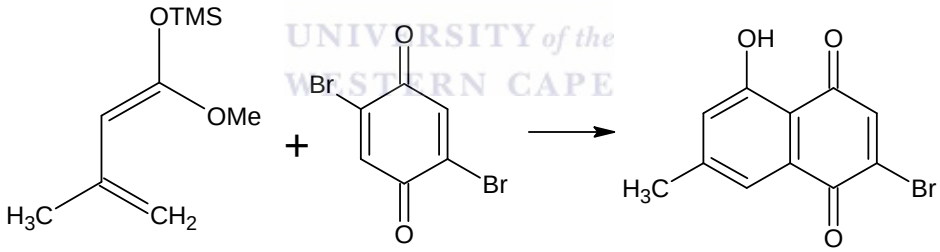

3.15 **3.5** **3.16**

Scheme 3.18

Spectral evidence for the structure of the adduct **3.16** includes a 1-proton singlet at 11.70ppm for the 5-OH group in the ^{1}H nmr spectrum. In the ^{13}C nmr spectrum, signals at 177.5 and 186.9ppm are assigned to the two quinone carbonyls. The proposed mechanism for the reaction is illustrated in Scheme **3.19**.

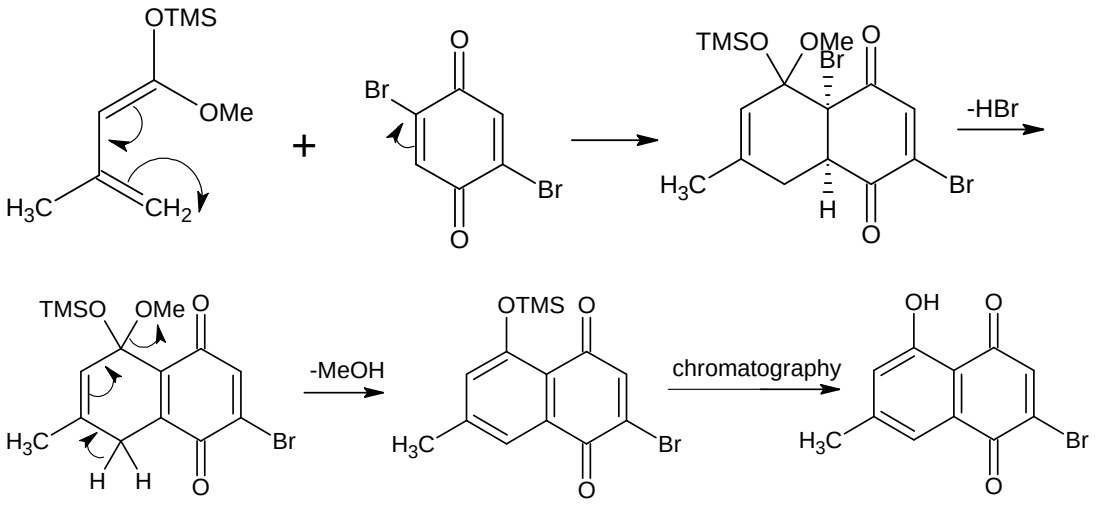

Scheme 3.19

The next step was the methylation of **3.16** to get 2-Bromo-5-methoxy-7-methyl-1,4-naphthoquinone **3.13** as reported by Jung *et al*.,[69] depicted in Scheme **3.20**.

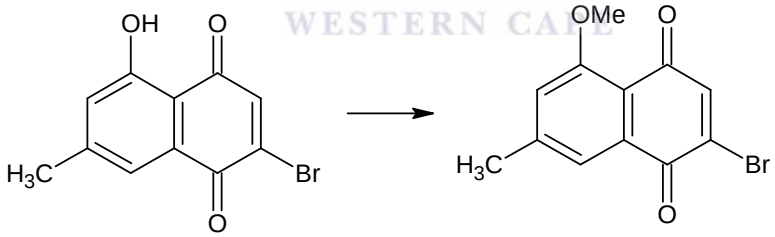

3.16 **3.13**

Scheme 3.20

A solution of hydroxynaphthoquinone **3.16** in benzene was treated with powdered Ag_2O and methyl iodide to afford 56% yield of the methoxynaphthoquinone **3.13**. Spectral evidence for the structure of product **3.13** includes a 3-proton singlet at 3.99ppm assigned to the methoxy group in the ^{1}H nmr spectrum. In the ^{13}C nmr spectrum, signals for the two quinone carbonyls viz., C-1 and C-4 appeared at 178.6 and 181.3ppm.

Section 3.2.2: Synthesis of 1,4,5-trimethoxy-7-methylnaphthalene-2-boronic acid 3.14

The next step was the synthesis of trimethoxyboronic acid **3.14**, which was to be coupled to quinone **3.13**. The synthetic protocol of the target boronic acid **3.14** is illustrated in Scheme **3.21**.

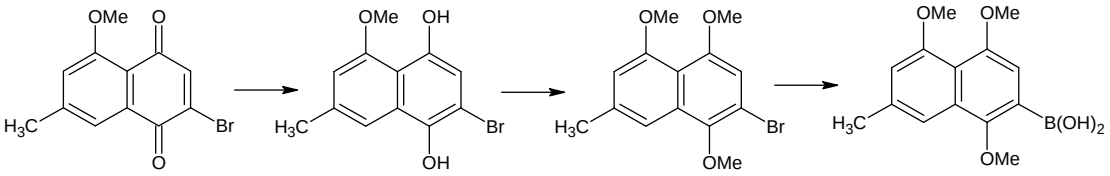

3.13 **3.18** **3.19** **3.14**

Scheme 3.21

The first step in this route was the reduction of **3.13** to naphthalenediol **3.18** as reported by Kesteleyn *et al.*,[68] shown in Scheme **3.22**.

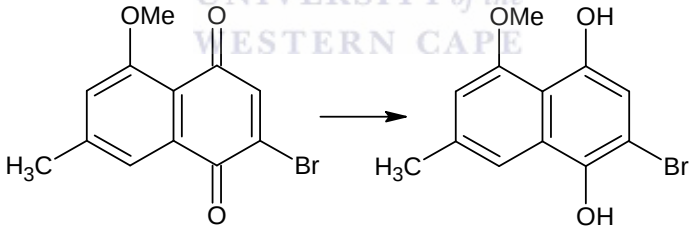

3.13 **3.18**

Scheme 3.22

A suspension of methoxynaphthoquinone **3.13** in dichloromethane was shaken in a separatory funnel with a freshly prepared solution of sodium dithionate in water to afford a 78% yield of naphthalenediol **3.18**. The resulting material was assigned the structure **3.18** based on the following spectral evidence. In the ^{1}H nmr spectrum, two peaks for 1-OH and 4-OH appeared at 5.43 and 8.91ppm. In the ^{13}C spectrum, signals for C-1 and C-4 appeared at 147.9 and 155.5ppm.

Subsequently methylation of **3.18** as reported by Jung *et al.*,[69] was effected as depicted in Scheme **3.23**.

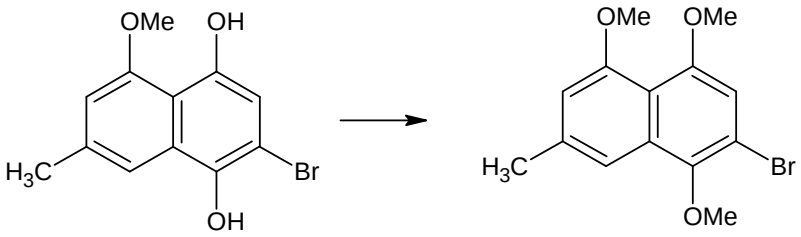

3.18 **3.19**

Scheme 3.23

A solution of naphthalenediol **3.18** in acetone was treated with anhydrous potassium carbonate and dimethyl sulphate and heated under reflux for 20h to afford an 82% yield of trimethoxynaphthalene **3.19**. Spectral evidence for the structure of compound **3.19** includes three methoxy signals at 3.91, 3.93 and 3.95ppm in the ^{1}H nmr spectrum while in the ^{13}C nmr spectrum, signals at 146.2, 153.8 and 157.3ppm were assigned to C-5, C-1 and C-4.

The method of Alo *et al.*,[70] was employed in the transformation of trimethoxynaphthalene **3.19** into the corresponding boronic acid **3.14** as shown in Scheme **3.24**.

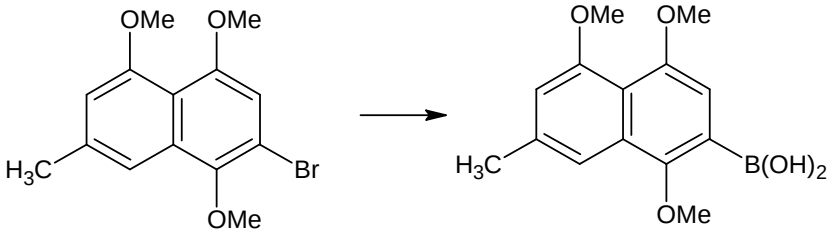

3.19 **3.14**

Scheme 3.24

A solution of trimethoxynaphthalene **3.19** in THF was treated with n-butyllithium and trimethyl borate at -78˚C and then stirred for 20h at room temperature after which the mixture was then cooled to 0˚C and treated with aqueous HCl (5% v/v) until the pH was approximately 6 to afford 75% yield of the boronic acid **3.14**. The boronic was not

characterized further by spectroscopy, but was used immediately in the next biaryl-coupling reaction.

Section 3.2.3: Coupled product

Next the two naphthalene subunits **3.13** and **3.14** were coupled together by using Suzuki methodology as reported by Miyaura *et al.*,[64, 65] to afford the biaxial binaphthalene unit **3.20** as illustrated in scheme **3.25**.

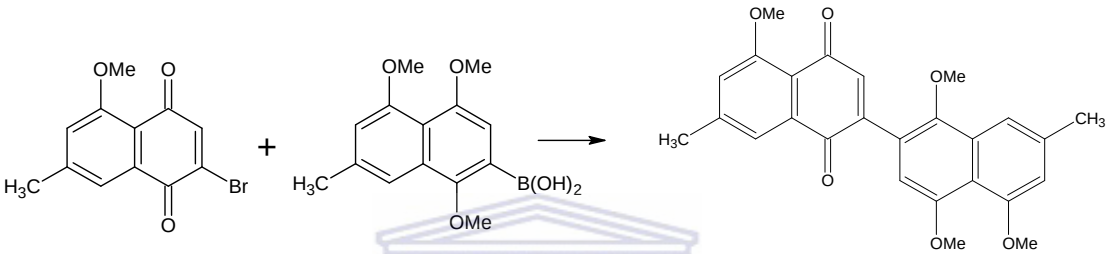

3.13 **3.14** **3.20**

Scheme 3.25

Thus a mixture of bromonaphthoquinone **3.13** and $Pd(PPh_3)_4$ in benzene was treated with an aqueous solution of sodium carbonate and trimethoxyboronic acid **3.14** in benzene at 24˚C and then heated under reflux for 16h to afford a 41% yield of the product **3.20**. The resulting material was assigned the structure **3.20** based on the following spectral evidence. In the ^{1}H nmr spectrum, a 6-proton singlet at 2.50ppm was assigned to both of the methyl groups and signals for the four methoxy groups appeared at 3.68, 3.94, 3.97 and 4.03ppm. In the ^{13}C spectrum, signals at 147.8, 153.4, 157.4, 159.8, 184.3 and 184.5ppm were assigned to C-5´, C-1´, C-4´, C-5, C-1 and C-4. A HRMS of 432.1546 supported the molecular formula $C_{26}H_{24}O_6$ (required 432.1572).

The final step in the synthesis of 2,2´-bis(5-methoxy-7-methyl-1,4-naphthoquinone) **3.12**, involved the oxidative demethylation of **3.20** as reported by Syper *et al.*,[71] as illustrated in Scheme **3.26**.

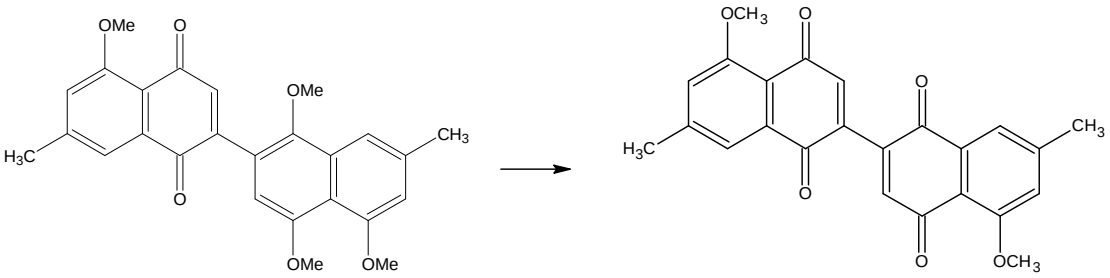

3.20 **3.12**

Scheme 3.26

A suspension of 2-(1′,4′,5′-trimethoxy-7′-methylnaphthalen-2′-yl)-5-methoxy-7-methyl-1,4-naphthoquinone **3.20** in a mixture of acetonitrile and water at 0˚C was treated with cerium(IV) ammonium nitrate in a mixture of acetonitrile and water and stirred for 30 min at 24˚C to afford a 34% yield of the product **3.12**. The resulting material was assigned the structure **3.12** based on the following spectral evidence. In the ^{1}H nmr spectrum, a 6-proton singlet at 2.49ppm was assigned to both CH_3-7´ and CH_3-7 and a 6-proton singlet at 4.02ppm was assigned to two methoxy groups. A singlet at 6.94ppm was assigned to H-6´ and H-6. In the ^{13}C spectrum, a signal at 22.5ppm was assigned to CH_3-7´ and CH_3-7 and a signal at 56.6ppm was assigned to two methoxy groups. A signal at 183.2ppm was assigned to (C-1´ and C-1) and a signal at 183.5ppm was assigned to (C-4´ and C-4). A HRMS of 402.1247 supported the molecular formula $C_{24}H_{18}O_6$ (required 402.1103).

Section 3.3: Synthesis of 2-(1´,4´-benzoquinon-2´-yl)-7-methyl-1,4-naphthoquinone 3.21

The next molecule that we decided to synthesize was benzoquinonenaphthoquinone **3.21**. This molecule differs from the previously synthesized molecule **3.1** with regard to it having a benzoquinone and not a naphthoquinone on the right hand ring as depicted in scheme **3.27**. These factors may affect its biological activity as an anti-TB and anti-cancer agent in comparison to the other analogues. The two retrosynthons for the molecule were quinone **3.2** and boronic acid **3.22**, shown in retro Scheme **3.27** below.

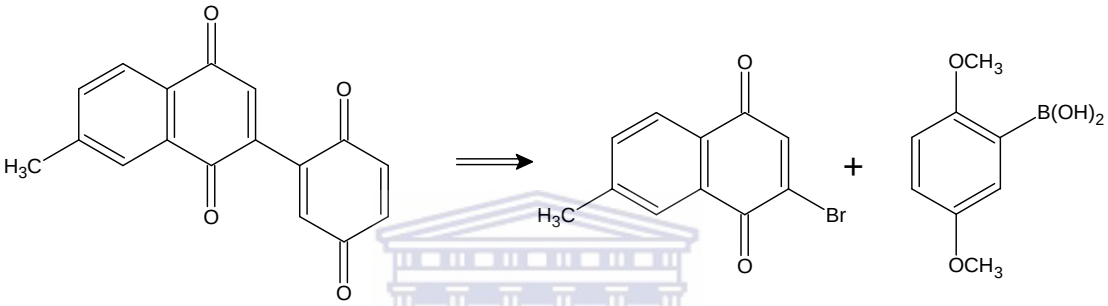

3.21 **3.2** **3.22**

Scheme 3.27

The proposed synthetic protocol of the target naphthoquinone **3.2** is already illustrated in Scheme **3.2**.

Section 3.3.1: Synthesis of 1,4-dimethoxybenzene-2-boronic acid 3.22

The envisaged route to boronic acid[70] **3.22** was expected to proceed according to Scheme **3.28**.

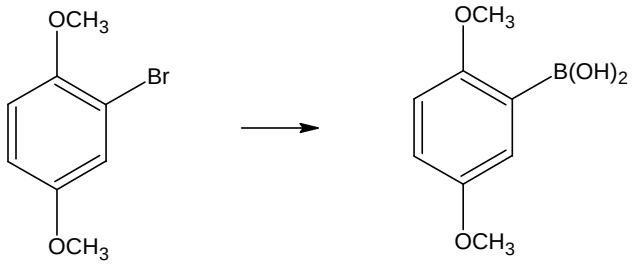

3.23 **3.22**

Scheme 3.28

A solution of 2-bromo-1,4-dimethoxybenzene **3.23** in THF was treated with n-butyllithium and trimethyl borate at -78˚C and then stirred for 20h at room temperature after which the cooled (0˚C) mixture was treated with an aqueous HCl (5% v/v) until the pH was approximately 6 to afford an 80% of yield of the boronic acid **3.22**. The resulting material was assigned the structure **3.22** based on the following spectral evidence. In the ^{1}H nmr spectrum, two methoxy signals appeared at 3.81 and 3.88ppm and a 2-proton broad singlet at 6.38ppm was assigned to the $B(OH)_2$ group. In the ^{13}C nmr spectrum, signals at 153.9 and 158.9ppm were assigned to C-1 and C-4. A HRMS of 182.0755 supported the molecular formula $C_8H_{11}BO_4$ (required 182.0752). The boronic was used immediately in the next biaryl-coupling reaction.

Section 3.3.2: Coupled product: Next the two aryl units **3.2** and **3.22** were coupled together to form naphthoquinone **3.24** by using Suzuki methodology as reported by Miyaura *et al.*,[64, 65] illustrated in Scheme **3.29**.

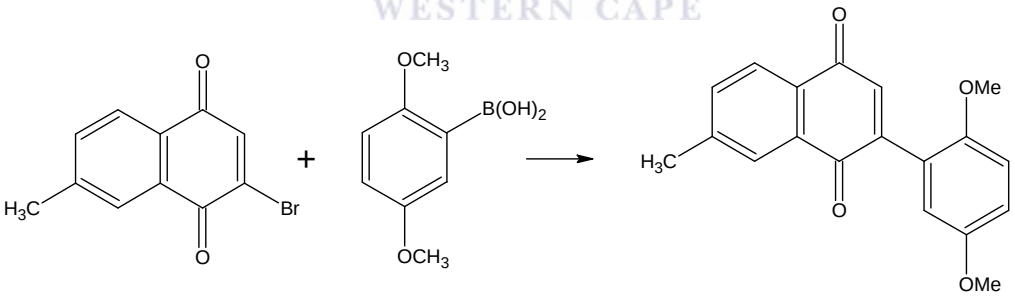

3.2 **3.22** **3.24**

Scheme 3.29

A mixture of 2-bromo-7-methyl-1,4-naphthoquinone **3.2** and $Pd(PPh_3)_4$ in benzene was treated with an aqueous solution of sodium carbonate and dimethoxyboronic acid **3.22** in benzene at 24˚C and heated under reflux for 16h to afford a 76% yield of the coupled product **3.24**. The resulting material was assigned the structure **3.24** based on the following spectral evidence. In the ^{1}H nmr spectrum, a 3-proton singlet at 2.51ppm was assigned to the C-7

methyl group and peaks at 3.74 and 3.79ppm were assigned to the two methoxy groups. In the ^{13}C spectrum, signals at 151.5, 153.5, 183.7 and 185.1ppm were assigned to C-1´, C-4´, C-1 and C-4. A HRMS of 308.1049 supported the molecular formula $C_{19}H_{16}O_4$ (required 308.1048).

The final step involved the oxidative demethylation of dimethyl ether **3.24** using a protocol reported by Syper *et al*.,[71, 68] depicted in Scheme **3.30**.

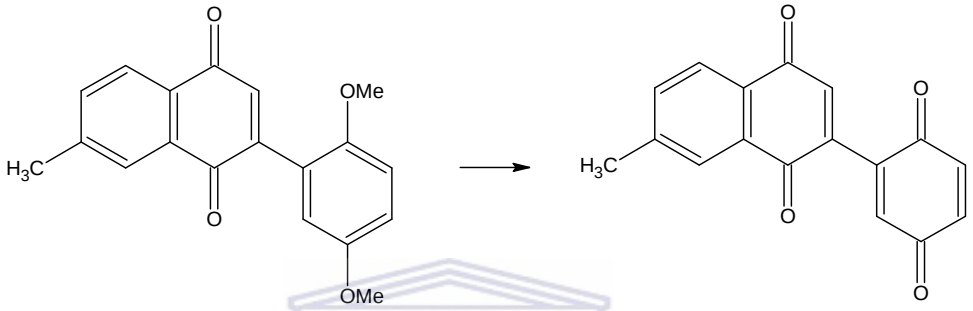

3.24 **3.21**

Scheme 3.30

A suspension of 2-(1´,4´-dimethoxybenzen-2´-yl)-7-methyl-1,4-naphthoquinone **3.24** in a mixture of acetonitrile and water at 0˚C was treated with cerium(IV) ammonium nitrate in a mixture of acetonitrile and water and stirred for 30 min at 24˚C to afford a 71% yield of the product **3.21**. Spectral evidence for the structure of biquinone **3.21** includes the disappearance of the two methoxy signals in the ^1H nmr spectrum. In the ^{13}C nmr spectrum, signals at 182.9, 183.8, 184.6 and 186.4ppm were assigned to C-1´, C-4´, C-1 and C-4 respectively. A HRMS of 278.0570 supported the molecular formula $C_{17}H_{10}O_4$ (required 278.0579).

Section 3.4: Synthesis of 2-(1´,4´-benzoquinon-2´-yl)-5-hydroxy-7-methyl-1,4-naphthoquinone 3.25

The next molecule that we decided to synthesize was binaphthoquinone **3.25**. This molecule differs from the previous molecule **3.21** with regard to it having the hydroxyl group at C-5.

Any difference in the biological activity of the compound in comparison to the previous molecule **3.21** would be due to the hydroxyl group. This should provide evidence as to whether the hydroxyl group is responsible for any enhanced biological activity of the compound. The two retrosynthons were quinone **3.13** and boronic acid **3.22** shown in retro Scheme **3.31**.

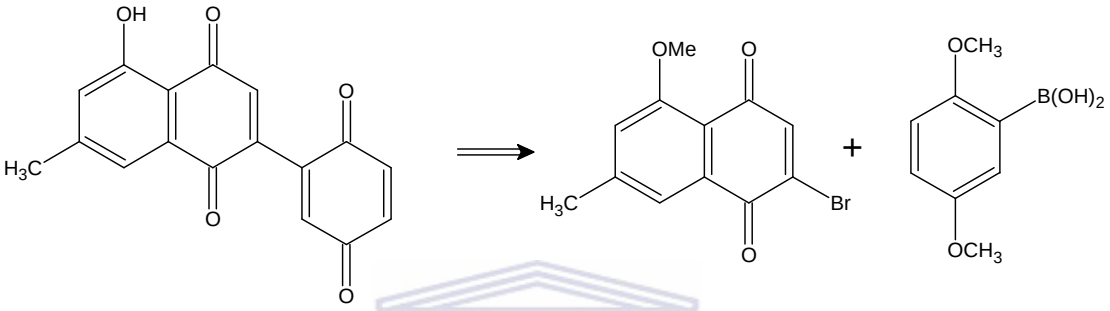

3.25 **3.13** **3.22**

Scheme 3.31

The proposed synthetic protocol of the target naphthoquinone **3.13** and boronic acid **3.22** are already illustrated in Scheme **3.16** and **3.28** respectively. In the first step, two aryl units were coupled together by using Suzuki methodology[64, 65] as shown in Scheme **3.32**.

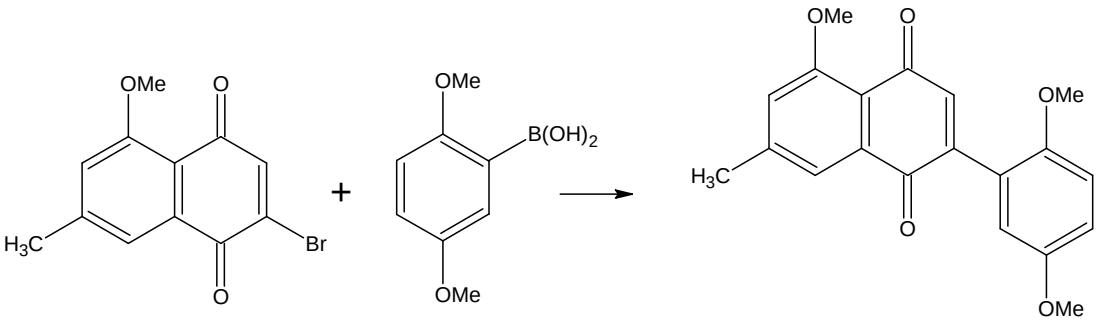

3.13 **3.22** **3.26**

Scheme 3.32

A mixture of 2-bromo-5-methoxy-7-methyl-1,4-naphthoquinone **3.13** and $Pd(PPh_3)_4$ in benzene was treated with an aqueous solution of sodium carbonate and dimethoxyboronic acid **3.22** in benzene at 24˚C and heated under reflux for 16h to afford a 32% yield of the product **3.26**. The resulting material was assigned the structure **3.26** based on the following spectral evidence. In the ^1H nmr spectrum, a 3-proton singlet at 2.46ppm was assigned to the C-7 methyl group and peaks at 3.71, 3.77 and 3.98ppm were assigned to three methoxy groups. In the ^{13}C spectrum, signals at 151.4, 153.4, 159.5, 183.8 and 184.2ppm were assigned to C-1´, C-4´, C-5, C-1 and C-4. A HRMS of 338.1143 supported the molecular formula $C_{20}H_{18}O_5$ (required 338.1154).

The next step was the oxidative demethylation of the dimethyl ether **3.26** by using a protocol reported by Syper *et al.*,[71, 68] and is illustrated in Scheme **3.33**.

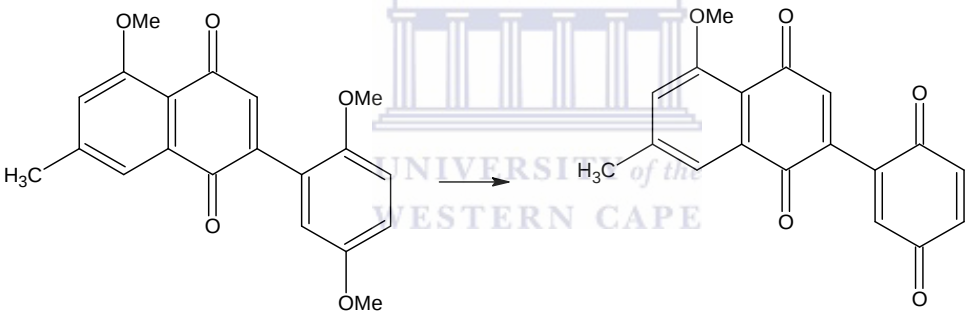

3.26 **3.27**

Scheme 3.33

A suspension of trimethoxyquinone **3.26** in a mixture of acetonitrile and water at 0˚C was treated with cerium(IV) ammonium nitrate in a mixture of acetonitrile and water and stirred for 30 min at 24˚C to afford a 72% yield of the product **3.27**. The resulting material was assigned the structure **3.27** based on the following spectral evidence. In the ^1H nmr (d_6-DMSO) spectrum a 1-proton doublet at 7.39ppm with *J* 2.6 was assigned to H-3´ and a 1-proton singlet at 7.48ppm was assigned to H-3. In the ^{13}C nmr (d_6-DMSO) spectrum, signals

at 154.7, 155.8, 160.5, 173.4 and 180.8ppm were assigned to C-5, C-1´, C-4´, C-1 and C-4. A HRMS of 308.0611 supported the molecular formula $C_{18}H_{12}O_5$ (required 308.0684).

Last step in the synthetic protocol involved the demethylation of the C-5 methoxy group and the method of Syper *et al*.,[71, 68] was adopted as depicted in Scheme **3.34**.

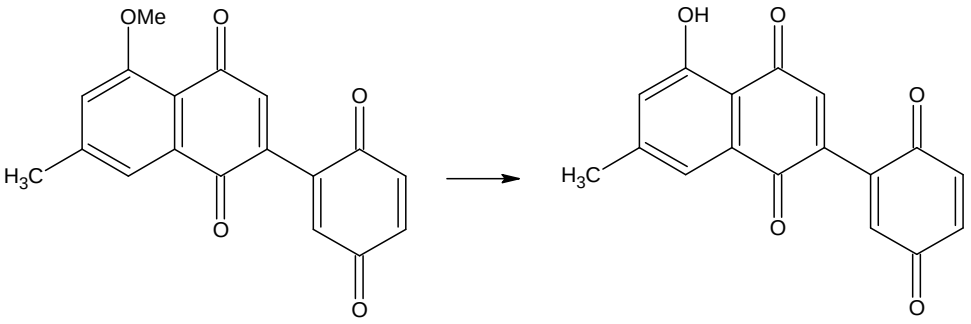

3.27 **3.25**

Scheme 3.34

A solution of methoxyquinone **3.27** in dry CH_2Cl_2 at 25˚C was treated with aluminium trichloride. The mixture was stirred at 25˚C for 24h, poured into water, and then acidified with dilute HCl to afford a 55% yield of the hydroxyquinone **3.25**. The resulting material was assigned the structure **3.25** based on the following spectral evidence. In the ^{1}H nmr (d_6-DMSO) spectrum, a skewed 2-proton doublet at 7.43ppm with *J* 2.4 was assigned to H-3´, which is overlaid by H-3, and a 1-proton singlet at 11.77ppm, which was assigned to the 5-OH. In order to clarify this signal unambiguously, the spectrum was also run in d_6-acetone. Thus in the ^{1}H nmr (d_6-acetone) spectrum, a 1-proton singlet at 7.16ppm was assigned to H-3, a 1-proton doublet at 7.62ppm with J 2.4 was assigned to H-3´ and a 1-proton singlet at 11.99ppm was assigned to 5-OH. In the ^{13}C nmr (d_6-DMSO) spectrum, signals at 153.5, 156.0, 161.4, 178.9 and 180.3ppm were assigned to C-5, C-1´, C-4´, C-1 and C-4. A HRMS of 294.0571 supported the molecular formula $C_{17}H_{10}O_5$ (required 294.0528).

Synthesis of naphthoquinone-naphthalene biaryl systems

The availability of commercially pure boronic acids allowed for the synthesis of naphthoquinone-naphthalene biaryl systems with a fair variety of groups attached to either of the naphthalenic nuclei. An evaluation of their biological activity against *M. tuberculosis* and certain cancer cell lines was consequently made possible which would provide guidelines in deducing the structure-activity relationship.

Section 3.5: Synthesis of 2-(6′-hydroxynaphthalen-2′-yl)-5-hydroxy-7-methyl-1,4-naphthoquinone 3.28

The first compound to be synthesized was **3.28**, which has two hydroxyl groups, the one on the naphthoquinone half and the other on the naphthalene moiety. In this synthesis, the first major step was the formation of 2-(6′-methoxynaphthalen-2′-yl)-5-methoxy-7-methyl-1,4-naphthoquinone **3.29**, which involved the Suzuki coupling[64, 65] between the naphthoquinone **3.13** and boronic acid **3.30** to afford a 90% yield of the quinone **3.29** as shown in Scheme **3.35**.

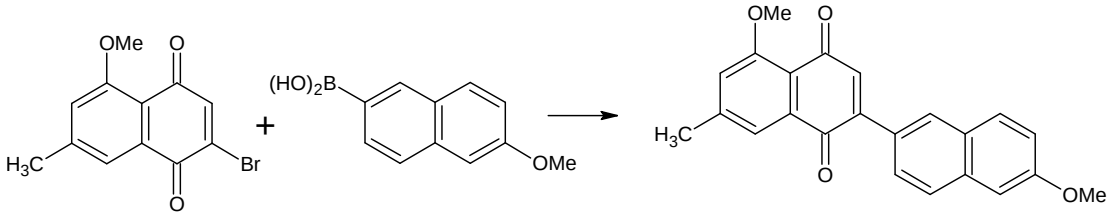

3.13 **3.30** **3.29**

Scheme 3.35

The resulting material was assigned the structure **3.29** based on the following spectral evidence. In the ^{1}H nmr spectrum, a signal at 2.51ppm was assigned to the 7- CH_3 and peaks at 3.95 and 4.03ppm were assigned to the two methoxy groups. In the ^{13}C nmr spectrum, signals at 158.9, 159.7, 184.4 and 185.3ppm were assigned to C-6´, C-5, C-1 and C-4. A HRMS of 358.1049 supported the molecular formula of $C_{23}H_{18}O_4$ (required 358.1204).

The next involved the demethylation of the C-5 OCH_3 group as reported by Kesteleyn *et al.*[74] as shown in Scheme **3.36**.

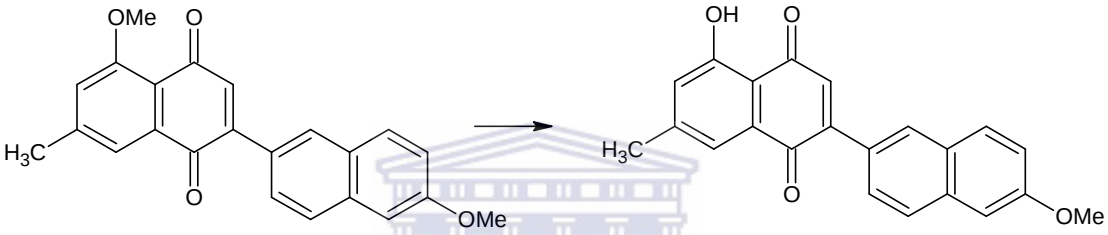

3.29 **3.31**

Scheme 3.36

Thus a solution of **3.29** in dry DCM was treated with boron tribromide to afford a 51% yield of the 5-hydroxyquinone **3.31**. The resulting material was assigned the structure **3.31** based on the following spectral evidence. In the ^{1}H nmr spectrum, there was only one signal for a methoxy group at 4.03ppm and the 1-proton singlet at 12.00ppm was assigned to 5-OH. In the ^{13}C nmr spectrum, signals at 155.1, 161.4, 184.2 and 189.5ppm were assigned to C-6´, C-5, C-1 and C-4. A HRMS of 343.0867 supported the molecular formula of $C_{22}H_{16}O_4$ (required 344.1048).

The final step involved the further demethylation of the C-6´ OCH_3 and in this instance the method of Kesteleyn *et al.*[74] was used to afford a 46% yield of the quinone 3.28 as illustrated in Scheme **3.37**.

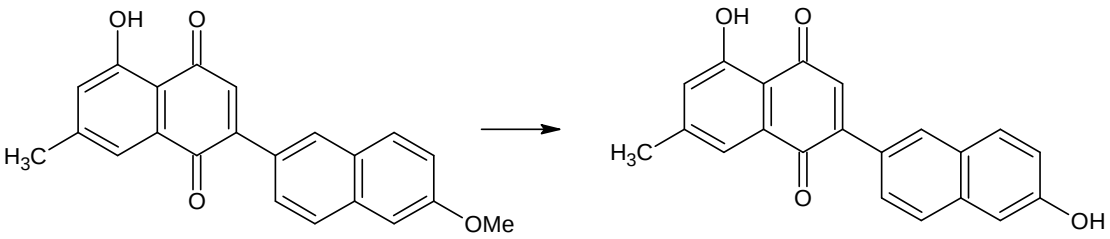

3.31 **3.28**

Scheme 3.37

The resulting material was assigned the structure **3.28** based on the following spectral evidence. In the ^{1}H nmr spectrum, the signals at 6.05 and 12.00ppm were assigned to 6´-OH and 5-OH. In the ^{13}C nmr spectrum, signals at 152.1, 161.4, 184.1 and 189.5ppm were assigned to C-6´, C-5, C-1 and C-4. A HRMS of 330.0872 supported the molecular formula of $C_{21}H_{14}O_4$ (required 330.0892).

Section 3.6: Synthesis of 2-(5´,10´-dioxydithianthren-1´-yl)-7-methyl-1,4-naphthoquinone 3.32

The second compound synthesized by using the commercially available boronic acid **3.33** was sulphone **3.32**. Suzuki coupling was employed in coupling bromoquinone **3.2** to boronic acid **3.33** in the first step as shown in Scheme **3.38**.

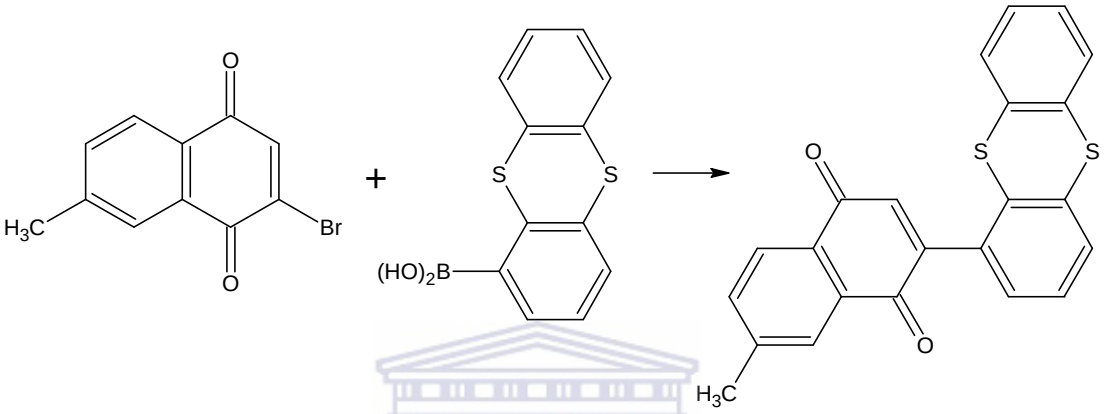

3.2 **3.33** **3.34**

Scheme 3.38

A mixture of **3.2** and $Pd(PPh_3)_4$ in benzene was treated with an aqueous solution of sodium carbonate and thiantherene-1-boronic acid **3.33** in benzene at 24˚C and heated under reflux for 16h to afford an 82% yield of the quinone **3.34**. The resulting material was assigned the structure **3.34** based on the following spectral evidence. In the ^1H nmr spectrum, a 5-proton multiplet at 7.27ppm was assigned to H-2´, H-3´, H-4´, H-7´ and H-8´. A M^+ in the HRMS of 386.0487 supported the molecular formula of $C_{23}H_{14}O_2S_2$ (required 386.0435).

The final step was the oxidation of the **3.34** by following the method reported by Nakayama et al.[75] as shown in Scheme **3.39**.

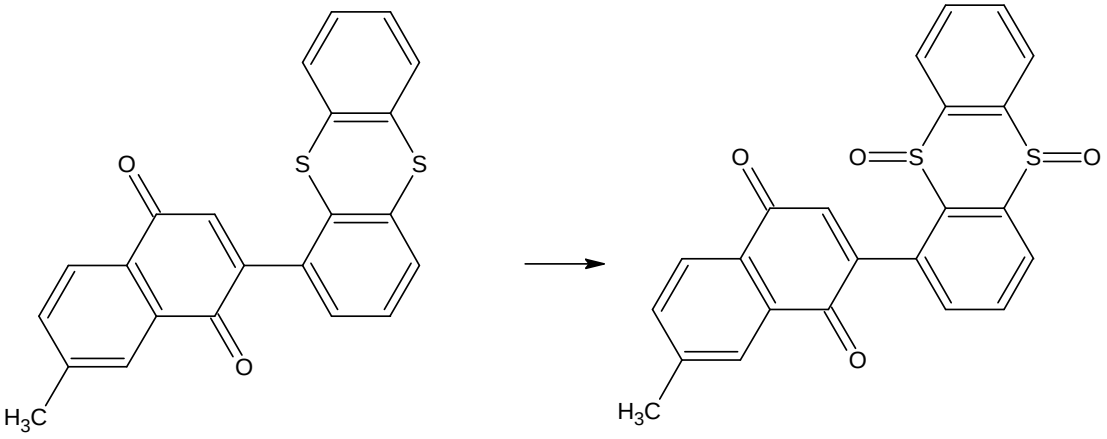

3.34 **3.32**

Scheme 3.39

A solution of **3.34** in DCM was treated with m-chloroperbenzoic acid to afford a 58% yield of the sulphone **3.32**. The resulting material was assigned the structure **3.32** based on the following spectral evidence. In the ir spectrum, peaks at 1164 and 1328 cm^{-1} were assigned to two S=O groups. A M^+ in the HRMS of 418.1630 supported the molecular formula of $C_{23}H_{14}O_4S_2$ (required 418.0334).

Section 3.7: Synthesis of 2-(5´,10´-dioxydithianthren-1´-yl)-5-methoxy-7-methyl-1,4-naphthoquinone 3.35

The other sulphone synthesized was **3.35** having an additional methoxy group at C-5 position. The initial step was the synthesis of 5-methoxy-7-methyl-2-(thianthren-1´-yl)-1,4-naphthoquinone **3.36** by using the Suzuki methodology[64, 65] as shown in Scheme **3.40**.

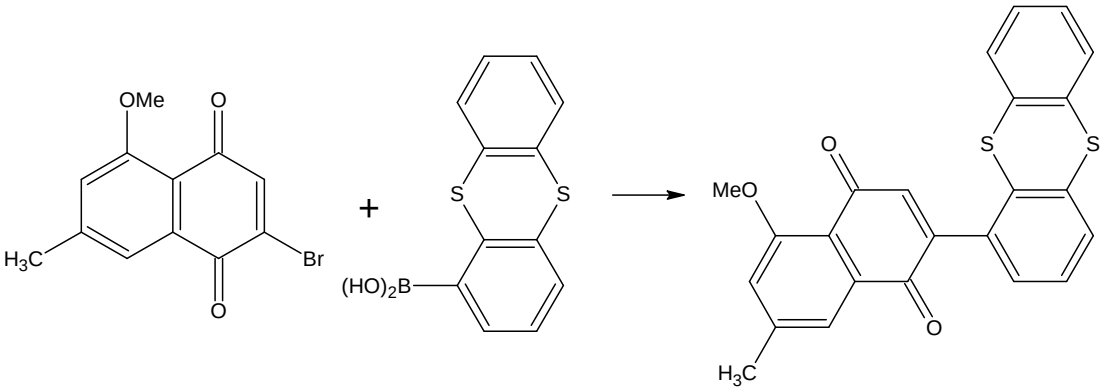

3.13 **3.33** **3.36**

Scheme 3.40

A mixture of **3.13** and $Pd(PPh_3)_4$ in benzene was treated with an aqueous solution of sodium carbonate and thianthrene-1-boronic acid **3.33** in benzene at 24˚C and heated under reflux for 16h to afford a 86% yield of the quinone **3.36**. The resulting material was assigned the structure **3.36** based on the following spectral evidence. In the ^{1}H nmr spectrum, a signal at 4.04ppm was assigned to the 5-OMe. A 5-proton multiplet at 7.27ppm was assigned to H-2´, H-3´, H-4´, H-7´ and H-8´. In the ^{13}C nmr spectrum, signals at 159.8, 183.8 and 183.9ppm were assigned to C-5, C-1 and C-4. A HRMS of 416.0498 supported the molecular formula of $C_{24}H_{16}O_3S_2$ (required 416.0541).

The next step involved the oxidation of **3.36** by following the method reported by Nakayama et al.[75] as shown in Scheme **3.41**.

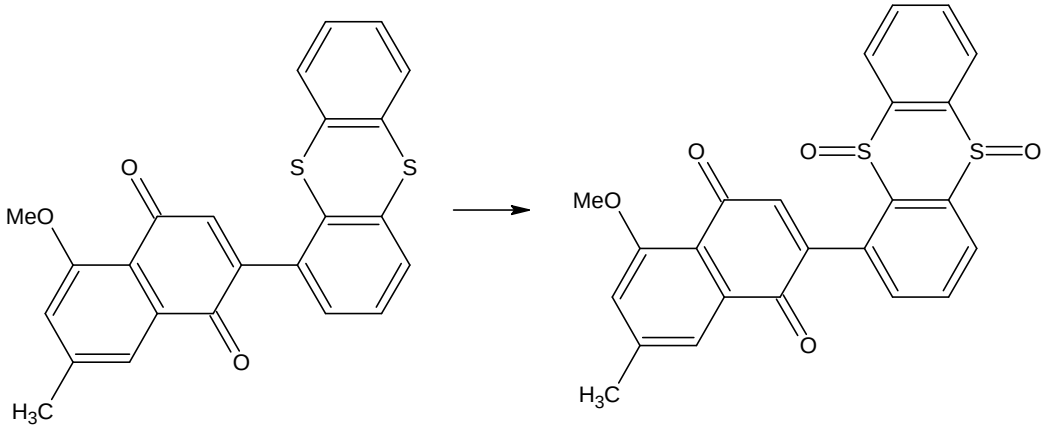

3.36 **3.35**

Scheme 3.41

A solution of **3.36** in DCM was treated with m-chloroperbenzoic acid to afford 64% yield of the sulphone **3.35**. The resulting material was assigned the structure **3.35** based on the following spectral evidence. In the ir spectrum, peaks at 1168 and 1326 cm^{-1} were assigned to two S=O groups. In the ^{1}H nmr spectrum, a signal at 4.04ppm was assigned to the 5-OMe. A 7-proton multiplet at 7.61ppm was assigned to H-3, H-8, H-2´, H-3´, H-7´, H-8´ and H-9´. In the ^{13}C nmr spectrum, signals at 160.0, 182.9 and 185.0ppm were assigned to C-5, C-1 and C-4. A HRMS of 448.1156 supported the molecular formula of $C_{24}H_{16}O_5S_2$ (required 448.0439).

Section 3.8: Synthesis of 5-hydroxy-7-methyl-2-(4′-methylnaphthalen-1′-yl)-1,4-naphthoquinone 3.37

The first step is the synthesis of 5-methoxy-7-methyl-2-(4′-methylnaphthalen-1′-yl)-1,4-naphthoquinone **3.39**, which involved Suzuki coupling[64, 65] as illustrated in Scheme **3.42**.

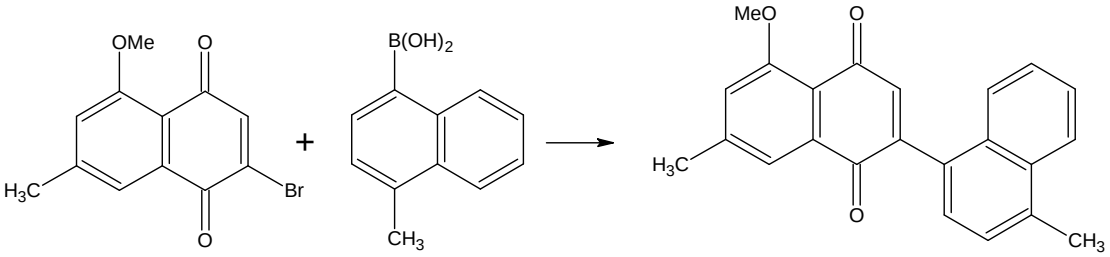

3.13 **3.38** **3.39**

Scheme 3.42

A mixture of **3.13** and $Pd(PPh_3)_4$ in benzene was treated with an aqueous solution of sodium carbonate and 4-methylnaphthalene-1-boronic acid **3.38** in benzene at 24˚C and heated under reflux for 16h to afford a 90% yield of the quinone **3.39**. The resulting material was assigned the structure **3.39** based on the following spectral evidence. In the ^1H nmr spectrum, singlets at 2.51 and 2.74ppm were assigned to 7-CH_3 and 4´-CH_3 while the 5-OMe signal appeared at 4.04ppm. In the ^{13}C nmr spectrum, signals at 159.8, 184.3 and 185.0ppm were assigned to C-5, C-1 and C-4. A HRMS of 342.1272 supported the molecular formula of $C_{23}H_{18}O_3$ (required 342.1255).

Demethylation of the **3.39** by the method reported by Kesteleyn *et al.*,[74] was then effected to produce the naphthol **3.37** as shown in Scheme **3.43**.

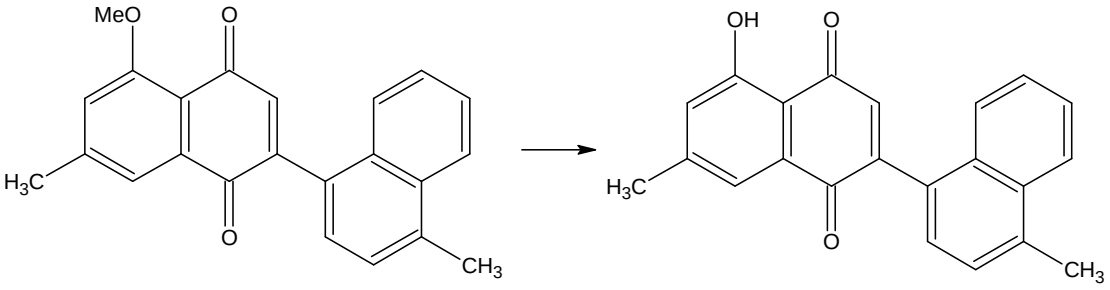

3.39 **3.37**

Scheme 3.43

A solution of **3.39** in dry DCM was treated with borontribromide to afford a 45% yield of the quinone **3.37**. The resulting material was assigned the structure **3.37** based on the following spectral evidence. In the ir spectrum, a broad signal at 3433 cm^{-1} was assigned to the 5-OH group. In the ^{1}H nmr spectrum, the peaks for the two aryl methyl groups appeared at 2.58 and 2.76ppm and a 1-proton singlet at 12.01ppm was assigned to 5-OH. A HRMS of 328.0170 supported the molecular formula of $C_{22}H_{16}O_3$ (required 328.1099).

Section 3.9: Synthesis of 2-(2´-naphthyl)- 5-hydroxy-7-methyl-1,4-naphthoquinone 3.40

The next compound synthesized was quinone **3.40**, which had only one hydroxyl group on the naphthoquinone half of the molecule. Again Suzuki coupling[64, 65] was employed for this purpose as shown in Scheme **3.44**.

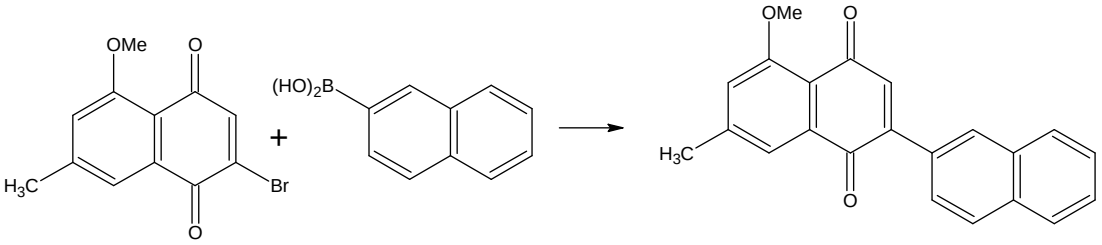

3.13 **3.41** **3.42**

Scheme 3.44

A mixture of **3.13** and $Pd(PPh_3)_4$ in benzene was treated with an aqueous solution of sodium carbonate and 2-naphthaleneboronic acid **3.41** in benzene at 24˚C and heated under reflux for 16h to afford an 88% yield of the quinone **3.42**. The resulting material was assigned the structure **3.42** based on the following spectral evidence. In the ^1H nmr spectrum, a signal at 4.03ppm was assigned to the C-5 methoxy group while a 1-proton singlet at 7.09ppm was assigned to H-3. A 2-proton multiplet at 7.54ppm was assigned to H-6´ and H-7´. A HRMS of 328.1181 supported the molecular formula of $C_{22}H_{16}O_3$ (required 328.1099).

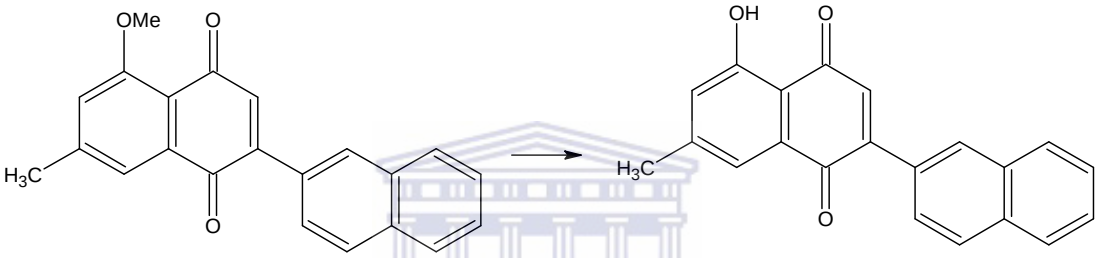

3.42 **3.40**

Scheme 3.45

Demethylation[74] was effected by treatment of a solution of **3.42** in dry DCM with borontribromide to afford a 37% yield of the quinone **3.40** (Scheme **3.45**). The resulting material was assigned the structure **3.40** based on the following spectral evidence. In the ir spectrum, a signal at 3340 cm^{-1} was assigned to the 5-OH group. In the ^1H nmr spectrum, the peak for the methoxy group was absent while a 1-proton singlet at 7.15ppm was assigned to H-3. A HRMS of 314.0898 supported the molecular formula of $C_{21}H_{14}O_3$ (required 314.0943).

Section 3.10: Synthesis of 2-(naphthalen-2′-yl)-7-methyl-1,4-naphthoquinone 3.43

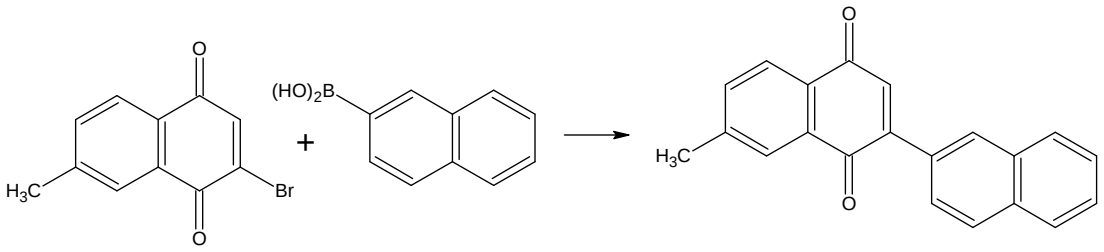

3.2 **3.41** **3.43**

Scheme 3.46

A mixture of **3.2** and $Pd(PPh_3)_4$ in benzene was treated with an aqueous solution of sodium carbonate and 2-naphthaleneboronic acid **3.41** in benzene at 24˚C and heated under reflux for 16h to afford an 86% yield of the quinone **3.43** (Scheme **3.46**). The resulting material was assigned the structure **3.43** based on the following spectral evidence. In the ^1H nmr spectrum, a signal at 2.53ppm was assigned to the C-7 methyl group and a 1-proton singlet at 7.16ppm was assigned to H-3. A HRMS of 298.1030 supported the molecular formula of $C_{21}H_{14}O_2$ (required 298.0993).

Section 3.11: Synthesis of 2-(4-methylnaphthalen-1′-yl)-7-methyl-1,4-naphthoquinone 3.44

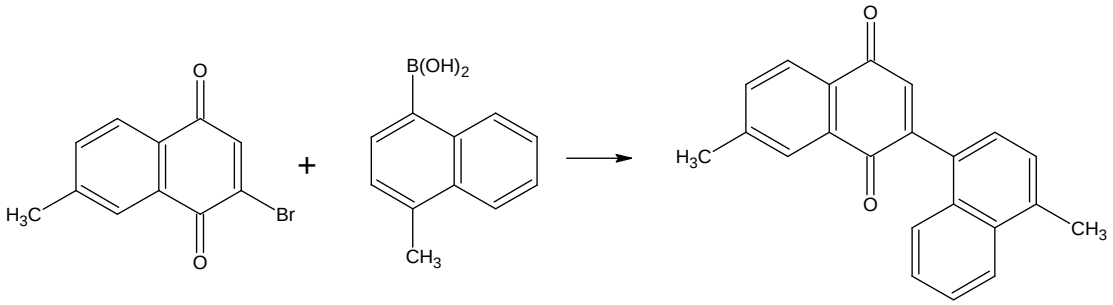

3.2 **3.38** **3.44**

Scheme 3.47

A mixture of **3.2** and $Pd(PPh_3)_4$ in benzene was treated with an aqueous solution of sodium carbonate and 4-methyl-1-naphthaleneboronic acid **3.38** in benzene at 24˚C and heated under reflux for 16h to afford a 90% yield of the quinone **3.44** as shown in Scheme **3.47**. The resulting material was assigned the structure **3.44** based on the following spectral evidence. In the ^1H nmr spectrum, the signals at 2.53ppm and 2.76ppm were assigned to CH_3-7 and CH_3-4′ and a 1-proton singlet at 7.07ppm was assigned to H-3. A HRMS of 312.1139 supported the molecular formula of $C_{22}H_{16}O_2$ (required 312.1150).

Section 3.12: Synthesis of 2-(naphthalen-2′-yl)-5-acetoxy-1,4-naphthoquinone 3.45

The two retrosynthons in Scheme **3.48** for the target quinone **3.45** are bromoquinone **3.46** and boronic acid **3.41**, which is commercially available.

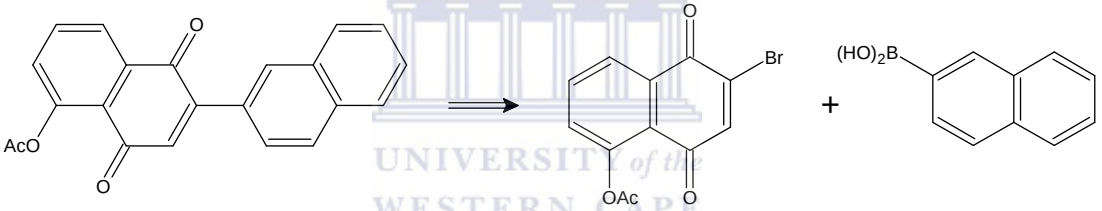

3.45 **3.46** **3.41**

Scheme 3.48

Section 3.12.1: Synthesis of 5-acetoxy-2-bromo-1,4-naphthoquinone 3.46

The proposed synthetic protocol of the target naphthoquinone **3.46** is illustrated in Scheme **3.49** below.

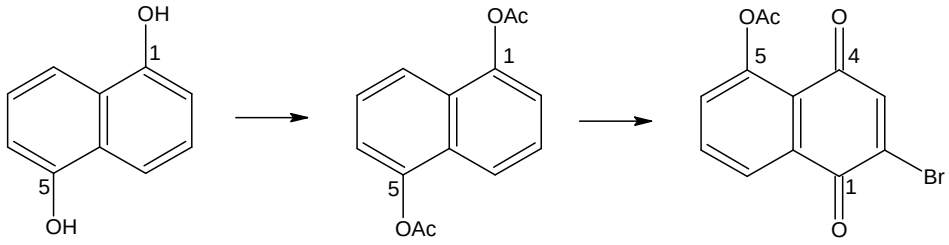

3.47 **3.48** **3.46**

Scheme 3.49

The first step was the synthesis of 1,5-diacetoxynaphthalene **3.48** as shown in Scheme **3.50**.

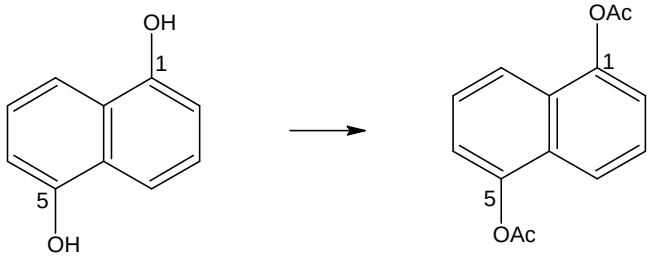

3.47 **3.48**

Scheme 3.50

1,5-Naphthalenediol **3.47** was treated with pyridine and acetic anhydride to afford 97% yield of the diacetate product **3.48** with m.p. 158-160˚C (from benzene). (Lit. m.p. 161˚C)[69]. In the ^{1}H nmr spectrum, a 6-proton singlet at 2.47ppm was assigned to the $–CO_2CH_3$ groups and the a 2-proton dd at 7.29ppm with *J* 7.2 and 1.2 was assigned to H-2 and H-6. In the ^{13}C nmr spectrum, the signal at 21.0ppm was assigned to the acetate $-CH_3$ groups. The signals at 146.7 and 169.2ppm were assigned to (C-1 and C-5) and (2 x C=O).

Next step was the oxidative bromination of the **3.48** by the method reported by Jung et al.[69] as shown in Scheme **3.51**.

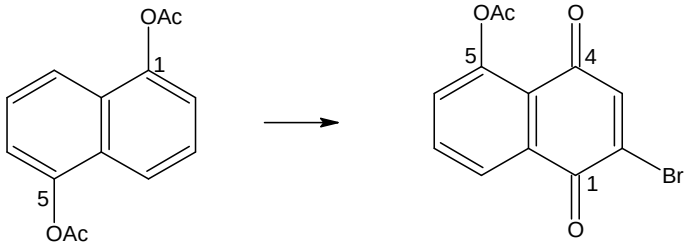

3.48 **3.46**

Scheme 3.51

A solution of 1,5-diacetoxynaphthalene **3.48** in warm acetic acid was treated with a solution of N-bromosuccinimide in acetic acid and water to afford 92% yield of the 5-acetoxy-2-bromo-1,4-naphthoquinone **3.46** with m.p. 156-157°C (Lit. m.p. 158˚C).[69] In the ^{1}H nmr spectrum, the signals at 2.44 and 7.39ppm were assigned to the $–CO_2CH_3$ group and H-3. In

the ^{13}C nmr spectrum, the signals at 169.2, 177.4 and 180.9ppm were assigned to [C=O (ester)], C-1 and C-4.

Section 3.12.2: Coupled product 3.45

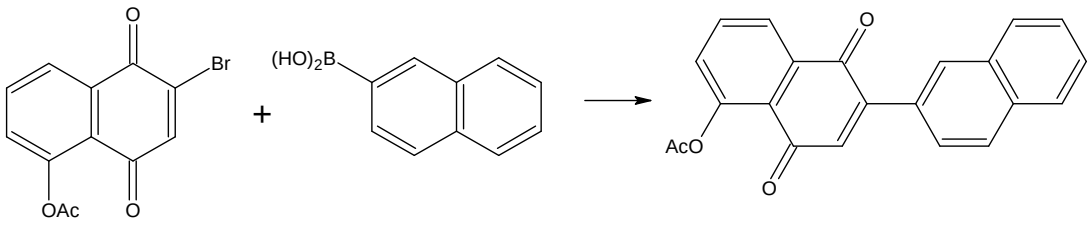

3.46 **3.41** **3.45**

Scheme 3.52

A mixture of **3.46** and $Pd(PPh_3)_4$ in benzene was treated with an aqueous solution of sodium carbonate and 2-naphthaleneboronic acid **3.41** in benzene at 24˚C and heated under reflux for 16h to afford 79% yield of the quinone **3.45** as shown in Scheme **3.52**. The resulting material was assigned the structure **3.45** based on the following spectral evidence. In the ^{1}H nmr spectrum, a 3-proton singlet at 2.49ppm was assigned to $–OCOCH_3$ group and a 3-proton multiplet at 7.58ppm was assigned to H-3´, H-6´ and H-7´. In the ^{13}C nmr spectrum, the signals at 169.4, 183.7 and 183.8 were assigned to (ester, C=O), C-1 and C-4. A HRMS of 342.0890 supported the molecular formula of $C_{22}H_{14}O_4$ (required 342.0892).

Section 3.13: Synthesis of 2-(4-methylnaphthalen-1′-yl)-5-acetoxy-1,4-naphthoquinone 3.49

Synthesis of quinone **3.49** involved the coupling[64, 65] of bromoquinone **3.46** and boronic acid **3.38** via the Suzuki protocol to afford the biaryl quinone **3.49** in 77% yield as shown in Scheme **3.53**.

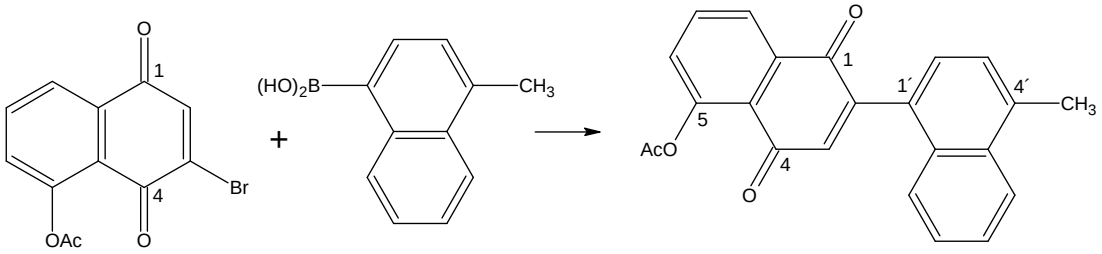

3.46 **3.38** **3.49**

Scheme 3.53

In the ^{1}H nmr spectrum of **3.49**, 3-proton signals at 2.49 and 2.75ppm were assigned to the ester-CH_3 and 4´-CH_3. A 2-proton multiplet at 7.35ppm was assigned to H-2´ and H-3´ and a 2-proton multiplet at 7.54ppm was assigned to H-6´ and H-7´. In the ^{13}C nmr spectrum, the signals at 19.6 and 21.1ppm were assigned to 4´- CH_3 and the ester-CH_3. The signals at 169.5, 183.7 were assigned to (ester, C=O) and (C-1 and C-4). A HRMS of 356.1049 supported the molecular formula of $C_{23}H_{16}O_4$ (required 356.1048).

Conclusion: The synthesis of two binaphthoquinone compounds viz., **3.1** and **3.12** has been achieved. The latter molecule has been synthesized by keeping in mind that the dimethyl ether derivative **1.27** of diospyrin was biologically more active than diospyrin **1.22** itself.[59] The synthesis of two further naphthoquinone-benzoquinone biaryl compounds viz., **3.21** and **3.25** has also been achieved. These quinones viz., **3.21** and **3.25** differ only by the C-5 hydroxyl

group and any enhanced biological activity of **3.25** as compared to **3.21** will thus be attributed to the hydroxyl group at C-5 position.

The synthesis of several naphthoquinone-naphthalene biaryl systems with different substituent groups has also been achieved. Evaluations of these molecules as antimycobacterial and anticancer agents would certainly assist in deducing the structure-activity relationship and thus determine future target molecules for synthesis.

Chapter 4: Experimental

Section 4.1: General

Nuclear magnetic resonance spectra were recorded using a Varian 200 MHz spectrometer. All spectra were recorded at 20°C in deuterocholoroform ($CDCl_3$) and *J* values are given in Hz. In the ^{1}H and ^{13}C spectra, assignments of signals with the same superscript are interchangeable. Mass spectra were recorded on a Finnigan-Matt Ion Trap Detector spectrometer at 70 eV with automatic gain control. High-resolution mass spectra were recorded on a modified AEI-902 High Resolution Mass Spectrometer at the University of the Witwatersrand, Johannesburg. Infrared spectra were recorded as Nujol mulls on a Perkin Elmer 1000PC Fourier Transform spectrometer. Melting points are uncorrected and were recorded on Fisher-Johns Melting Point Apparatus.

Column chromatography was carried out using Merck Kieselgel 60 (70-230 mesh) as dry columns. Preadsorption was carried out on Merck kieselgel 60 (35-70 mesh). Preparative layer chromatography was performed on glass plate coated with silica gel with UV254 as a 1.0 mm thick layer, while thin layer chromatography was carried out on aluminium plates coated with Merck Kieselgel 60 F_{254}. The residue obtained upon workup refers to material obtained from the dried (magnesium sulphate) organic extract after filtration and solvent removal. Hexane refers to the fraction of boiling point 68°C -72°C. All solvents were purified by distillation and, if necessary, were dried according to standard methods.

2-Bromo-7-methyl-5,5,8,8-tetrahydro-1,4-naphthoquinone 3.6

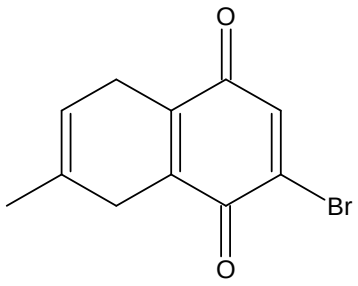

3.6

To a solution of 2,5-dibromo-1,4-benzoquinone **3.5** (2.68 g, 10.0 mmol) in 20 ml of THF at 24°C under nitrogen was added a solution of isoprene **3.4** (0.68 g, 10.0 mmol) in 10 ml of THF drop-wise over 15 minutes. The resulting solution was heated under reflux for 8h and then cooled down to 24°C. The residue obtained upon workup was chromatographed using EtOAc:hexane (1:19) to afford quinone **3.6** (1.64 g, 64%) as bluish black needles, m.p. 73-75°C (from ethanol). υ_{max} 1660 (m, C=O), 1651 (m, C=O), 1601 (w, Ar) and 1585 cm^{-1} (w, Ar); δ_H 1.77 (3H, s, CH_3-7), 3.05 (4H, m, H-5 and H-8), 5.48 (1H, m, H-6) and 7.24 (1H, s, H-3). δ_C 22.9 (CH_3), 25.3 (C-5)[a], 29.5 (C-8)[a], 116.6 (C-6), 130.2 (C-2)[b], 137.2 (C-7)[b], 137.9 (C-3), 139.4 (C-4a)[c], 140.2 (C-8a)[c], 179.3 (C-1)[d], 184.5 (C-4)[d]. (HRMS: Found M^+ 251.9787; C, 52.4 ; H, 3.5. Calc. for $C_{11}H_9BrO_2$: M 251.9785; C, 52.2; H, 3.6%).

2-Bromo-7-methyl-1,4-naphthoquinone 3.2

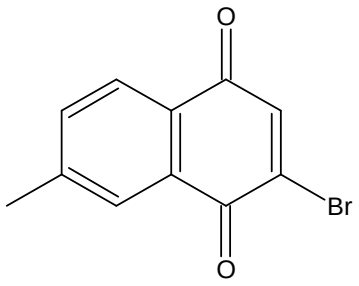

3.2

A mixture of 2-bromo-7-methyl-5,5,8,8-tetrahydro-1,4-naphthoquinone **3.6** (1.82 g, 7.1 mmol), chloranil (1.74 g, 7.1 mmol) and 30 ml of benzene was heated under reflux for 30h. The residue obtained upon workup was chromatographed using EtOAc:hexane (1:19) to afford quinone **3.2** (1.35 g, 75%) as yellow needles, m.p. 124 - 126°C (from ethanol). υ_{max} 1674 (s, C=O), 1650 (s, C=O), 1597 (m, Ar) and 1587 cm^{-1} (m, Ar); δ_H 2.51 (3H, s, CH_3-7), 7.49 (1H, s, H-3), 7.57 (1H, dd, *J* 8.0 and 1.2, H-6), 7.96 (1H, d, *J* 1.2, H-8) and 7.98 (1H, d, *J* 8.0, H-5). δ_C 21.9 (CH_3), 127.2 (C-3)[a], 128.3 (C-6)[a], 129.7 (C-2)[b], 131.0 (C-7)[b], 135.2 (C-5)[c], 139.9 (C-4a)[d], 140.5 (C-8)[c], 145.6 (C-8a)[d], 179.0 (C-1)[e] and 182.4 (C-4)[e]. (HRMS: Found M^+ 251.9631; C, 52.7; H, 2.6. Calc. for $C_{11}H_7BrO_2$: M 251.9629; C, 52.6; H, 2.8%).

2-Bromo-7-methyl-1,4-naphthalenediol 3.9

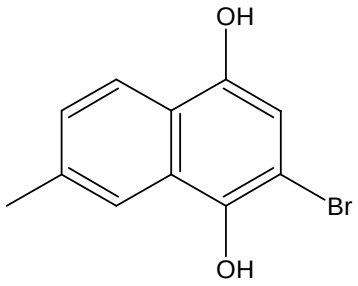

3.9

To a stirred suspension of 2-bromo-7-methyl-1,4-naphthoquinone **3.2** (1 g, 3.98 mmol) in 40 ml of ethanol at 50°C was added a solution of tin(II) chloride (3.1 g, 13.9 mmol) in concentrated HCl (5 ml). After stirring for 45 min at the same temperature, the reaction mixture was poured into cold water (150 ml), and the solid material was filtered and washed with water to afford the product **3.9** (0.77g, 77%) as white needles, m.p. ~115°C (decomp, from benzene). υ_{max} 3297 (m, -OH) and 1595 cm^{-1} (m, Ar); δ_H 2.54 (3H, s, CH_3-7), 5.56 (1H, s, -OH), 6.81 (1H, s, H-3), 7.36 (1H, dd, *J* 8.5 and 1.6, H-6), 7.95 (1H, d, *J* 1.6, H-8) and 7.97 (1H, d, *J* 8.5, H-5). δ_H [d_6-acetone] 2.50 (3H, s, CH_3-7), 6.92 (1H, s, H-3), 7.36 (1H, dd, *J* 8.4 and 1.6, H-6), 7.77 (1H, s, 1-OH)[a], 7.98 (1H, d, *J* 1.6, H-8), 8.07 (1H, d, *J* 8.4, H-5) and 8.83 (1H, s, 4-OH)[a]. δ_C [d_6-acetone] 12.9 (CH_3), 95.4 (C-2), 101.8 (C-3)[a], 113.0 (C-6)[a], 114.2 (C-5)[a], 115.4 (C-4a)[b], 118.4 (C-8a)[b], 119.3 (C-8)[a], 128.0 (C-7)[b], 133.8 (C-1)[c] and 138.9 (C-4)[c]. (HRMS: Found M^+ 251.9782; C, 52.4 ; H, 3.3. Calc. for $C_{11}H_9BrO_2$: M 251.9785; C, 52.2; H, 3.6%).

2-Bromo-1,4-dimethoxy-7-methylnaphthalene 3.10

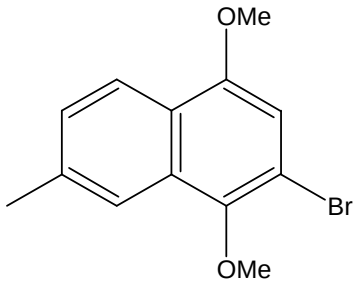

3.10

To a solution of 2-bromo-7-methyl-1,4-naphthalenediol **3.9** (0.73 g, 2.89 mmol) in dry acetone (20 ml) was added anhydrous potassium carbonate (4.79 g, 34.68 mmol). Dimethylsulphate (1.82 g, 1.36 ml, 14.40 mmol) was then added in one portion and the mixture was heated and vigorously stirred under reflux for 20h. It was then cooled down to 25°C, filtered and the filtrate was concentrated under reduced pressure. The residue was dissolved in 50 ml of ether, and triethylamine (1.46 g, 2.0 ml, 14.40 mmol) was added. After being stirred for 20 min at 25°C, the solution was washed with 1M HCl (2 X 20 ml) and water (1 X 25 ml). The residue obtained upon workup was chromatographed using EtOAc:hexane (1:5) to afford the product **3.10** (0.62g, 77 %) as colourless needles, m.p. 73-74°C (form ethanol). υ_{max} 1626 (w, Ar) and 1587 cm^{-1} (m, Ar); δ_H 2.54 (3H, s, CH_3-7), 3.94 (3H, s, OMe), 3.96 (3H, s, OMe), 6.81 (1H, s, H-3), 7.33 (1H, dd, *J* 8.4 and 1.6, H-6), 7.81 (1H, d, *J* 1.6, H-8) and 8.09 (1H, d, *J* 8.4, H-5). δ_C 22.0 (CH_3), 55.9 (OMe), 61.4 (OMe), 107.3 (C-3), 112.1 (C-2)[a], 121.0 (C-6)[b], 122.6 (C-5)[b], 124.1 (C- 4a)[a], 128.0 (C- 8)[b], 129.3 (C-8a)[a], 137.4 (C- 7)[a], 150.6 (C-1)[c] and 152.4 (C-4)[c]. (HRMS: Found M^+ 280.0099; C, 55.7 ; H, 4.6. Calc. for $C_{13}H_{13}BrO_2$: M 280.0098; C, 55.5; H, 4.7%).

1,4-dimethoxy-7-methylnaphthalene-2-boronic acid 3.3

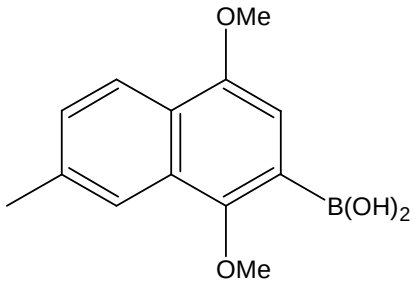

3.3

n-Butyllithium (1.67 ml, 1.28M, 2.14 mmol, 1.2 mol equiv) was added drop-wise to a stirring solution of 2-bromo-1,4-dimethoxy-7-methylnaphthalene **3.10** (500 mg, 1.78 mmol) in dry THF (10 ml) at -78˚C. The reaction was stirred at this temperature under N_2 for 15 min, during which time the mixture colour went from colourless to lime green. Trimethyl borate (1.0 ml, 0.92 g, 8.90 mmol, 5.0 mol equiv) was then added drop-wise causing the reaction mixture to become clear again. The reaction mixture was stirred at -78˚C for a further 30 min and then allowed to warm to 24˚C over 20h. The reaction mixture was then cooled to 0˚C and aqueous HCl (5% v/v) was added until the pH was approximately 6. The aqueous phase was extracted with DCM (3×30 ml) to afford the product **3.3** (308 mg, 70%) that was used immediately in the further reaction. δ_H 2.52 (3H, s, CH_3-7), 3.55 (3H, s, OMe), 3.81 (3H, s, OMe), 5.58 (2H, s, $B(OH)_2$), 6.57 (1H, s, H-3), 7.57 (1H, dd, *J* 8.0 and 1.2, H-6), 7.97 (1H, d, *J* 1.2, H-8) and 8.02 (1H, d, *J* 8.0, H-5).

Palladium-tetrakis(triphenylphosphine) 3.50

Into a dry 200 ml Schlenk tube containing argon was placed DMSO (120-130 ml) and the solvent was degassed at least five times by a sequence of vacuum – argon replenishment. To the solvent was added $PdCl_2$ (1.77 g, 9.98 mmol) followed by triphenylphosphine (13.1 g, 49.9 mmol). The solution was once again degassed several times and the stopper on the Schlenk tube was replaced by a new septum. The slurry was then heated and at about 150°C the $PdCl_2$ was completely solubilised however some PPh_3 remained undissolved. Dissolution of all components occurred at about 170°C thus producing a homogenous orange solution. The solution was removed from the oil bath and without delay hydrazine hydrate (2.0 g, 40 mmol) was added by means of a syringe via the septum. Vigorous effervescence of the reaction mixture occurred during the addition and the solution immediately darkened in colour.

Whilst stirring, the solution was allowed to cool without external cooling and eventually $Pd(PPh_3)_4$ precipitated as bright yellow crystals. The solution was allowed to cool to room temperature and then rapidly filtered (under argon). The filtrate was washed twice with cold ethanol (2 x 20 ml, degassed), then washed twice with cold ether (2 x 20 ml, degassed) and dried overnight in a sintered glass funnel by passing a stream of dry nitrogen gas through the solid to afford the product **3.50** (10.40 g, 90%) as bright yellow solid.

2-(1´,4´-Dimethoxy-7-methylnaphthalen-2´-yl)-7-methyl-1,4-naphthoquinone 3.11

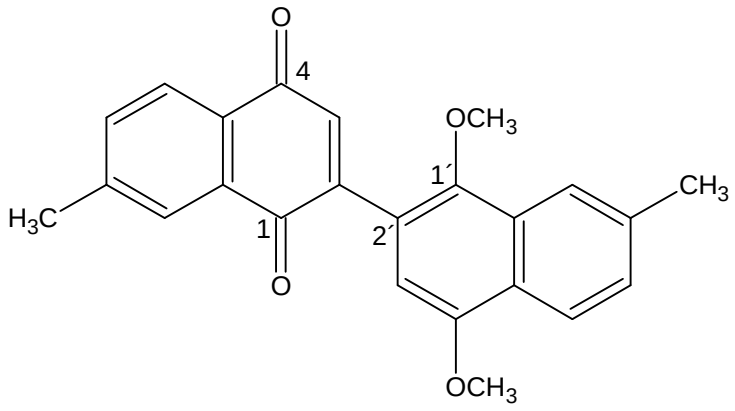

3.11

A mixture of 2-bromo-7-methyl-1,4-naphthoquinone **3.2** (314 mg, 1.25 mmol) and $Pd(PPh_3)_4$ (150 mg, 0.13 mmol) in benzene (20 ml) was stirred for 0.5h at 24˚C under nitrogen. An aqueous solution of sodium carbonate (2M, 1.0 ml) and boronic acid **3.3** (307 mg, 1.25 mmol) in benzene (20 ml) were added successively. The mixture was heated under reflux for 16h with vigorous stirring. The resulting mixture was extracted with DCM. The residue obtained upon workup was chromatographed using EtOAc:hexane (3:7) to afford quinone **3.11** (190mg, 41%) as red crystals. m.p. 141-143°C (from EtOAc/Hexane). υ_{max} 1664 (s, C=O), 1657 (m, C=O) and 1597 cm^{-1} (m, Ar); δ_H 2.53 (3H, s, CH_3-7´), 2.55 (3H, s, CH_3-7), 3.74 (3H, s, OMe), 3.97 (3H, s, OMe), 6.56 (1H, s, H-3´), 7.17 (1H, s, H-3), 7.38 (1H, dd, *J* 8.4 and 1.4, H-6´), 7.59 (1H, dd, *J* 7.6 and 1.0, H-6), 7.87 (1H, d, *J* 1.4, H-8´) 8.00 (1H, d, *J* 1.0, H-8), 8.05 (1H, d, *J* 7.6, H-5) and 8.16 (1H, d, *J* 8.4, H-5´). δ_C 21.9 (CH_3), 22.0 (CH_3), 55.7 (OMe), 62.4 (OMe), 104.0 (C-3´), 108.8 (C-2´), 118.0 (C-2), 121.5 (C-6)[a], 122.4 (C-6´)[a], 126.3 (C-5´)[b], 127.4 (C-8´)[b], 128.7 (C-3)[b], 130.0 (C-7´)[c], 130.3 (C-4a´)[c],132.5 (C-8a´)[c], 134.5 (C-5)[d], 136.8 (C-7)[d], 137.5 (C-8)[d], 145.0 (C-1´)[e], 147.7 (C-4a)[e], 147.9 (C-8a)[e], 151.7 (C-4´)[e], 184.4 (C-1)[f] and 185.1 (C-4)[f]. (HRMS: Found M^+ 372.1299; C, 77.7; H, 5.2. Calc. for $C_{24}H_{20}O_4$: M 372.1361; C, 77.4; H, 5.4%).

2,2´-Bis(7-methyl-1,4-naphthoquinone) 3.1

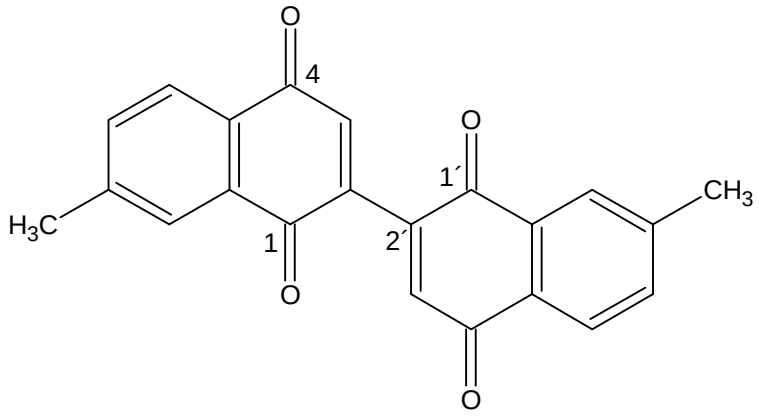

3.1

A suspension of 2-(1´,4´-dimethoxy-7-methylnaphthalen-2´-yl)-7-methyl-1,4-naphthoquinone **3.11** (200 mg, 0.54 mmol) in a mixture of acetonitrile (18 ml) and water (8 ml) was cooled to 0˚C. Over the course of 10 min a cooled solution of cerium(IV) ammonium nitrate (1.10 g, 2.0 mmol) in a mixture of acetonitrile (12 ml) and water (12 ml) was added to the suspension. The reaction mixture was stirred for 20 min and allowed to warm to 24˚C over 30 min. The mixture was diluted with water and extracted with DCM. The residue obtained upon workup was chromatographed using EtOAc:hexane (2:3) to afford quinone **3.1** (30mg, 15%) as yellow crystals. m.p. 179-181°C (from ethanol). υ_{max} 1668 (s, C=O), 1657 (s, C=O) and 1599 (m, Ar) and 1587 cm^{-1} (m, Ar); δ_H 2.52 (3H, s, CH_3-7´)[a], 2.54 (3H, s, CH_3-7)[a], 6.93(1H, s, H-3´)[b], 7.26 (1H, s, H-3)[b], 7.60 (2H, dd, *J* 8.2 and 2.0, H-6´ and H-6), 7.93 (1H, d, *J* 2.0, H-8/8´), 8.01 (1H, d, *J* 8.2, H-5´/5) 8.03 (1H, d, *J* 2.0, H-8/8´) and 8.05 (1H, d, *J* 8.2, H-5/5´). δ_C 21.9 (CH_3), 29.7 (CH_3), 126.7 (C-3´)[a], 127.4 (C-3)[a], 127.6 (C-6´)[a], 128.2 (C-6)[a], 129.2 (C-2´)[b], 129.8 (C-2)[b], 131.0 (C-7´)[c], 131.7 (C-7)[c], 135.0 (C-5´)[d], 135.4 (C-5)[d],137.8 (C-4a´)[e], 138.1 (C-8a´)[e], 140.0 (C-4a)[e], 144.3 (C-8a)[e], 145.5 (C-8´)[f], 145.8 (C-8)[f], 177.3 (C-1´)[g], 180.0 (C-4´)[g], 182.0 (C-1)[g] and

183.8 (C-4)[g]. (HRMS: Found M^+ ; C, 77.1; H, 4.3. Calc. for $C_{22}H_{14}O_4$: M 342.0892; C, 77.2; H, 4.1%).

1-Methoxy-3-methyl-1-trimethylsilyloxy-1,3-butadiene 3.15

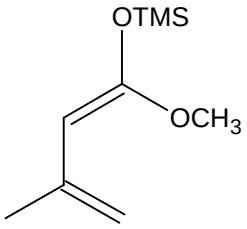

3.15

Methyl-3-methyl-2-butenoate **3.17** (2.85 g, 25 mmol) in THF (10 ml) was added drop-wise over 30 min to a solution of lithiumdiisopropylamide at -78˚C, prepared by addition of a hexane solution of n-butyllithium (18.3 ml, 1.5M, 27.5 mmol) to diisopropylamine (2.5 g, 25 mmol) in THF (60 ml). The mixture was stirred for 0.5h at the same temperature, after which trimethylsilyl chloride (4.07 g, 4.76 ml, 37.5 mmol) and triethylamine (1 ml) were added. The temperature was allowed to rise to 24˚C, and the reaction mixture was stirred for 2h after which hexane (100 ml) was added. The solution was filtered to remove the precipitated LiCl. The filtrate was concentrated to afford the product **3.15** (3.72 g, 80%) used immediately in the further reaction.

2,5-Dibromo-1,4-benzoquinone 3.5

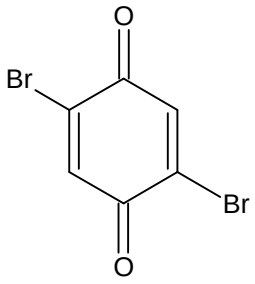

3.5

To a solution of 1,4-dimethoxybenzene **3.7** (10 g, 72.5 mmol) in acetic acid (20 ml) was added drop-wise a solution of bromine (23.15 g, 7.44 ml, 145 mmol) in acetic acid (7 ml) at 24˚C. The reaction mixture was stirred for 2h, then cooled down to 24˚C and filtered to afford 2,5-dibromo-1,4-dimethoxybenzene **3.8** (15.69 g). The filtrate was diluted with water (15 ml) and extracted with DCM, which was washed with a 10% aqueous solution of $NaHCO_3$, dried over $MgSO_4$ and evaporated, yielding an additional amount (2.86 g) of the product **3.8**. The combined fractions (18.55 g, 62.7 mmol) was dissolved in acetonitrile (150 ml) and heated. A solution of cerium (IV) ammonium nitrate (75 g, 136.8 mmol) in 300 ml of water was added drop-wise to the boiling solution of the 2,5-dibromo-1,4-dimethoxybenzene in acetonitrile. The reaction mixture was left to cool down at 24˚C while stirring for 30 min. The solid material was filtered and washed with water to afford quinone **3.5** (15.21g, 82%) as yellow solid, m.p. 159-160˚C (from EtOAc/hexane). (Lit.[66] m.p. 160-161˚C). δ_H 7.48 (2H, s, H-3 and H-6). δ_C 137.2 (C-2 and C-5)[a], 137.9 (C-3 and C-6)[a] and 177.0 (C-1 and C-4).

2-Bromo-5-hydroxy-7-methyl-1,4-naphthoquinone 3.16

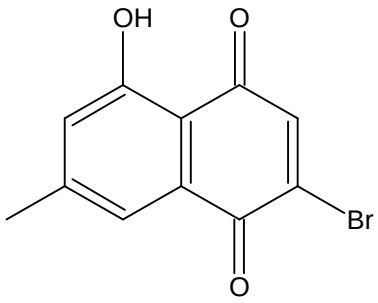

3.16

To a solution of 2,5-dibromo-1,4-benzoquinone **3.5** (3.99 g, 15.0 mmol) in dry THF (30 ml) at 0°C under N_2 was added a solution of 1-methoxy-3-methyl-1-trimethylsilyloxy-1,3-butadiene **3.15** (2.58 g, 15.0 mmol) in dry THF (15 ml) drop-wise over 1h. The resulting solution was stirred at 25˚C for 8h. The residue obtained upon workup was chromatographed using EtOAc:hexane (1:4) to afford the quinone **3.16** (2.31 g, 57%) as an orange red solid, m.p. 131-133˚C (from EtOAc/hexane). (Lit.[41] m.p. 132-133.5˚C). υ_{max} 1672 (s, C=O), 1633 (m, C=O), 1575 (m, Ar) and 1567 cm^{-1} (m, Ar). δ_H 2.43 (3H, s, CH_3-7), 7.08 (1H, d, *J* 1.4, H-6), 7.44(1H, s, H-3), 7.52 (1H, d, *J* 1.4, H-8) and 11.70 (1H, s, 5-OH). δ_C 22.2 (CH_3), 112.7 (C-2)[a], 122.4 (C-3)[b], 124.8 (C-6)[b], 130.5 (C-7)[a], 140.4 (C-8)[b], 140.5 (C-4a)[c], 148.6 (C-8a)[c], 162.0 (C-5), 177.5 (C-1)[d] and 186.9(C-4)[d].

2-Bromo-5-methoxy-7-methyl-1,4-naphthoquinone 3.13

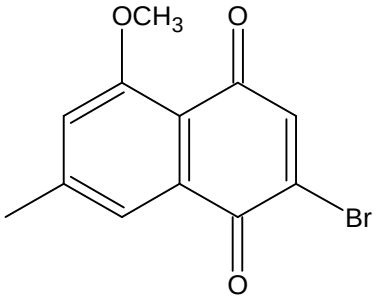

3.13

A mixture of 2-bromo-5-hydroxy-7-methyl-1,4-naphthoquinone **3.16** (2.31 g, 8.64 mmol), powdered Ag_2O (13.91 g, 60.48 mmol) and methyl iodide (6.31 g, 2.68 ml, 43.2 mmol) in benzene (50 ml) was stirred and heated under reflux for 1h. After filtration, the residue obtained upon workup was chromatographed using EtOAc:hexane (1:4) to afford quinone **3.13** (1.36 g, 56%) as yellow solid, m.p. 168-170˚C (form ethanol). (Lit.[69] m.p. 168.5-170˚C). δ_H 2.48 (3H, s, CH_3-7), 3.99 (3H, s, OMe), 7.12 (1H, d, *J* 1.2, H-6), 7.36 (1H, s, H-3) and 7.62 (1H, d, *J* 1.2, H-8). δ_C 22.4 (CH_3), 56.6 (OMe), 119.0 (C-3)[a], 121.6 (C-6)[a], 133.0 (C-2)[b], 136.7 (C-4a)[b], 142.5 (C-8)[a], 146.7 (C-7)[b], 146.8 (C-8a)[b], 160.3 (C-5), 178.6 (C-1)[c] and 181.3 (C-4)[c].

2-Bromo-5- methoxy-7-methyl-1,4-naphthalenediol 3.18

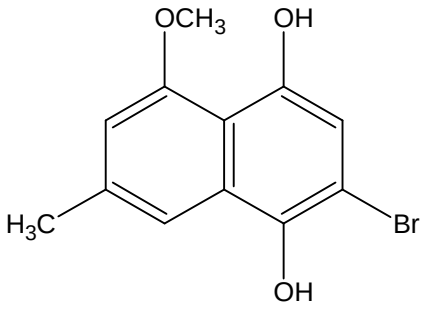

3.18

A suspension of 2-bromo-5-methoxy-7-methyl-1,4-naphthoquinone **3.13** (1.1 g, 3.91 mmol) in dichloromethane (100 ml) was shaken in a separatory funnel with a freshly prepared solution of sodium dithionite (10.2 g, 58.65 mmol) in water (150 ml). After the mixture was shaken (3 x 50 ml), the organic layer was separated, dried over $MgSO_4$ and then concentrated in vacuo to afford the product **3.18** (0.86 g, 78%) as a white solid which is used in the next reaction without purification. δ_H 2.49 (3H, s, CH_3-7), 4.04 (3H, s, OMe), 5.43 (1H, br s, 1-OH)[a], 6.67 (1H, d, *J* 1.2, H-6), 6.84 (1H, s, H-3), 7.58 (1H, d, *J* 1.2, H-8) and 8.91 (1H, s, 4-OH)[a]. δ_C 21.8 (CH_3), 55.8 (OMe), 104.9 (C-2)[a], 107.1 (C-3)[b], 110.6 (C-6)[b], 115.0 (C-8)[b], 126.2 (C-7)[a], 136.2 (C-4a)[c], 140.4 (C-8a)[c], 142.3 (C-5)[c], 147.9 (C-1)[d] and 155.5 (C-4)[d].

2-Bromo-1,4,5-trimethoxy-7-methylnaphthalene 3.19

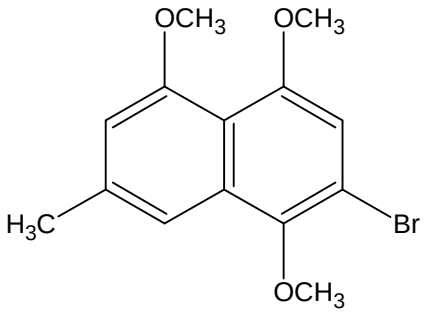

3.19

A mixture of 2-bromo-5-methoxy-7-methyl-1,4-naphthalenediol **3.18** (1.0 g, 3.53 mmol) in dry acetone (50 ml), anhydrous potassium carbonate (5.85 g, 42.40 mmol) and dimethylsulphate (3.55 g, 28.24 mmol) was vigorously stirred and heated under reflux for 20h. The reaction mixture was then cooled to 25°C, filtered and the filtrate was concentrated under reduced pressure. The residue obtained was dissolved in 50 ml of ether and Et_3N (2.86 g, 3.92 ml, 28.24 mmol) was added. After being stirred for 20 min at 24°C, the solution was washed with 1M HCl (2 x 20 ml) and water (1 x 25 ml). The residue obtained upon workup was chromatographed using EtOAc:hexane (1:4) to afford the product **3.19** (0.90 g, 82%) as colourless solid, m.p. 94-96˚C (form EtOAc/hexane). (Lit. m.p. 95-96˚C). δ_H 2.50 (3H, s, CH_3-7), 3.91 (3H, s, OMe), 3.93 (3H, s, OMe), 3.95 (3H, s, OMe), 6.72 (1H, d, *J* 1.2, H-6), 6.83 (1H, s, H-3) and 7.46 (1H, d, *J* 1.2, H-8). δ_C 22.0 (CH_3), 56.3 (OMe), 56.6 (OMe), 60.9 (OMe), 108.9 (C-3)[a], 109.0 (C-6)[a], 112.5 (C-2)[b], 113.7 (C-8)[a], 115.8 (C-7)[b], 131.7 (C-4a)[c], 137.6 (C-8a)[c], 146.2 (C-5), 153.8 (C-1)[d] and 157.3 (C-4)[d].

1,4,5-Trimethoxy-7-methylnaphthalene-2-boronic acid 3.14

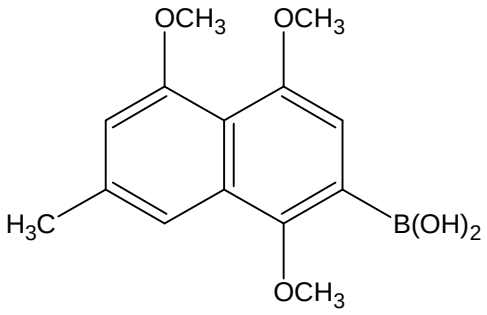

3.14

n-Butyllithium (2.90 ml, 1.32M, 3.88 mmol, 1.1 mol equiv) was added drop-wise to a stirred solution of 2-bromo-1,4,5-trimethoxy-7-methylnaphthalene **3.19** (1.1 g, 3.53 mmol) in dry THF (15 ml) at -78˚C. The reaction was stirred at this temperature under N_2 atmosphere for 15 min during which time the colour of the mixture went from colourless to lime green. Trimethyl borate (2.0 ml, 1.83 g, 17.65 mmol, 5.0 mol equiv) was then added drop-wise causing the reaction mixture to become clear again. The reaction mixture was stirred at -78˚C for a further 30 min and then allowed to warm to 24˚C over 20h. The reaction mixture was the cooled to 0˚C and aqueous HCl (5% v/v) was added until the pH was approximately 6. The aqueous phase was extracted with DCM (3×30 ml) to afford the product **3.14** (0.73 g, 75%) that was immediately used without further purification.

2-(1′,4′,5′-Trimethoxy-7′-methylnaphthalen-2′-yl)-5-methoxy-7-methyl-1,4-naphthoquinone 3.20

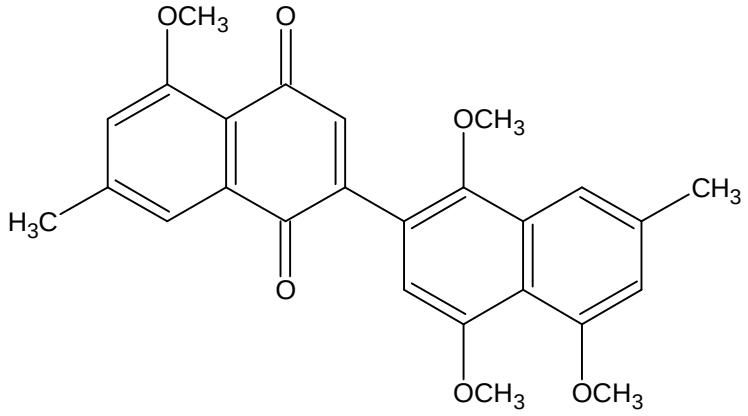

3.20

A mixture of 2-bromo-5-methoxy-7-methylnaphthoquinone **3.13** (800 mg, 2.9 mmol) and $Pd(PPh_3)_4$ (340 mg, 0.30 mmol) in benzene (30 ml) was stirred for 0.5h at 24˚C under nitrogen. An aqueous solution of Na_2CO_3 (2M, 3.0 ml) and boronic acid **3.14** (780 mg, 2.80 mmol) in benzene (20 ml) were added successively. The mixture was heated under reflux for 16h with vigorous stirring. The residue obtained upon workup was chromatographed using EtOAc:hexane (1:1) to afford quinone **3.20** (510 mg, 41%) as reddish brown needles, m. p. 84-86˚C (from EtOAc:hexane). υ_{max} 1668 (m, C=O), 1651 (m, C=O) and 1599 cm^{-1} (m, Ar); δ_H 2.50 (6H, s, CH_3-7′ and CH_3-7), 3.68 (3H, s, OMe), 3.94 (3H, s, OMe), 3.97 (3H, s, OMe), 4.03 (3H, s, OMe), 6.61 (1H, s, H-3′), 6.76 (1H, d, *J* 1.2, H-6′), 7.07 (1H, s, H-3), 7.13 (1H, d, *J* 1.0, H-6), 7.50 (1H, d, *J* 1.0, H-8) and 7.66 (1H, d, *J* 1.2, H-8′). δ_C 22.3 (CH_3), 22.4 (CH_3), 56.6 (OMe), 56.8 (OMe), 57.0 (OMe), 62.1 (OMe), 106.6 (C-3′)[a], 110.1 (C-6′)[a], 114.6 (C-8′)[a], 117.5 (C-2′)[b], 118.0 (C-2)[b], 118.2 (C-3)[a], 120.8 (C-6)[a], 122.8 (C-7′)[c], 131.4 (C-7)[c], 134.7 (C-4a′)[c], 137.2 (C-8a′)[c], 139.6 (C-8)[a], 145.2 (C-4a)[d], 146.4 (C-8a)[d], 147.8 (C-5′)[d], 153.4 (C-1′)[e], 157.4 (C-4′)[e],

159.8 (C-5)[e], 184.3 (C-1)[f] and 184.5 (C-4)[f]. (HRMS: Found M^+ 432.1546; C, 72.1; H, 5.4. Calc. for $C_{26}H_{24}O_6$: M 432.1572; C, 72.2; H, 5.6%).

2,2′-Bis(5-methoxy-7-methyl-1,4-naphthoquinone) 3.12

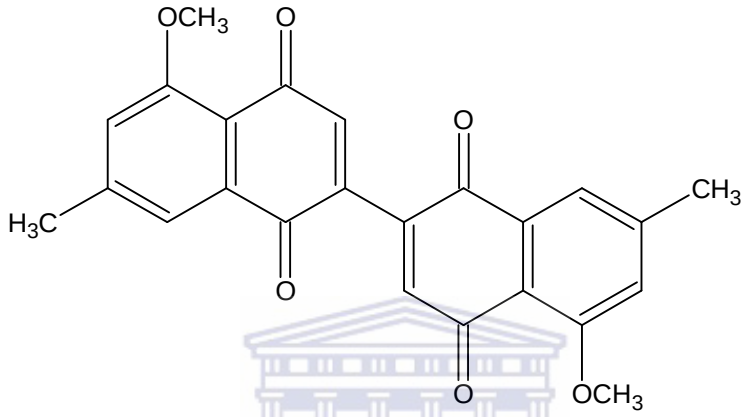

3.12

A suspension of 2-(1′,4′,5′-trimethoxy-7′-methylnaphthalen-2′-yl)-5-methoxy-7-methyl-1,4-naphthoquinone **3.20** (250 mg, 0.58 mmol) in a mixture of acetonitrile (18ml) and water (8 ml) was cooled to 0˚C. Over the course of 20 min a cooled solution of cerium (IV) ammonium nitrate (1.0 g, 1.80 mmol) in a mixture of acetonitrile (10 ml) and water (10 ml) was added to the suspension. The reaction mixture was stirred for 20 min and allowed to warm to 25˚C over 30 min. The mixture was diluted with water and extracted with DCM. The residue obtained upon workup was chromatographed using EtOAc:hexane (1:1) to afford quinone **3.12** (80 mg, 34%) as yellow crystals, m. p. 219˚C (decomp.) (from EtOAc:hexane). υ_{max} 1668 (m, C=O) and 1652 (m, C=O); δ_H 2.49 (6H, s, CH_3-7′ and CH_3-7), 4.02 (6H, s, 2 x OMe), 6.94 (2H, s, H-6′ and H-6), 7.13 (2H, s, H-3′ and H-3), 7.58 (2H, s, H-8′ and H-8). δ_C 22.5 (CH_3-7′ and CH_3-7), 56.6 (2 x

OMe), 118.6 (C-6′ and C-6)[a], 120.8 (C-3′ and C-3)[a], 131.0 (C-2′ and C-2)[b], 135.1 (C-7′ and C-7)[b], 139.8 (C-8′ and C-8), 141.1 (C-4a′ and 4a)[c], 146.9 (C-8a′ and 8a)[c], 160.0 (C-5′ and C-5), 183.2 (C-1′ and C-1)[d] and 183.5 (C-4′ and C-4)[d]. (HRMS: Found M^+ 402.1247; C, 71.4; H, 4.6. Calc. for $C_{24}H_{18}O_6$: M 402.1103; C, 71.6; H, 4.5%).

1,4-Dimethoxybenzene-2-boronic acid 3.22

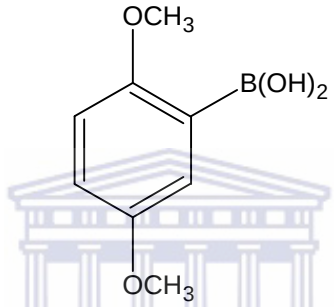

3.22

n-Butyllithium (3.84 ml, 1.32M, 5.06 mmol, 1.1 mol equiv) was added drop-wise to a stirring solution of 2-bromo-1,4-dimethoxybenzene **3.23** (1.0g, 4.60 mmol) in THF (10 ml) at -78˚C. The reaction was stirred at this temperature under N_2 for 10 min, during which the colour of the mixture went from colourless to lime green. Trimethyl borate (2.58 ml, 2.39 g, 23.0 mmol, 5.0 mol equiv) was then added drop-wise by syringe causing the reaction mixture to become clear again. The reaction mixture was stirred at -78˚C for a further 30 min and then allowed to warm to 24˚C over 2h. The reaction mixture was then cooled to 0˚C and aqueous HCl (5% v/v) was added until the pH was approximately 6. The aqueous phase was extracted with DCM (3×30 ml) to afford the product **3.22** (671 mg, 80%) as white crystals, m.p. 86-87°C (from benzene). υ_{max} 3227 (s, -OH) and 1503 cm^{-1} (s, Ar); δ_H 3.81 (3H, s, OMe), 3.88 (3H, s, OMe), 6.38 (2H, br s,

$B(OH)_2$), 6.85 (1H, d, *J* 8.6, H-6), 6.99 (1H, dd, *J* 8.6 and 2.8, H-5) and 7.39 (1H, d, *J* 2.8, H-3). δ_C 55.8 (OMe), 56.1 (OMe), 111.3, 118.7, 120.8 (C-2, C-3, C-5 and C-6), 153.9 (C-1)[a] and 158.9 (C-4)[a]. (HRMS: Found M^+ 182.0755; C, 52.6; H, 6.2. Calc. for $C_8H_{11}BO_4$: M 182.0752; C, 52.8; H, 6.1%).

2-(1´,4´-Dimethoxybenzen-2´-yl)-7-methyl-1,4-naphthoquinone 3.24

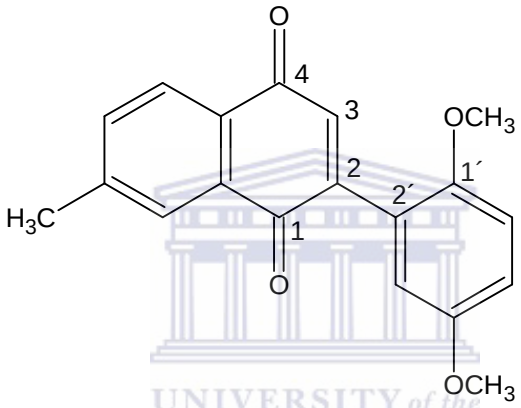

3.24

A mixture of 2-bromo-7-methyl-1,4-naphthoquinone **3.2** (700 mg, 2.80 mmol) and $Pd(PPh_3)_4$ (335 mg, 0.29 mmol) in benzene (30 ml) was stirred for 0.5h at 25˚C under Nitrogen. An aqueous solution of sodium carbonate (2M, 3.0ml) and 1,4-dimethoxybenzene-2-boronic acid **3.22** (500 mg, 2.74 mmol) in benzene (20 ml) were added successively. The mixture was heated under reflux for 16h with vigorous stirring. The resulting cooled mixture was extracted with DCM. The residue obtained upon workup was chromatographed using EtOAc:hexane (1:5) to afford quinone **3.24** (652 mg, 76%) as reddish brown crystals, m.p. 63-64˚C (from ethanol). υ_{max} 1663 (s, C=O), 1655 (m, C=O) and 1599 cm^{-1} (s, Ar); δ_H 2.51 (3H, s, CH_3-7), 3.74 (3H, s, OMe), 3.79 (3H, s, OMe), 6.81 (1H, d, *J* 2.6, H-3´), 6.94 (1H, s, H-3)[a], 6.94 (1H, m, H-6´)[a], 6.97 (1H, m, H-5´)[a],

7.56(1H, dd, *J* 8.2 and 2.0, H-6), 7.94 (1H, d, *J* 2.0, H-8) and 8.01 (1H, d, *J* 8.2, H-5). δ_C 21.8 (CH_3), 55.8 (OMe), 56.4 (OMe), 112.6 (C-3′)[a], 115.9 (C-6′)[a], 116.1 (C-5′)[a], 124.4 (C-2′)[b], 126.2 (C-3)[c], 127.3 (C-6)[c], 130.0 (C-2)[b], 132.5 (C-7)[b], 134.3 (C-8)[c], 136.8 (C-5)[c], 144.8 (C-4a)[d], 147.8 (C-8a)[d], 151.5 (C-1′)[e], 153.5 (C-4′)[e], 183.7 (C-1)[f] and 185.1 (C-4)[f]. (HRMS: Found M^+ 308.1049; C, 74.2; H, 5.3. Calc. for $C_{19}H_{16}O_4$: M 308.1048; C, 74.0; H, 5.5%).

2-(1′,4′-Benzoquinon-2′-yl)-7-methyl-1,4-naphthoquinone 3.21

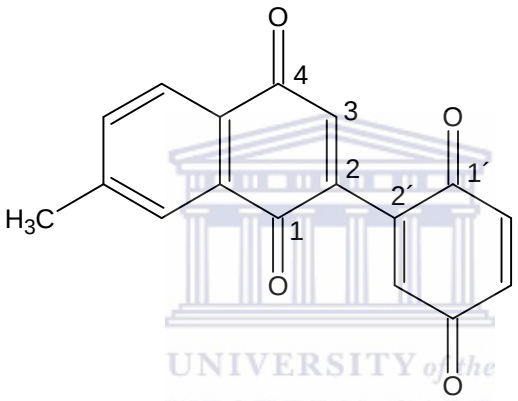

3.21

A suspension of 2-(1′,4′-dimethoxybenzen-2′-yl)-7-methyl-1,4-naphthoquinone **3.24** (450 mg, 1.45 mmol) in a mixture of acetonitrile (40 ml) and water (16 ml) was cooled to 0˚C. Over the course of 20 min, a cooled solution of cerium (IV) ammonium nitrate (2.4 g, 4.37 mmol) in a mixture of acetonitrile (25 ml) and water (25 ml) was added to the suspension. The reaction mixture was stirred for 20 min and allowed to warm to 25˚C over 30 min. The mixture was diluted with water and extracted with DCM (3×30 ml). The residue obtained upon workup was chromatographed using EtOAc:hexane (1:4) to afford quinone **3.21** (290 mg, 71%) as yellow crystals, m.p. 155-157°C (from ethanol). υ_{max} 1668 (s, C=O), 1658 (m, C=O), 1599 (s, Ar) and

1580 cm^{-1} (m, Ar); δ_H 2.52 (3H, s, CH_3-7), 6.89 (3H, br s, H-3′, H-5′ and H-6′), 6.97 (1H, s, H-3), 7.59 (1H, dd, *J* 8.0 and 2.0, H-6), 7.92 (1H, d, *J* 2.0, H-8) and 8.01(1H, d, *J* 8.0, H-5). δ_C 21.9 (CH_3), 126.6 (C-5′)[a], 127.4 (C-6′)[a], 129.8 (C-2′)[b], 131.8 (C-2)[b], 135.0 (C-3′)[c], 135.5 (C-6)[c], 136.6 (C-8)[c], 136.9 (C-5)[c], 138.0 (C-3)[c], 141.3 (C-4a)[d], 142.2 (C-8a)[d], 145.6 (C-7)[d], 182.9 (C-1′)[e], 183.8 (C-4′)[e], 184.6 (C-1)[e] and 186.4 (C-4)[e]. (HRMS: Found M^+ 278.0570; C, 73.2; H, 3.4. Calc. for $C_{17}H_{10}O_4$: M 278.0579; C, 73.3; H, 3.6%).

2-(1′,4′-Dimethoxybenzen-2′-yl)-5-methoxy-7-methyl-1,4-naphthoquinone 3.26

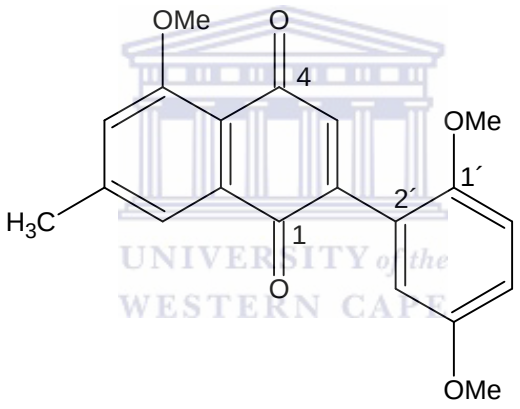

3.26

A mixture of 2-bromo-5-methoxy-7-methyl-1,4-naphthoquinone **3.13** (760 mg, 2.70 mmol) and $Pd(PPh_3)_4$ (320 mg, 0.28 mmol) in benzene (30 ml) was stirred for 0.5h at 24˚C under Nitrogen. An aqueous solution of sodium carbonate (2M, 3.0 ml) and 1,4-dimethoxybenzene boronic acid **3.22** (500 mg, 2.70 mmol) in benzene (20 ml) were added successively. The mixture was heated under reflux for 16h with vigorous stirring. The resulting cooled mixture was extracted with DCM. The residue obtained upon workup was chromatographed using EtOAc:hexane (3:7) to afford quinone **3.26** (290 mg, 32%) as reddish brown crystals, m.p. 147-149˚C (from ethanol).

υ_{max} 1668 (m, C=O), 1649 (s, C=O) and 1603 cm^{-1} (m, Ar); δ_H 2.46 (3H, s, CH_3), 3.71 (3H, s, OMe), 3.77 (3H, s, OMe), 3.98 (3H, s, OMe), 6.79 (1H, dd, *J* 2.4 and 0.6, H-3′), 6.86 (1H, s, H-3), 6.90 (2H, m, H-5′ and H-6′), 7.08 (1H, d, *J* 2.0, H-6) and 7.58 (1H, d, *J* 2.0, H-8). δ_C 22.2 (CH_3), 55.7 (OMe), 56.3 (2 x OMe), 112.5 (C-3′)[a], 115.7 (C-5′)[a], 116.0 (C-6′)[a], 117.7 (C-2′), 117.9 (C-6)[b], 120.4 (C-8)[b], 123.9 (C-2)[c], 134.6 (C-7)[c], 138.8 (C-3)[b], 145.3 (C-4a)[d], 146.1 (C-8a)[d], 151.4 (C-1′)[e], 153.4 (C-4′)[e], 159.5 (C-5)[e], 183.8 (C-1)[f] and 184.2 (C-4)[f]. (HRMS: Found M^+ 338.1143; C, 69.9; H, 5.6. Calc. for $C_{20}H_{18}O_5$: M 338.1154; C, 71.0; H, 5.4%).

2-(1′,4′-Benzoquinon-2′-yl)-5-methoxy-7-methyl-1,4-naphthoquinone 3.27

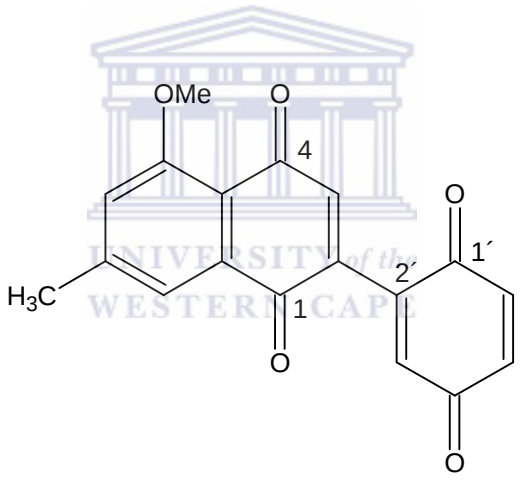

3.27

A suspension of 2-(1′,4′-dimethoxybenzene-2′-yl)-5-methoxy-7-methyl-1,4-naphthoquinone **3.26** (290 mg, 0.86 mmol) in a mixture of acetonitrile (25 ml) and water (10 ml) was cooled to 0˚C. Over the course of 10 min, a cooled solution of cerium (IV) ammonium nitrate (1.44 g, 2.62 mmol) in a mixture of acetonitrile (15 ml) and water (15 ml) was added to the suspension. The reaction mixture was stirred for 20 min and allowed to warm to 25˚C over 30 min. The mixture was diluted with water and extracted with DCM. The residue obtained upon workup was

chromatographed using EtOAc:hexane (2:3) to afford quinone **3.27** (191mg, 72%) as orange crystals, m.p. >300°C (from ethanol). υ_{max} 1667 (m, C=O), 1646 (w, C=O), 1597 (w, Ar) and 1577 cm^{-1} (m, Ar); δ_H [d_6-DMSO] 2.42 (CH_3), 3.90 (OMe), 7.03 (1H, dd, *J* 8.8 and 2.6, H-5′), 7.34 (1H, d, *J* 2.0, H-6), 7.39 (1H, d, *J* 2.6, H-3′), 7.48 (1H, s, H-3), 7.66 (1H, d, *J* 8.8, H-6′) and 9.91 (1H, d, *J* 2.0, H-8). δ_C [d_6-DMSO] 21.7 (CH_3), 56.3 (OMe), 106.3 (C-5′)[a], 113.5 (C-6′)[a], 116.7 (C-2′)[b], 118.3 (C-3′)[a], 119.4 (C-2)[b], 119.8 (C-3)[c], 120.8 (C-7), 122.9 (C-6)[c], 134.9 (C-8), 146.9 (C-4a)[d], 149.5 (C-8a)[d], 154.7 (C-5), 155.8 (C-1′)[e], 160.5 (C-4′)[e], 173.4 (C-1)[f] and 180.8 (C-4)[f]. (HRMS: Found M^+ 308.0611; C, 70.0; H, 4.0. Calc. for $C_{18}H_{12}O_5$: M 308.0684; C, 70.1; H, 3.9%).

2-(1′,4′-Benzoquinon-2′-yl)-5-hydroxy-7-methyl-1,4-naphthoquinone 3.25

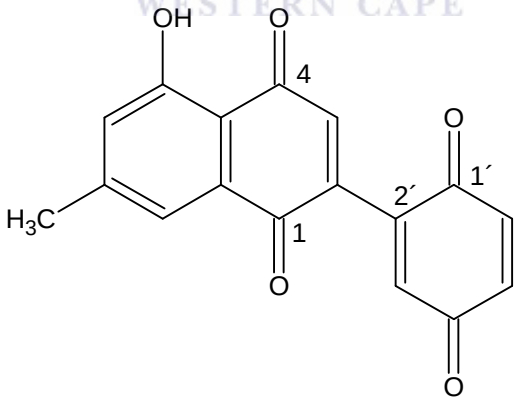

3.25

To a solution of 2-(1′,4′-benzoquinon-2′-yl)-5-methoxy-7-methyl-1,4-naphthoquinone **3.27** (150 mg, 0.49 mmol) in dry CH_2Cl_2 (20 ml) at 25˚C under nitrogen was added aluminum trichloride (2.61 g, 19.6 mmol). The mixture was stirred at 25˚C for 24h, poured into water, then acidified

with dilute HCl, and extracted with DCM. The residue obtained upon workup was chromatographed using EtOAc:hexane (1:5) to afford quinone **3.25** (78mg, 55%) as red crystals, m.p. >300°C (from EtOAc:hexane). υ_{max} 1650 (w, C=O), 1643 (m, C=O) and 1565 cm^{-1} (w, Ar); δ_H [d_6-DMSO] 2.40 (3H, s, CH_3), 7.09 (1H, dd, *J* 9.0 and 2.4, H-5′), 7.15 (1H, d, *J* 2.0, H-6), 7.43 (2H, d, *J* 2.4, H-3′, overlaid by H-3), 7.72 (1H, d, *J* 9.0, H-6′), 9.97 (1H, d, *J* 2.0, H-8) and 11.77 (1H, s, 5-OH). δ_H [d_6-acetone] 2.48 (3H, s, CH_3), 7.16 (1H, s, H-3), 7.22 (1H, dd, *J* 9.2 and 2.4, H-5′), 7.56 (1H, d, *J* 2.2, H-6), 7.62 (1H, d, J 2.4, H-3′), 7.68 (1H, d, *J* 9.2, H-6′), 8.93 (1H, d, *J* 2.2, H-8) and 11.99 (1H, s, 5-OH). δ_C [d_6-DMSO] 21.5 (CH_3), 106.1 (C-5′)[a], 113.0 (C-2′), 113.7 (C-6′)[a], 119.3 (C-3′)[b], 120.4 (C-3)[b], 123.0 (C-6)[c], 123.3 (C-2), 124.0 (C-7)[c], 133.0 (C-8), 148.4 (C-4a)[d], 150.1 (C-8a)[d], 153.5 (C-5), 156.0 (C-1′)[e], 161.4 (C-4′)[e], 178.9 (C-1)[f] and 180.3 (C-4)[f]. (HRMS: Found M^+ 294.0571; C, 69.5; H, 3.6. Calc. for $C_{17}H_{10}O_5$: M 294.0528; C, 69.4; H, 3.4%).

2-(6′-Methoxynaphthalen-2′-yl)-5-methoxy-7-methyl-1,4-naphthoquinone 3.29

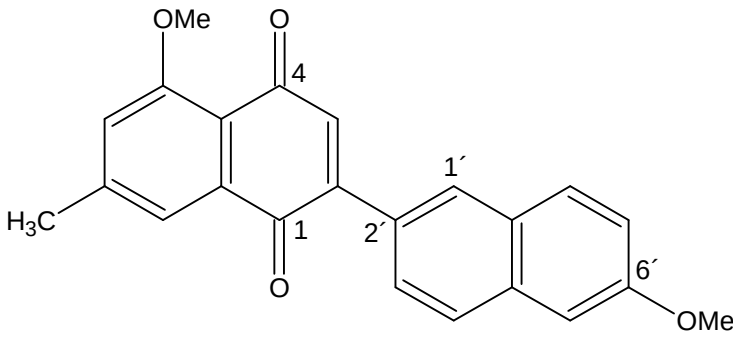

3.29

A mixture of 2-bromo-5-methoxy-7-methyl-1,4-naphthoquinone **3.13** (351 mg, 1.25 mmol) and $Pd(PPh_3)_4$ (130 mg, 0.11 mmol) in benzene (15 ml) was stirred for 0.5h at 24°C under nitrogen.

An aqueous solution of Na_2CO_3 (2M, 1 ml) and 6-methoxynaphthalene-2-boronic acid **3.30** (238 mg, 1.18 mmol) in benzene (10 ml) were added successively. The mixture was heated under reflux for 16h with vigorous stirring. The residue obtained upon workup was chromatographed using EtOAc:hexane (2:3) to afford quinone **3.29** (401 mg, 90%) as orange red needles, m. p. 179-181°C (from ethanol). υ_{max} 1663 (s, C=O), 1645 (m, C=O) and 1604 cm^{-1} (s, Ar); δ_H 2.51 (3H, s, 7- CH_3), 3.95 (3H, s, 6′-OMe)[a], 4.03 (3H, s, 5-OMe)[a], 7.07 (1H, s, H-3), 7.13 (1H, d, *J* 1.2, H-6), 7.18 (2H, m, H-5′- and H-7′)[b], 7.62 (1H, dd, *J* 8.4 and 1.8, H-3′), 7.67(1H, d, *J* 1.2, H-8), 7.80 (2H, m, H-4′ and H-8′)[b] and 8.07 (1H, d, *J* 1.8, H-1′). δ_C 22.5 (7-CH_3), 55.5 (6′-OMe)[a], 56.6 (5-OMe)[a], 105.8 (C-2), 118.3 (C-3)[b], 119.5 (C-6)[b], 120.8 (C-1′)[b], 121.9 (C-2′), 126.9 (C-4′)[c], 127.0 (C-5′)[c], 128.4 (C-4a′)[d], 128.6 (C-8a′)[d], 129.5 (C-7′)[c], 130.4 (C-8′)[c], 135.0 (C-7), 135.3 (C-3′)[c], 137.2 (C-8)[c], 145.6 (C-4a)[e], 146.3 (C-8a)[e], 158.9 (C-6′)[f], 159.7 (C-5)[f], 184.4 (C-1)[g] and 185.3 (C-4)[g]. (HRMS: Found M^+ 358.1049; C, 77.2; H, 5.0. Calc. for $C_{23}H_{18}O_4$: M 358.1204; C, 77.1; H, 5.1%).

5-Hydroxy-2-(6-methoxynaphthalen-2′-yl)-7-methyl-1,4-naphthoquinone 3.31

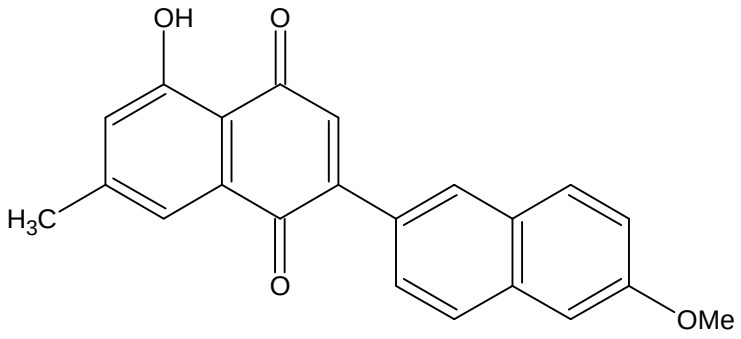

3.31

To a solution of 2-(6′-methoxynaphthalen-2′-yl)-5-methoxy-7-methyl-1,4-naphthoquinone **3.29** (250 mg, 0.70 mmol) in dry DCM (20 ml) was added borontribromide (1M solution in CH_2Cl_2, 0.9 ml, 0.9 mmol) drop-wise at -78ºC under nitrogen. The mixture was stirred for 3h at 25ºC, poured into ice water, acidified to litmus, extracted with DCM and the combined organic phase was washed with water. The residue obtained upon workup was chromatographed using EtOAc:hexane (1:4) to afford quinone **3.31** (122 mg, 51%) as reddish brown needles, m. p. 262-263°C (from ethanol). υ_{max} 1665 (s, C=O), 1644 cm^{-1} (m, C=O); δ_H 2.48 (3H, s, 7-CH_3), 4.07 (3H, s, 6′-OMe), 7.12 (2H, m, H-3 and H-6), 7.26 (1H, d, *J* 1.0, H-5′), 7.33 (1H, dd, *J* 8.4 and 1.0, H-7′), 7.55 (1H, d, *J* 1.2, H-1′), 7.71 (1H, dd, *J* 8.8 and 1.2, H-3′), 7.92 (1H, d, *J* 8.4, H-8′), 8.10 (1H, d, *J* 1.0, H-8), 8.29 (1H, d, *J* 8.8, H-4′) and 12.00 (1H, s, 5-OH). δ_C 22.3 (7-CH_3), 57.0 (6′-OMe), 113.2 (C-2)[a], 114.1 (C-3)[b], 121.1 (C-1′)[c], 124.0 (C-3′)[c], 126.6 (C-4′)[c], 127.9 (C-5′)[c], 128.9 (C-2′)[a], 129.0 (C-4a′)[d], 129.2 (C-8a′)[d], 130.1 (C-7′)[c], 130.2 (C-8′)[c], 132.2 (C-7)[b], 133.9 (C-6)[b], 135.1 (C-8)[b], 148.3 (C-4a and C-8a)[e], 155.1 (C-6′)[f], 161.4 (C-5)[f], 184.2 (C-1)[g] and 189.5 (C-4)[g]. (HRMS: Found M^+ 343.0867; C, 76.5; H, 4.7. Calc. for $C_{22}H_{16}O_4$: M 344.1048; C, 76.7; H, 4.7%).

2-(6′-Hydroxynaphthalen-2′-yl)-5-hydroxy-7-methyl-1,4-naphthoquinone 3.28

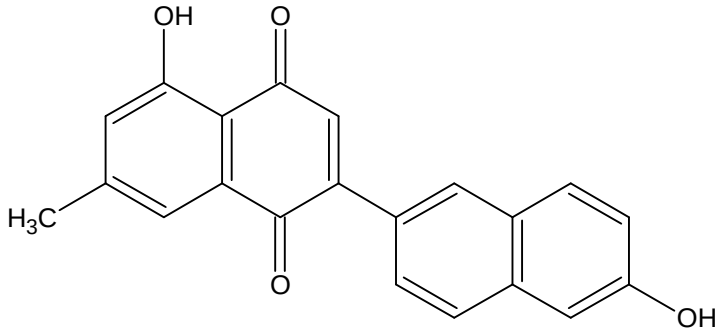

3.28

To a solution of 2-(6′-methoxynaphthalen-2′-yl)-5-hydroxy-7-methyl-1,4-naphthoquinone **3.31** (400 mg, 1.11 mmol) in dry DCM (20 ml) was added borontribromide (1M solution in CH_2Cl_2, 2.44 ml, 2.44 mmol) drop-wise at -78ºC under nitrogen. The mixture was stirred for 3h at 25ºC, poured into ice water, acidified to litmus, extracted with DCM and the combined organic phase was washed with water. The residue obtained upon workup was chromatographed using EtOAc:hexane (1:4) to afford quinone **3.28** (178 mg, 46%) as reddish brown needles, m. p. 236-238°C (form EtOAc/hexane). υ_{max} 1664 (s, C=O), 1642 cm^{-1} (m, C=O); δ_H 2.47 (3H, s, 7-CH_3), 6.05 (1H, bs, 6′-OH), 7.12 (2H, m, H-3 and H-6), 7.32 (1H, dd, *J* 8.8 and 1.0, H-7′), 7.36 (1H, d, *J* 1.0, H-5′), 7.55 (1H, d, *J* 1.2, H-1′), 7.73 (1H, dd, *J* 9.2 and 1.2, H-3′), 7.83 (1H, d, *J* 8.8, H-8′), 8.12 (2H, m, H-4′ and H-8) and 12.00 (1H, s, 5-OH). δ_C 22.3 (7-CH_3), 117.2 (C-2)[a], 118.0 (C-3)[b], 121.1 (C-1′)[c], 124.0 (C-3′)[c], 125.7 (C-4′)[c], 128.1 (C-5′)[c], 128.3 (C-2′)[a], 129.0 (C-4a′)[d], 129.2 (C-8a′)[d], 130.2 (C-7′)[c], 130.3 (C-8′)[c], 132.2 (C-7)[b], 133.1 (C-6)[b], 135.1 (C-8)[b], 148.1 (C-4a)[e], 148.2 (C-8a)[e], 152.1 (C-6′)[f], 161.4 (C-5)[f], 184.1 (C-1)[g] and 189.5 (C-4)[g]. (HRMS: Found M^+ 330.0872; C, 76.5; H, 4.2. Calc. for $C_{21}H_{14}O_4$: M 330.0892; C, 76.4; H, 4.3%).

7-Methyl-2-(thianthren-1´-yl)-1,4-naphthoquinone 3.34

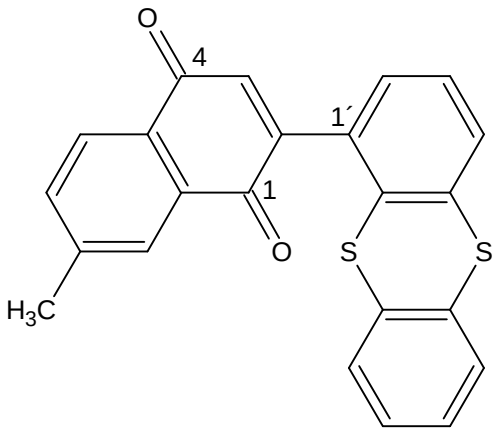

3.34

A mixture of 2-bromo-7-methyl-1,4-naphthoquinone **3.2** (260 mg, 1.03 mmol) and $Pd(PPh_3)_4$ (115 mg, 0.10 mmol) in benzene (10 ml) was stirred for 0.5h at 24˚C under nitrogen. An aqueous solution of Na_2CO_3 (2M, 1 ml) and thiantherene-1-boronic acid **3.33** (260 mg, 1.00 mmol) in benzene (15 ml) were added successively. The mixture was refluxed for 16h with vigorous stirring. The residue obtained upon workup was chromatographed using EtOAc:hexane (1:4) to afford quinone **3.34** (330 mg, 82%) as a yellow solid, m.p. 208-209°C (from EtOAc/hexane). υ_{max} 1671 (m, C=O), 1660 (s, C=O), 1599 (m, Ar); δ_H 2.55 (3H, s, CH_3-7), 6.93 (1H, s, H-3), 7.27 (5H, m, H-2´, H-3´, H-4´, H-7´ and H-8´), 7.51 (1H, dd, *J* 8.0 and 1.2, H-6) 7.61 (2H, m, H-6´ and H-9´), 8.01 (1H, d, *J* 1.2, H-8) and 8.07 (1H, d, *J* 8.0, H-5). δ_C 21.9 (7-CH_3), 126.4 (C-3)[a], 126.6 (C-2)[b], 127.4 (C-2´)[c], 127.6 (C-3´)[c], 127.8 (C-4´)[c], 127.9 (C-6´)[c], 128.63 (C-7´)[c], 128.64 (C-8´)[c], 128.9 (C-9´)[c], 129.9 (C-5)[a], 130.0 (C-1´)[b], 132.1 (C-7), 134.1 (C-6)[a], 134.8 (C-10a´)[d], 135.2 (C-4a´)[d], 135.8 (C-5a´)[d], 136.2 (C-9a´)[d], 136.9 (C-8)[a], 145.3 (C-4a)[e], 148.8 (C-8a)[e], 183.6 (C-1)[f] and 184.8 (C-4)[f]. (HRMS: Found M^+ 386.0487; C, 71.6; H, 3.5. Calc. for $C_{23}H_{14}O_2S_2$: M 386.0435; C, 71.5; H, 3.7%).

2-(5′,10′-Dioxydithianthren-1′-yl)-7-methyl-1,4-naphthoquinone 3.32

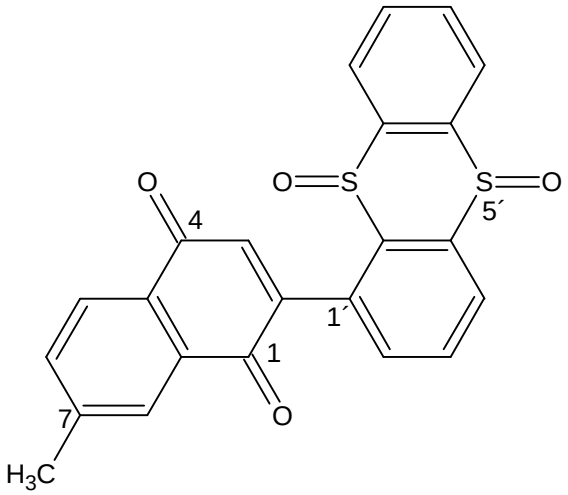

3.32

A mixture of 2-(thianthren-1′-yl)-7-methyl-1,4-naphthoquinone **3.34** (150 mg, 0.39 mmol) and m-chloroperbenzoic acid (2 mol equiv., 135 mg) in DCM (20 ml) was stirred for 2h at 25˚C and thereafter the organic acids were extracted into aqueous sodium hydrogen carbonate and the dried DCM yielded a residue upon workup which was chromatographed using EtOAc:hexane (1:4) to afford sulphone **3.32** (94 mg, 58%) as orange needles, m.p. 115-117˚C (from EtOAc/hexane). υ_{max} 1671 (m, C=O), 1658 (s, C=O), 1592 (m, Ar), 1164 (w, S=O) and 1328 (w, S=O); δ_H 2.50 (3H, s, CH_3-7), 6.84 (1H, s, H-3), 7.35 (7H, m, H-5, H-6, H-8, H-6′, H-7′, H-8′ and H-9′), 7.61 (1H, dd, *J* 7.6 and 1.4, H-2′), 7.83 (1H, t, *J* 7.6, H-3′) and 8.19 (1H, dd, *J* 7.6 and 1.4, H-4′). δ_C 21.1 (7-CH_3), 123.5 (C-2)[a], 125.8 (C-3)[b], 127.4 (C-2′)[c], 127.8 (C-3′)[c], 128.0 (C-4′)[c], 128.7 (C-6′ and C-7′)[c], 129.0 (C-8′)[c], 129.7 (C-9′)[c], 130.1 (C-5)[b], 134.0 (C-1′)[a], 134.2 (C-7)[a], 134.9 (C-6)[b], 135.1 (C-10a′)[d], 135.8 (C-4a′)[d], 136.2 (C-5a′)[d], 137.2 (C-9a′)[d], 138.0 (C-8)[a], 147.7 (C-4a)[e], 149.4 (C-8a)[e], 182.7 (C-1)[f] and 183.5 (C-4)[f]. (HRMS: Found M^+ 418.1630; C, 66.2; H, 3.5. Calc. for $C_{23}H_{14}O_4S_2$: M 418.0334; C, 66.0; H, 3.4%).

5-Methoxy-7-methyl-2-(thianthren-1′-yl)- 1,4naphthoquinone 3.36

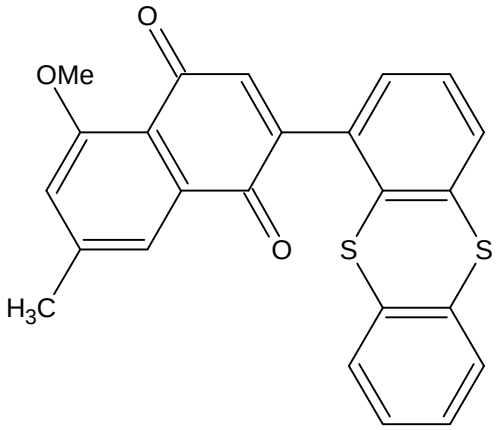

3.36

A mixture of 2-bromo-5-methoxy-7-methyl-1,4-naphthoquinone **3.13** (351 mg, 1.25 mmol) and $Pd(PPh_3)_4$ (148 mg, 0.12 mmol) in benzene (10 ml) was stirred for 0.5h at 24˚C under nitrogen. An aqueous solution of Na_2CO_3 (2 M, 1 ml) and thiantherene-1-boronic acid **3.33** (306 mg, 1.18 mmol) in benzene (15 ml) were added successively. The mixture was heated under reflux for 16h with vigorous stirring. The residue obtained upon workup was chromatographed using EtOAc:hexane (2:3) to afford quinone **3.36** (420 mg, 86%) as a yellow solid, m. p. 203-204˚C (from EtOAc/hexane). υ_{max} 1670 (m, C=O), 1658 (s, C=O); δ_H 2.52 (3H, s, CH_3-7), 4.04 (3H, s, OMe), 6.83 (1H, d, *J* 1.4, H-6), 7.16 (1H, s, H-3), 7.27 (5H, m, H-2′, H-3′, H-4′, H-7′ and H-8′), 7.49 (1H, dd, *J* 7.4 and 1.4, H-6′), 7.59 (1H, dd, *J* 7.6 and 1.8, H-9′), 7.67 (1H, d, *J* 1.4, H-8). δ_C 22.3 (7-CH_3), 56.5 (OMe), 118.4 (C-6)[a], 120.8 (C-3)[b], 127.4 (C-2′)[c], 127.7 (C-3′)[c], 127.9 (C-4′)[c], 128.3 (C-2)[c], 128.6 (C-6′)[c], 128.7 (C-7′)[c], 128.9 (C-8′)[c], 129.8 (C-9′)[a], 131.5 (C-1′)[b], 134.2 (C-10a′)[d], 134.6 (C-4a′)[d], 135.3 (C-7)[d], 136.2 (C-5a′)[d], 136.9 (C-9a′)[d], 139.0 (C-8)[a], 146.4 (C-4a)[e], 146.6 (C-8a)[e], 159.8 (C-5), 183.8 (C-1)[f] and 183.9 (C-4)[f]. (HRMS: Found M^+ 416.0498; C, 69.4; H, 3.8. Calc. for $C_{24}H_{16}O_3S_2$: M 416.0541; C, 69.2; H, 3.9%).

2-(5′,10′-Dioxydithianthren-1′-yl)-5-methoxy-7-methyl-1,4-naphthoquinone 3.35

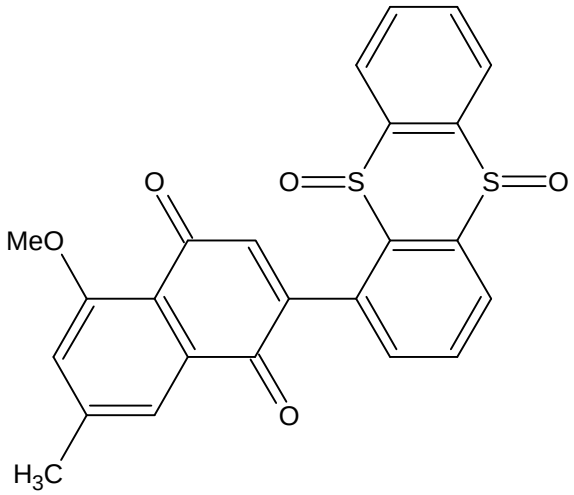

3.35

A mixture of 2-(thianthren-1′-yl)-5-methoxy-7-methyl-1,4-naphthoquinone **3.36** (162 mg, 0.39 mmol) and m-chloroperbenzoic acid (2 mol equiv., 135 mg) in DCM (20 ml) was stirred for 2h at 25˚C and thereafter the organic acids were extracted into aqueous sodium hydrogen carbonate and the dried DCM yielded a residue upon workup which was chromatographed using EtOAc:hexane (1:4) to afford sulphone **3.35** (112 mg, 64%) as orange needles, m.p. 112-114˚C (from EtOAc/hexane). υ_{max} 1671 (m, C=O), 1660 (s, C=O), 1168 (w, S=O) and 1326 (w, S=O); δ_H 2.54 (3H, s, CH_3-7), 4.04 (3H, s, OMe), 7.19 (1H, s, H-6), 7.61 (7H, m, H-3, H-8, H-2′, H-3′, H-7′, H-8′ and H-9′), 8.24 (1H, dd, *J* 7.6 and 1.4, H-6′), 8.32 (1H, dd, *J* 7.6 and 1.2, H-4′). δ_C 22.4 (7-CH_3), 56.5 (OMe), 119.0 (C-3)[a], 120.9 (C-6)[a], 126.0 (C-2′)[b], 127.1 (C-3′)[b], 128.8 (C-4′)[b], 130.3 (C-6′)[b], 131.2 (C-7′)[b], 131.8 (C-8′)[b], 132.1 (C-9′)[b], 132.2 (C-10a′)[c], 133.1 (C-4a′)[c], 133.4 (C-5a′)[c], 139.1 (C-9a′)[c], 140.4 (C-8)[d], 143.3 (C-4a)[c], 147.0 (C-8a)[c], 160.0 (C-5), 182.9 (C-1)[e] and 185.0 (C-4)[e]. (HRMS: Found M^+ 448.1156; C, 64.4; H, 3.5. Calc. for $C_{24}H_{16}O_5S_2$: M 448.0439; C, 64.3; H, 3.6%).

5-Methoxy-7-methyl-2-(4-methylnaphthalen-1′-yl)-1,4-naphthoquinone 3.39

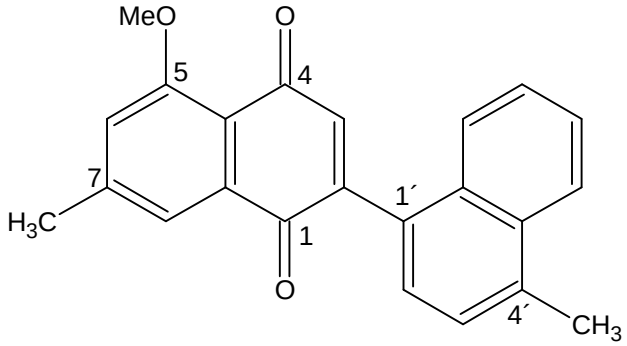

3.39

A mixture of 2-bromo-5-methoxy-7-methyl-1,4-naphthoquinone **3.13** (351 mg, 1.25 mmol) and $Pd(PPh_3)_4$ (148 mg, 0.12 mmol) in benzene (20 ml) was stirred for 0.5h at 24˚C under nitrogen. An aqueous solution of Na_2CO_3 (2M, 1 ml) and 4-methylnaphthalene-1- boronic acid **3.38** (220 mg, 1.18 mmol) in benzene (10 ml) were added successively. The mixture was heated under reflux for 16h with vigorous stirring. The residue obtained upon workup was chromatographed using EtOAc:hexane (2:3) to afford quinone **3.39** (428 mg, 90%) as a yellow solid, m.p. 228-230°C (from EtOAc/hexane). υ_{max} 1659 (s, C=O), 1648 (m, C=O) and 1597 cm^{-1} (m, Ar); δ_H 2.51 (3H, s, 7-CH_3), 2.74 (3H, s, 4′-CH_3), 4.04 (3H, s, OMe), 6.98 (1H, s, H-3), 7.15 (1H, d, *J* 1.0, H-6), 7.44 (4H, m, H-2′, H-3′, H-6′ and H-7′), 7.65 (2H, m, H-5′ and H-8) and 8.06 (1H, dd, *J* 8.0 and 1.0, H-8′). δ_C 19.7 (4′-CH_3), 22.4 (7-CH_3), 56.6 (OMe), 118.1 (C-2)[a], 118.4 (C-3)[b], 120.9 (C-2′)[c], 124.7 (C-3′)[c], 126.01 (C-5′)[c], 126.04 (C-6′)[c], 126.1 (C-7′)[c], 126.2 (C-8′)[c], 127.2 (C-4′)[c], 130.2 (C-1′)[a], 131.6 (C-4a′)[d], 132.7 (C-8a′)[d], 134.5 (C-7)[d], 136.4 (C-6)[b], 140.1 (C-8)[b], 146.5 (C-4a)[e], 147.4 (C-8a)[e], 159.8 (C-5), 184.3 (C-1)[f] and 185.0 (C-4)[f]. (HRMS: Found M^+ 342.1272; C, 80.8; H, 5.4. Calc. for $C_{23}H_{18}O_3$: M 342.1255; C, 80.7; H, 5.3%).

5-Hydroxy-7-methyl-2-(4-methylnaphthalen-1′-yl)-1,4-naphthoquinone 3.37

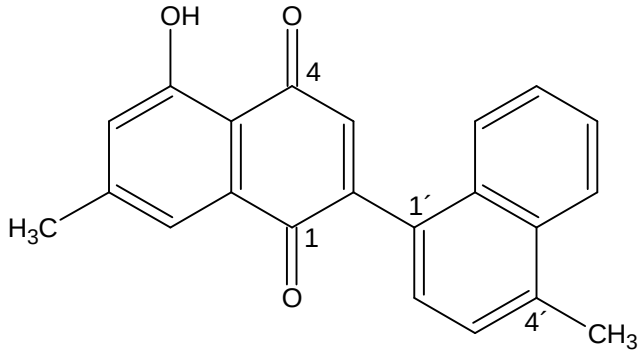

3.37

To a solution of 2-(4-Methylnaphthalen-1′-yl)-5-methoxy-7-methyl-1,4-naphthoquinone **3.39** (390 mg, 1.13 mmol) in dry CH_2Cl_2 (20 ml) was added BBr_3 (1M solution in CH_2Cl_2, 1.3 ml, 1.3 mmol) drop-wise at -78ºC under nitrogen. The mixture was then stirred for 3h at 25ºC, poured into ice water, acidified to litmus, extracted with CH_2Cl_2 and the combined organic phase was washed with water. The residue obtained upon workup was chromatographed using EtOAc:hexane (1:4) to afford hydroxyquinone **3.37** (170 mg, 45%) as a red coloured solid, m.p. 182-183°C (from EtOAc/hexane). υ_{max} 3433 (bs, -OH), 1665 (m, C=O) and 1634 cm^{-1} (m, C=O); δ_H 2.58 (3H, s, 7-CH_3), 2.76 (3H, s, 4′-CH_3), 7.09 (2H, m, H-3 and H-6), 7.43 (4H, m, H-2′, H-3′, H-6′ and H-7′), 7.63 (2H, m, H-5′ and H-8), 8.07 (1H, dd, *J* 7.6 and 0.8, H-8′) and 12.01 (1H, s, 5-OH). δ_C 19.7 (4′-CH_3), 24.2 (7-CH_3), 121.1 (C-2)[a], 121.6 (C-3)[b], 124.0 (C-1′)[a], 124.6 (C-2′)[c], 125.9 (C-3′ and C-5′)[c], 126.1 (C-6′)[c], 126.3 (C-7′)[c], 127.2 (C-8′)[c], 129.7 (C-4′)[c], 130.0 (C-4a′)[d], 131.3 (C-8a′)[d], 132.7 (C-7)[d], 137.0 (C-6)[b], 137.3 (C-8)[b], 148.1 (C-4a)[e], 151.1 (C-8a)[e], 161.6 (C-5), 183.5 (C-1)[f] and 189.6 (C-4)[f]. (HRMS: Found M^+ 328.0170; C, 80.3; H, 5.0. Calc. for $C_{22}H_{16}O_3$: M 328.1099; C, 80.5; H, 4.9%).

2-(2′-Naphthyl)- 5-methoxy-7-methyl-1,4-naphthoquinone 3.42

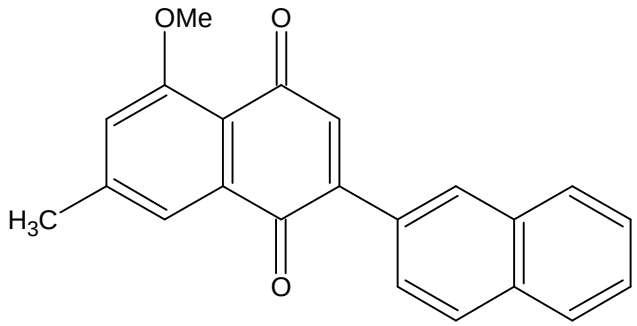

3.42

A mixture of 2-bromo-5-methoxy-7-methyl-1,4-naphthoquinone **3.13** (351 mg, 1.25 mmol) and $Pd(PPh_3)_4$ (148 mg, 0.12 mmol) in benzene (20 ml) was stirred for 0.5h at 25˚C under nitrogen. An aqueous solution of Na_2CO_3 (2M, 1 ml) and 2-naphthaleneboronic acid **3.41** (203 mg, 1.18 mmol) in benzene (10 ml) were added successively. The mixture was heated under reflux for 16h with vigorous stirring. The residue obtained upon workup was chromatographed using EtOAc:hexane (2:3) to afford quinone **3.42** (358 mg, 88%) as a yellow solid, m. p. 172-173°C (from ethanol). υ_{max} 1658 (s, C=O) and 1651 cm^{-1} (m, C=O); δ_H 2.52 (3H, s, CH_3-7), 4.03 (3H, s, OMe), 7.09 (1H, s, H-3), 7.13 (1H, d, *J* 1.4, H-6), 7.54 (2H, m, H-6′ and H-7′)[a], 7.66 (2H, m, H-5′ and H-8′)[a], 7.89 (3H, m, H-1′, H-3′ and H-4′)[a] and 8.13 (1H, d, *J* 1.4, H-8). δ_C 22.5 (CH_3), 56.6 (OMe), 118.3 (C-6)[a], 120.8 (C-3)[a], 126.3 (C-1′)[b], 126.6 (C-3′)[b], 127.3 (C-4′)[b], 127.8 (C-6′)[b], 128.1 (C-7′)[b], 128.8 (C-5′)[b], 129.6 (C-8′)[b], 130.8, 133.2, 133.9, 134.8 (C-2′, C-2, C-4a′, C-8a′ and C-7), 137.8 (C-8), 145.7 (C-4a)[c], 146.5 (C-8a)[c], 159.7 (C-5), 184.3 (C-1)[d] and 185.2 (C-4)[d]. (HRMS: Found M^+, 328.1181; C, 80.7; H, 4.8. Calc. M for $C_{22}H_{16}O_3$: 328.1099; C, 80.5; H, 4.9%).

2-(2´-Naphthyl)- 5-hydroxy-7-methyl-1,4-naphthoquinone 3.40

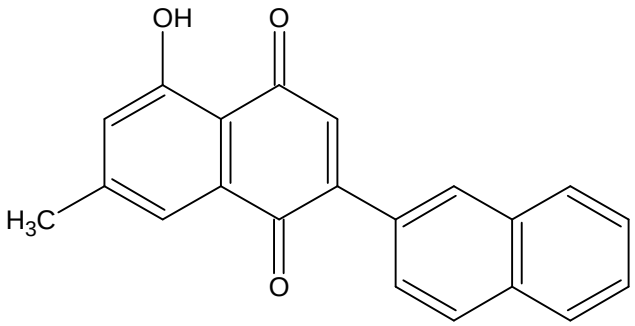

3.40

To a solution of 2-(2´-naphthyl)- 5-methoxy-7-methyl-1,4-naphthoquinone **3.42** (310 mg, 0.94 mmol) in dry DCM (20 ml) was added borontribromide (1M solution in CH_2Cl_2, 1 ml) drop-wise at -78ºC under nitrogen. The mixture was stirred for 4h at 25ºC, poured into ice water, acidified to litmus, extracted with DCM and the combined organic phase was washed with water. The residue obtained upon workup was chromatographed using EtOAc:hexane (3:7) to afford quinone **3.40** (110 mg, 37%) as orange red needles, m. p. 216-218°C (form EtOAc/hexane). υ_{max} 3340 (s, -OH), 1651 (s, C=O) and 1644 cm^{-1} (m, C=O); δ_H 2.58 (3H, s, CH_3-7), 7.15 (1H, s, H-3), 7.26 (1H, d, *J* 1.2, H-6), 7.59 (4H, m, H-1´, H-3´, H-6´ and H-7´)[a], 7.91 (3H, m, H-4´, H-5´ and H-8´)[b] and 8.12 (1H, d, *J* 1.2, H-8). δ_C 24.4 (CH_3), 121.1 (C-6)[a], 121.6 (C-3)[a], 126.1 (C-1´)[b], 126.8 (C-3´)[b], 127.6 (C-2´)[c], 127.7 (C-4´)[b], 127.8 (C-6´)[b], 128.3 (C-7´)[b], 129.0 (C-5´)[b], 130.2 (C-8´)[b], 130.3 (C-2)[c], 130.4 (C-7)[a], 133.0 (C-4a´)[c], 134.1 (C-8a´)[c], 134.9 (C-8), 148.1 (C-4a)[c], 149.3 (C-8a)[c], 158.0 (C-5), 183.8 (C-1)[d] and 189.5 (C-4)[d]. (HRMS: Found M^+ 314.0898; C 80.4; H 4.4. Calc. M for $C_{21}H_{14}O_3$: 314.0943; C, 80.2; H, 4.5%).

2-(Naphthalen-2′-yl)-7-methyl-1,4-naphthoquinone 3.43

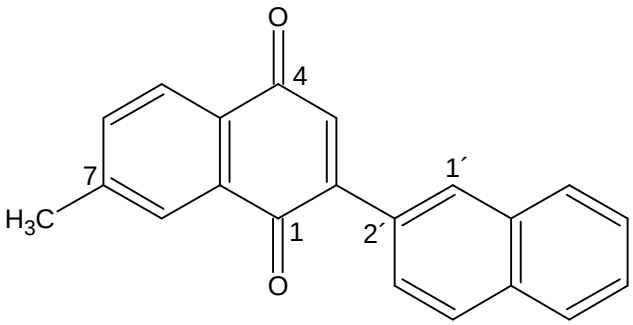

3.43

A mixture of 2-bromo-7-methyl-1,4-naphthoquinone **3.2** (314 mg, 1.25 mmol) and $Pd(PPh_3)_4$ (148 mg, 0.11 mmol) in benzene (10 ml) was stirred for 0.5h at 24˚C under nitrogen. An aqueous solution of Na_2CO_3 (2M, 1 ml) and 2-naphthaleneboronic acid **3.41** (203 mg, 1.18 mmol) in benzene (5 ml) were added successively. The mixture was heated under reflux for 16h with vigorous stirring. The residue obtained upon workup was chromatographed using EtOAc:hexane (1:4) to afford quinone **3.43** (319 mg, 86%) as yellow needles, m.p. 169-170˚C (form EtOAc/hexane). υ_{max} 1658 (s, C=O) and 1652 cm^{-1} (m, C=O); δ_H 2.53 (3H, s, CH_3-7), 7.16 (1H, s, H-3), 7.59 (4H, m, H-1′, H-3′, H-6′ and H-7′), 7.99 (6H, m, H-4′, H-5′, H-8′, H-5, H-6 and H-8). δ_C 22.0 (CH_3-7), 126.3 (C-3)[a], 126.4 (C-1′)[a], 126.7 (C-3′)[a], 127.4 (C-4′)[a], 127.5 (C-5′)[a], 127.8 (C-6′)[a], 128.2 (C-4a′)[b], 128.9 (C-7′)[a], 129.8 (C-8′)[a], 130.1 (C-2′)[b], 131.1 (C-8a′)[b], 132.6 (C-2)[b], 133.1 (C-7)[c], 134.0 (C-6)[c], 134.7 (C-5)[c], 135.6 (C-8)[c], 145.1 (C-4a)[d], 148.0 (C-8a)[d], 185.0 (C-1)[e] and 185.1 (C-4)[e]. (HRMS: Found M^+ 298.1030; C, 84.5; H, 4.8. Calc. for $C_{21}H_{14}O_2$: M 298.0993; C, 84.5; H, 4.7%).

2-(4-Methylnaphthalen-1′-yl)-7-methyl-1,4-naphthoquinone 3.44

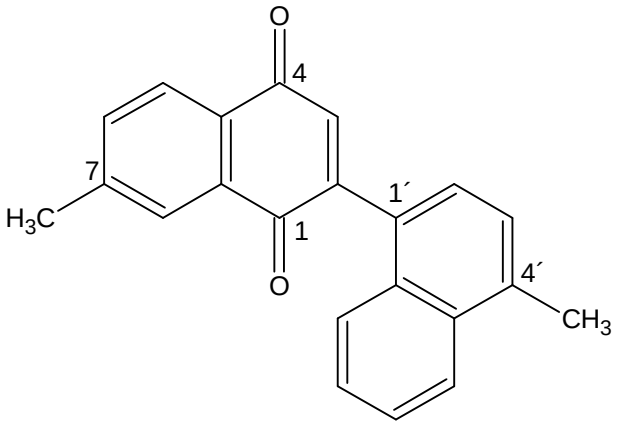

3.44

A mixture of 2-bromo-7-methyl-1,4-naphthoquinone **3.2** (314 mg, 1.25 mmol) and $Pd(PPh_3)_4$ (148 mg, 0.11 mmol) in benzene (20 ml) was stirred for 0.5h at 24˚C under nitrogen. An aqueous solution of Na_2CO_3 (2M, 1 ml) and 4-methyl-1-naphthaleneboronic acid **3.38** (220 mg, 1.18 mmol) in benzene (10 ml) were added successively. The mixture was heated under reflux for 16h with vigorous stirring. The residue obtained upon workup was chromatographed using EtOAc:hexane (1:4) to afford quinone **3.44** (352 mg, 90%) as red needles, m.p. 109-111°C (from EtOAc/hexane). υ_{max} 1660 (s, C=O) and 1652 cm^{-1} (m, C=O); δ_H 2.53 (3H, s, CH_3-7)[a], 2.76 (3H, s, CH_3-4′)[a], 7.07 (1H, s, H-3), 7.49 (6H, m, H-2′, H-3′, H-5′, H-6′, H-7′ and H-8′), 7.97 (1H, d, *J* 0.8, H-8) and 8.08 (2H, dd, *J* 8.2 and 0.8, H-5 and H-6). δ_C 19.7 (7-CH_3), 21.9 (4′-CH_3), 124.6 (C-3)[a], 125.9 (C-2′)[b], 126.0 (C-3′)[b], 126.1 (C-5′)[b], 126.2 (C-6′)[b], 126.4 (C-7′)[b], 127.0 (C-8′)[b], 127.5 (C-4′)[b], 130.1 (C-1′)[c], 130.3 (C-2)[c], 131.5 (C-4a′)[d], 132.3 (C-8a′)[d], 132.7 (C-7)[d], 134.6 (C-5)[a], 136.5 (C-6)[a], 137.9 (C-8)[a], 145.1 (C-4a)[e], 149.7 (C-8a)[e], 184.8 (C-1)[f] and 185.0 (C-4)[f]. (HRMS: Found M^+ 312.1139; C, 84.5; H, 5.0. Calc. for $C_{22}H_{16}O_2$: M 312.1150; C, 84.6; H, 5.2%).

1,5-Diacetoxynaphthalene 3.48

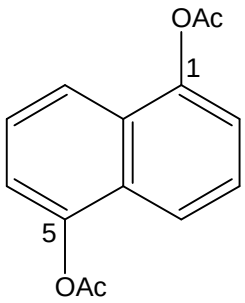

3.48

1,5-Naphthalenediol **3.47** (5.0 g, 31.2 mmol) was dissolved in pyridine (25 ml, 306 mmol) and acetic anhydride (25 ml, 265 mmol). The solution was stirred for 12h at 24˚C under nitrogen, and then the remaining acetic anhydride was quenched by addition of water. The solution was then filtered and the solid obtained was washed with ethyl alcohol:water (1:19) and dried in the air to afford the product **3.48** (7.39 g, 97%) as a light brown coloured solid, m.p. 158-160˚C (from benzene). (Lit.[69] m.p. 161˚C); δ_H 2.47 (6H, s, 2 x -CH_3), 7.29 (2H, dd, *J* 7.2 and 1.2, H-2 and H-6), 7.51 (2H, dd, *J* 7.8 and 7.2, H-3 and H-7) and 7.79 (2H, dd, *J* 7.8 and 1.2, H-4 and H-8). δ_C 21.0 (2 x -CH_3), 118.8 (C-2 and C-6), 119.3 (C-3 and C-7), 126.0 (C-4 and C-8), 128.1 (C-4a and C-8a), 146.7 (C-1 and C-5) and 169.2 (2 x C=O).

5-Acetoxy-2-bromo-1,4-naphthoquinone 3.46

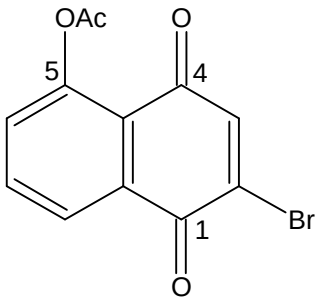

3.46

A solution of 1,5-diacetoxynaphthalene **3.48** (2.4 g, 10.0 mmol) in warm acetic acid (100 ml) was added drop-wise to a solution of N-bromosuccinimide (7.2 g, 40.0 mmol) in acetic acid (200 ml) and water (100 ml) at 65°C. The solution was stirred for 1h at the same temperature and cold water (200 ml) was then added. The solution was extracted with DCM (4 x 50 ml) and the combined extracts were washed with water (4 x 200 ml). The residue obtained upon workup was chromatographed using EtOAc: hexane (1:4) to afford quinone **3.46** (2.7 g, 92%) as a yellow solid, m.p. 156-157°C (Lit.[69] m.p. 158˚C); δ_H 2.44 (3H, s, -CH_3), 7.39 (1H, s, H-3), 7.42 (1H, dd, *J* 8.2 and 1.6, H-6), 7.77 (1H, dd, *J* 8.2 and 8.0, H-7) and 8.14 (1H, dd, *J* 8.0 and 1.4, H-8). δ_C 21.0 (-CH_3), 123.2 (C-3), 126.3 (C-2)[a], 130.3 (C-6)[a], 132.6 (C-4a)[b], 134.9 (C-7)[a], 138.5 (C-8a)[b], 141.4 (C-8)[a], 149.9 (C-5), 169.2 [C=O (ester)], 177.4 (C-1)[c] and 180.9 (C-4)[c].

2-(Naphthalen-2′-yl)-5-acetoxy-1,4-naphthoquinone 3.45

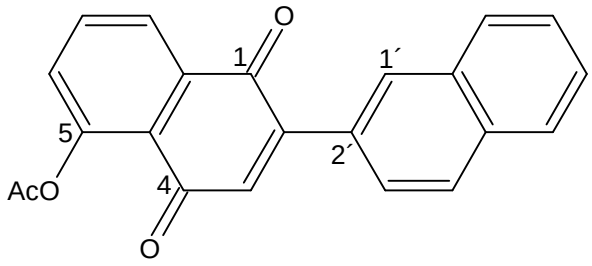

3.45

A mixture of 2-bromo-5-acetoxy-1,4-naphthoquinone **3.46** (150 mg, 0.51 mmol) and $Pd(PPh_3)_4$ (60 mg, 0.052 mmol) in benzene (15 ml) was stirred for 0.5h at 24˚C under nitrogen. An aqueous solution of Na_2CO_3 (2M, 0.5 ml) and 2-naphthaleneboronic acid **3.41** (86 mg, 0.50 mmol) in benzene (10 ml) were added successively. The mixture was heated under reflux for 16h with vigorous stirring. The residue obtained upon workup was chromatographed using EtOAc:hexane (1:4) to afford quinone **3.45** (137 mg, 79%) as yellow needles, m.p. 182-183°C (from ethanol). υ_{max} 1772 (m, C=O), 1668 (m, C=O), 1657 (s, C=O) and 1610 cm^{-1} (w, Ar); δ_H 2.49 [3H, s, $-CH_3$ (ester)], 7.07 (1H, s, H-3), 7.43 (1H, dd, *J* 8.2 and 1.0, H-6), 7.58 (3H, m, H-3′, H-6′ and H-7′)[a], 7.80 (1H, dd, *J* 8.2 and 9.2, H-7), 7.90 (3H, m, H-4′, H-5′ and H-8′)[a], 8.11 (1H, d, *J* 1.0, H-1′) and 8.18 (1H, dd, *J* 9.2 and 1.2, H-8). δ_C 21.1 [ester,$-CH_3$), 123.5 (C-2)[a], 125.6 (C-3)[b], 126.1 (C-1′)[c], 126.6 (C-3′)[c], 127.4 (C-4′)[c], 127.7 (C-5′)[c], 128.1 (C-6′)[c], 128.8 (C-7′)[c], 129.5 (C-8′)[c], 129.8 (C-6)[b], 130.3 (C-2′)[d], 133.0 (C-4a′)[d], 133.9 (C-8a′)[d], 134.3 (C-4a)[d], 134.7 (C-7)[b], 136.5 (C-8)[b], 146.9 (C-8a)[d], 149.2 (C-5), 169.4 (ester, C=O) and 183.7 (C-1)[e] and 183.8 (C-4)[e]. (HRMS: Found M^+ 342.0890; C, 77.4; H, 4.0. Calc. for $C_{22}H_{14}O_4$: M 342.0892; C, 77.2; H, 4.1%).

2-(4-Methylnaphthalen-1′-yl)-5-acetoxy-1,4-naphthoquinone 3.49

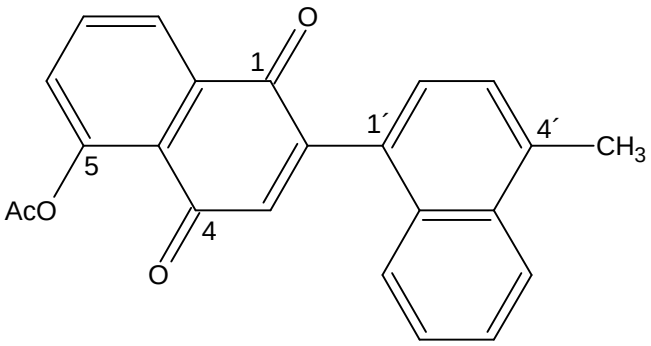

3.49

A mixture of 2-bromo-5-acetoxy-1,4-naphthoquinone **3.46** (150 mg, 0.51 mmol) and $Pd(PPh_3)_4$ (60 mg, 0.052 mmol) in benzene (15 ml) was stirred for 0.5h at 24˚C under nitrogen. An aqueous solution of Na_2CO_3 (2M, 0.5 ml) and 4-methyl-1-naphthaleneboronic acid **3.38** (93 mg, 0.50 mmol) in benzene (10 ml) were added successively. The mixture was heated under reflux for 16h with vigorous stirring. The residue obtained upon workup was chromatographed using EtOAc:hexane (1:4) to afford quinone **3.49** (140 mg, 77%) as reddish brown needles, m.p. 173-174°C (from ethanol). υ_{max} 1769 (m, C=O), 1667 (w, C=O), 1655 (s, C=O), 1613 (w, Ar) and 1592 cm^{-1} (w, Ar); δ_H 2.49 [3H, s, $-CH_3$ (ester)], 2.75 (3H, s, 4′-CH_3), 6.98 (1H, s, H-3), 7.35 (2H, m, H-2′ and H-3′)[a], 7.45 (1H, dd, *J* 8.0 and 1.0, H-6), 7.54 (2H, m, H-6′ and H-7′)[b], 7.65 (1H, dd, *J* 7.4 and 1.4, H-5′)[c], 7.80 (1H, dd, *J* 8.0 and 7.6, H-7), 8.07 (1H, dd, *J* 7.4 and 1.4, H-8′)[c] and 8.15 (1H, dd, *J* 7.6 and 1.0, H-8). δ_C 19.6 (4′- CH_3), 21.1 [ester,-CH_3), 123.6 (C-2)[a], 124.6 (C-3)[b], 125.7 (C-2′)[c], 125.9 (C-3′)[c], 126.0 (C-5′)[c], 126.1 (C-6′)[c], 126.3 (C-7′)[c], 127.1 (C-8′)[c], 129.6 (C-6)[b], 131.4 (C-1′)[a], 132.7 (C-4a′)[d], 134.1 (C-8a′)[d], 134.8 (C-7)[b], 136.7 (C-4′)[d], 138.9 (C-8)[b], 147.2 (C-4a)[e], 148.6 (C-8a)[e], 149.4 (C-5)[e], 169.5 (ester, C=O) and 183.7 (C-1 and C-4). (HRMS: Found M^+ 356.1049; C, 77.5; H, 4.6. Calc. for $C_{23}H_{16}O_4$: M 356.1048; C, 77.5; H, 4.5%).

Chapter 5: Evaluation of the compounds as anti-mycobacterial agents

This chapter describes details of the methods used to investigate the antimycobacterial activities of synthesized test compounds. Initially, two fast growing stains of mycobacterium viz., *Mycobacterium smegmatis* and *Mycobacterium aurum* were used to determine the activities using the broth micro-dilution method. Literature revealed that different strains of bacteria respond differently to the induced compounds. This insight led us to investigate the activities of the synthesized compounds on a clinical strain of *M. tuberculosis* using the radiometric BACTEC method and an exploratory analysis is thus presented.

Section 5.1: Materials and Methods

Broth micro-dilution methodology was performed in 96-well plates using 7H9 Middlebrook broth. Each sample was tested in duplicate in two separate assays, including a third, organism-free, replicate in each plate to allow for background colour arising from each compound. The test compounds were prepared in concentrations of 1mg/ml in 18% DMSO/82% sterile distilled water. Normally compounds would be dissolved in 10% DMSO, but these compounds precipitated out of solution at this concentration. A solvent control was prepared in the same manner. The concentration of compounds used in the assay ranged from 2µg/ml – 250µg/ml (8 half dilutions tested in total). Ciprofloxacin **1.8** was used as a positive control. MICs were determined as the lowest concentration at which 100% inhibition of organism growth occurred.

Section 5.1.1: Media composition

Middlebrook 7H10 agar: Add 3.8g of Middlebrook 7H10 (DIFCO ^{TM}) and 1mg of glycerol to 180ml distilled water. Sterilize by autoclaving at 121°C for 15 minutes. Once cooled, added 10% OADC (Becton Dickinson; oleic acid, albumin, dextrose, catalase).

1x Middlebrook 7H9: Add 0.94g Middlebrook 7H9 (DIFCO^{TM}) and 0.4ml glycerol (Merck) to 180ml distilled water. Sterilize by autoclaving at 121°C for 15 minutes. Once cooled, added 10% OADC (Becton Dickinson; oleic acid, albumin, dextrose, catalase).

Section 5.1.2: Organism preparation for experimentation

A single glycerol stock of *M.aurum* A+ (Pasteur Institute) and *M. smegmatis* (clinical strain) was used to inoculate two supplemented Middlebrook 7H10 agar (7H10 + 10% OADC) plates. The plates were incubated at 37°C for 4 days and loosely sealed in a plastic packet to avoid dehydration. A single colony was used to inoculate 5ml supplemented 1x 7H9 broth, which was grown at 37°C for 72 h. **Section 5.1.3: Broth micro-dilution method**

To flat-bottomed 96-well plates, 100µl of 2x 7H9 broth (double the recommended strength) supplemented with 20% OADC was added to each well using a multi-channel pipette, except for the medium control well to which 200µl of 1x7H9 supplemented with 10% OADC was added. For the drug and solvent controls, as well as the test samples, 100µl of the respective sample was added to the first well of the column. A multi-channel pipette was used to perform serial doubling dilutions from the top to the bottom of the plate by transferring 100µl aliquots and mixing thoroughly at each step. The final 100µl was discarded. A stock concentration of 62.5µg/ml of ciprofloxacin **1.8** was used as the drug control. The optical density (OD) of the 72 h liquid culture was adjusted to 0.125 at 550nm,[76] using the supplemented 1x 7H9 broth as a 'blank'. 100µl of the diluted culture was added to every well of the microtitre plate excluding the wells of

the first column that serve as the medium control. The plates were loosely sealed in plastic bags to prevent dehydration and incubated at 37°C for 48 h for *M. smegmatis* and 72 h for *M. aurum*. The plates were then removed from the incubator and 40µl of a 0.4 mg/ml solution of p-iodonitrotetrazolium salt (INT; Fluka) was added to each well of the plate.[77] The tetrazolium salt turns red in the presence of metabolizing organism. The plates were left sealed in plastic packets and were checked after 6 and 18 h to avoid dehydration and contamination. The lowest concentration containing no indication of red as a result of INT was deemed to be the MIC. IC_{50} values can be determined with the use of a micro-plate reader set at a wavelength of 620 nm (nanometer). Strongly coloured extracts/compounds affect these readings and therefore an organism-free column should be included for each concentration of each sample.

Section 5.1.4: Results

Seven synthetic analogues of diospyrin **1.22** were tested for activity against two strains of mycobacterium. Ciprofloxacin **1.8** was used as the positive control. The positive control should have an MIC less than 2µg/ml. The negative control demonstrated that the highest concentration of DMSO tested (4.5%) did not affect bacterial growth. The antibiotic, medium and organism controls were acceptable throughout experimentation. The MIC values obtained from duplicate experiments were used to generate a measure of the final average activity of the compounds. The results of the analysis are presented in Table 5.1.

Table 5.1 The MIC's of the test compounds against *M. smegmatis* and *M. aurum*. All concentrations are expressed in µg/ml.

Compound	*M. smegmatis*	*M. aurum*
3.34	>250	>250
3.21	125	125
3.25	>250	>250
3.40	250	>250
3.45	>250	>250
3.32	>250	>250
3.43	>250	>250

Section 5.1.5: Discussion

All the tested compounds did not appear to have very good activity against the two mycobacteria. Compound **3.21** had the best activity, with an MIC of 125µg/ml. Promising anti-mycobacterials should have activity under 10µg/ml, so this activity would not justify further investigation with regard to anti-mycobacterials. Due to the high concentrations at which activity was noted, if at all, IC_{50} values (the concentration at which 50% of organism is killed) were not determined.

The ability of mycobacteria to develop multi-drug resistance in some strains shows that different strains of mycobacteria respond selectively towards different drugs. It is thus possible that the above two strains of mycobacteria were not responsive to the compounds administered and that perhaps these compounds might act against other strains of mycobacteria. To test this hypothesis, the test compounds were further tested on another clinical strain of mycobacterium by employing radiometric BACTEC method.

Section 5.2: The radiometric BACTEC method:

All work was carried out in the Biosafety Level 3 laboratory of the Division of Molecular Biology and Human Genetics of the University of Stellenbosch. A clinical isolate of *M. tuberculosis* was also selected from a bank of genetically well-characterized (according to their

IS6110 fingerprint profile) strains located in the Division of Molecular Biology and Human Genetics of the University of Stellenbosch for the evaluations.[78] The strain was drug sensitive to Isoniazid **1.1** and Rifampicin **1.2**.

The 7H9 middlebrook mycobacterial growth medium, which contains the ^{14}C-labeled substrate (palmitic acid) as a source of carbon, was used for the testing. Growth of the organism leads to the consumption of the substrate, with subsequent release of $^{14}CO_2$ into the atmosphere above the medium in the sealed vial; the BACTEC TB-460 instrument (Becton Dickinson and Company, USA) detects the amount of $^{14}CO_2$ and records it as a growth index (GI) on a scale of 0-999.

Compounds to be tested for antimycobacterial activity were filter sterilized through 0.22 micron syringe filters (millex LG) The *M. tuberculosis* clinical strain 1432 was grown on Lowenstein-Jensen culture medium for 4 weeks.[79] After incubation at 37°C, bacteria were collected, suspended in 7H9 mycobacterial growth medium and the bacterial suspension added to a BACTEC vial containing BACTEC 12B growth medium (Becton Dickinson, USA). Growth was monitored every 24 h until a GI value of 400-500 was reached. A volume of 0.1ml of this culture was added to a new BACTEC vial and the growth monitored every 24 h until a GI value of 500 was reached.[80] This culture was the primary culture and was used for testing bacterial viability against a variety of inhibitors. 0.1ml of inhibitor was added to a BACTEC vial to give a final concentration of 125 µg/ml. A 1:11 dilution with DMSO was made of the compounds to give a final concentration of 12 µg/ml and 0.1ml of this was added to a BACTEC vial. BACRWC vials were incubated at 37°C and the GI was monitored every 24 h. A GI below 10 was considered as negative growth and above 10 as positive growth. The GI of the treated samples was compared to a control containing sterile DMSO. The control experiments have shown that the final amount of DMSO (1%) in the media had no effect on the growth of *M. tuberculosis.*

Section 5.2.1: Results

The GI of the bacteria was measured over a period of 5 days, with a skip of the fourth day. Fig 5.1 represents the effect of compounds on the growth of mycobacterium.

Fig 5.1 Effect of test compounds in concentration of 5 mg/ml on the growth of the clinical strain of mycobacterium measured over a period of 5 days

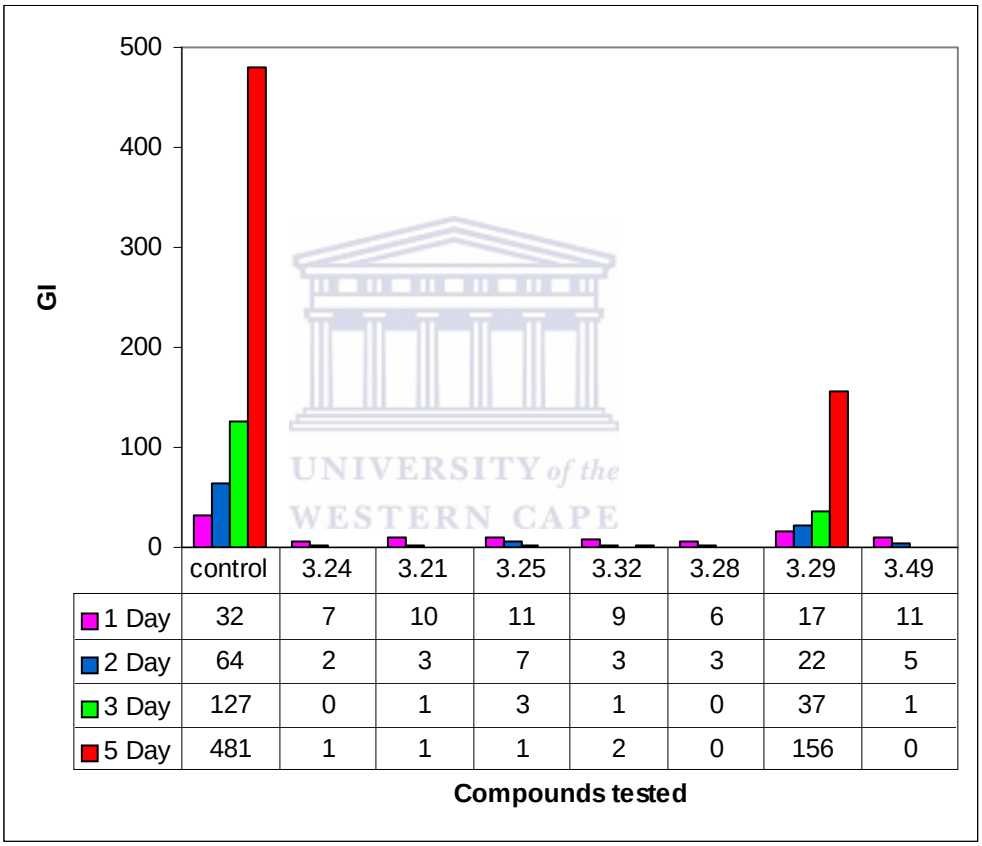

	control	3.24	3.21	3.25	3.32	3.28	3.29	3.49
1 Day	32	7	10	11	9	6	17	11
2 Day	64	2	3	7	3	3	22	5
3 Day	127	0	1	3	1	0	37	1
5 Day	481	1	1	1	2	0	156	0

The control has a normal doubling rate every 24 h. The graph in Fig 5.1 reveals that all the compounds except **3.29** have the ability to inhibit the growth of mycobacterium (clinical strain 1432) tested. This is not a true indicator of inhibitory activity since the compounds were added in very high concentration. To observe the true activity of the test compounds, dilutions were made

up to a factor of eleven i.e. 12 µg/ml. The activity of the diluted compounds in BACTEC vials was measured for the same period of time as that of the undiluted ones.

Fig 5.2 Effect of the test compounds with a 1:11 dilution on the growth of the clinical strain 1432 of mycobacterium measured over a period of 5 days

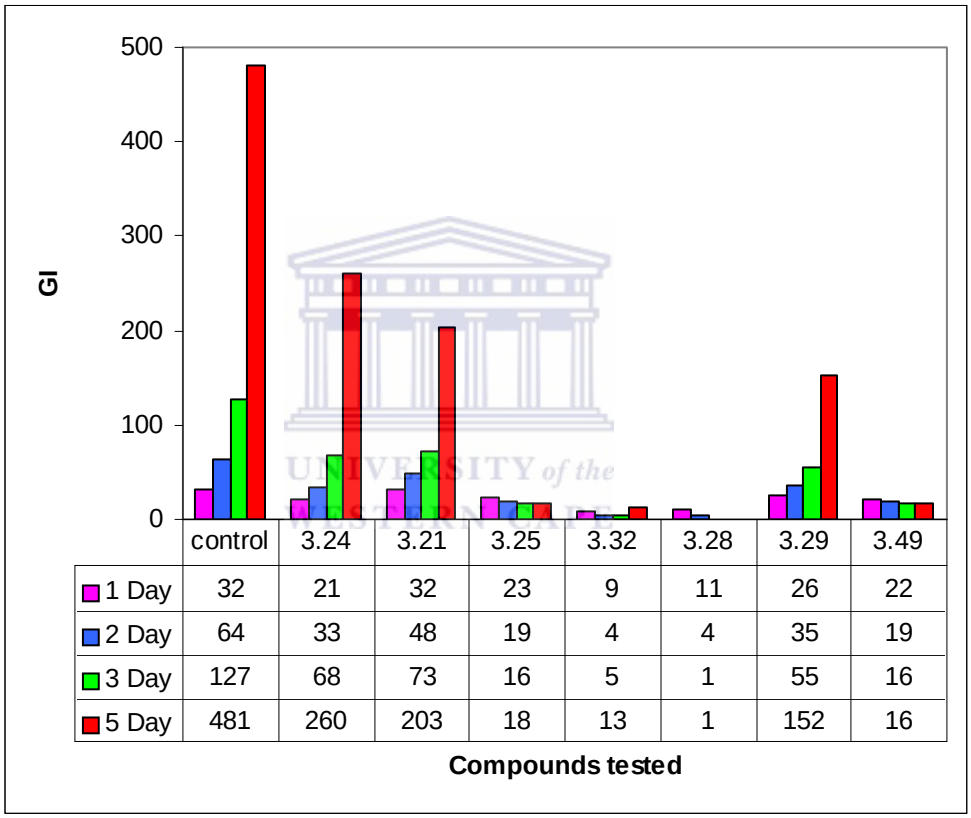

	control	3.24	3.21	3.25	3.32	3.28	3.29	3.49
1 Day	32	21	32	23	9	11	26	22
2 Day	64	33	48	19	4	4	35	19
3 Day	127	68	73	16	5	1	55	16
5 Day	481	260	203	18	13	1	152	16

It is clear from Fig 5.2 that compounds **3.32** and **3.28** demonstrate the most promising activity. These are bactericidal even at 1:11 dilution. Most of the samples show inhibition of growth at a concentration of 5 mg/ml but at 1:11 dilution, although reduced considerably, growth of cells continues. Even if the diluted versions of the test compounds other than **3.32** and **3.28** show some

growth inhibition they only appear to be bacteristatic at 12 µg/ml, a concentration much to high to even consider developing it as a drug.

The results of the analysis Fig 5.1 and Fig 5.2 reveal that the different strains of bacteria respond differently to the treatment regimes. Some of the compounds were common in two methods viz., **3.21, 3.25**, and **3.32** and others were unique to each methodology, viz., **3.24**, **3.28, 3.29 and 3.49** were tested using BACTEC method and **3.34**, **3.40**, **3.43 and 3.45** were tested using micro-dilution method. Since the two methods used to evaluate the anti-mycobacterial activities of the test compounds are entirely different in terms of their underlying principle, the results of these methods cannot be compared directly. However, a conclusion can be made based upon activities measured in the various strains of mycobacterium. It is observed here that the test compound **3.28** has enhanced activity against the clinical strain 1432 of mycobacterium as compared to all other compounds. It was further observed that binaphthoquinone types of compounds generally show good activity. This is the first time to our knowledge that biaryl compounds having as one half a naphthoquinone unit and as the other half, a naphthalene unit that also shows good activity. It is also the first time to our knowledge that sulphone **3.32** has been tested for its anti-mycobacterial activity and is now reported to show promising activity. Compounds **3.24**, **3.21** and **3.29** did not demostrate potent inhibition of the strains of mycobacterium tested. However, these are preliminary results and further indepth testing is required to unfold the true effects of compounds **3.32** and **3.28** to confirm that the observed effects are not due to cytotoxicity. As far as the different methods that were used are concerned, both are well standardized and routinely used in mycobacterium testing. The advantage of using a liquid medium is that there is more cell-to-drug contact.

Section 5.3: Discussion

Quinonoid compounds, by virtue of their facile redox cycle capacity, are known to possess wide-ranging anti-mycobacterial activities, however, the underlying mechanism of action is still unknown. More than 2000 naturally occurring quinones, for example - anthraquinones, naphthoquinones, and benzoquinones are now known and widely distributed in nature as pigments and as intermediates in cellular respiration and photosynthesis.[81, 82] Some quinones have important roles in the biochemistry of energy production and serve as vital links during electron transport. Most quinones, which are aromatic compounds present in bacteria and eukaryotes,[83] are often involved in electron transport and include, ubiquinones and menaquinones.[84]They provide a defense role as a result of their effectiveness at inhibiting the growth of bacteria, fungi, or parasites .[85- 88] Therefore, a number of them have been shown to possess physiological activities as antimicrobial and anticancer compounds.[89] The mechanism of toxicity is still under investigation, but two theories viz., redox cycling and reductive alkylation dominate the literature,[90] with some quinones proposed to exhibit one or both mechanisms.

Redox cycling is the concept in which compounds catalytically cycle and generate oxidative radicals or reactive oxygen species (ROS), such as hydrogen peroxide and superoxide, which then damage the cell. NADPH oxidases, also known as NOX proteins, produce ROS in response to exogenous stimuli. NADPH oxidases catalyze the univalent reduction of O_2 to produce O_2^-, which is rapidly converted to H_2O_2.[91]

Fig 5.3 Redox cycling of NADH or NAD(P)H and quinone.

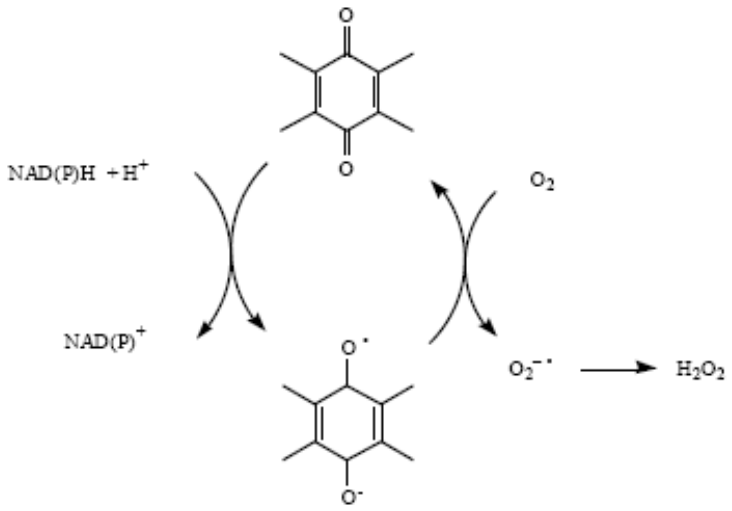

Lin[92] introduced the term "bioreductive alkylation" and this hypothesis was formalized by Moore to explain the biological activity of several natural products.[93] Moore's emphasis lay in the use of naturally occurring and synthetic quinones as potential bioreductive alkylating agents. The cytotoxic effect of these quinones can be viewed as occurring over three steps as shown in Scheme **5.1**.

1. The quinone undergoes an *in vivo* bioreduction to the hydroquinone.

2. Mesomerically assisted cleavage of a benzylic substituent by formal loss of HX results in the formation of a quinone methide.

3. Michael addition of the biological nucleophiles such as DNA, proteins or carbohydrates to the reactive enone system of the quinone methide results in the formation of covalent adducts.

Finally, after the cytotoxic effect of the quinone has been carried out, oxidation of the resulting adduct results in its biologically inactive quinone form, which is now covalently bonded to the biological target i.e. bacteria. Because of this, the cell is no longer able to carry out its normal function or to replicate, thus leading to cell death.

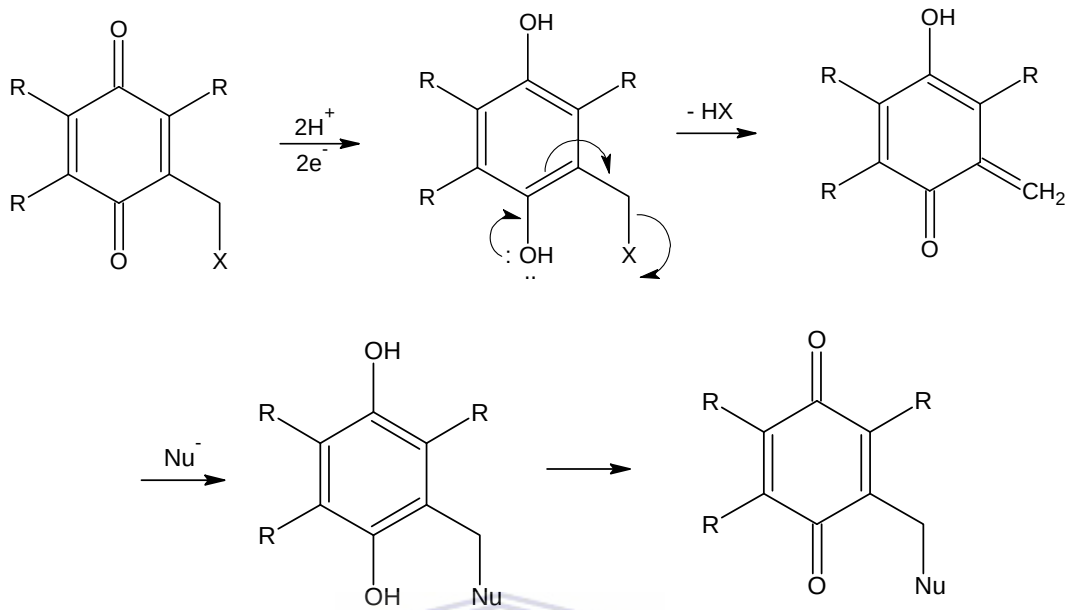

Scheme 5.1

Conclusion:

Quinone compounds are intermediates in many pathways of gene regulation, enzyme protein induction, feedback control, and waste product elimination in addition to the role as substrates and products in metabolism. Quinones play a pivotal role in energy metabolism, many other key processes, and even in chemotherapy where redox cycling drugs are utilized. However, the molecular mechanisms involved in quinone cytotoxicity and pharmaceutical activity are still mostly unknown. Their widespread use as antibiotics, antiparasitic agents, antitumor agents, and a variety of other agents makes it imperative to understand their effects on cellular function. Until this is clarified, it is not possible to use a rational approach to search for or design more effective quinone agents with less side-effects, and the current approach of random screening and analog development will continue to dominate current research.

Chapter 6: Introduction to Apoptosis

Apoptosis, or programmed cell death, is a normal component of the development and health of multicellular organisms. Cells die in response to a variety of stimuli and during apoptosis they do so in a controlled, regulated fashion including membrane blebbing, cell shrinkage, protein fragmentation, chromatin condensation and DNA degradation followed by rapid engulfment of corpses by neighbouring cells. This makes apoptosis distinct from another form of cell death called necrosis in which uncontrolled cell death leads to lysis of cells, inflammatory responses and, potentially, to serious health problems. Apoptosis, by contrast, is a process in which cells play an active role in their own death (which is why apoptosis is often referred to as cell suicide).

Section 6.1: The development of the term *apoptosis*

In 1964, term *programmed cell death* was introduced, proposing that cell death during development follows a sequence of controlled steps leading to locally and temporally defined self-destruction and is not of an accidental nature.[94] Kerr, Wyllie and Currie in 1972 coined the term *apoptosis* in order to describe the morphological processes leading to controlled cellular self-destruction .[95] The apoptotic mode of cell death is an active and defined process, which plays an important role in the development of multicellular organisms and in the regulation and maintenance of the cell populations in tissues under physiological and pathological conditions.[96]

Section 6.2: The importance of apoptosis

A complex and sophisticated interplay of cells forms multicellular organisms and during maintenance of the biological systems cells die in routine and the way in which most cells die is conserved from worm to mammal. During maintenance of body about 10 billion of our cells die

on a normal day to balance the number of new cells that arise through mitosis. During development, many cells are produced in excess, which eventually undergo programmed cell death and thereby contribute to sculpturing many organs and tissues.[97]

Apoptosis represents a process of great biological importance, being involved also in differentiation, development, proliferation, homoeostasis, regulation and function of the immune system. Thus, failures in apoptosis may result in autoimmune diseases, neoplasia and spreading of viral infections. Conversely, excessive apoptosis has been associated with other sorts of diseases, such as AIDS, neurodegenerative disorders and ischaemic diseases.[98]

Section 6.3: Characteristic morphological features of apoptosis

Apoptotic cells are characterized by morphological changes viz., the cell shrinks, shows deformation and looses contact with its neighboring cells. The cell chromatin condenses and marginates at the nuclear membrane, the plasma membrane is blebbing or budding, and finally the cell is fragmented into compact membrane-enclosed structures, called 'apoptotic bodies' which contain cytosol, the condensed chromatin, and organelles (Fig 6.1). The macrophages engulf the apoptotic bodies and are removed from the tissue without causing an inflammatory response. The sequential morphological changes are result of molecular and biochemical events within the cell undergoing apoptosis leading to activation of proteolytic enzymes, which eventually mediate the cleavage of DNA into small fragments.[99] The other mode of cell death is necrosis and in this type of cell death the cells suffer a major insult, resulting in a loss of membrane integrity, swelling and disrupture of the cells. During necrosis, the cellular contents are released uncontrolled into the cell's environment which results in damage of surrounding cells and a strong inflammatory response in the corresponding tissue.[96]

Fig 6.1 Hallmarks of the apoptotic and necrotic cell death process.[100]

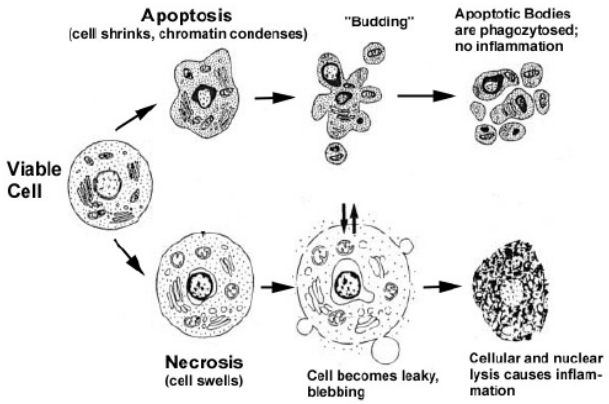

Apoptosis can be triggered by various stimuli from outside or inside the cell, e.g. by ligation of cell surface receptors, by DNA damage as a cause of defects in DNA repair mechanisms, treatment with cytotoxic drugs or irradiation, by a lack of survival signals, contradictory cell cycle signalling or by developmental death signals. There are four main groups of stimuli (Fig 6.2) for apoptosis.[101-109]

Fig 6.2 Possible mechanisms through which apoptosis can be induced (Apoptosis, Phil Dash, http://www.sgul.ac.uk/depts/immunology/~dash/apoptosis/)

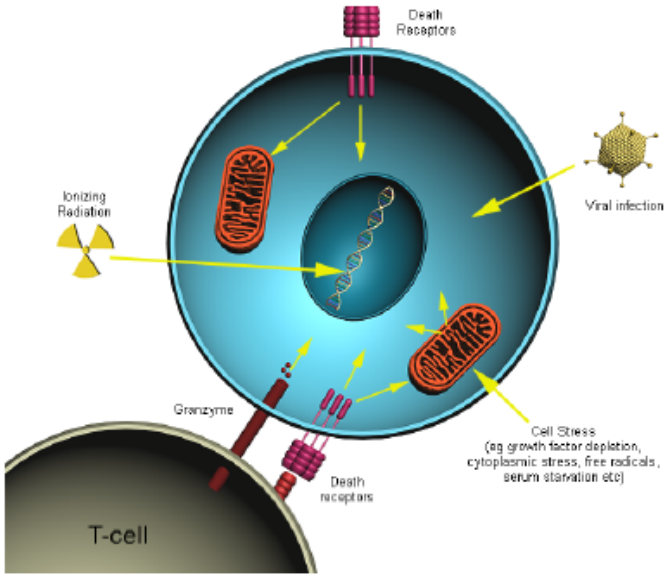

The first group of stimuli includes ionizing radiations and anticancer drugs, which are alkylating in action and cause DNA damage. The second group of stimuli induces apoptosis via receptor mechanisms, either by receptor activation mediated by glucocorticoids (acting on the thymus).[104] tumor necrosis factor-a (TNF-a), or by withdrawal of growth factors (nerve growth factor and interleukin (IL)-3).[105, 106] The third group of stimuli includes biochemical agents that include phosphatases and kinase inhibitors (e.g. calphostin C, staurosporine) and act via enhancing the downstream components of the apoptotic pathway [102]. The heat, ultraviolet light and oxidizing agents (super oxide anion, hydrogen peroxide) are classified as the fourth group of stimuli and have property to cause direct cell membrane damage. Excessive production of reactive oxygen species (ROS), such as superoxide, hydrogen peroxide and the hydroxyl radicals, produces free radicals that damage lipid membranes, proteins and nucleic acids. Many of these stimuli cause necrosis in larger doses.[107, 108]

Following an appropriate stimulus, the first stage or `decision phase' of apoptosis is the genetic control point of cell death. The cells, which do not recover during first stage after getting stimulus, enter the second stage or `execution' phase, which is responsible for the morphological changes of apoptosis. Although several pathways have been suggested to be involved in the process of apoptosis, two pathways have been the targets of extensive studies i.e signalling via mitochondria, and signaling via 'death-receptors' such as CD95 or Fas and these pathways trigger the cell to enter the first stage of apoptosis. The pathways are both further discussed below; however, it would firstly be prudent to introduce the major players in apoptosis, the caspases. Actually, cell death only can be strictly defined to follow a classical apoptotic mode if execution of cell death is dependent on caspase activity.[96]

Section 6.4: Caspases are key players of apoptosis

The term caspases is derived from Cysteine-dependent aspartate-specific proteases i.e. they cleave proteins, and their catalytical activity depends on a critical cysteine-residue within a highly conserved active-site pentapeptide QACRG, and the caspases have a property to specifically cleave their substrates after Aspartate residues. In mammals 14 different members of the caspase-family have been identified so far, whereas this number is limited to seven in Drosophila.[110, 111] According to a unified nomenclature, the caspases are referred to in the order of their publication: caspase-1 is ICE (Interleukin-1ß-Converting Enzyme), the first mammalian caspase identified.[112, 113]

The caspases are synthesized as inactive zymogens, so called procaspases, and carry a pro-domain followed by a large and a small subunit separated by a linker peptide. The procaspases are proteolytically cleaved between the large and small subunit, which result in separate small and large subunits. A heterotetramer consisting of two small and two large subunits then forms an active caspase.

The pro-domain is also frequently but not necessarily removed during the activation process. The pro-apoptotic caspases can be divided into the group of initiator caspases including procaspases-2, -8, -9 and –10, and into the group of executioner caspases including procaspases-3, -6, and –7. Whereas the executioner caspases possess only short pro-domains, the initiator caspases possess long pro-domains, containing death effector domains (DED) in the case of procaspases-8 and –10 or caspase activated recruitment domains (CARD) as in the case of procaspase-9 and procaspase-2.[114]

Fig 6.3 Hypothetical hierarchy of caspases[114]

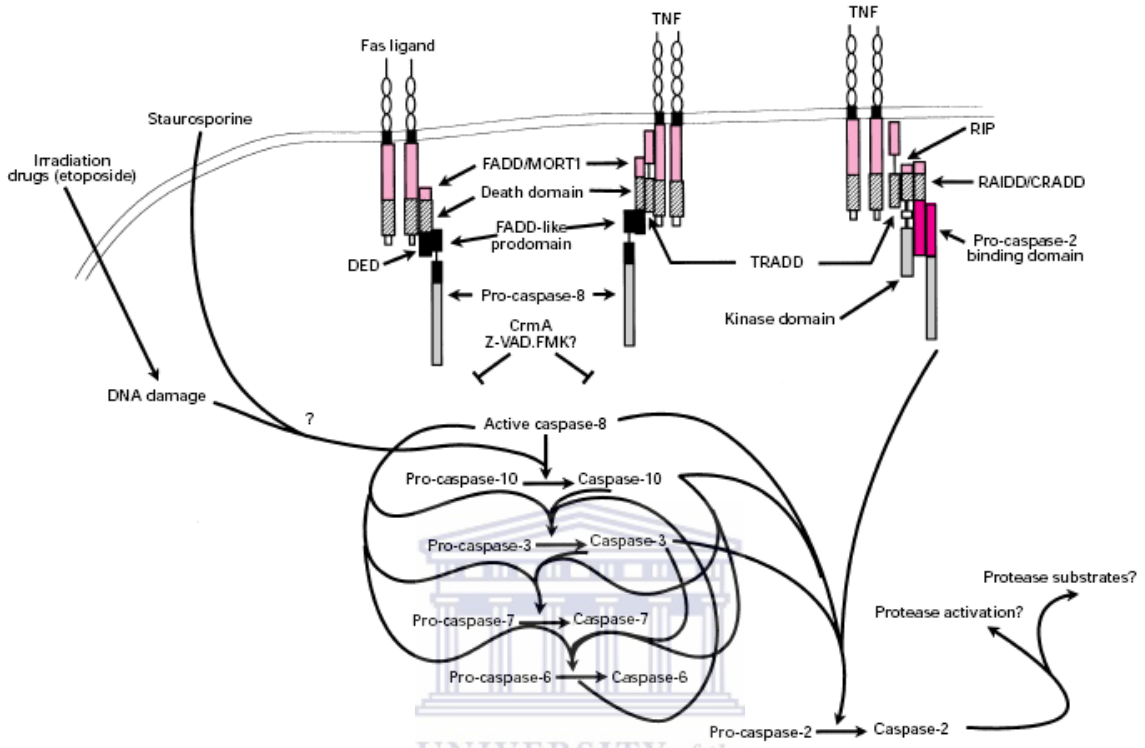

After receiving the death inducing signal the death inducing signaling complexes are activated and recruit the initiator caspases via their pro-domains either in response to the ligation of cell surface death receptors (extrinsic apoptosis pathways) or in response to signals originating from inside the cell (intrinsic apoptosis pathways).

Section 6.5: Pathways of apoptosis

Section 6.5.1: The extrinsic (receptor) pathway

The cell surface has death receptors that are activated in response to a stimulus and transmit apoptotic signals after binding to specific ligands. The extrinsic apoptosis pathway mediates this process. The extrinsic apoptosis pathway involves procaspase-8 which is recruited by its death effector domains (DEDs) to the death inducing signaling complex (DISC), a membrane

receptor complex formed to the ligation of a member of the tumor necrosis factor receptor (TNFR) family. This superfamily has several death receptors including TNFR-1, Fas/CD95 and the TRAIL receptors DR-4 and DR-5. Several procaspase-8 molecules bound to DISC are joined in close proximity and then activate each other by autoproteolysis. The signal is then transmitted through conserved death domain (DD), which is the cytoplasmic part of the death receptor. The DDs harboured by adapter molecules like FADD (Fas-activated Death Domain) or TRADD (Toll receptor activated death domain) are recruited to the DDs of the activated death receptor, and form the DISC and the local concentration of several procaspase-8 molecules at the DISC leads to their autocatalytic activation and release of active caspase-8. The caspase-8 is now ready for acting on downstream effector caspases, which subsequently cleave specific substrates resulting in apoptosis (Fig 6.4). The cells possessing the ability to induce apoptosis via direct caspase-dependent pathway are classified as type I cells. In type II cells, the signal coming from the activated receptor does not directly mediate a caspase signaling cascade and the signal is processed via mitochondria-dependent apoptotic pathway. The Bcl-2 gene family member Bid links the caspase signaling cascade and the mitochondrial pathway. Bid is cleaved by caspase-8 into the truncated form (t-BID), which translocates to the mitochondria where it acts in concert with the pro-apoptotic Bcl-2 family members Bax and Bak to induce the release of cytochrome c and other mitochondrial pro-apoptotic factors into the cytosol.[110]

Fig 6.4 Receptor-mediated caspase activation at the DISC (ApoReview, Introduction to Apoptosis, Andreas Gewies, 2003, http://www.celldeath.de/encyclo/aporev/aporev.htm**)**

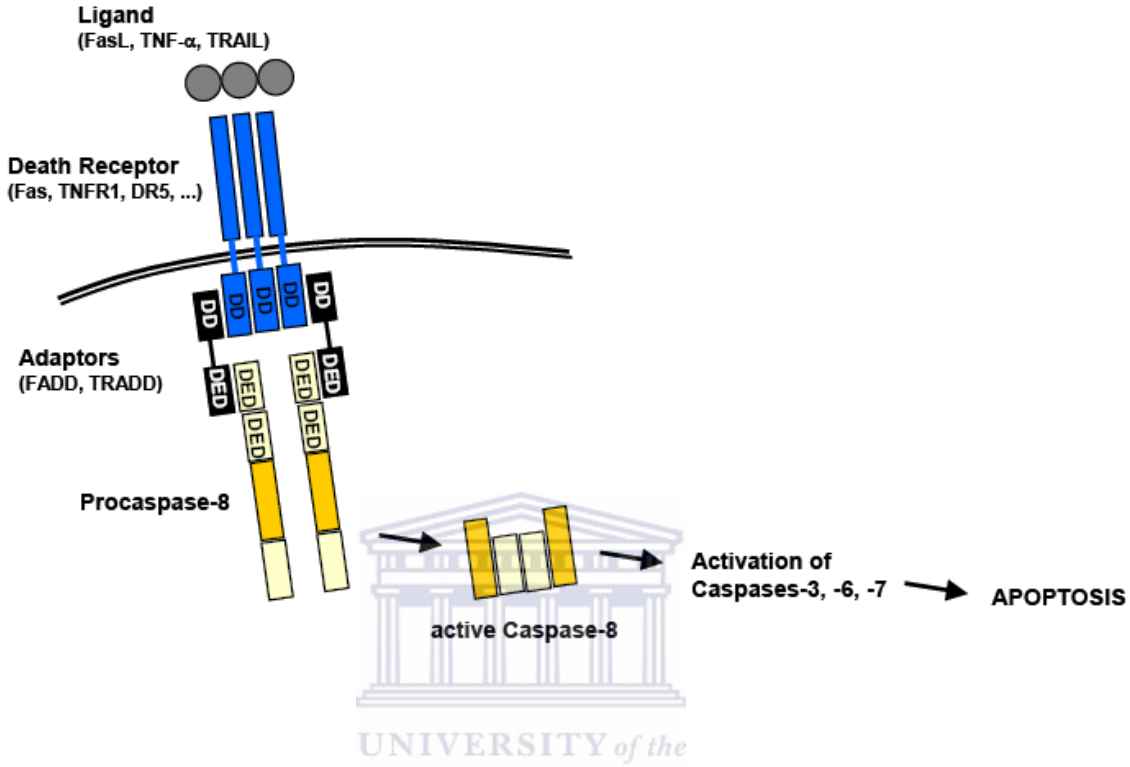

Section 6.5.2: The intrinsic (mitochondrial) pathway

The main initiator caspase in the intrinsic apoptosis pathways is procaspase-9, which is activated downstream of mitochondrial pro-apoptotic events at the apoptosome. The apoptosome is a cytosolic death signalling protein complex that is formed upon release of cytochrome C from the mitochondria.[115] In cancer, DNA damage caused by chemotherapy and irradiation activates the intrinsic pathway. Other stimuli for intrinsic pathway mediated apoptosis include hypoxia, defective cell cycle events, and deprivation of growth factors.

Fig 6.5 Mitochondria-mediated caspase activation at the apoptosome (Apoptosis, Phil Dash, http://www.sgul.ac.uk/depts/immunology/~dash/apoptosis/**)**

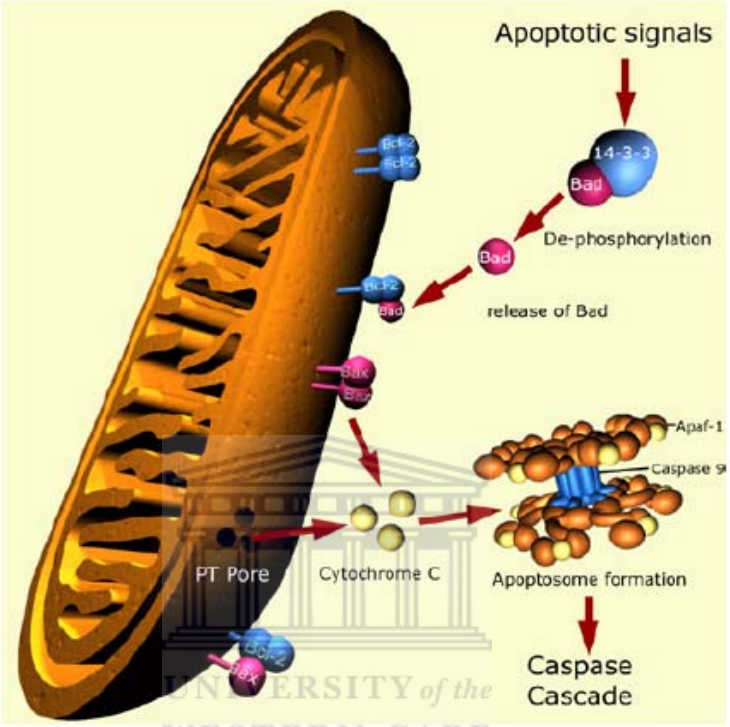

In response to an apoptotic stimulus, Bax (the prototypic pro-apoptotic protein), undergoes homodimerization and oligodimerization and inserts into the mitochondrial membrane and the increased permeabilization results in loss of membrane potential, which consequently lead to release of apoptogenic factors including cytochrome c, ATP, and SMAC/DIABLO (second mitochondria-derived activator of caspase/direct IAP binding protein with low pI). The binding of nucleotide-binding domain of apoptotic protease-activating factor 1 (APAF1) to ATP result in the formation of large oligomers (heptamers). Cytochrome c binds to APAF1 and through a CARD in APAF1, binds to a complementary CARD on procaspase-9 leading to activation of caspase 9 (Fig 6.5) and of the downstream "executioner" caspases 3, 6, and 7.[110] These activated caspases auto-induce activation of themselves as well as downstream caspases and the proteolytic

cascade, that ultimately cleaves substrates essential for cell viability, results in the characteristic biochemical and morphological changes of apoptosis.

Section 6.6: Regulation of apoptosis signaling

As described in the previous sections, the process of apoptosis is activated after encountering a specific death-inducing signal. This suggests that the apoptosis signaling pathways in viable cells are kept in an inactive state and are only turned on in response to a death stimulus. This further suggests that there must be some regulatory signals, which promote survival of cell and suppress the cell death in normal circumstances. Various growth factors, hormones and nutrients help to maintain homeostasis in organisms. It has been shown that the survival signals enhance the expression and/or activity of anti-apoptotic regulatory molecules thereby keeping in check the activation of pro-apoptotic factors.[116, 117] Follows the description of some of the anti-apoptotic molecules and mechanisms.

Section 6.6.1: The Bcl-2 family

This is the family of oncogenes that inhibits cell death rather than promoting proliferation. The discovery of this gene family demonstrated for the first time that the pathway toward tumorigenesis depends not only on the ability to escape growth control but also depends on the ability to prevent apoptosis.[118] The Bcl-2 family of proteins can be characterized by the presence of conserved sequence motifs known as Bcl-2 homology domains (BH1 to BH4). In mammals, up to 30 members have been identified under this family of which some belong to a group of pro-survival members and others to a group of pro-apoptotic members.[119] The pro-apoptotic group of Bcl-2 members is comprised of two subgroups: first, the Bax-subfamily, which consists of Bax, Bak, and Bok all possessing the domains BH1, BH2, and BH3, and the second known as the

BH3-only proteins (Bid, Bim, Bik, Bad, Bmf, Hrk, Noxa, Puma, Blk, BNIP3, and Spike) all of which have only the short BH3 motif, an interaction domain that is both necessary and sufficient for their killing action.[120, 121] The central function of mammalian Bcl-2 family members is to prevent mitochondrial membrane loss and to control the release of mitochondrial proteins into the cytoplasm.[120]

In summary, a current model of how Bcl-2 family members regulate apoptosis can be described as follows (Fig 6.6): specific apoptotic stress signals trigger the activation of particular BH3-only proteins which then interact with anti-apoptotic members on the outer mitochondrial membrane resulting in the release of Bax-like pro-apoptotic factors. Bax-like factors undergo a conformational change (possibly assisted by some BH3-only proteins), and then insert themselves into the outer mitochondrial membrane to provoke the release of apoptogenic factors.[119]

Fig 6.6 Role of various apoptosis related genes (ApoReview, Introduction to Apoptosis, Andreas Gewies, 2003, http://www.celldeath.de/encyclo/aporev/aporev.htm)

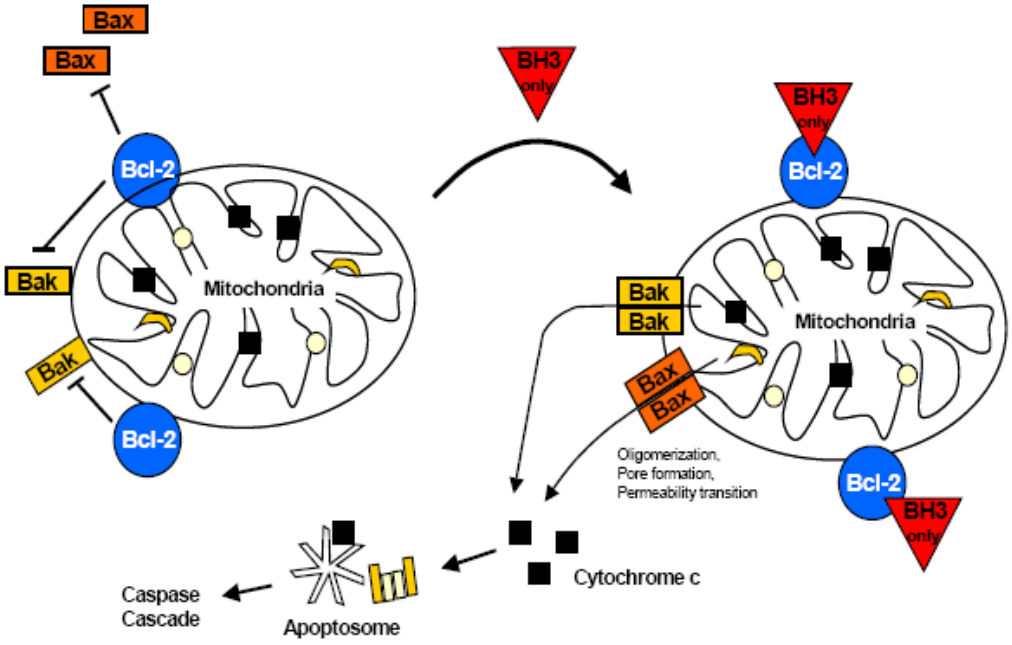

Section 6.6.2: Regulation of apoptosis by IAPs

IAPs (inhibitors of apoptosis proteins) are a family of anti-apoptotic proteins transactivated by transcription factor NF-κB, which is also a regulator of anti-apoptotic proteins such as Bcl-2, Bcl-X_L, and A1. [122, 123] In humans, eight IAPs have been identified so far, including among others NAIP, c-IAP1, c-IAP2, XIAP and survivin. The anti-apoptotic properties of IAPs are conferred by the interaction between the baculovirus IAP repeat (BIR) domains and caspases. BIR domain is a conserved 70 amino acids motif and through binding of this domain the XIAP, c-IAP1 and c-IAP2 are thought to directly inhibit caspases-3, -7, and –9.[124]

Section 6.6.3: Mitochondria as central regulator of intrinsic apoptosis pathways

Mitochondria has been demonstrated to have a key role in the integration and propagation of death signals originating from inside the cell such as DNA damage, oxidative stress, starvation, as well as those induced by chemotherapeutic drugs.[125, 126] One of the common events in mitochorial mediated apoptosis is the disruption of the mitochondrial inner transmembrane potential ($\Delta\psi$) as well as the so called permeability transition (PT) (defined as a sudden increase of the inner mitochondrial membrane permeability to solutes with a molecular mass below approximately 1.5 kDa). The influx of water into the mitochondrial matrix leads to osmotic mitochondrial swelling causing rupturing of the outer mitochondrial membrane and result in the release of pro-apoptotic proteins from the mitochondrial intermembrane space into the cytoplasm.[127] Released proteins include cytochrome c, which activates the apoptosome and therefore the caspase cascade. In addition to the release of mitochondrial factors these changes in membrane potential also affect the biochemical homeostasis of the cell: ATP synthesis is stopped, redox molecules such as NADH, NADPH, and glutathione are oxidized, and reactive

oxygen species (ROS) are increasingly generated.[128] Increased levels of ROS directly cause the oxidation of lipids, proteins, and nucleic acids, thereby enhancing the disruption of $\Delta\psi$ as part of a positive feedback.[129] Since PT, loss of $\Delta\psi$, and release of mitochondrial proteins are of central importance in mediating and enhancing apoptotic pathways, those mitochondrial events must be kept under strict control of regulatory mechanisms which are in many ways dependent on members of the Bcl-2 family.

Section 6.7: Disease as a consequence of dysregulated apoptosis

Dysregulation of apoptotic signaling has been linked to several diseases. The insufficient apoptosis leads to cancer (cell accumulation, resistance to therapy, defective tumor surveillance by the immune system), autoimmunity (failure to eliminate autoreactive lymphocytes), persistent infections (failure to eradicate infected cells), whereas excessive apoptosis contributes to neurodegeneration (Alzheimer's disease, Parkinson's disease, Huntington's disease, amyotrophic lateral sclerosis), autoimmunity (uncontrolled apoptosis induction in specific organs), AIDS (depletion of T lymphocytes), and ischaemia (stroke, myocardial infarction).[130] Mutations in the genes have been linked with the malfunctioning of the death machinery and several mutations in apoptosis genes have been identified as a causing or contributing factor in human diseases.[131]

Defective apoptosis pathways contribute to formation, progression, and metastasis of tumors as well as the as well as contribute to multi-drug resistance during cancer therapy. The impairment of apoptosis checkpoints also contribute to tumorigenesis.[132, 133]

As an example and as already mentioned, Bcl-2 was the first apoptosis-related gene that was recognized to play a role in tumorigenesis, and indeed, Bcl-2 is over expressed in a variety of cancers, contributing to cancer cell survival through direct inhibition of apoptosis.[134, 135] Conversely, mutated or down regulated Bax and Bak are observed in certain cancers[136, 137] and

disruption of those genes promotes tumorigenesis in mice.[138] During the past few years of research, p53 has emerged as a central checkpoint for apoptosis and is inactivated in more than 50% of all human cancers.[139] The tumor suppressor protein p53 is activated as a transcription factor in response to e.g. oncogene activation, hypoxia and especially DNA damage, resulting in growth arrest and/or apoptosis by stimulating the expression of various p53 target genes such as p21, Bax, Puma, Noxa, Apaf-1, Fas, and DR5[140] or by repressing the expression of anti-apoptotic proteins, e.g. Bcl-2, Bcl-XL or surviving.[141, 142] Recent evidence suggests transcription-independent p53 apoptosis pathways in which p53 translocates to the mitochondria, interacts with Bcl-X_L, induces PT and the release of cytochrome c.[143]

In non-stressed and undamaged cells, p53 is present at low cellular concentrations and it is retained in the cytosol.[144] In response to cellular stress (such as DNA damage), p53 is phosphorylated at specific serine/threonine residues, and thus p53 is stabilized and activated.[145] Moreover, p53 is central to oncogene-induced cell death because it is induced by oncogenes such as c-myc, adenovirus E1A, and ras as well as by loss of the retinoblastoma tumor suppressor pRb.[146] All those oncogenes activate the transcription factor E2F-1, which not only can promote cell cycle progression and proliferation but at the same time directly triggers expression of the tumor suppressor ARF which leads to stabilization and activation of p53.[147] This explains in part why oncogene activation not always leads to uncontrolled cell proliferation but under certain circumstances to the stabilization of p53 and activation of cell death..[148]

Section 6.8: Cell cycle regulation

The homeostasis is not only important at physiological and biochemical level, also the maintenance of genome stability is essential for normal cell proliferation. Genome stability is compromised by genotoxic agents that damage DNA, resulting in the direct or indirect induction of DNA breaks. Somatic cells are continually dividing via a highly ordered and regulated process called the cell cycle. The cell cycle comprises of four phases namely; G1 (cell grows), S (DNA replication), G2 (cell prepares to divide) and the M phase (cell division) (illustrated in figure 6.7). Cell cycle progression through these replication events is stalled at the G1/S checkpoint, the intra-S-phase checkpoint or the G2/M checkpoint if DNA damage induced by the drugs and other sources activates the DNA repair mechanism.

The G1/S checkpoint prevents cells from entering the S phase in the presence of stress, thus inhibiting replication. The exact pathway of cell cycle arrest depends on the kind of stress induced. The intra-S-phase checkpoint prevents cells from entering the G2 phase in the presence of stress encountered during replication or stress that escaped the G1/S checkpoint. The G2/M checkpoint prevents cells from entering the M phase in the presence of stress.

DNA damage can activate checkpoint pathways that lead to cell cycle arrest in the G1, S or G2 phases of the cell cycle.[149-152] DNA breaks can occur after an interference with the DNA replication machinery.[153, 154] Inhibition of the elongation stage of DNA replication activates the replication checkpoint which is closely related to the S phase DNA damage checkpoint, and leads to cell cycle arrest.[151, 155] The mechanisms proposed to generate DNA breaks during the elongation phase of DNA replication rely on events arising from the inhibition of replication fork progression.[156,157] At present, it is unclear what kind of DNA structure is detected at the

replication checkpoint; inhibition of replication elongation has been shown to result in the accumulation of single stranded stretches of DNA in yeast,[158] and can also lead to the formation of double-strand breaks (DSBs) in bacteria,[159] yeast[158] and higher eukaryotes.[154]

Fig 6.7 Cell cycle phases (Blue stars represent checkpoints)

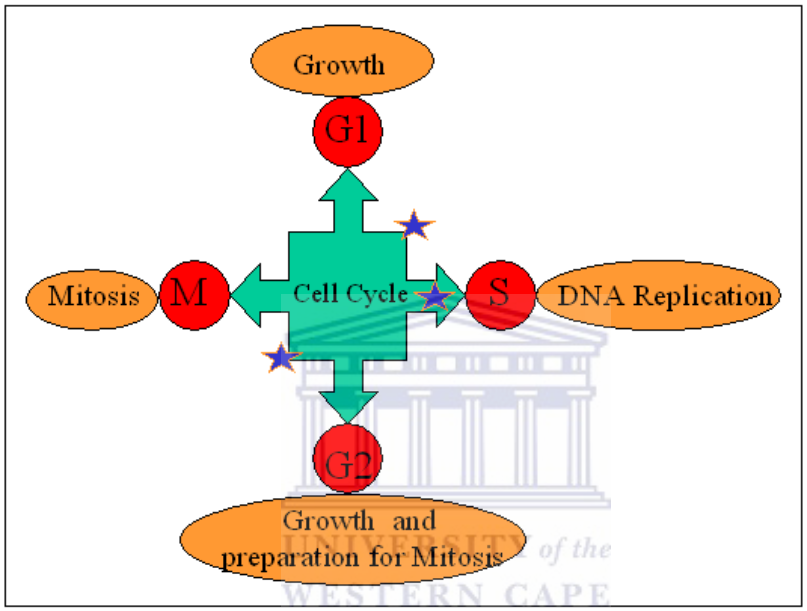

Gaining insight into the mechanisms and alterations by which components of the apoptotic machinery contribute to pathogenic processes, should allow the development of more effective, higher specificity and therefore better-tolerable therapeutic approaches. Those may include the targeted activation of pro-apoptotic tumour suppressors or alternatively the blockade of antiapoptotic oncogenes in the case of cancer, whereas for the treatment of premature cell death during e.g. neurodegeneration the inhibition of pro-apoptotic key components such as the caspases might be promising.[130] The universality of the genetic programme controlling apoptosis has helped to rapidly analyse the regulation of apoptosis in different tissues and diseases. While there are high expectations about possible therapeutics that might be targeted against apoptosis regulating factors, the ubiquitous nature of the event also sets limitations to the possible measures.

Section 6.9: Plant-derived anti-cancer drugs

For centuries, medicinal plants have been the biggest source of relief from several ailments. During recent years the extraction of active compounds from the plant extracts has been an area of active research and several currently used drugs for cancer are either directly extracted compounds or are derivatives of these compounds. The web page (http://biotech.icmb.utexas.edu/botany/chemtab.html) provides very succinct information about the plant-derived compounds. Some of the currently used plant-derived compounds in cancer treatment are summarized below:

Section 6.9.1: Paclitaxel (6.1) and Docetaxel (6.2)

These drugs were originally extracted from the bark of the *Taxus brevifolius* . Docetaxel (6.2) is a derivative of Paclitaxel **6.1** and is twice as effective in causing G_2-M arrest during cell cycle as compared to the parent compound. Paclitaxel **6.1** is used to treat breast, ovarian, lung and oesophageal cancers. [161]

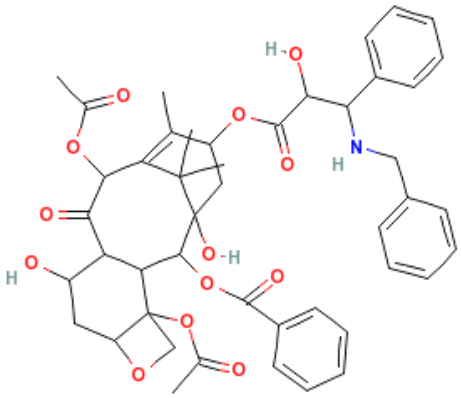

6.1

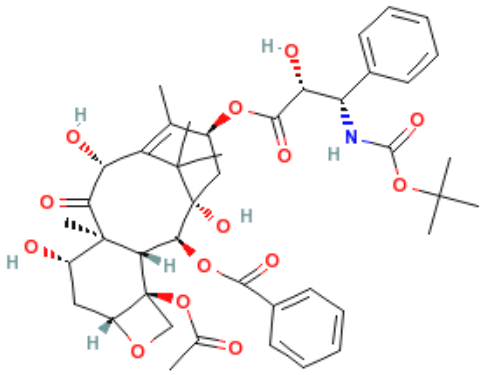

6.2

Docetaxel **6.2**, is also an intravenous drug that is being tested on carcinomas of the bladder, cervix, lung, and ovaries, on malignant melanoma; and on non-Hodgkin's lymphoma.

Section 6.9.2: Camptothecin 6.3 and Topotecan 6.4

Camptothecin **6.3** is a quinoline-based alkaloid isolated from the bark of the C*amptotheca acuminata* (Nyssaceae). Camptothecin **6.3** and its derivatives aminocamptothecin, CPT-11 [irinotecan], DX-8951f, and topotecan **6.4** act as DNA topoisomerase-I inhibitors and target the cell during S–phase of cell cycle.[162]

Topotecan **6.4** is approved to use for the treatment of advanced ovarian cancers, and irinotecan HCl as a treatment for metastatic cancer of the colon or rectum.

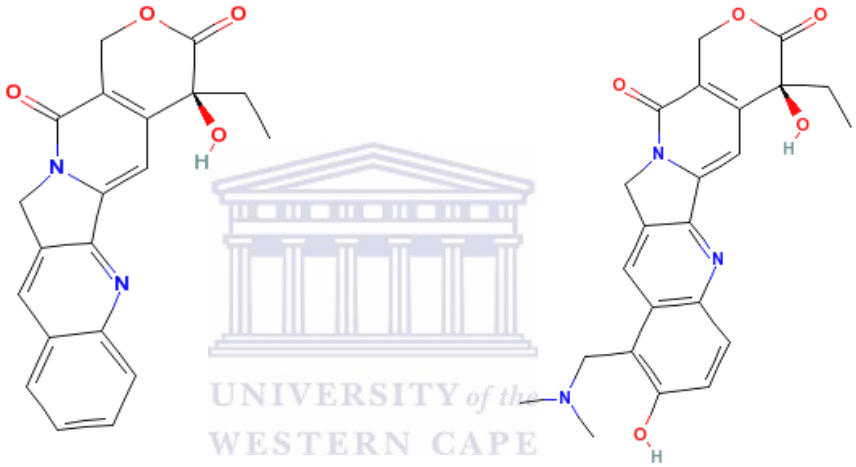

6.3 **6.4**

Section 6.9.3: Colchicine **6.5**, a water-soluble alkaloid and mitosis inhibitor, was isolated from the C*olchicum autumnale.*

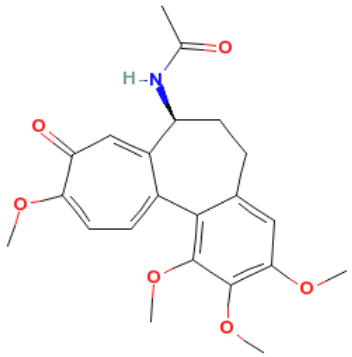

6.5

Cancer cells divide more rapidly than normal cells and thus are more susceptible to being poisoned by mitotic inhibitors such as colchicines **6.5**, paclitaxel **6.1**, and the Vinca alkaloids.[163] However, colchicines **6.5** has proven to have a fairly narrow range of effectiveness as a chemotherapy agent, so its only FDA-approved for use in the treatment of gout.

Section 6.9.4: Podophyllotoxin 6.6 and etoposide 6.7

Podophyllotoxin **6.6** was extracted from the P*odophyllum peltatum* (Berberidaceae). Etoposide **6.7**is a derivative of podophyllotoxin **6.6** and both block the cell cycle in G1 phase and the S phase and induce breaks in DNA via an interaction with DNA topoisomerase II.[164] Podophyllotoxin **6.6** has been found effective against genital infection caused by the human papillomavirus (HPV). Etoposide **6.7** is used mainly to treat testicular cancer. It is also used to treat chorionic carcinomas, lymphomas and malignant melanomas.[165]

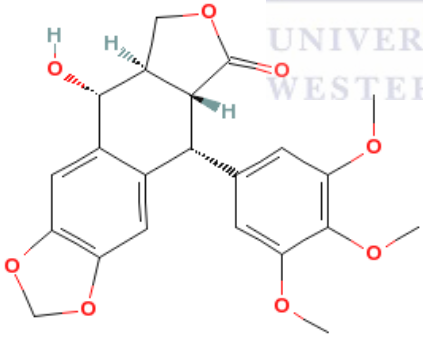

6.6

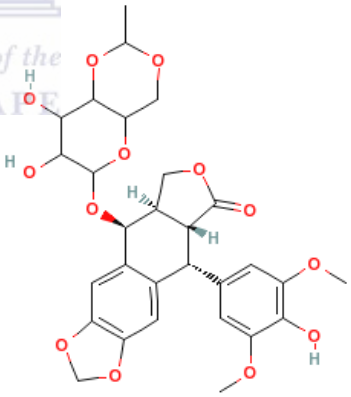

6.7

Section 6.9.5: Tetrahydrocannabinol 6.8

Tetrahydrocannabinol (THC) **6.8** was first extracted from *Cannabis sativa* (Cannabaceae). THC's derivative Delta-trans-tetrahydrocannabinol commonly known as Dronabinol is recognized as an appetite stimulant and anti-nausea/vomiting (antiemetic) agent.[166]

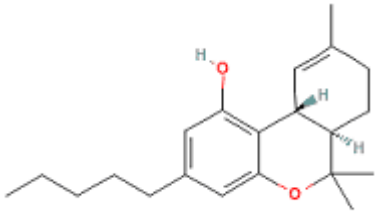

6.8

It inhibits nerve impulse that causes nausea and is used to treat chemotherapy related nausea and glaucoma.

Section 6.9.6: Vinblastine 6.9, vincristine 6.10 and vindesine 6.11

Vinblastine **6.9** and vincristine **6.10** are alkaloids found in the *Catharanthus roseus*. Vindesine **6.11** is a semi-synthetic derivative of vinblastine **6.9** and all of these alkaloids works by inhibiting mitosis in metaphase.

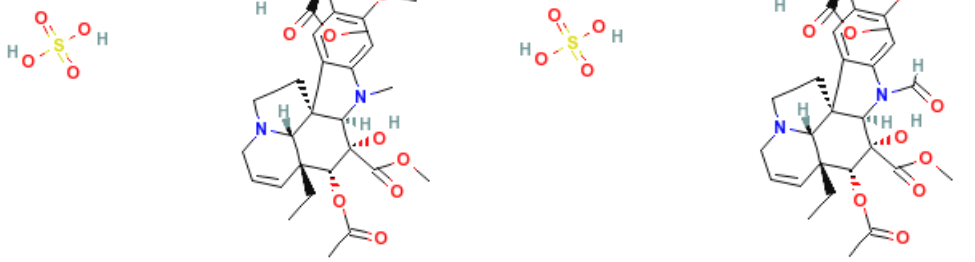

6.9 **6.10**

Vinblastine **6.9** is useful for treating Hodgkin's disease, lymphocytic lymphoma, histiocytic lymphoma, advanced testicular cancer and advanced breast cancer. Vincristine **6.10** is used mainly to treat acute leukemia, neuroblastoma, Hodgkin's disease and other lymphomas.

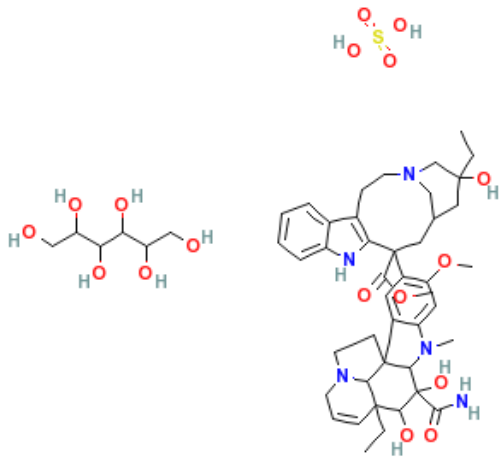

6.11

Vindesine **6.11** is used to treat melanoma and lung cancers. It is also effective in treating uterine squamous cell carcinomas.

Current plant derived anti-cancer drugs primarily target cell cycle phases and thus their toxicity is not restricted to cancer cells. Clinical application of these drugs has been partially successful, as they have been administered in phases and in combination with other anti-cancer agents. The research community thus endeavors to identify site specific, non-toxic novel anti-cancer drugs that target the underlying genetic components of malignancy in an effort to overcome the cytotoxic effects of conventional drugs.

In recent years, apoptosis has become an important issue in biomedical research. The rate of apoptosis significantly affects the life span of normal as well as cancer cells within a living system. Because apoptosis is a discrete manner of cell death that differs from necrotic cell death and is regarded as an ideal way to eliminate damaged cells, agents that can modulate apoptosis may be used for the management and therapy of cancer by modulating the steady-state cell population.

Chapter 7: Evaluation of the compounds for Apoptosis

The objective of this section is for the purposes of undertaking preliminary screening for anti-cancer activity of the synthesized analogues of diospyrin **1.22**, which has demonstrated encouraging anti-tumor activity. The literature indicates that with a few modifications to the basic structure, the anti-tumor activity of diospyrin **1.22** can be enhanced.[167] In the present study, a few novel analogues of diospyrin **1.22** viz., **3.20, 3.21, 3.25, 3.32** were synthesized and subjected to anti-tumor evaluation. The Biotechnology department of University of the Western Cape, Cape Town has in house facilities available to undertake apoptosis analysis. The choice of the cell lines was restricted to the routinely used cell lines in the department. Thus, this chapter reports on the cytotoxicity (via the neutral red colorimetric assay) of test compounds on the 'normal' non-transformed mammalian cell line; the CHO (Chinese Hamster Ovaries) cell line and apoptosis activity (via APOpercentage™ assay, Biocolor Ltd) on three cancer cell lines namely; MCF-7 (human breast adenocarcinoma), HeLa (human cervical carcinoma), MG-63 (human bone osteosarcoma). The cytotoxic and apoptotic activity was used to identify the synthetic analogue having the most significant anti-cancer activity. This pro-apoptotic activity was conclusively demonstrated with more specific markers of apoptosis namely; the externalisation of phosphatidylserine, DNA fragmentation and cell cycle apoptosis.

Section 7.1: Material Used

Section 7.1.1: General chemicals and assay kits

Active Caspase – 3 FITC Mab Apoptosis Kit	BD Biosciences
APOpercetage™ apoptosis assay	Biocolor Ltd

Crystal Violet	Sigma
DMSO (Dimethyl sulphoxide)	Sigma
Ampicillin	Roche
APO-DIRECT™ Kit	Roche
Propidium Iodide (1 mg/ml in 3.8 mM sodium citrate)	Sigma
RNase	Roche
Phosphate Buffer Saline (PBS) (Ca^{++}, Mg^{++} free)	Sigma
Camptothecin	Sigma

Section 7.1.2 Tissue culture media components and cell lines

Invitrogen supplied tissue culture media:

Dulbecco's modified eagle medium (DMEM) with 4500mg/l glucose and Glutamax™

Nutrient mix Ham's F12 with L-glutamine

RPMI 1640 medium with L-glutamine

100x penicillin streptomycin

Foetal calf serum (FCS)

Media composition:

Complete Ham's F12 = Ham's F12 + 0.2 % penicillin streptomycin + 5 % FCS

Complete DMEM = DMEM + 0.2 % penicillin streptomycin + 10 % FCS

Complete RPMI = RPMI + 0.2 % penicillin streptomycin + 10 % FCS

Table 7.1 The cell lines used during apoptosis analysis

Species	Cell lines	Medium	Serum
Hamster	CHO 22	Hams F12	5 % FCS
Human	HeLa	DMEM	10 % FCS
Human	MCF7	RPMI 1640	10 % FCS
Human	MG-63	DMEM	10 % FCS

Section 7.2: General Methods for cell culturing and various apoptosis assays

Section 7.2.1: Thawing of cells

The frozen cell filled cryovials were removed from storage at -150^{o}C and immediately thawed in a 37^{o}C water bath. The contents of the vials were then transferred into a 15 ml tube containing 5 ml Hams F12 media. The 15 ml tube was centrifuge for 2min. @ 2000rpm. The supernatant was discarded whilst the pellet was re-dissolved in 5 ml relevant media (specific for different cell lines) that was transferred to a 25cm^2 tissue culture flask for incubation. All the cell lines used were adherent and were incubated at 37^{o}C in a humidifier atmosphere of 5 % CO_2.

Section 7.2.2: Trypsinization of cells

Once cells reach confluency, cells need to be trypsinized (or potentially die of overcrowding). The media in the flask was then discarded. Cells were washed with trypsin, then allowed to trypsinized with 3 ml of 0.0625 % trypsin in hood. After 3 min., 12 ml of media was added to the trypsin (to stop trypsinization). The cells were split into three 25cm^2 tissue culture flasks for incubation (media in flasks are topped up to a minimum of five milliliters).

Section 7.2.3: Freezing of cells

To ensure continuity of cell lines, cells were grown to confluency and then stored at -150^{o}C. To store cells they were trypsinized after which the pellet was re-dissolved in a 10 % DMSO and 90 % media mixture. The suspensions were aliquoted into 2 ml cryovials, then stored at -150^{o}C.

Section 7.2.4: Seeding of cells

Once cells have been thawed and incubated in a 25cm^{2} tissue culture flask, they will be left for 48 h to 72 h to grow to confluency. The cells can then be used for various experiments and are ready to be seeded in the appropriate well plates for testing. That is, cells are trypsinized, and are then counted using a Hausser Scientific Fuchs Rosenthal Ultra Plane Hemocytometer using crystal violet dye and seeded at a concentration of 2.5x10^{4} cells per well. When 6, 24 or 96 well plates were used 2 ml, 500 µl or 100 µl of cells were seeded respectively. Cells were incubated overnight at 37^{o}C for 24 h.

Section 7.2.5: Dissolving compounds

The compounds were dissolved in DMSO to obtain a final concentration of 100µl. This was the stock solution and further required dilutions were made from this stock. The stock was stored at -20 ^{o}C and the dissolved compounds were stable during storage.

Section 7.3: Tests authenticating the induction of apoptosis

Section 7.3.1: Cytotoxicity assay

CHO cells were seeded in 96 well tissue culture plates and treated with compounds of concentrations ranging from 0.625µM to 10µM for 24 h with in triplicate. The supernatants were removed from the well, cells were washed with PBS and 100 µl of neutral red solution (100 µg/

ml, in serum free media) was added to each well. The plates were incubated for 2 h at 37°C. Wells were washed rapidly with 100 µl, 1 % paraformaldehyde. Nutrient red (NR) dye from the cells was extracted by adding 100 µl of NR desorb to each well. The plates were incubated for 15min. and then placed on a shaker for an additional 30 min. before determining the optical density at 540 nm (OD_{540}) on a multi-well spectrophotometer. Cytotoxicity is calculated as follows:

$$\% \text{ cytotoxicity} = \frac{\text{Abs of negative control} - \text{Abs of treated cells}}{\text{Abs of negative control}}$$

Where Abs = Absorbance measured using spectrophotometer

Section 7.3.2: APOpercentage™ assay

The APOpercentage dye was prepared by adding 15.9 ml media to 0.1 ml APOpercentage dye. Cells were seeded in 24 well tissue culture plates and tested for 24 h with concentrations ranging from 0.625µM to 10µM in triplicate. After the cells were treated with the test compound, the supernatant was removed and placed in 15 ml tubes. Cells were washed with 1 ml PBS and trypsinized with 300 µl trypsin. Cells were centrifuged @ 3000 rpm for 5 min. Cells were re-suspended in 200 µl of the prepared APOpercentage dye, followed by incubation for 30 min. at 37°C. The cells were washed with 2 ml PBS to remove excess dye. The cells were analyzed within one hour on a (Fluorescent Activated Cell Sorting) FACScan instrument using CELLQuest PRO software (BD Biosciences). The cell fluorescence was measured by flow cytometry using the FL2 channel and a minimum of 10 000 events was acquired per sample.

Section 7.3.3: APO-DIRECT™ Kit (DNA fragmentation)

The cells were seeded in 6 well tissue culture plates and cells were exposed to the required concentration of the compounds (**3.20, 3.21, 3.25, 3.32**) for 48 h and 72h. After the cells were treated with the compound, cells were trypsinized and re-suspended in 5 ml of 1 % (w/v) paraformaldehyde in PBS and placed on ice for 15 min. The cells were centrifuged @ 3000 rpm for 5 min. and the supernatant was discarded. The cells were washed twice in 5 ml of PBS followed by centrifugation @ 3000 rpm for 5 min. The cells were re-suspended in 0.5 ml of PBS and 5 ml of ice-cold 70 % (v/v) ethanol was added drop by drop and cells were stored in 70 % (v/v) ethanol at –20^{o}C for 48 h. The cells were removed from storage and centrifuged at 3000 rpm for 5 min. at room temperature and supernatant was discarded and cells were re-suspended in 1 ml of wash buffer supplied with the kit. The cells were centrifuged as before and the supernatant agsin discarded and the washing with wash buffer was repeated. The cell pellet was resuspended in 50 ml of the staining solution (prepared as described in table 7.2). The cells were incubated in the staining solution for 60 min at 37^{o}C. At the end of the incubation, 1 ml of rinse buffer was added to each tube and the cells centrifuged as before. The supernatant was removed by aspiration. The treatment with rinse buffer was repeated and the cells were re-suspended in 0.5 ml of the Propidium Iodide (PI)/RNase A solution. The cells were incubated in the dark for 30 min. at room temperature. The cells were analysed in Propidium Iodide/RNase solution within 3 h on FACScan instrument using CELLQuest PRO software after time intervals 48 and 72 h.

Table 7.2 APO-DIRECT^{TM} kit staining solution

Staining Solution	1 Assay (µl)	4 Assay (µl)
TdT reaction	10	40
TdT enzyme	0.75	3
Fluorescein-dUTP	8	32
dH_2O	32	128
Total volume	50.75	203

Section 7.3.4: Cell Cycle analysis with Propidium Iodide (PI):

The cells were seeded in 6 well tissue culture plates and cells were induced with 10 µM concentration of the compound for 24 h, 48 h and 72h. After completion of incubation, the cells were gently trypsinized using 500 µl trypsin. The trypsinized cells were then harvested and were washed with 5 ml of PBS using centrifugation. The cell pellet was re-suspended in 200 µl PBS and 4 ml ice-cold 70% ethanol was added drop-wise to prevent aggregation of cells and was mixed well. The cells were fixed at -20^{o} C for at least 48 h. After the fixation, the cells were washed with 5 ml 1x PBS by centrifuging at 3000 rpm for 5 minutes. The cells were re-suspended in PI master mix and were incubated at 37^{o} C for 30 minutes. The cells were stored on ice until analysed by FACScan instrument using CELLQuest PRO software (BD Biosciences). The cell fluorescence was measured by flow cytometry using the FL2 channel and a minimum of 10 000 events was acquired per sample.

PI Master Mix (10 ml):

PBS	9.5 ml
RNase	100 µl
PI	400 µl

Section 7.4: Results

Section 7.4.1: Screening cytotoxic effects of compounds using the neutral red (NR) assay

The cytotoxicity of a compound is believed to be an indicator of its apoptotic potential. The cytotoxicity test is routinely used in the preliminary screening of the compounds extracted from plants and their anti-cancer activities. The neutral red (NR) cytotoxicity assay is a cell viability assay based on the ability of viable cells to incorporate and bind the NR dye. NR is a weak cationic dye that penetrates cell membranes by non-ionic diffusion and accumulates intracellularly at the anionic sites in the lysosomal matrix. Alterations in the cell membrane or the sensitive lysosomal membrane lead to lysosomal fragility.[168, 169] As a consequence, only cells that are intact (viable) will bind NR dye i.e. the viable cells with an intact lysosomal membrane will be stained with the dye while the dead cells with lysosomal membrane damage will not be labelled. It thus follows that the dye trapped within live cells can be released, quantified and expressed as a function of cell death.

Fig 7.1 shows the percentage of apoptotic cells in CHO cell line observed in response to various concentrations of compounds. The compound **3.32** showed the maximum killing (60%) at a 5 µM concentration followed by a sharp increase in cytotoxicity by **3.20** at 10 µM. Two other compounds **3.21** and **3.25** had no cytotoxic effects on the CHO cells under similar conditions.

Fig 7.1 Test compounds screened for cytotoxicity on CHO cell line

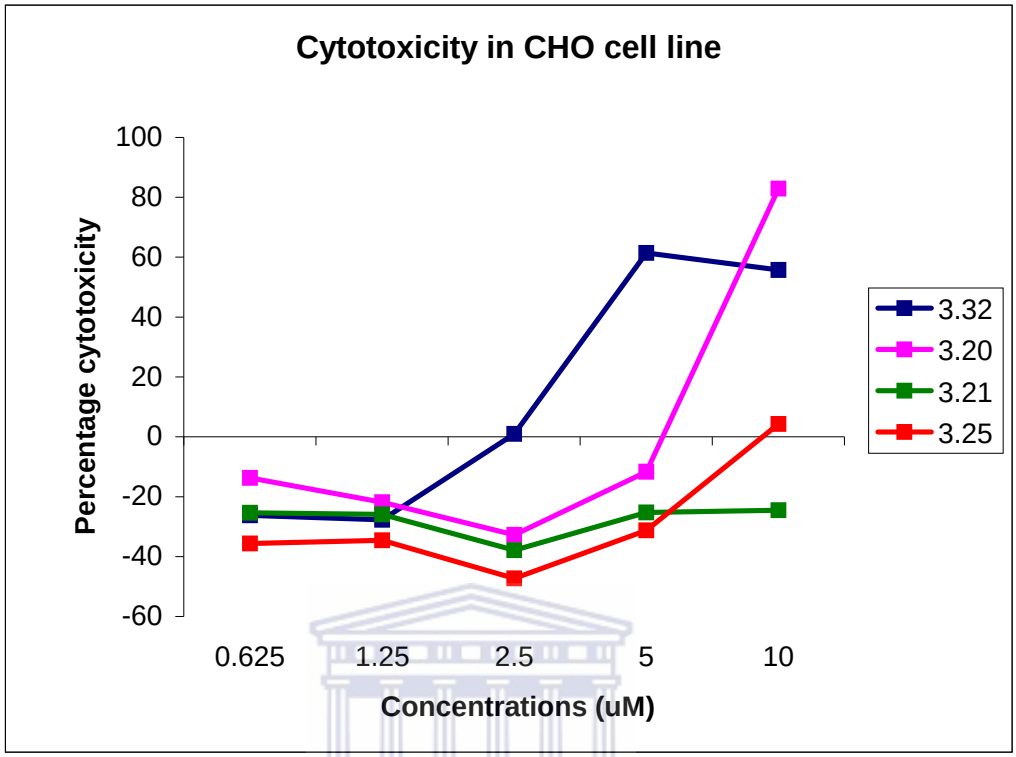

The cytotoxicity test is considered a preliminary test for screening compounds as potential apoptosis inducers. However, a recent study by M Essack, Masters thesis, UWC, submitted in 2007, demonstrated that cytotoxicity is not such a good indicator of apoptotic potential of a compound. Keeping this in mind, it was decided to perform apoptosis analysis on all four compounds as shown in Fig 7.1.

Section 7.4.2: TheAPOpercentage™ assay

Apoptosis may be defined as programmed cell death characterized by certain morphological features such as membrane asymmetry and attachment, condensation of the chromatin, and internucleosomal cleavage of DNA. In cells at early stage of apoptosis, the membrane phospholipid phosphatidylserine (PS) is externalized to the outer-leaflet of the plasma membrane. The APOpercentage™ assay is a dye uptake assay, which stains apoptotic cells with a red dye

(Biocolor Ltd). This exposure of the PS allows the unidirectional uptake of the APOpercentage™ dye.[170] As a consequence, only cells that have undergone apoptosis i.e. externalization of phosphatidylserine; will be dye labeled, whereas the normal and necrotic cells that are present remain unlabelled. The experiments were performed in triplicates and the average was used to represent killing.

Fig 7.2 indicates that all four test compounds have different apoptotic abilities in CHO cells. The compounds **3.32** and **3.20** showed maximum induction of apoptosis in CHO cells at 5 μM, with not much change at 10 μM. Compound **3.25** was also active with 90% of apoptotic cells at 10 μM. An initial increase was observed followed by a decrease in case of compound **3.21**.

Fig 7.2 Test compounds screened for apoptosis activity on the CHO cell line

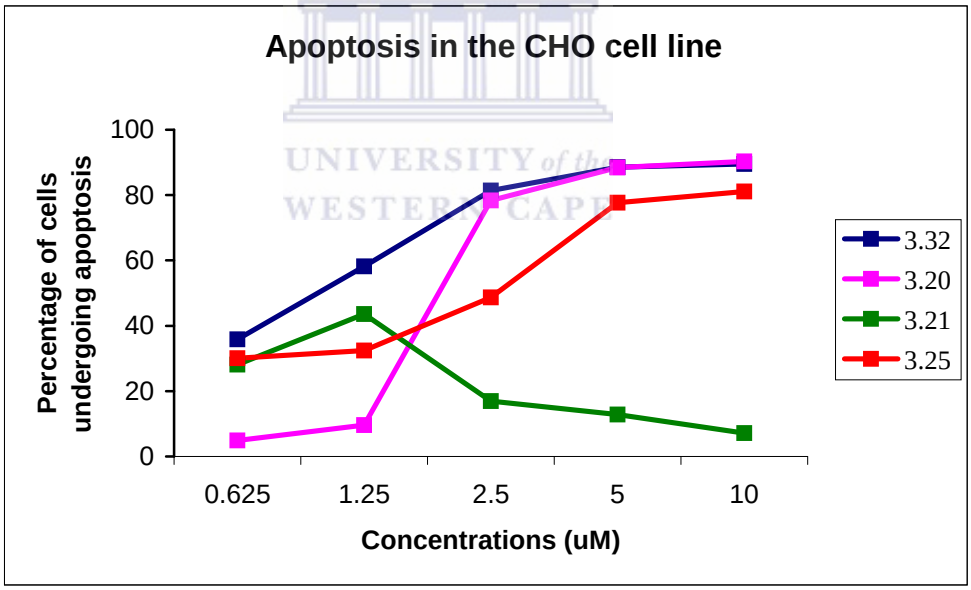

Compound **3.25** showed negligible cytotoxicity, but when observing the percentage of cells undergoing apoptosis measured using the APOpercentage assay (Fig 7.2) it is clear that compound **3.25** do have apoptotic potential.

In Fig 7.3 it can be clearly seen that compound **3.32** induced apoptosis in MCF-7 cells (65%) in relation to the other two compounds that caused a less than 20% of cells to undergo apoptosis

even at a concentration of 10 μM. The important observation here is the selective killing induced by compound **3.32** against MCF-7, which is a breast cancer cell line and is deficient in caspase-3.[171] This selectivity could be contributed to in part, the underlying mechanisms of apoptosis.

Fig 7.3 Test compounds screened for apoptosis activity on MCF-7 cell line

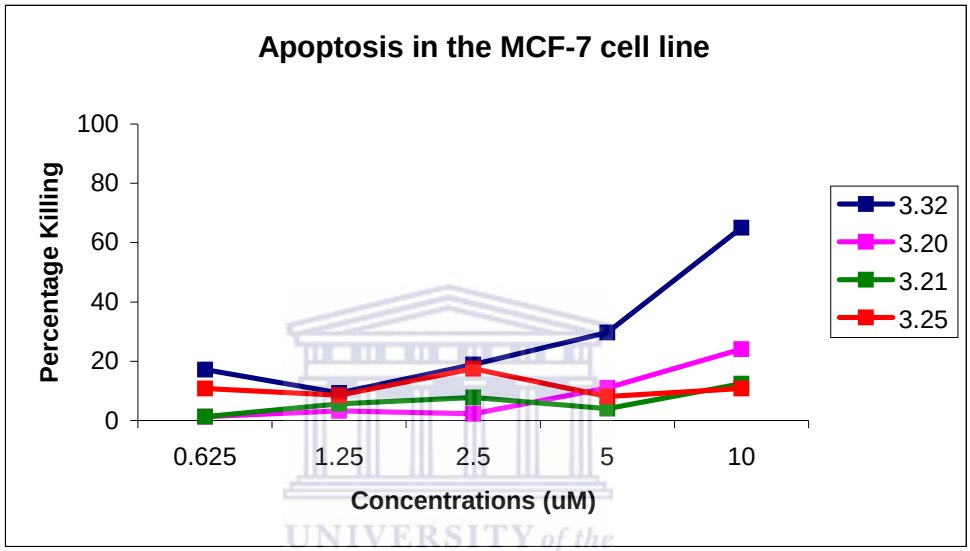

Fig 7.4 indicates that compound **3.25** displayed the highest apoptosis activity (67%) at 10 μM. In this case compounds **3.20**, **3.21** and **3.32** all displayed negligible apoptosis activity.

Fig 7.4 Test compounds screened for apoptosis activity on the HeLa cell line

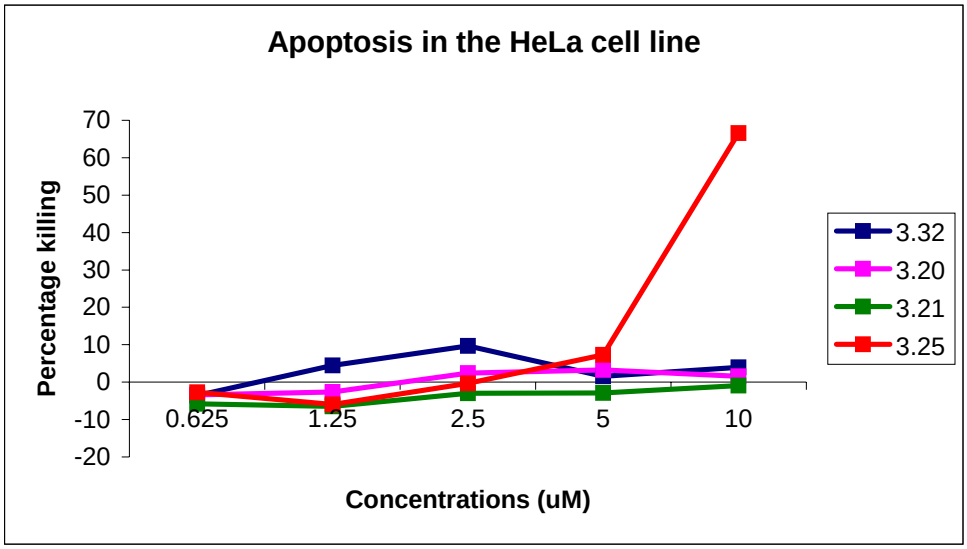

In culture, **3.25** have been shown to selectively kill HeLa cells (70%) at a concentration of 10 μM. This selective killing could be due to different signalling pathways used by the various compounds in the different cancer cells.

Fig 7.5 Test compounds screened for apoptosis activity on the MG-63 cell line

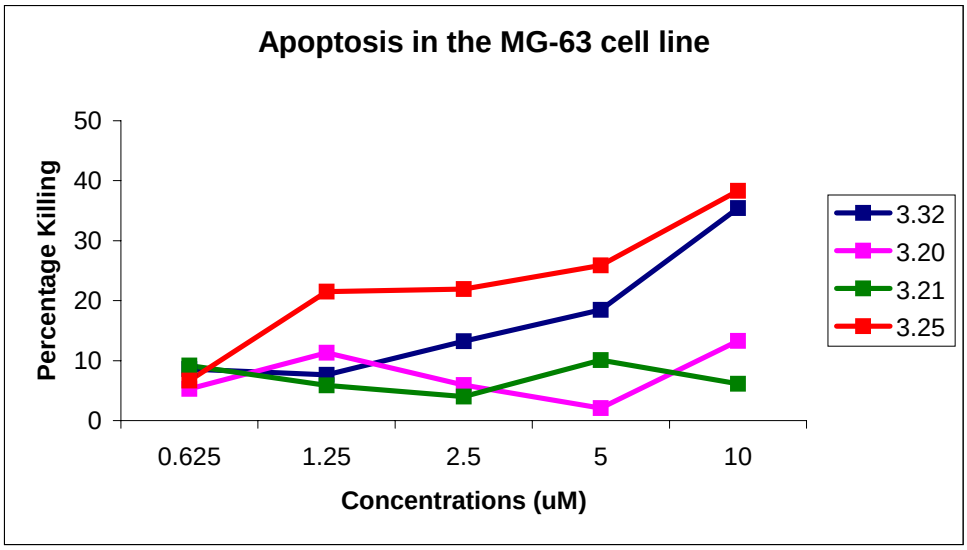

In Fig 7.5 it is obvious that compounds **3.25** and **3.32** displayed apoptosis activity (above 35%) in relation to the other two compounds in MG-63 cell line that only caused 10% of the cells to become apoptotic.

The results for the CHO cell line proved that the cytotoxicity test (Fig 7.1) is not that reliable since **3.25** displays significant apoptosis activity but negligible cytotoxicity, indicating that this compound would have been mistakenly eliminated during the initial screening process. Test compounds **3.32**, **3.20** and **3.21** induced the highest degree of apoptosis activity for the CHO cell line as opposed to MCF-7 and HeLa cells which displayed the maximum apoptosis with test compounds **3.32** and **3.25** respectively. This is to be expected, as the CHO cell line is a 'normal' animal cell line that should not have any mutations affecting its ability to undergo apoptosis, that is; it should have a larger array of apoptosis inducers. Also, MCF-7 in particular has been characterized with caspase-3 gene mutation.[171] From the extensive coverage of the most common extrinsic and intrinsic pathways in section 6.5 it can be inferred that these pathways commonly converge at caspase-3. This highlights the reason why the presence of caspase-3 is recognized as a hallmark of apoptosis and accounts for the high resistance to apoptosis inducers displayed by the MCF-7 cell line. It can thus be deduced that test compound **3.32** can induce an apoptotic pathway independent of caspase-3. Test compound **3.25** was found to be most active apoptosis inducer for the HeLa cell line. Additionally, **3.32** and **3.25** are both active in MG-63 cell line at a 10 μM concentration, indicating that **3.32** might have both a caspase-3-dependent and a caspase-3-independent mode of action, since **3.32** is also active in the caspase-3 deficient cancer cell line MCF-7. An analysis of the above graphs reveals that the compounds have selective killing properties in different cell lines. The purpose of the above analyses was to identify a lead compound, which could be subjected to further testing for identifying downstream apoptotic

signals. Since **3.25** has shown outstanding results in three of the cell lines, it was therefore decided to perform further analyses for testing the specific hallmarks of apoptosis, using this compound at a 10 μM concentration. Since test compound **3.25** was most active in HeLa cell line, it is logical to use this cell line for performing downstream apoptosis analyses.

Section 7.5: Screening 3.25 for specific markers of apoptosis

Section 7.5.1: DNA fragmentation

The fragmentation of the genomic DNA is a late event during apoptosis. DNA fragmentation is a result of active caspase-3 mediated cleavage of ICAD (Inhibitor of CAD) to activate CAD (caspase-activated deoxyribonuclease), which is responsible for the fragmentation of the DNA.[172, 173] The APO-DIRECT™ Kit allows for the detection and quantification of DNA breaks by FACS analysis. DNA fragmentation during apoptosis exposes 3' -hydroxyl groups in terminal positions. This characteristic can be used to differentiate apoptotic cells from viable cells by labelling the DNA breaks with fluorescein-tagged deoxyuridine triphosphate nucleotides (F-dUTP). The enzyme, terminal deoxynucleotidyl transferase (TdT), catalyzes a template-independent addition of deoxyribonucleoside triphosphates to the 3' -hydroxyl terminal groups of double- or single-stranded DNA.[174]Consequently, the apoptotic cells that contain DNA breaks will fluoresce. Results can be acquired and analysed in the form of a histogram or dot plot. For the results obtained in histogram form, normal cells will fluoresce in the first decade (10^1), whilst a horizontal fluorescent shift along the X-axis from the first decade (10^1) to the second decade (10^2) or third decade (10^3) is expected for apoptotic cells. In the case of results obtained as a dot plot, the normal convention of this display is to put DNA (Linear Red Fluorescence) on the X-axis and the F-dUTP (Log Green Fluorescence) on the Y-axis, apoptotic cells will display an

increase in fluorescence of fluorescein by shifting vertically up along the Y-axis. The graph is divided into two regions R3 and R2 corresponding to the percentage of apoptotic and normal cells respectively.

HeLa cells were plated in 6 well tissue culture plates. The cells were induced with test compound **3.25** and the standard positive control camptothecin **6.3**. The results for DNA fragmentation were obtained after treating the cells with test compound for 48 h and 72 h. The reason for choosing these time points was that DNA fragmentation is a late event during the process of apoptosis and it was observed that most cells were in early stage of apoptosis after 24 h (as demonstrated by APOpercentage assay).

Fig 7.6 DNA fragmentations in untreated control HeLa cells after 48 h

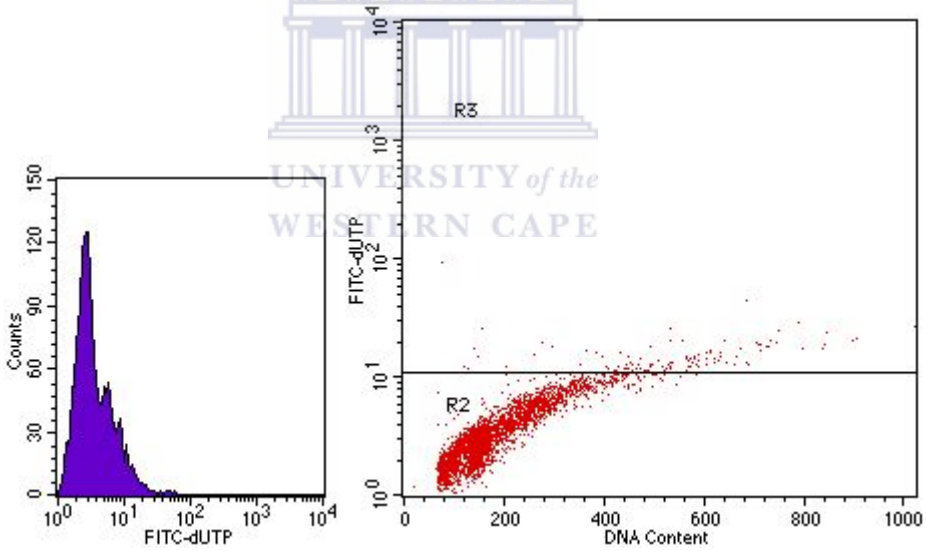

R3 = apoptotic cells (3.85%)

Fig 7.6 suggests that the cells in the normal state do undergo apoptosis but only a small percentage of cells (3.85%) dies during normal growth cycles. This is the control index for us to compare all apoptosis percentage levels obtained after induction of apoptosis by **3.25** compound.

Fig 7.7 DNA fragmentations in positive control (treated for 48 h with 10 µM camptothecin 6.3)

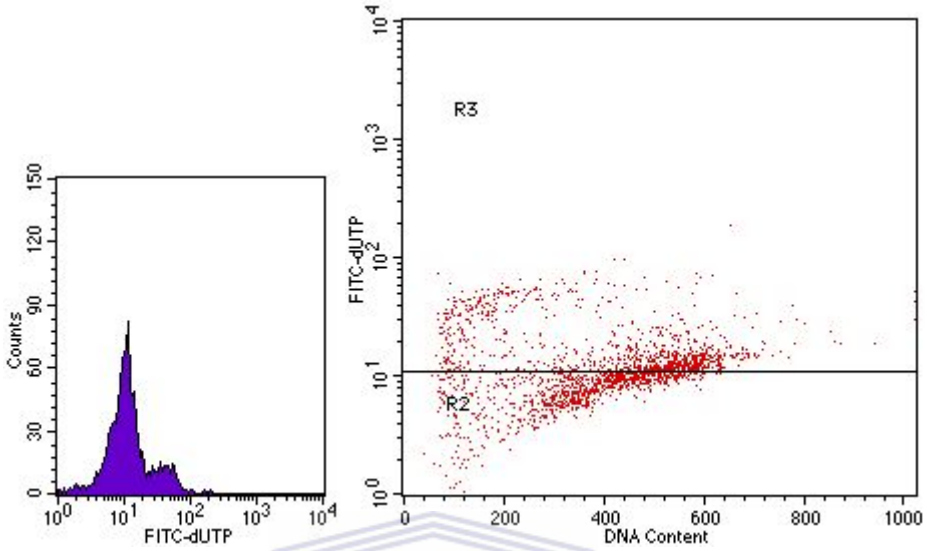

R3 = apoptotic cells (51.68%)

In Fig 7.7 it can be seen that the positive control shows a significant increase in F-dUTP staining. This is denoted by an increase in the fluorescence of fluorescein. Camptothecin **6.3** is a DNA topoisomerase-I inhibitor and induces apoptosis at very low concentration. In the present study, a killing of about 51.68% was observed in the HeLa cell line after treatment for 48 h. This is visible from the histogram shift from first decade (10^1) to the second decade (10^2). Another indicator is the spreading of cells towards the Y-axis in the dot plot. The more the DNA fragments, the higher will be the percentage of cells shown in region R3.

Fig 7.8 demonstrates the DNA strand breaks in HeLa cells treated for 48 hr with 10 µM of test compound **3.25**, which in turn induced DNA fragmentation in 93.51% of the HeLa cells, compared to the 3.85% for the untreated cells.

Fig 7.8 DNA fragmentations in HeLa cells treated for 48 h with 10 µM 3.25

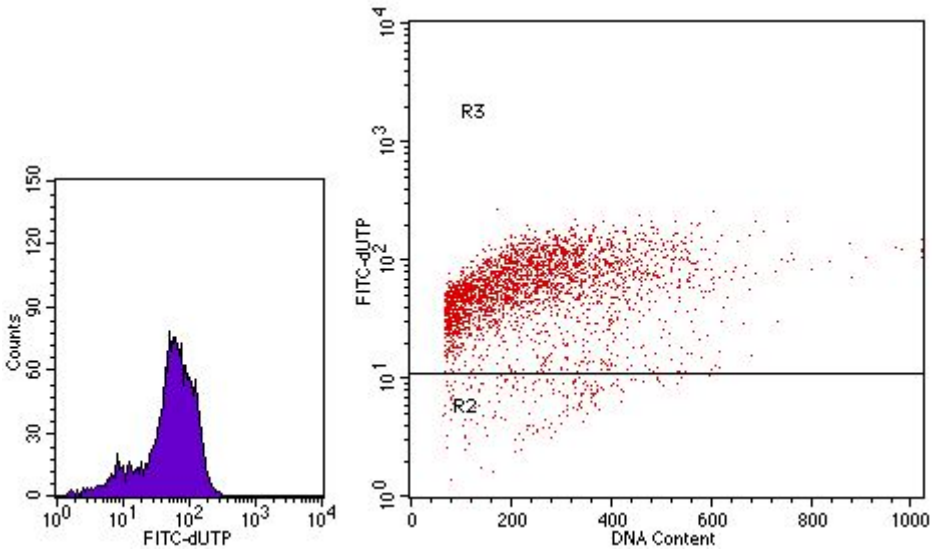

R3 = apoptotic cells (93.51%)

The above graphs in Fig 7.8 show that the compound **3.25** has the potential to kill about 94% HeLa cells via apoptosis within 48 h of treatment. This shows that with treatment of compound **3.25 at a concentration of 10 µM**, about 94% of HeLa cell population under investigation was in a late apoptosis phase, as represented by DNA fragmentation, which is a late apoptosis event. Since all the cells in a population do not undergo similar cell cycle phases at the same time (meaning that the cells in a population divide at different time intervals), it is appropriate to analyze the cells at different time intervals. Thus, the DNA fragmentation analyses were performed on HeLa cells after treatment with compound **3.25** for 72 h and also after treatment with standard compound viz., camptothecin **6.3**.

The untreated control after 72 h showed a minimal increase in the percentage of apoptotic cells (7.74%) as presented in Fig 7.9.

Fig 7.9 DNA fragmentation in untreated HeLa cells after 72 h

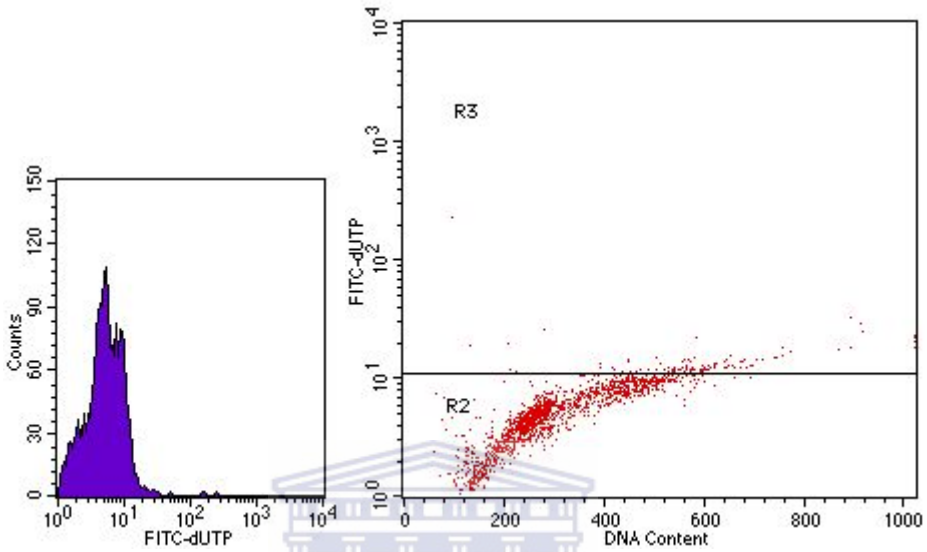

R3 = apoptotic cells (7.74%)

Fig 7.10 DNA fragmentation in HeLa cells treated for 72 h with 10 µM camptothecin 6.3

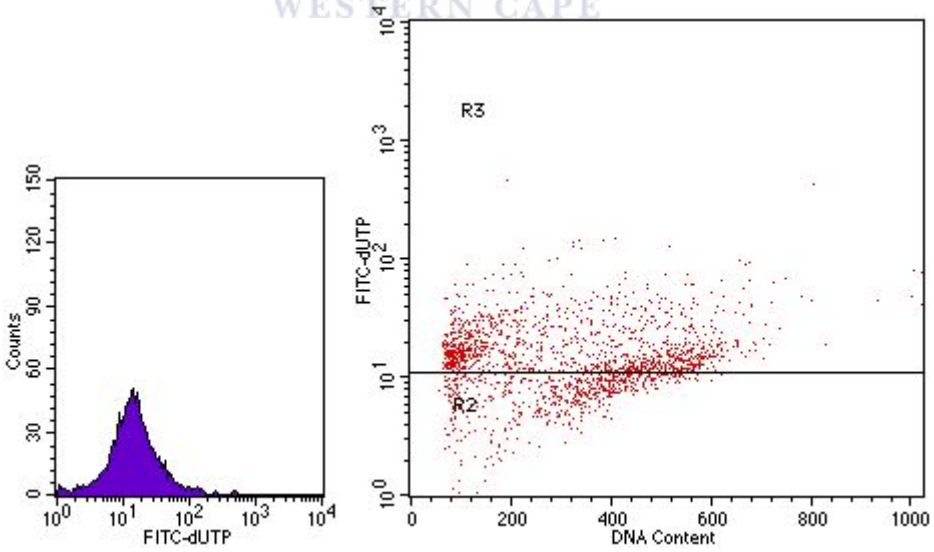

R3 = apoptotic cells (66.32%)

Fig 7.10 demonstrates DNA strand breaks in cells treated for 72 h with 10 µM of camptothecin **6.3**, which induced DNA fragmentation in 66.32% of the cells, compared to the 7.74% for the

untreated cells. This is visible from both the histogram and dot plot.

Fig 7.11 demonstrates DNA strand breaks in cells treated for 72 h with 10 µM **3.25**, which induced DNA fragmentation in 98.94% of the cells, compared to the 7.74% for the untreated cells.

Fig 7.11 DNA fragmentation in HeLa cells treated for 72hr with 10 µM 3.25

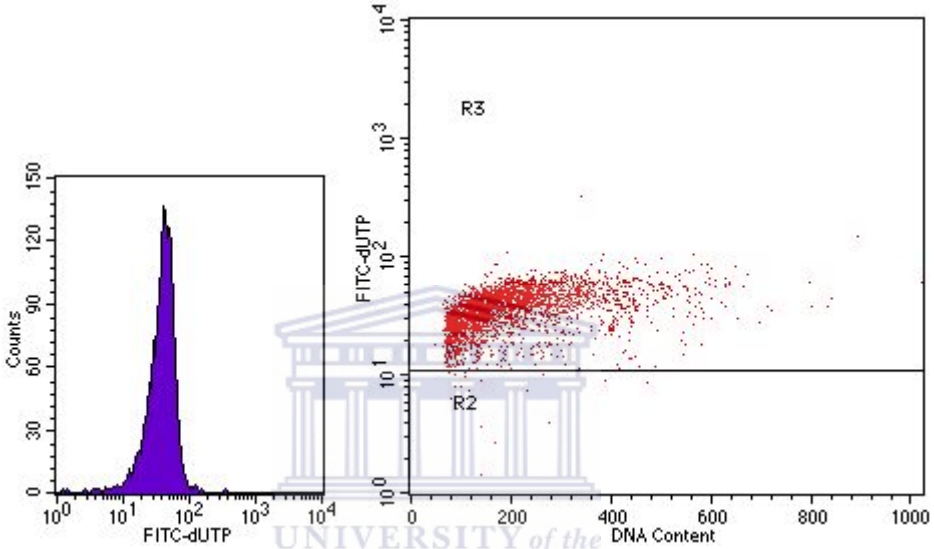

R3 = apoptotic cells (98.94%)

About 99% of HeLa cells were found to be in the late apoptosis stage after **3.25** induction for 72h. This shows that the test compound **3.25** has the potential to kill 99% of HeLa cells in the culture after 72 hr of induction. The histogram has shifted to the second decade (10^2) and the corresponding dot plot representation has most of the cells shifted towards the Y-axis in region R3. This is a clear proof of apoptotic potential of **3.25**.

Section 7.5.2: Cell cycle analysis:

Cell cycle checkpoints are the pathways which regulate the completion of specific events in one phase of cell cycle before entering the next phase during the eukaryotic cell cycle progression.. These checkpoints also serve as sites where cells can arrest to repair any damage, responding to an exogenous cellular stress signal and making use of essential growth factors, hormones or

nutrients. If the cells fails to repair the damage during arrest at checkpoints, it could activate the pathways leading to apoptosis and the defects in cell cycle checkpoints have been reported to result in gene mutations, chromosome damage and ultimately contribute to tumorigenesis. [175]

DNA damaging agents trigger checkpoints that produce arrest in G1, and G2, stages of the cell cycle. The G1, and G2, phases of the cycle represented the "gaps" in the cell cycle that occur between the two obvious landmarks, DNA synthesis and mitosis. In the first gap, G1, phase, the cell is preparing for DNA synthesis. S phase cells are synthesizing DNA and therefore have double DNA content. Cells can also arrest in S phase, which leads to a prolonged S phase with slowed DNA synthesis. The G2, phase is the second gap in the cell cycle during which the cell prepares for mitosis or M phase. Arrest in G1, allows repair before DNA replication, whereas arrest in G2, allows repair before chromosome separation in mitosis.[176]

The cell cycle assay is performed by tagging the DNA with the PI dye as explained in the section 7.3.4. The underlying mechanism used to label the DNA fragments during apoptosis is explained in DNA fragmentation assay in section 7.5.1 above. Results can be acquired and analysed in the form of a histogram or dot plot. The graph is divided into four regions M1, M2, M3 and M4 corresponding to sub-G1, G1, S and G2 phases respectively. The sub-G1 represents the apoptotic cells whereas the G1 represents the first phase of cell cycle in which cell prepares itself for DNA synthesis. The second phase in cell cycle is the S phase i.e. synthesis phase during which the DNA is synthesized. The third phase of cell cycle is the G2 phase, when cell prepares for entering the mitosis and divides into two. For the results obtained in histogram form, normal cells will fluoresce in the M2, M3 and M4 regions whilst a horizontal backward fluorescent shift along the X-axis is expected for apoptotic cells. The normal convention of this display is to put DNA vertically (Linear Red Fluorescence) on the Y-axis and the FL2-H (PI Fluorescence) horizontally

on the X-axis, apoptotic cells will display an increase in fluorescence of fluorescein by shifting vertically up along the Y-axis as a peak before the G1 peak.

To elucidate the mechanism behind the anti-tumor activity of **3.25**, the effect of **3.25** on the viability and cell-cycle progression of HeLa cells was investigated. HeLa cells were plated in 6 well tissue culture plates. The cells were exposed to test compound **3.25** at a concentration of 10 µM and the standard camptothecin **6.3** at a concentration of 10µM. The cells were analysed on a FACScan instrument using CELLQuest PRO software after time intervals 24, 48 and 72 h.

Fig 7.12 Cell cycle analysis of untreated HeLa cells after 24 h

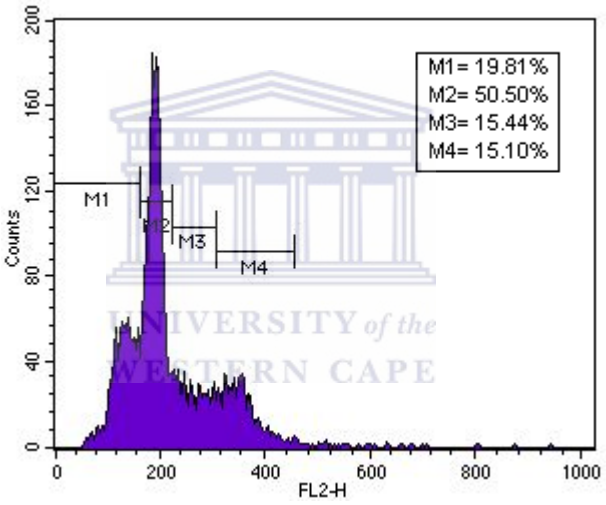

Where FL2-H = PI fluorescence

It is shown in Fig 7.12 that M1 has 19.81% cells, which is the percentage of apoptotic cells in normal untreated control. This will be an index for measuring apoptosis in treated samples. If the percentage of cells in M1 region in treated cells is increased, this will be an indicator of the apoptosis during cell cycle. In untreated control most of the cells were found to be in G1 phase of cell cycle.

Fig 7.13 represents the distribution of cells in various phases of cell cycle after treatment with 10 µM camptothecin **6.3** for 24 h. It is visible that in positive control more cells are present in M1

region representing the percentage of apoptotic cells. The observed increase in percentage of cells in M3 region reveals that after treatment with camptothecin **6.3**, the cells were possibly arrested in the S phase of cell cycle, as in line with the previous report.[177]

Fig 7.13 Cell cycle analysis of HeLa cells treated with 10 µM camptothecin 6.3 for 24 h

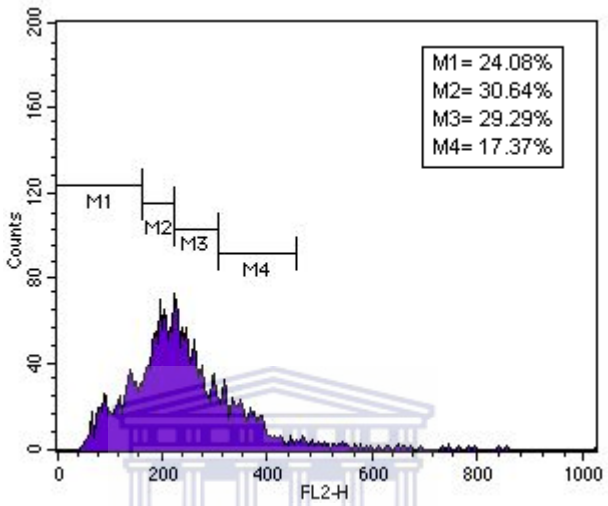

The effect of compound **3.25** on cell cycle of HeLa cells is presented in Fig 7.14. As is visible from graph that after treatment with compound **3.25**, about 47% cells are present in M2 region as compared to the 50.50% in untreated control and 30.64% in camptothecin **6.3** treated positive control.

Fig 7.14 Cell cycle analysis of HeLa cells treated with 10 µM 3.25 for 24 h

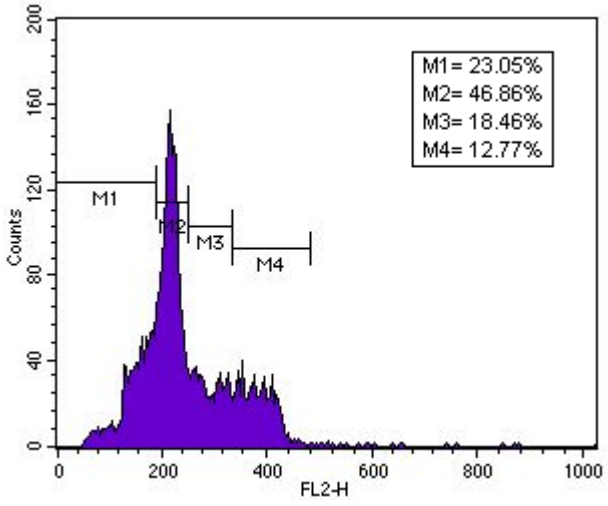

There is approximately same percentage of cells in G1 phase as observed in Fig 7.14 as compared to the untreated cells (Fig 7.12). To observe the long-term effects of the test compound **3.25**, the cell cycle analysis was extended to 48 and 72 h.

Fig 7.15 Cell cycle analysis of untreated HeLa cells after 48 h

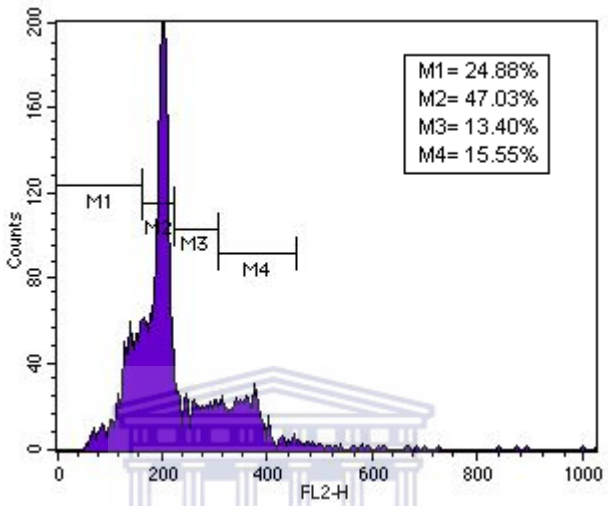

Fig 7.15 represents the percentages of cells in various phases of cell cycle in untreated control after 48 h. The Fig 7.15 shows that percentages of the cells in various regions of the graph are not much changed as compared to untreated control after 24 h (Fig 7.12). The percentages of cells in various phases of cell cycle and cells undergoing apoptosis after treatment with camptothecin **6.3** are represented in Fig 7.16. This graph also doesn't show much change in percentages of cells as compared to the cells treated with camptothecin **6.3** for 24 h Fig 7.13.

Fig 7.16 Cell cycle analysis of HeLa cells treated with 10 µM camptothecin 6.3 for 48 h

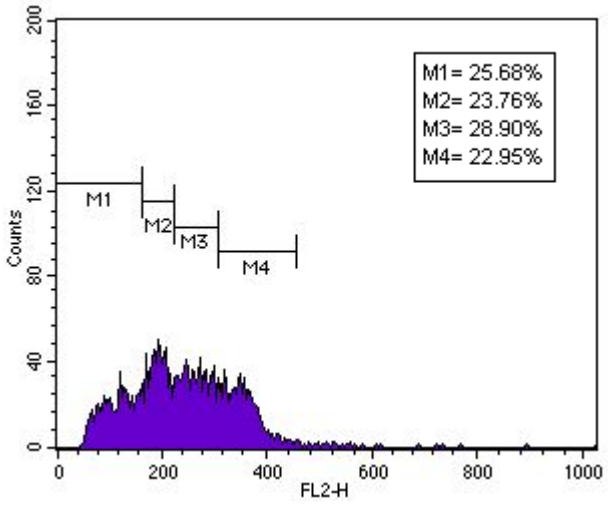

The cells after treatment with camptothecin **6.3** for 48 h could possibly be in S and G2 phases of cell cycle as revealed by the increase in percentage of cells in regions M3 and M4 respectively as compared to the untreated control after 48 h.

The percentages of cells in various phases of cell cycle after treatment with test compound **3.25** for 48 h are shown in Fig 7.17.

Fig 7.17 Cell cycle analysis of HeLa cells treated with 10 µM 3.25 for 48 h

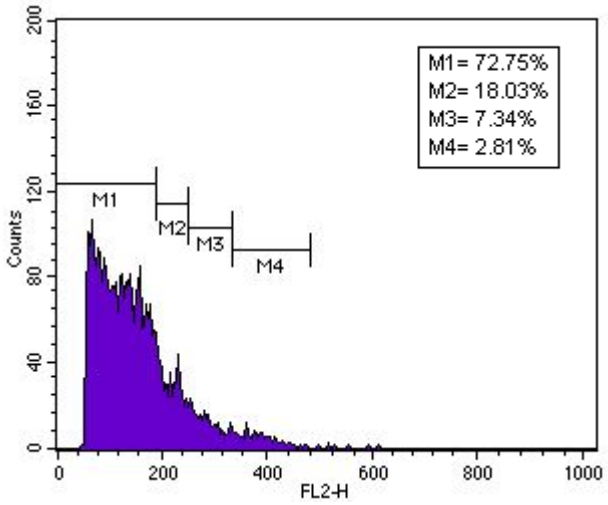

Fig 7.17 explains that after treatment of test compound for 48 h, a greater percentage (72.75%) of HeLa cells undergo apoptosis. This is represented as a peak in M1 region of the graph. It is

visible that about 28% (percentage of cells in M2, M3 and M4 regions) cells are present in the sample after treatment with compound **3.25** for 48 h.

The analysis was extended to 72 h and Fig 7.18 shows the results obtained after leaving the untreated cells in the media for 72 h.

Fig 7.18 Cell cycle analysis of untreated HeLa cells after 72 h

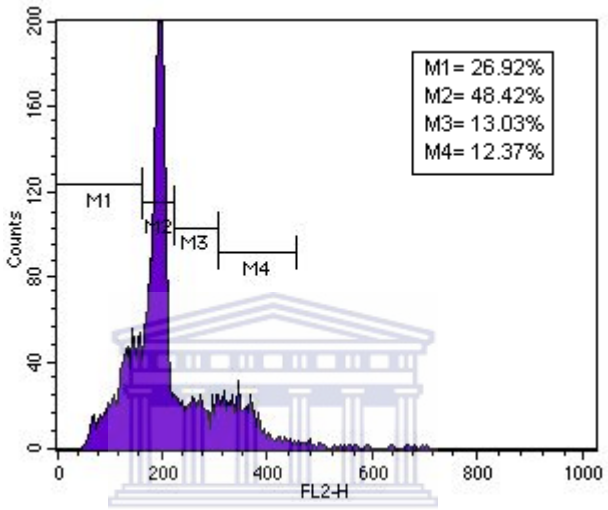

As is clear from Fig 7.18 that the normal untreated cells have approximately the same number of cells in various phases of cell cycle even after 72 h. The number of apoptotic cells (as represented in M1 region of graph) has increased as compared to shown in Fig 7.12. In comparison to this, the percentages of cells in various phases of cell cycle are changed in cells treated with camptothecin **6.3** for 72 h.

Fig 7.19 Cell cycle analysis of HeLa cells treated with 10 µM camptothecin 6.3 for 72 h

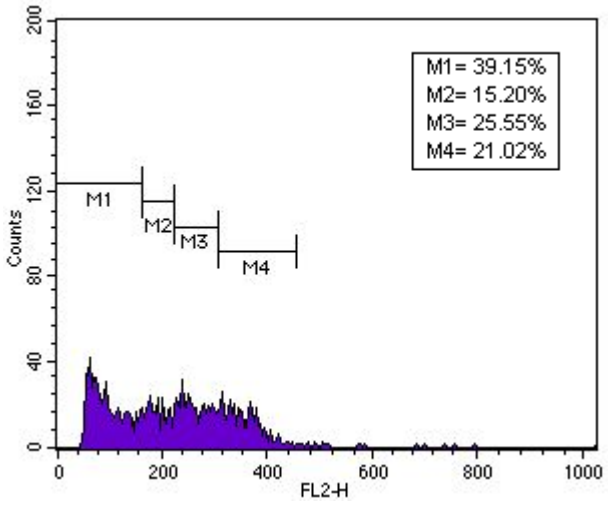

The Fig 7.19 shows that about 40% of the HeLa cells have undergone apoptosis after induction with camptothecin **6.3** for 72 h. Similar effects are observed in cells treated with test compound **3.25** for 72 h.

Fig 7.20 shows that after 72 h of treatment with test compound **3.25**, approximately 80% cells were apoptotic. This is clear from the sharp peak observed in M1 region corresponding to sub-G0 or apoptotic phase. The percentages of the cells in G1, S and G2 phases of cell cycle are markedly decreased as observed in M2, M3 and M4 regions of the graph respectively.

Fig 7.20 Cell cycle analysis o HeLa cells treated with 10 µM 3.25 for 72 h

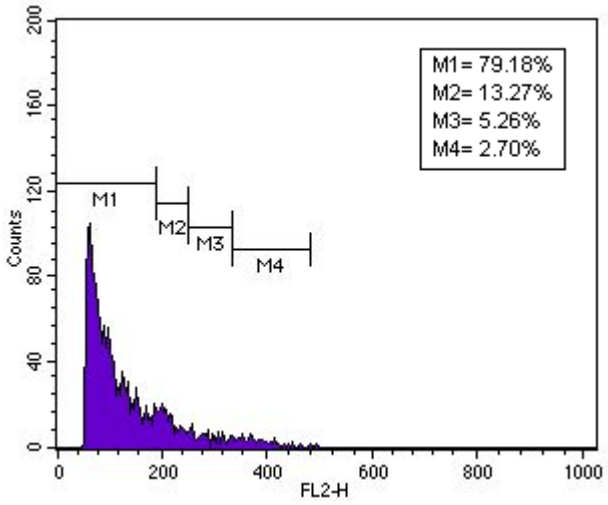

The results of the cell cycle analysis reveal that the test compound **3.25** has the ability to induce apoptosis when induced for longer periods, as well as limiting the population of cells in G1 phase of the cell cycle when treated for shorter time periods. Another highlight of the analysis is that the compound **3.25** has enhanced apoptotic potential as compared to the camptothecin **6.3**, which is a known inducer of apoptosis.

Section 7.6: Discussion

Quinones occur widely in animals, plants and microorganisms, and often carry out indispensable roles in the biochemistry of energy production by providing vital links in the respiratory chain of living cells. These compounds act as inhibitors of electron transport, uncouplers of oxidative phosphorylation, and give rise to a wide range of antiproliferative activies.[178]

Quinones comprise the second largest class of anti-tumor agents currently in use. Studies have demonstrated that these drugs kill the tumor cells through apoptosis.[167] In the present study, **3.25**, an analogue of diospyrin **1.22** has been shown to have potential apoptotic activity against two human cancer cell lines derived from human cervical carcinoma and human bone osteosarcoma at a concentration of 10 µM. This compound is more active compared to diospyrin **1.22**, as the latter

has been shown to have anti-tumor activity (IC_{50}) at 100 μM after 48 h of treatment.[52] The compound **3.25** is also much more active than the other derivatives of diospyrin **1.22** tested so far. The derivatives of diospyrin **1.22** were shown to have IC_{50} values in the acute myeloblastic leukemia (HL-60) cell line at concentrations of 64 μM for diospyrin dimethyl ether, 54 μM for hydroquinonoid derivative and 30 μM for diospyrin diethyl ether derivative after 48h of treatment respectively. In a recently published study,[55] the aminoquinonoid derivative **1.29** of diospyrin **1.22** exhibited IC_{50} values of 0.06μM, i.e. thus inhibited growth of 50% of Ehrlich ascites carcinoma (EAC) after 16 hr *in vitro*. This shows that the amino group enhances the anti-tumor activity immensely. Since the analogues of diospyrin **1.22** have never been synthesized and tested for the anti-tumor activity, the present study we have undertaken is considered to be unique.

Several mechanisms have been proposed for the action of quinones. One of the operating mechanisms for quinones has been associated with oxidative stress.[179-182] Quinonoid compounds can act as prodrugs through 'bioreductive alkylation' which involves two-electron reductions to the hydroquinones which in turn would react with biological nucleophiles like DNA and proteins. Since the **3.25** compound structurally differs from the **3.21** compound involving the OH group only, this may explain the higher activity associated with **3.25**, compared to **3.21.** The present study also supports the hypothesis that the OH group enhances the anti-tumor activities associated with quinonoids. Another possible mechanism could be the one-electron reduction of a quinonoid compound, to produce a semiquinone radical which in turn would generate reactive oxygen species causing dramatic changes in mitochondrial transmembrane potential and other associated events signaling cell death.[52]

The diospyrin **1.22** is a specific inhibitor of DNA topoisomerase[49] as camptothecin **6.3**. DNA topoisomerase enzymes have been recognized as potential chemotherapeutic targets and several naphthoquinonoid natural products have been found to be topoisomerase active.[41, 52, 182, 183] Topoisomerase I is primarily known as a DNA nicking/closing enzyme capable of resolving topological constraints in DNA. Its ability to relax supercoiled DNA and its implication in chromatin (de)condensation have already been discussed.[184] In addition to DNA, topoisomerase I interacts with different protein partners, among which are p53, nucleolin, and various other nuclear proteins.[185] One key feature of this enzyme is its capacity to perform reactions via two distinct activity domains on both DNA and a class of proteins called SR proteins implicated in RNA splicing, such as the SF2/ASF splicing factor.[186-189] With DNA, topoisomerase I functions as a phosphodiesterase, introducing simple strand breaks and then as a ligase to reseal the break after the DNA has been conformationally manipulated.[190] With SR proteins, topoisomerase I acts as a kinase to phosphorylate their arginine-serine-rich domain, as has been shown for the SF2/ASF splicing factor.[186, 191]

For a long time, the DNA cutting activity of topoisomerase I has attracted the attention of chemists and pharmacologists because the characterization in the early 1980s of the plant alkaloid camptothecin **6.3** which acts as a potent and specific inhibitor of topoisomerase I. Camptothecin **6.3** promotes DNA cleavage by topoisomerase I through the stabilization of topoisomerase I phosphotyrosine-DNA intermediates. The accumulation of DNA breaks activates specific molecular circuits through the nucleus, cytoplasm, and mitochondria, leading to apoptotic cell death, mostly in rapidly proliferating tumor cells. The majority of the topoisomerase I inhibitors reported thus far intervene at the level of DNA-topoisomerase I complex, through stabilization of the covalent intermediate whereby the enzyme is covalently attached to the DNA via a phosphotyrosyl linkage. This intermediate complex is selectively trapped by camptothecin **6.3** or

other drugs referred to as poisons, such as certain indolocarbazoles and indenoisoquinolines. Diospyrin does not belong to this group of poisons. Its action certainly results from a direct interaction with the enzyme, as suggested for isodiospyrin.[192]

Selective inhibition of topoisomerase I from *L. donovani* has been reported with diospyrin,[57] and, the related compound isodiospyrin, extracted from *Diospyros morrisiana*, was shown to inhibit human topoisomerase I.[192] These two studies suggested that the diospyrin-type biaryl molecule interacts directly with topoisomerase I but not with its DNA partner as is frequently the case with other inhibitors like camptothecin **6.3**. Most interestingly, it was reported that isodiospyrin antagonizes camptothecin-induced DNA cleavage mediated by topoisomerase I and strongly inhibits the kinase activity of the enzyme toward SF2/ASF.[192] Since the synthesized compounds in the present study are analogues of diospyrin **1.22** and are diospyrin-like compounds, it is possible that they might also act as inhibitors of topoisomerase I activity.

Another possible mechanism of action of quinines involves glutathione. Glutathione transferases (GSTs) are multifunctional enzymes that catalyse conjugation of a wide variety of electrophilic endogenous and exogenous compounds with the tripeptide glutathione (GSH).[193] The GSH conjugates are more hydrophilic and can therefore be excreted easily, thus facilitating the cells to get rid of exogenous chemicals. Thus, the cancer cells become less responsive to the drugs administered. GSTs also protect cells by sequestering compounds through high affinity binding.[194] In human liver, GSTs make up between 4%-10% of the total cytosolic protein. Due to their abundance in the cell, GSTs are likely to interact with novel compounds presented to them as evidenced by their broad substrate specificity. The overexpression of GSTs has been implicated in resistance to alkylating anticancer type drugs.[195] Diospyrin **1.22** has been found to inhibit the human GSTs *in vitro*[196]and it also possess anti-tumor activity, which makes it an ideal candidate for a comprehensive testing regime as a potential anti-tumor drug. It could be thus

inferred from previous studies that co-administration of diospyrin **1.22** with an alkylating anti-cancer drug could inhibit tumor growth and at the same time prevent resistance to the co-drug by inhibiting GST-mediated detoxication of the latter.

In the present investigation, the effect of the test compounds on expression of apoptosis regulating genes (p53, Bax, bcl-2 etc.) is unknown and thus a more detailed study at expression level could shed some light on the underlying mechanism of action of these compounds. Since the induction of apoptosis following chemotherapy is associated with the activation of pro-apoptotic genes and the suppression of anti-apoptotic genes, attenuation of pro-apoptotic genes and increases in anti-apoptotic genes causes resistance to apoptosis. Thus, to increase the therapeutic effect of cancer chemotherapy, the assessment of molecular mechanisms and targeting apoptosis-related genes may lead to new strategies for the enhancement of the anti-tumor effect.

Section 7.7: Summary

The aim of this study was to test the pro-apoptotic activity and therefore also the anti-cancer activity of synthetic analogues of diospyrin **1.22**. The results demonstrated that not all of the compounds were active in all the cell lines available for the study. The selective killings represent the different apoptotic pathways initiated after induction with each of the test compounds. Furthermore, it was also observed that compounds that are cytotoxic are not necessarily pro-apoptotic, that is, cell death induced by these compounds may be a consequence of necrotic rather than apoptotic cell death. For example, compound **3.20** has been found to be cytotoxic in CHO cells, whereas it was unable to induce apoptosis in the cancer cell lines tested. Also, the non-cancerous CHO cells were more sensitive to the effects of compound **3.20** than the cancer cell lines themselves. Test compounds **3.25** and **3.32** demonstrated much higher apoptotic activity

than the other two compounds **3.20** and **3.21**. Compound **3.25** has displayed the ability to induce specific markers of apoptosis in HeLa cells such as phosphatidylserine externalization, DNA fragmentation and apoptosis at the level of cell cycle. Test compound **3.32** is the only one that induced apoptosis in the MCF-7 cell line that is characterized by caspase-3 gene mutation. This ability of **3.32** to induce apoptosis in the MCF-7 cell line indicates that it compound has the ability to induce apoptosis via caspase-3 independent pathways respectively. It is known that compounds that act on the basic apoptosis machinery do not induce apoptosis in all cells and this may be due to the differential expression of various pro- and anti-apoptosis factors in normal versus cancer cells and may thus provide a strategy for selectively targeting cancer cells.

Conclusion: Above analyses has revealed that the synthesized analogues of diospyrin **1.22** in the present study have the potential to induce apoptosis in various cancer cell lines *in vitro.* The activity of test compound **3.25** is dose and time dependent and at 10 µM concentration, the compound induced apoptosis in 67% HeLa cells in 24h, which is more enhanced than diospyrin (100 µM for 48h induction). After 72h of treatment with test compound **3.25**, about 99% of HeLa cells were found to be in late apoptosis stages as revealed by DNA fragmentation. Additionally test compound **3.25** might have chemotherapeutic potential, which needs a more detailed and comprehensive investigation. Other compounds **3.20**, **3.21** and **3.32** were also found to be apoptotic and the subsequent detailed analysis of these compounds was beyond the scope of this thesis. We believe that a complete analysis at the mechanism level could unravel the chemotherapeutic potential of these compounds.

References

1. Mohan A, Sharma S. K., *Jaypee Brothers Medical Publishers*, **2001**, 14-29
2. Madison B. M., *Biotech. Histochem.*, **2001**, *76(3)*, 119-25
3. Raja A, *Indian J. Med. Res.*, **2004**, *October*, 213-232
4. WHO, **2004**, *www.who.int/mediacentre/factsheets*
5. Medical Research Council, *www.mrc.ac.za*
6. Mahmoudi A, Iseman M. D., *JAMA*, **1993**, *270*, 65-68
7. Marris E., *Nature*, **2006**, *443*, 131
8. Hong Kong Chest Services/ British Medical Research Council, *Tubercle*, **1979**, *60*, 201-210
9. Blumberg H. M., Burman W. J., Chaisson R. E., Daley C. L., Etkind S. C., Friedman L. N., American Thoracic Society/Centers for Disease Control and Prevention/ Infectious Diseases Society of America, *Am. J. Respir. Crit. Care Med.*, **2003**, *167*, 603-662.
10. Chan E. D., Iseman M. D., *BMJ*, **2002**, *325*, 1282-1286
11. Nunn P., Kibuga D., Gathna S., Brindle R., Imalingat A., Wasunna K., *Lancet*, **1991**, *337*, 627-630
12. Alangaden, G. J., Lerner S. A., *Clin. Infect. Dis.*, **1997**, *25*, 1213-1221
13. Grassi, C., *Exp. Opin. Investig. Drugs*, **1997**, *6*, 1211-1226
14. Ji B., Lounis N., Truffot-Pernot C., Grosset J., *Antimicrob. Agents Chemother.*, **1995**, *39*, 1341-1344
15. Rastogi N., Goh K. S., Bryskier A., Devallois A., *Antimicrob. Agents Chemother.*, **1996**, *40*, 1610-1616
16. Watanabe A., Tokue Y., Takahashi H., Kikuchi T., Kobayashi T., Gomi K., Fujiwara S., Nukiwa T., *Antimicrob. Agents Chemother.*, **1999**, *43*, 1767-1768

17. Haruaki T., Katsumasa S., Tatsuya A., Hiroko K., Shin K., Mitsunori S., *Antimicrob. Agents Chemother.*, **1999**, *43*, 3001-3004

18. Saito H., *Drugs*, **1999**, *58, 2*, 400-401

19. Lipsky B. A., Baker C. A., *Clin. Infect. Dis.*, **1999**, *28*, 352-364

20. Diekema D. J., Jones R. N., *Drugs*, **2000**, *59*, 7-16

21. Iseman M. D., *Eur. Respir. J.*, **2002**, *20*, 87-94

22. Stover C. K., Warrener P., van Devanter D. R., *Nature*, **2000**, *405*, 962-966

23. Espinal M. A., Dye C., Raviglione M., Kochi A., *Int. J. Tuberc. Lung Dis.*, **1999**, *3*, 561-563

24. O'Brien R. J., Vernon A. A., *Am. J. Respir. Crit. Care Med.*, **1998**, *157*, 1705-1707

25. Ulubelen A., Topcu G., Johansson C. B., *Journal of Natural Products*, **1997**, *60*, 1275-1280

26. Delaha E. C., Garagusi V. F., *Antimicrob. Agents Chemother.*, **1985**, *27 (4)*, 485-486

27. Ulubelen A. E., Tuzlaci E., Johanson C., *Journal of Natural Products*, **1988**, *51 (6)*, 1178-1183

28. Cantrell C. L., Lu T., Fronczek F. R., Fischer N. H., *Journal of Natural* Products, **1996**, *59*, 1131-1136

29. Grange J. M., Snell N. J. C., *Journal of Ethnopharmacology*, **1996**, *50*, 49–53

30. Houghton P. J., Woldermariam T. Z., Watanabe Y., Yates M., *Planta Medica*, **1999**, *65*, 250–254

31. Olenick J. G., Cook T. M., Hahn F. E., *Journal of Bacteriology*, **1971**, *107*, 528–534

32. Bintu O. A., Adesogan K. E., Okogun J. I., *Planta Medica*, **1996**, *62 (4)*, 352–353

33. Chantrapromma S, Fun H-K, Koysomboonc S, Chantrapromm K, *Acta Cryst.*, **2006**, *E62*, 1984–1986

34. Lall N., Meyer J. J. M., *Journal of Ethnopharmacology*, **1999**, *66*, 347-354

35. Lall N., Meyer J. J. M., *Journal of Ethnopharmacology*, **2001**, *78*, 213-216

36. Tran T., Saheba E., Arcerio A. V., Chavez V., Li Q., Martinez L. E., Primm T. P., *Bioorg. Med. Chem.*, **2004**, *12*, 4809-4813

37. Adeniyi B. A., Fong H. H. S., Pezzuto J. M., Luyengi L., Odelola H. A., *Phytotherapy Research*, **2000**, *14*, 112-117

38. Kapil R. S., Dhar M. M., *J. Sci. Industr. Res.*, **1961**, *20B*, 498-500

39. Ganguly A. K., Govindachari T. R., *Tetrahedron Lett.*, **1966**, 3373-3376

40. Sidhu G. S., Pardhasaradhi M., *Indian J. chem.*, **1970**, *8*, 569-571

41. Yoshida M., Mori K., *Eur. J. Org. Chem.*, **2000**, 1313-1317

42. Harrison W. T. A., Musgrave O. C., *Acta Cryst.*, **2004**, *C60*, 399-401

43. Lillie T. J., Musgrave O. C., Skoyles D., *J. Chem. Soc. Perkin Trans. I*, **1976**, 2155-2161

44. Adams R., Teeter H. M., *J. Am. Chem. Soc.*, **1940**, *62*, 2188-2190

45. Lall N., Sarma M. D., Hazra B., Meyer J. J. M., *Journal of Antimicrobial Chemotherapy*, **2003**, *51*, 435-438

46. Sharma V. K., *Tubercle*, **1990**, *71*, 293-295

47. Hartwell J. L., *Lloydia*, **1969**, *32*, 153

48. Hazra B., Sur P., Sur B., Banerjee A., Roy D.K., *J. Indian Chem. Soc.*, **1981**, *58*, 627

49. Fallas A. L., Thomson R. H., *J. Chem. Soc.*, **1968**, *C*, 2279

50. Hazra B., Pal S., Banerjee A., *J. Med. Sci. Res.*, **1994**, *22*, 351-353

51. Hazra B., Pal S., Banerjee A., *J. Med. Sci. Res.*, **1994**, *22*, 621-623

52. Chakrabarty S., Roy M., Hazra B., Bhattacharya R. K., *Cancer Letters*, **2002**, *188*, 85-93

53. Hazra B., Sur P., Roy D. K., Sur B., Banerjee A., *Planta Medica*, **1984**, *51*, 295-297

54. Hazra B., Pal S., Banerjee A., Ray R., Bhattacharya R. K., *Phytother. Res.*, **1996**, *10*, 393-397

55. Sarma M. D., Ghosh R., Patra A., Sharma P., Ghoshal N., Hazra B., *Bioorg. Med. Chem.*, **2006**, doi: 10.1016/j.bmc.2006.07.041

56. Cushion M. T., Collins M., Hazra B., Kaneshiro E. S., *Antimicrobial Agents and Chemotherapy*, **2000**, *44*, 713-719

57. Ray S., B. Hazra B. Mittra A. Das, Majumder H. K.**,** *Mol. Pharmacol.*, **1998**, *54*, 994–999

58. Yardley V., Snowdon D., Croft S., Hazra B.**,** *Phytother. Res.*, **1996**, *10*, 559–562

59. Hazra B., Golenser J., Nechemiya O., Bhattacharya S., Azzam T., Domb A., Frankenburg S., *Indian Journal of Pharmacology*, **2002**, *34*, 422-427

60. Croft S. L., Evans A. T., Neal R. A., *Ann. Trop. Med. Parasitol.*, **1985**, *79*, 651-688

61. Hazra B., Ghosh R., Banerjee A., Kirby G. C., Warhurst D. C., Phillipson J. D., *Phytotherapy Research*, **1995**, *9(1)*, 72-74

62. Stille J. K., *Angew. Chem Int Ed*, **1986**, *25*, 508

63. Saito S., Sakai M., Miyaura N., *Tetrahedron Lett*, **1996**, *37*, 2993

64. Miyaura N., Yanagi T., Suzuki A., *Synth Commun*, **1981**, *11*, 513-519

65. Miyaura N., Suzuki A., *Chem Rev*, **1995**, *95*, 2457-2487

66. Lopez-Alvarado P., Avendano C., Menendez C., *Syn. Comm.*, **2002**, *32*, 3233-3239

67. Ho T-I., Chen G-P., Lin Y-C., Lin Y-M., Chen F-C., *Phytochemistry*, **1986**, *25*, 1988-1989

68. Kesteleyn B., de Kimpe N., Puyrelde L. V., *J. Org. Chem.*, **1999**, *64*, 1173-1179

69. Jung M. E., Hagenah J. A., *J. Org. Chem.*, **1987**, *52*, 1889-1902

70. Alo B. I., Kandil A., Patil P. A., Sharp M. J., Siddiqui M. A., Snieckus V., *J. Org. Chem.*, **1991**, *56*, 3763-3768

71. Syper L., Kloc K., Mlochowski J., Szulc Z., *Synthesis*, **1979**, 521-522

72. Hartmut L., *Liebigs Annalen der Chemie*, **1985**, *2*, 251-274

73. Casey C. P., Jones C. R., Tukada H., *J. Org. Chem.*, **1981**, *46*, 2089-2092

74. Kesteleyn B., de Kimpe N. D., *J. Org. Chem.*, **2000**, *65*, 640-644

75. Nakayama J., Mizumura A., Yokomori Y., Krebs A., Schutz K., *Tetrahedron Letters*, **1995**, *36(47)*, 8583-8586

76.Chung Y. C., Kobayashi T., Kanai H., Akiba T., Kudo T., *Appl. Environ. Microbiol.*, **1995**, *61*, 1502–1506

77. Eloff J. N., *Planta Medica*, **1998**,*64*, 711 –713

78. Warren R., Richardson M., Sampson S., Hauman J. H., Beyers N., Donald P. R., van Helden P.D., *J. Clin. Microbiol.*, **1996**, *34*, 2219-2224

79. Somoskovi A., Magyar P., *J. Clin. Microbiol.*, **1999,** *37*,1366-1369

80. Siddiqi, S. H., 460TB system. Product and procedure manual. Becton Dickinson and Company, Maryland, USA, **1995**

81. Morton R. A., Ed, Biochemistry of Quinones. New York, Academic Press, **1965**

82. Nohl H., Jordan W., Youngman R. I., *Adv. Free Rad. Biol. Med.*, **1986**, *2*,211-279

83. O'Brien P. J., *Chem. Biol. Interact.*, **1991**, *80*, 1-41

84. Meganathan R., *Vitam. Horm.*, **2001**, *61*, 173-218

85. Kersten W., *Prog. Mol. Subcell. Biol.*, **1971**, *2*, 48-57

86. Olenick C. G., Hahn F. E., *Ann. NY Acad. Sci.*, **1974**, *235*, 542-552

87. Rich S., In: Torgeson DC. ED, New York, Academic Press, **1969**

88. Martin Y. C., Bustard T. M., Lynn K. R., *J. Med. Chem.*, **1973**, *16*, 1089-1093

89. Pardee A. B., Li Y. Z., Li C. J., *Cancer Drug Targets*, **2002**, *2*, 227-242

90 Seung S. A., Lee J. Y., Lee M. Y., Park J. S., Chung J. H., *Chem. Biol. Interact.*, **1998**, *113*, 133-144

91. Koyama, J., *Recent Patents on Anti-Infective Drug Discovery*, **2006**, *1*, 113-125

92 Lin A. J., Cosby, L. A., Shansky C. W., Sartorelli, A. C., *J. Med. Chem*., **1972**, *15*, 1247-1252

93. Moore, H. W., *Science*, **1977**, *197*, 527-532

94. Lockshin R. A., Williams C. M., *Nat. Rev. Mol. Cell Biol.*, **1964**, *2(7)*, 545-550

95. Kerr J. F., Wyllie A. H., Currie A. R., *Br. J. Cancer.*, **1972**, *26(4)*, 239-257

96. Leist M., Jaattela M., *Nat. Rev. Mol. Cell Biol.*, **2001,** *2(8)*, 589-598

97. Meier P., Finch A., Evan G., *Nature*, **2000**, *407(6805)*, 796-801

98. Fadeel B., Gleiss B., Hogstrand K., Chandra J., Wiedmer T., Sims P.J., Henter J. I., Orrenius S., Samali A., *Biochem. Biophys. Res. Commun.*, **1999a,** *266(2)*, 504-511

99. Saraste A., Pulkki K., *Cardiovasc. Res.*, **2000,** *45(3)*, 528-537

100. Van Cruchten S., Van Den Broeck W., *Anat. Histol. Embryol.*, **2002,** *31(4)*, 214-223

101. Pitchard D. M., Watson A. J. M., *Pharmacological Therapeutics*, **1996,** *72*, 149-169

102. Savitz S. I., Daniel B. A., Rosenbaum M.D., *Neurosurgery*, **1998,** *42*, 555-572

103. Wyllie A. H., *Bri. Med. Bull.*, **1997**, *53*, 451-465

104. Wyllie A., *Nature*, **1980**, *284*, 555-556

105. Rudin C. M., Thompson C. B., *Ann. Rev. Med.*, **1997**, *48*, 267-281

106. MacLellan W. R., Schneider M. D., *Circul. Res.* **1997**, *81*: 137-144

107. Haimovitz-Friedman A., Kan C., Enleiter D., *J. Exp. Med.*, **1994**, *180*, 525-535

108. Santana P., PenÄa L. A., Haimovitz-Friedman A., *Cell*, **1996,** *86*,189-199

109. Narula J., Kharbanda S., Khaw B. A., *Chest*, **1997,** *112*, 1358-1362

110. Denault J. B., Salvesen G. S., *Chem. Rev.*, **2002,** *102(12)*, 4489-4500

111. Richardson H., Kumar S., *J. Immunol. Methods*, **2002,** *265(1-2)*, 21-38

112. Creagh E. M., Martin S. J., *Biochem. Soc. Trans.*, **2001,** *29(6)*, 696-702

113. Miura M., Zhu H., Rotello R., Hartwieg E. A., Yuan J., *Cell*, **1993,** *75(4)*, 653-660

114. Cohen G. M., *Biochem. J.*, **1997**, *326*, 1-16

115. Salvesen G. S., Renatus M., *Dev. Cell*, **2002b,** *2(3)*, 256-257

116. Ameisen J. C., *Cell Death Differ.*, **2002,** *9(4)*, 367-393

117. Raff M. C., Barres B. A., Burne J. F., Coles H. S., Ishizaki Y., Jacobson M. D., *Science*, **1993,** *262(5134)*, 695-700

118. Vaux D. L., Cory S., Adams J.M., *Nature*, **1988,** *335(6189)*, 440-442

119. Borner C., *Mol. Immunol.*, **2003,** *39(11)*, 615-647

120. Cory S., Dams J. M., *Nat. Rev. Cancer.*, **2002,** *2(9)*, 647-656

121. Mund T., Gewies A., Schoenfeld N., Bauer M. K., Grimm S., *Faseb J.*, **2003,** *17(6)*, 696-698

122. Heckman C. A., Mehew J. W., Boxer L. M., *Oncogene*, **2002,** *21(24)*, 3898-3908

123. Karin M., Lin A., *Nat. Immunol.*, **2002,** *3(3)*, 221-227

124. Salvesen G. S., Duckett C. S., *Nat. Rev. Mol. Cell. Biol.*, **2002a,** *3(6)*, 401-410

125. Kaufmann S. H., Earnshaw W. C., *Exp. Cell. Res.*, **2000,** *256(1)*, 42-49

126. Wang X., *Genes. Dev.*, **2002,** *15(22)*, 2922-2933

127. Bernardi P., Scorrano L., Colonna R., Petronilli V., Di Lisa F., *Eur. J. Biochem.*, **1999,** *264(3)*, 687-701

128. Kroemer G., Reed J. C., *Nat. Med.*, **2000,** *6(5)*, 513-519

129. Marchetti P,. Decaudin D., Macho A., Zamzami N., Hirsch T., Susin S. A., Kroemer G., *Eur. J. Immunol.*, **1997,** *27(1)*, 289-296

130. Reed J. C., *Nat. Rev. Drug. Discov.*, **2002,** *1(2)*, 111-121

131. Mullauer L., Gruber P., Sebinger D., Buch J., Wohlfart S., Chott A., *Mutat. Res.*, **2001,** *488(3)*, 211-231

132. Hanahan D., Weinberg, R.A., *Cell*, **2000,** *100(1)*, 57-70

133. Wang X. W., *Anticancer Res.*, **1999,** *19(6A)*, 4759-4771

134. Hockenbery D., Nunez G., Milliman C., Schreiber R. D., Korsmeyer S.J., *Nature*, **1990,** *348(6299)*, 334-336

135. Reed J. C., *J. Clin. Oncol.,* **1999,** *17(9),* 2941-2953

136. Kondo S., Shinomura Y., Miyazaki Y., Kiyohara T., Tsutsui S., Kitamura S., Nagasawa Y., Nakahara M., Kanayama S., Matsuzawa Y., *Cancer Res.,* **2000,** *60(16),* 4328-4330

137. Rampino N., Yamamoto H., Ionov Y., Li Y., Sawai H., Reed J. C., Perucho M., *Science,* **1997,** *275(5302),* 967-969

138. Yin C., Knudson C. M., Korsmeyer S.J, van Dyke T., *Nature,* **1997,** *385(6617),* 637-640

139. Hainaut P., Hollstein M., *Trends Mol. Med.,* **2000,** *8(8),* 385-389

140. Vousden K. H., Lu X., *Nat. Rev. Cancer,* **2002,** *2(8),* 594-604

141. Hoffman W. H., Biade S., Zilfou J. T., Chen J., Murphy M., *J. Biol. Chem.,* **2002,** *277(5),* 3247-3257

142. Wu Y., Mehew J. W., Heckman C. A., Arcinas M. Boxer L. M., *Oncogene,* **2001,** *20(2),* 240-251

143. Mihara M., Erster S., Zaika A., Petrenko O., Chittenden T., Pancoska P., Moll U.M., *Mol. Cell.,* **2003,** *11(3),* 577-590

144. Chene P., *Nat. Rev. Cancer*., **2003,** *3(2),* 102-109

145. Schon O., Friedler A., Bycroft M., Freund S. M., Fersht A.R., *J. Mol. Biol.,* **2002,** *323(3),* 491-501

146. Henriksson M., Selivanova G., Lindstrom M., Wiman K. G, *Apoptosis,* **2001,** *6(1-2),* 133-137

147. Ginsberg D., *FEBS Lett.,* **2002,** *529(1),* 122-125

148. Eischen C. M., Weber J.D., Roussel M. F., Sherr C. J., Cleveland J. L., *Genes Dev.,* **1999,** *13(20),* 2658-2669

149. Bartek J., Lukas J., *Curr. Opin. Cell Biol.***2001a,** *13,* 738-747

150. Bartek J., Lukas, J., *FEBS Lett.,* **2001b**, *490*, 117-122

151. Nyberg K. A., Michelson R. J., Putnam C. W., Weinert T. A., *Annu. Rev. Genet.*, **2002**, *36*, 617-656

152. O'Connell M. J., Walworth N. C., Carr A. M., *Trends Cell Biol.*, **2000**, *10*, 296-303

153. Michel B., Ehrlich S. D., Uzest M., *EMBO J.*, **1997**, *16*, 430-438

154. Saintigny Y., Delacote F., Vares G., Petitot F., Lambert S., Averbeck D., Lopez B. S., *EMBO J.*, **2001**, *20*, 3861- 3870

155. Osborn A.J., Elledge S. J., Zou L., *Trends Cell Biol.*, **2002**, *12*, 509-516

156. Hyrien O., *Biochimie*, **2000**, *82*, 5-17

157. Rothstein R., Michel B., Gangloff S., *Genes Dev.*, **2000**, *14*, 1-10

158. Sogo J. M., Lopes M., Foiani M., *Science*, **2002**, *297*, 599-602

159. Michel B., Ehrlich S. D., Uzest M., *EMBO J.*, **1997**, *16*, 430-438

160. Schiff P. B., Horwitz S. B., *Proc. Natl. Acad. Sci.*, **1980,** 77, 1561-1565

161. Vacca A., Ribatti D., Iurlaro M., Merchionne F., Nico B., Ria R., Dammacco F., *J. Hemat. Stem Cell Res.*, **2002,** 11, 103-118

162. Morris E. J., Geller H.M., *J. Cell Biol.*, **1996,** *134*, 757-770

163. Jordan M. A., Wilson L., *Curr. Opin. Cell Biol.*, **1998,** *10*, 123-130

164. Clark P. I., Slevin M. L., *Clin. Pharmacokinet.*, **1987,** *12*, 223-252

165. Henwood J. M., Brogden R. N., *Drugs*, **1990,** *39*, 438-490

166. Ekert H., Waters K. D., Jurk I. H., Mobilia J., Loughnan P., *Med. J.*, **1979,** *2*, 657-659

167. Borenfreund E., Puerner J.A., *Toxicol. Lett.*, **1985**, *24*, 119- 124

168. Triglia D., Wegener P. T., Harbell J., Wallace K., Matheson D., Shopsis C., *Alternative Methods in Toxicology*. A. M. Goldberg, ed. Mary Ann Liebert, Inc., New York, **1989,** *7*, 357-365

169. Fadok V. A., Voelker D. R., Campbell P.A., Cohen J. J., Bratton D. L., Henson P. M., *Journal of Immunology*, **1992**, *148*, 2207-2216

170. Kurokawa M., Koyama A. H., Yasuoka S., Adachi A**.**, *International Journal of Molecular Medicine,* **1999**, *3*, 527-530

171. Jenike RU., Sprengert ML., Wati MR., Porter AG., *J. Biol. Chem.* **1998,** *273*, 9357-9360

172. Sakahira H., Enari M., Nagata S., *Nature,* **1998**, *391*, 96-99

173. Eschenfeldt W. H., Puskas R. S., Berger S. L., *Methods in Enzymology*. Academic Press. **1987**

174. Pietenpol J. A., Stewart Z. A., *Toxicology,* **2002**, *181*, 475-481

175. Schaffer K. A., *Vet. Path.,* **1998**, *01*, 35:461-478

176. Poot M., Hiller K-H., Heimpel S., Hoehn H., *Experimental Cell Research*, **1995**, *218*, 326- 330

177. Powis G., *Free Radic. Biol. Med.,* **1989,** *6*, 63

178. de Abreu F. C., Ferraz P. A. L., Goulart M. O. F., *J. Braz. Chem. Soc.* **2002,** *13*,19

179. Rogers D., Hopfinger A. J., *J. Chem. Inf. Comput. Sci.* **1994,** *34*, 854

180. Rogers D., In: J. Devillers, Ed., *Genetic Algorithms in Molecular Modeling*, Academic Press, London, **1996,** 87–107

181. Sanyal U., Bhattacharyya S., Patra A., Hazra B., *J. Chromatogr.,* **2003,** *1017*, 225

182. Wang J. C., *Nat. Rev. Mol. Cell. Biol.,* **2002,** *3***,** 430-440

183. Tazi J., Rossi F., Labourier E., Gallouzi I., Brunel C., Antoine E., *J. Mol. Med.,* **1997,** *75***,** 786-800

184. Rossi F., Labourier E., Forné T., Divita G., Derancourt J., Riou J.F., Antoine E., Cathala G., Brunel C., Tazi J., *Nature,* **1996,** *381***,** 80-82

185. Chen H. J., Hwang J., *Eur. J. Biochem.,* **1999,** *265***,** 367-375

186. Andersen F., Tange T., Sinnathamby T., Olesen J., Andersen K., Westergaard O., Kjems J., Knudsen B., *J. Mol. Biol.,* **2002,** *322***,** 677-686

187. Soret J., Tazi J., *Prog. Mol. Subcell. Biol.,* **2003,** *31***,** 89-126

188. Champoux J. J., *Ann. Rev. Biochem.,* **2001,** *70,* 369-413

189. Labourier E., Rossi F., Gallouzi I.E., Allemand E., Divita G., Tazi J. *Nucleic Acids Res.*, **1998,** *26,* 2955-2962

190. Ting C. Y., Hsu C. T., Hsu H. T., Su J. S., Chen T. Y., Tarn W. Y., Kuo Y. H., Whang-Peng J., Liu L.F., Hwang J., *Biochem. Pharmacol.,* **2003,** *66,* 1981-1991

191. Van Bladeren P.J., *Chem. Biol. Interact.*, **2000,** *129*, 61-76

192. Schipper D. L., Wagenmans M. J. H., Wagener D. J. T., Peters W. H. M., *Int. J. Oncol.*, **1997**, *10*, 1261-1264

193. Burg D., Mulder G. J., *Drug. Metab. Rev.*, **2002**, *34*, 821-863

194. Hayeshi R., Mukanganyama S., Hazra B., Abegaz Hasler J., *Phytotherapy Research*, **2004**, *18*, 877-883